



UNIVERSITÀ  
DEGLI STUDI  
DI TRIESTE

# **Substituent-Dependent Stereoselective Synthesis of Hexa-Functionalised Borazine Derivatives**

## **PhD Thesis**

XXVIII Ciclo del Dottorato di Ricerca in Scienze e  
Tecnologie Chimiche e Farmaceutiche  
PhD School in Chemical and Pharmaceutical Sciences  
and Technologies

**María Mercedes Lorenzo García**

**May 2017**





**UNIVERSITÀ DEGLI STUDI DI TRIESTE**

**XXVIII CICLO DEL DOTTORATO DI RICERCA IN**

**SCIENZE E TECNOLOGIE CHIMICHE E  
FARMACEUTICHE**

**SUBSTITUENT-DEPENDENT  
STEREOSELECTIVE SYNTHESIS OF  
HEXA-FUNCTIONALISED BORAZINES**

Settore scientifico-disciplinare: CHIM/06

DOTTORANDA  
MARÍA MERCEDES LORENZO GARCÍA

COORDINATORE  
PROF. MAURO STENER

SUPERVISORE DI TESI  
PROF. DAVIDE BONIFAZI

CO-SUPERVISORE DI TESI  
PROF. PAOLO TECILLA

*46 T. uille*

**ANNO ACCADEMICO 2015 / 2016**



## Acknowledgements

*First of all, I'd like to thank my supervisor, **Pr. Davide Bonifazi**, for giving me the great opportunity to pursue my doctoral studies in his group. It has been a pleasure to work in this international environment. Thank you for guiding me during this experience, and for being always so enthusiastic and motivated by science.*

*Great thanks to **Pr. Tatiana Da Ros**, **Prof. Mario Grassi** and **Prof. Aurelio Mateo-Alonso** for being part of my doctoral commission. I would also like to thank **Pr. Alain Krief** and **Pr. Jorge Parola** for accepting to evaluate this manuscript.*

*Thanks to **Pr. Maurizio Prato** for accepting me in his big community. Besides, I would like to thank **Pr. Da Ros**, for all the support and help during my time in Trieste, as well as **Pr. Krief**, for the all the advices and chemistry discussions about my project, during my time in Namur.*

*I would like to thank Prato's group for this amazing experience. It has been a pleasure to work with you all, guys. Thank you! I always felt I was part of a big family, in all senses. Thanks to the people in Pharmacy and in Chemistry. I wish you all the best!*

*Me gustaría dar las gracias, de una manera especial, a la comunidad española del grupo. Gracias, chicos. **Alex**, todavía me acuerdo del primer día que llegaste y revolucionaste todo. Gracias por tantos momentos, por cuidarme como si de una hermanita pequeña se tratase. Por dejarnos siempre acampar en tu casa y que la sintiéramos como nuestra. **Joselete**, muchas gracias por haberte mostrado siempre tan dispuesto a ayudar en todo ¡Y por ese pollo al curry tan rico! **Caroline**, ¡La supermamá! Muchas gracias por haber cuidado tanto de esta gran familia. **Dani**, por todo lo que llevamos recorrido y disfrutado juntos, y por lo que seguro aún nos queda. Muchas gracias. **Arturo** ¿qué te voy a decir? Tu llegada a Trieste hizo el Lab 157 mucho más ameno y alegre. Gracias por todo. **Manu**, **Jenni**, **Nuria**, trajisteis la alegría y el entusiasmo para hacer de mi último periodo en Trieste uno de los mejores momentos de este doctorado.*

Sois geniales. **Jesús**, muchas gracias por haber formado parte de esta experiencia, mexicanito lindo. No me puedo dejar al resto de españolitos que formasteis también parte de esta aventura: **Martu, Laura**, muchas gracias. **Cris**, mi jerezana: ¡qué arte! Gracias por haber traído la alegría del sur a Trieste. **Mauro, Elena**: un placer haberos conocido.

This experience would not have been the same without 'The Chicas' group'. You have given this adventure meaning. Each one of you has been fundamental and very helpful along these years. **Agni**, your contagious craziness made our life better. **Vale**, how can I define it? Your passionate way to face life has captivated me; thanks for the period in Namur, you made my days better. **Tanja**, 'chiqui mía', you have been my fundamental partner in this experience, specially this last year, supporting me every day, even in the most difficult moments. THANK YOU. **Cris y Ana**... ¿qué deciros a vosotras? **Ana**, después de todo lo que hemos compartido es difícil destacar algo en concreto por lo que darte las gracias. Pienso que ser compañeras de piso durante esta experiencia nos ha unido de una manera particular. Muchas gracias por todo. **Cris**, ains mi Cris. Gracias de corazón por tu amistad incondicional desde el primer día; por tus motivadoras ganas de aprender. **Maribel**, a ti te tengo que dar las gracias por haber aparecido en mi vida y ser uno de los mayores regalos de este doctorado. GRACIAS CHICAS.

I am lucky to have been part of Lab 1 in Namur. From the first to the last, you were able to create such a nice working atmosphere. Thanks to 'The Borazine Team'. My pleasure to work in the same field than you. We have created an amazing family. **Jonathan** (Jorge), my first contact with this group, my supervisor. You have taught me your way to love the Chemistry, to be perseverant, and to keep the hope on what we do, always smiling and happy. **Hamid**, my dear **Hamid** ('estamos de vacaciones en Marbella'). You are amazing, always kind and helpful. Thanks. **Davide, Francesco**: what should I say to you? Vi voglio tanto bene, ragazzi. Grazie mille di tutto. **Florent, Riccardo**, thanks for being part of this amazing Lab. Finally, I would like to thank **Laure-Elie**. You are the example of how a colleague can become your best friend. Thanks for being always by my side. Thank you also for your help with this manuscript.

Many thanks to the rest of the members of the COMS, who contributed to this experience. Thank you **Rosaria, Valentina, Federica, Irene, Daphne, Dario, Adrian**. No me puedo olvidar de dar las gracias a **Marta**, ¡gracias por todo! Mi estancia en Namur no habría sido igual sin nuestras conversaciones en la facultad, nuestros millones de viajes y de aventuras. Gracias también a **Celia** y a **Mireia**, por esos sábados tan divertidos.

Besides, I would like to thank the people in Cardiff. This last year here has been extremely enriching. Thanks **Lou, Alex, Andrea, Rodolfo, Elissa, Oliwia, Olessia, Dmitry, Andrey, Elisa, Deborah and Fermi. Nicolas**, thank you for your collaboration in the project. **Antoine**, thanks a lot for the time dedicated to this manuscript, for each correction and advice. Thanks **Cataldo**, you are amazing. My pleasure to have met you! **Jacopo**, the new member of the borazine family, your enthusiasm will make you arrive anywhere you wish!

También quiero dar las gracias a mi grupito, la familia que yo elegí. Sois lo más bonito que uno puede tener en la vida. Cada uno de vosotros, con vuestras peculiaridades, habéis contribuido a hacerme feliz en tantas y tantas ocasiones. Mil experiencias juntos, millones de historias y momentos que nos han hecho lo que somos hoy en día. Gracias **Belén, Jesús, Félix, María Cifo, Silvita, Vero**. A ti, **Celia**, te quiero agradecer de una manera particular tu constante presencia en este último y difícil año. Gracias por haber estado día tras día apoyándome, por creer siempre en mí. Gracias también a mis Estrellitas. **Inma, Laura**, suerte la mía por contar con gente como vosotras.

Gracias a mis compañeras de piso. **Soni, Merian, Inmita**, gracias por seguir a mi lado. Lo que aquel piso unió... Gracias por quererme y mimarme con tanto esmero, por vuestras visitas, por los viajes juntas, por las quedadas, por los innumerables mensajes de ánimo. Gracias **Paquitina**, desde el primer momento fuiste el fichaje perfecto. Me llenas siempre de alegría. **Anita**, gracias a ti también, bonita, por estar siempre tan presente.

Gracias a mi familia, en especial a **mis cuatro puntos cardinales**, porque sin entender muy bien la razón por la que me marché de España, me habéis esperado cada vez que volvía con la más grande de las sonrisas y el más fuerte de los abrazos. Gracias abuelillos por vuestros consejos escondidos en cada una de las historias (batallitas) que me habéis contado. Es siempre un placer aprender tanto de la vida escuchándoos. Quiero incluir aquí a mi tía **Amparo**, una mujer culta donde las haya, enamorada de su trabajo y de su familia. Me quedo con el recuerdo de mis viajes a Barcelona, de las charlas en vuestra biblioteca, con todas vosotras. Gracias tía. Gracias a los **Fajardo-Lorenzo** por estar a mi lado en esta aventura; desde el primer día, mandando a vuestra pequeñaja en el grupo de apoyo moral junto a mi hermana; hasta el último, ayudando siempre en todo. Gracias a mi tía **Amparo** y a mi tío **Pedro** por tanto cariño.

Gracias **Bea**, mi complemento perfecto, por hacer siempre todo y más para ayudarme, por tu inmensa bondad y generosidad. Gracias a ti también, **Antonio**.

*Finalmente, querría agradecer a mis padres todo el apoyo que me han dado siempre. Por estar día tras día detrás de mi pantalla dispuestos a escucharme, animarme y ayudarme con todo. Por todo vuestro amor. **Papi**, por ser un guerrero que se enfrenta cada día a la vida con valentía, y por enseñarme que nunca hay que darse por vencido y que tengo que luchar para conseguir mis sueños. A ti **mami**, gracias por enseñarme tanto, por tu fuerza y por tu energía que siempre me guían; por ser el espejo en el que mirarme y el pilar en el que sostenerme.*

*“Mi suerte es andar de un sitio para otro y adaptarme a nuevos suelos. Creo que lo logro porque tengo puñados de mi tierra en las raíces y siempre los llevo conmigo”*

*Isabel Allende. Mi país inventado.*

*Thank you everyone*

*Gracias a todos*

*María Mercedes*

## Table of Contents

<i>List of Abbreviations</i> .....	V
<i>Abstract</i> .....	VII
<i>Riassunto</i> .....	IX

### CHAPTER 1- Introduction

1.1. Generalities .....	1
1.2 Synthesis of the Borazine Core .....	4
1.2.1 [1+1'+1+1'+1+1'] Hexamerisation via Dehydrogenation Reactions .....	5
1.2.2 [1+1'+1+1'+1+1'] Hexamerisation via Condensation Reactions .....	7
1.2.3 [2+2+2] Trimerisation Reaction.....	8
1.2.3.a Via Formation of Iminoboranes as Precursors .....	8
1.2.3.b Via Formation of Aminoboranes as Precursors .....	12
1.2.3.c Via Trimerisation from a BN- Phenanthrene Derivative .....	12
1.3 Reactivity of the Borazine Core .....	13
1.3.1 General Considerations about the Chemical Stability and Reactivity of the B <sub>3</sub> N <sub>3</sub> Core .....	13
1.3.2. Electrophilic Addition Reactions at the Borazine Core .....	14
1.3.3. Exchange Reactions at the Boron Sites .....	15
1.4 Building an 'Outer Shell': Peripheral Functionalisation of the 'Inner Shell' ..	18
1.5 A Reactivity Chart for Bis-Substituted Borazines: Compatible Reagents and Conditions.....	20
1.6 Materials and Applications .....	23
1.5.1 Materials for Optoelectronic Device .....	24
1.5.2 Self-Assembled Architectures at the Solid State and on Surfaces .....	25
1.5.3 Materials for H <sub>2</sub> Storage.....	29
1.7 Outline of the dissertation .....	31
1.8 References .....	32

## CHAPTER 2- *Substituent-Dependent Stereoselective Synthesis of Hexa-Functionalised Borazine Derivatives*

2.1	Introduction.....	40
2.2	Research Aim.....	42
2.3	Results and Discussion .....	44
2.3.1	Study of the Steric Protection using Bis- <i>B-ortho</i> -Substituted Groups...	44
2.3.2	Study of the Steric Protection using Mono- <i>Ortho</i> -Substituted groups ..	52
2.3.2.a	Syntheses of Borazine Derivatives containing Long-Range <i>ortho</i> -Substituents (Silyl Protected acetylene moieties) .....	52
2.3.2.b	Synthesis of Borazine 2-17 using a Triazene Moiety for the Steric Protection .....	57
2.3.2.c	Study of the Isomerisation Process in Borazine 2-15 from <i>cc</i> to <i>ct</i> .....	58
2.3.2.c.1	Variable Temperature Analysis .....	58
2.3.2.c.2	Calculation of $k$ and $\Delta G^\ddagger$ at 50 °C.....	61
2.3.2.c.3	Study of the Isomerisation Process.....	62
2.3.2.d	Syntheses of Borazine Derivatives containing Short-Range <i>ortho</i> -Substituents .....	71
2.3.4	Study of the Effect of the <i>ortho</i> -Substituent in the Stereoselectivity of the Process .....	77
2.3.4.a	Proposed explanation for the stereoselective process .....	79
2.3.5.b	LROs: triazene, acetylene TMS, acetylene TIPS.....	84
2.3.4.c	SROs: Me.....	85
2.3.4.d	SROs: OMe.....	86
2.3.4.e	SROs: Me, and LROs: acetylene TMS.....	87
2.3.5	Reactivity of the Borazine Core against Different Nucleophiles .....	88
2.3.5.a	Comparative Study of the Process in Terms of Nucleophilicity of the ArLi Reagent .....	88
2.3.5.b	Comparative Study of the Process in Terms of the Steric Hindrance of the ArLi Reagent.....	90
2.3.6	Mono-Protected Borazine Derivatives: Stability and Chemical Tools for the Formation of an 'Outer Shell'.....	91
2.3.6.a	Stability of the Borazine Core .....	91
2.3.6.b	Chemical Tools for the Formation of the 'Outer Shell' .....	92
2.3.6.c	Toward extended BNC-hybrids .....	96
2.4	Conclusions and Perspectives .....	99
2.5	References .....	101

## CHAPTER 3 - Scanning the Effect of *ortho*-Substituted *N*-aryl rings on the Formation of the Borazine Ring

3.1	Introduction.....	104
3.1.1	Mono- <i>ortho</i> -substituted Aniline Moieties .....	104
3.1.2	Bis- <i>ortho</i> -substituted Aniline Moieties .....	105
3.2	Research Aim .....	107
3.3	Results and Discussion .....	108
3.3.1	Formation of the BN-core from Aniline as Amino Precursor.....	108
3.3.2	Formation of the BN-core from mono-substituted Anilines as Amino Precursor.....	110
3.3.2.a	Formation of the BN-core from 2-methylaniline.....	110
3.3.2.a.1	Functionalisation with mono short-range <i>ortho</i> -substituted aryl species .....	111
3.3.2.a.2	Functionalisation with bis short-range <i>ortho</i> -substituted aryl species .....	113
3.3.2.a.3	Functionalisation with mono long-range <i>ortho</i> -substituted aryl species .....	116
3.3.2.b	Formation of the BN-core from 2-isopropylaniline as Amino Precursor.....	118
3.3.2.c	Study of the Formation of the BN-core from 2- <i>tert</i> -butylaniline as Amino Precursor.....	120
3.3.2.d	Study of the Formation of the BN-core from mono long-range <i>ortho</i> -substituted Aniline as Amino Precursor.....	122
3.3.3	Study of the formation of the BN-core from bis-substituted Anilines as Amino Precursor .....	123
3.4	Conclusions .....	126
3.5	References .....	127

## CHAPTER 4- Experimental Part

4.1	Instrumentation .....	129
4.2	Material and General Methods .....	132
4.3	Experimental Procedures .....	133
4.4	$^1\text{H}$ , $^{11}\text{B}$ , $^{13}\text{C}$ , and $^{19}\text{F}$ NMR spectra .....	178



## List of Abbreviations

Ar	Aryl
[A]	Concentration of molecule A
br	broad signal (NMR)
B.P.	Boiling point
Bu	Butyl
°C	Degree Celsius ( $0\text{ }^{\circ}\text{C} = 273.16\text{ K}$ )
cal	Calories
CH <sub>2</sub> Cl <sub>2</sub>	Dichloromethane
CHCl <sub>3</sub>	Chloroform
CDCl <sub>3</sub>	Deuterated chloroform
CHX	Cyclohexane
CPD	tetraphenylcyclopentadienone
d	Doublet (NMR)
ESI	ESI Electrospray ionisation
Et <sub>2</sub> O	Diethylether
EtOAc	Ethyl acetate
EtOH	Ethanol
eV	Electronvolt ( $1\text{ eV} = 1.602 \times 10^{-19}\text{ J}$ )
EWG	Electron withdrawing group
g	Gram
h	Planck constant
HOMO / LUMO	Highest occupied molecular orbital / Lowest occupied molecular orbital
h	Hour
HR	High resolution
<i>i.e.</i>	<i>id est</i> (latin) – that is to say
<i>i</i> -Pr	Isopropyl
IR	Infra-red
J	Joules

K	Degree Kelvin
k	Rate constant, kilo ( $10^3$ )
$k_B$	Boltzmann constant
L	Liter
ln	Natural logarithm
LRoS	Long-range <i>ortho</i> -substituents
m	Milli ( $10^{-3}$ ), multiplet (NMR)
M	Molar
Me	Methyl
MHz	Megahertz
min	Minute
mg	Milligram
Mes	Mesityl (2,4,6-trimethylphenyl)
M.P.	Melting point
MeOH	Methanol
MALDI	Matrix-assisted laser desorption/ionisation
MS	Mass spectrometry
NMR	Nuclear magnetic resonance
OTBDMS	<i>O-Tert</i> -butyldimethylsilyl
PAHs	polycyclic aromatic hydrocarbons
Ph	Phenyl
R	Substituent
r.t.	Room temperature
s	Seconds, singlet (NMR)
SRoS	Short-range <i>ortho</i> -substituent
T	Temperature
t	Time, triplet (NMR)
THF	Tetrahydrofuran
TIPS	Triisopropylsilane
TLC	Thin layer chromatography
TMS	Trimethylsilane
vdW	van der Waals
$\lambda$	Wavelength
$\delta$	Chemical shift (NMR)

## ABSTRACT

In the growing field of polycyclic aromatic hydrocarbons, the doping by heteroatoms has emerged as one of the most versatile approaches to tune the optoelectronic properties of the materials. In particular, borazine derivatives attracted a lot of attention in the last years. While their synthesis, functionalisation and possible use in a broad spectrum of applications have previously been investigated, the effect of different substituents on the formation of the borazine ring and its functionalisation at the boron site has yet to be addressed. This doctoral thesis aims at filling this gap through an in-depth study of the synthesis of novel borazines derivatives.

Before addressing the detailed investigations of this thesis work, *Chapter I* of this manuscript introduces a brief insight into the history and generalities of borazines in the literature since its discovery in 1926 by *Stock* and *Pohland*. This Chapter also includes the description of the synthetic approaches used for their production, as well as the chemical properties, stability and material applications.

The *Chapter II* of this manuscript describes the investigations developed toward the elucidation of the substituent's effect during the **functionalisation at the boron site** of the borazine core. Following a  $[1+1'+1+1'+1+1']$  hexamerisation route toward the formation of the borazine core (using an amino precursor and boron trichloride), the latter can be further functionalised by the addition of a nucleophile, which leads to the formation of stable borazine derivatives. Accordingly, the synthesis of multiple borazine moieties has been performed, using only one type of amino-precursor (aniline) and different organometallic derivatives during the functionalisation step. These organometallic moieties consist of aryl groups that contain one or two *ortho*-substituents, which allow for a partial- or full-protection of the borazine core, respectively. In the first case, the control of the stereoselectivity in a reaction in which two different isomers (*cc* and *ct*) can be formed, is the main focus of this study. Finally, the **chemical compatibility** and the **stability** of this novel class of partially-protected borazine moieties developed along this doctoral thesis is also discussed (Figure A.1).

Encouraged by the results obtained in *Chapter II*, the study developed in *Chapter III* aims at bringing light to the effect of the substituents on the **formation of the borazine core** together with the subsequent functionalisation toward the preparation of stable borazine moieties. For this purpose, the formation of the borazine core has been followed by reaction of different amino-precursors with boron trichloride. The later functionalisation at the boron site can lead to the formation of stable borazine derivatives, depending on the nature of the amino precursor (Figure A.1).

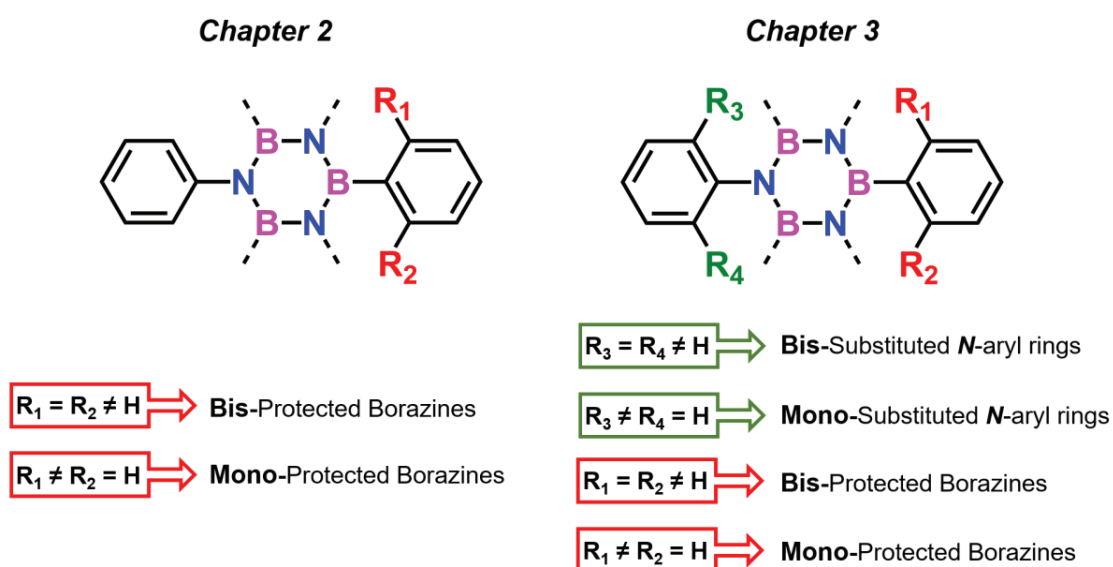


**Figure A.1** – Schematic representation of the work developed in this doctoral thesis.

## RIASSUNTO

All'interno del campo di studio degli idrocarburi policiclici aromatici, il doping con eteroatomi è emerso come uno degli approcci più versatili per modificare le proprietà optoelettroniche dei materiali. In particolare, i derivati di borazine hanno attratto molta attenzione negli ultimi anni. Mentre la loro sintesi, funzionalizzazione, e possibile impiego in una vasta gamma di applicazioni è stato già investigato, il ruolo che diversi sostituenti hanno nella formazione dell'anello borazinico e nella funzionalizzazione degli atomi di boro deve ancora essere assegnato. Questa tesi di dottorato ha lo scopo di rimediare a questa mancanza attraverso lo studio della sintesi di nuovi derivati borazinici.

Prima di focalizzarsi nella ricerca svolta in questo lavoro, il *Capitolo I* di questo manoscritto è volto all'introduzione di informazioni generali riguardanti la storia della borazina nella letteratura scientifica dal momento in cui fu scoperta da Stock e Pohland nel 1926. Il Capitolo I include anche la descrizione delle proprietà chimiche, stabilità, applicazione per la fabbricazione di materiali e approcci sintetici usati per la produzione di derivati borazinici.

Il *Capitolo II* descrive l'investigazione dell'effetto dei sostituenti durante la funzionalizzazione degli atomi di boro del nucleo borazinico. Utilizzando un precursore amminico e tricloruro di boro, la formazione dell'anello borazinico avviene seguendo una esamerizzazione di tipo  $[1+1'+1+1'+1+1']$ . Il nucleo borazinico formatosi può essere ulteriormente funzionalizzato tramite addizione di un nucleofilo, che conferisce stabilità al derivato borazinico. A questo scopo, una serie di borazine è stata sintetizzata usando lo stesso precursore amminico (anilina) e utilizzando diversi derivati organometallici per la funzionalizzazione finale. I reagenti organometallici scelti consistono in gruppi arilici contenenti uno o due sostituenti in posizione orto, consentendo così una protezione parziale o intera del nucleo di boro e azoto. Nel caso dei derivati parzialmente protetti, l'oggetto principale dello studio è costituito dal controllo della stereoselettività nella reazione in cui due isomeri (cc e ct) possono essere formati. Un'ulteriore discussione viene inoltre intrapresa a riguardo della compatibilità chimica e la stabilità di questa nuova classe di derivati borazinici con protezione parziale (Figura A.1).

Incoraggiati dai risultati ottenuti nel *Capitolo II*, lo studio intrapreso nel *Capitolo III* è volto alla delucidazione dell'effetto dei sostituenti nella formazione del nucleo borazinico e alla seguente funzionalizzazione di questo verso la preparazione di borazine stabili. Per questo motivo, la formazione di diverse borazine è stata ottenuta tramite reazione di diversi precursori amminici con tricloruro di boro. In questo caso la funzionalizzazione finale può portare alla formazione di derivati stabili a seconda del precursore amminico inizialmente usato (Figura A.1).

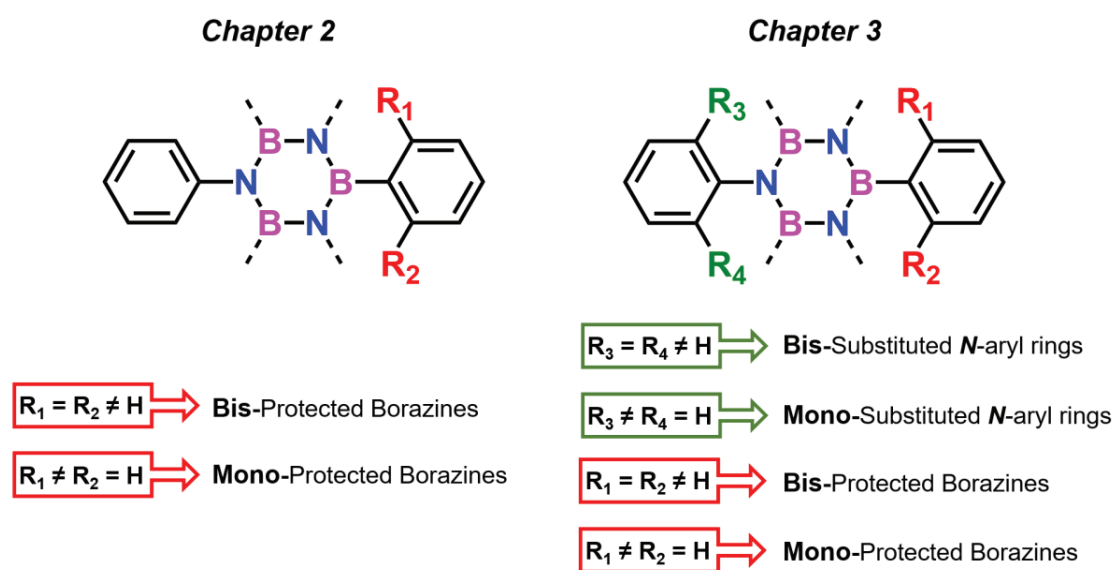


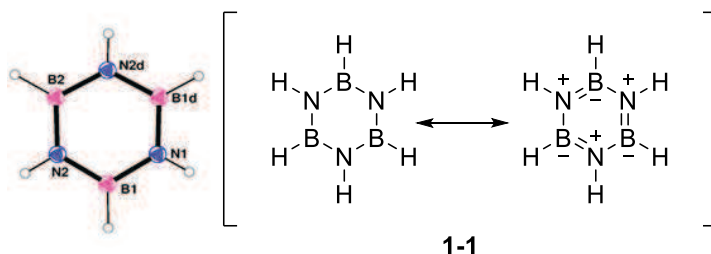
**Figura A.1** – Rappresentazione schematica del lavoro sviluppato in questa tesi di dottorato.

# CHAPTER 1

## Introduction

### 1.1. Generalities

Borazine ( $\text{H}_3\text{B}_3\text{N}_3\text{H}_3$ , molecule **1-1**, Scheme **1.1**), firstly isolated by *Stock* and *Pohland* in 1926, is often named “inorganic benzene” due to its similarities with its carbon analogue, benzene. It is a planar hexagonal ring, consisting of three boron atoms and three nitrogen atoms in alternate positions of a regular cycle. Each of its atom presents a  $sp^2$ -hybridisation, where the nitrogen atom has five electrons with a lone pair, and the boron atoms has three, with an empty  $p$  orbital available. As benzene, borazine is liquid at room temperature, shows equalised bond lengths (1.40 Å for benzene, and 1.44 Å for borazine, with the latter being between B–N single bond at 1.51 Å and B–N double bond at 1.31 Å) and shares a planar hexagonal structure.<sup>[1–3]</sup>



**Scheme 1.1** – Left: ORTEP representation of borazine **1-1**,<sup>[4]</sup> right: resonance forms for borazine **1-1**.

Notwithstanding, borazine shows only a weakly aromatic character,<sup>[5,6]</sup> thus displaying lower intrinsic stability that favour its hydrolysis to boric acid and ammonia under typical atmospheric moisture conditions. Another difference between borazine and its all-carbon analogue resides in the strong polar character of the B–N bonds with a dipole of 5.2 D and bond dissociation energy of 27.2 kcal mol<sup>-1</sup>,<sup>[7–9]</sup> resulting from the electron donation of the nitrogen atoms to the electrophilic boron centres. This strong polar bond imparts a series of peculiar physical and structural properties to the  $\text{H}_3\text{B}_3\text{N}_3\text{H}_3$ . Namely, a widening of the HOMO-LUMO gap (6.2 eV compared to 6.0 eV for benzene) along with an increase of the HOMO energy level with respect to

that of benzene (ionization potentials measured by photoelectron spectroscopy as 10.1 eV for borazine, compared to 9.25 eV for benzene).<sup>[10,11]</sup> This makes borazine a good UV emitter, displaying a significantly blueshifted absorption spectra if compared to those of oligophenylenes.<sup>[12]</sup> Similarly, the change in the electron density on the nitrogen atoms dictates a peculiar reactivity of the borazine core that greatly differ from that of classical aromatic compounds.<sup>[13]</sup>

After a series of publications during the 1960's and 1970's, where borazine's fundamental structural, reactivity and electronic properties were firstly approached in depth,<sup>[14–16]</sup> it was only in the 1990's that substituted borazines started to gather interest from the scientific community as precursors for boron nitride (BN) ceramics, in particular hexagonal boron nitride (h-BN), the insulating analogue of graphene.<sup>[17–19]</sup> In 2005, the first investigations of borazine derivatives as active materials in optoelectronic devices started to appear.<sup>[20]</sup>

Following vigorous synthetic developments of polyaromatic hydrocarbons (PAHs),<sup>[21]</sup> nanoribbons<sup>[22–28]</sup> and graphene,<sup>[29–31]</sup> the substitution (*i.e.* doping) of  $sp^2$ -carbon atoms with heteroatoms<sup>[32–35]</sup> has emerged as one of the most versatile approaches to tune the optoelectronic properties of graphitic materials. This has prompted a deep research in the field, rediscovering the use of the isoelectronic and isostructural B-N couples as doping units to trigger the electronic properties<sup>[36–41]</sup> of the all- $sp^2$ -carbon materials, leading to hybrids CBN monolayers.<sup>[42–45]</sup>

In particular, borazine derivatives and BN-doped PAHs (*e.g.*, azaborines,<sup>[46,47]</sup> borazapyrene,<sup>[48,49]</sup> borazaphenanthrene,<sup>[50,51]</sup> borazanaphthalene<sup>[52–56]</sup>) is now increasingly attracting the chemists' attention for their exploitation in a broad spectra of applications like UV-emitting OLEDs, materials for H<sub>2</sub> storage, ceramics, coatings, and in supramolecular chemistry for engineering new functional architectures both in solution and at interfaces. Figure 1.1 summarises the evolution of the yearly publication concerning borazine and its derivatives, with a clear steady increase in the recent years (sourced from SciFinder).

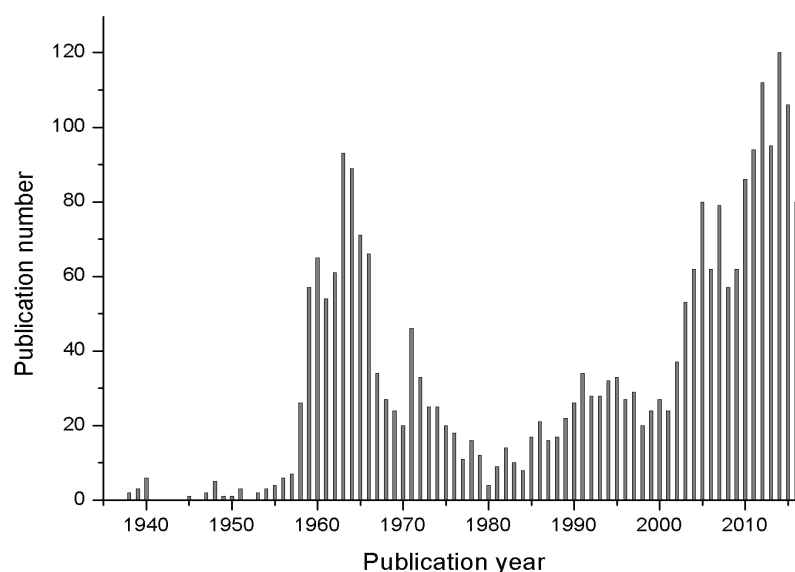


**Figure 1.1** - Histogram representation of the yearly appearance of publication about borazine and its derivatives until December 2016 (data taken from SciFinder).

This Chapter aims to give a general, yet concise, overview about the synthesis, organic reactivity and materials applications of borazine and its derivatives.<sup>[57]</sup> In particular, through a detailed description of the most significant examples coming from our group and others, we intend to show that, despite the intrinsic sensitivity of the borazine core towards hydrolysis, borazine derivatives can be rationally functionalised through a large variety of organic reactions (*e.g.*, metal-catalysed cross-coupling, nucleophilic addition and/or substitutions, photocyclisation, thermal dehydrogenation, electrophilic substitutions) being compatible with commonly used organic transformations employed in the Chemistry of protecting groups (*e.g.*, hydrogenation, fluoride, weak bases, metal-based reductions, hydrides, thermal cleavages to name a few).

This allowed the preparation of a large selection of scaffolds that has expanded the spectrum of different applications where borazine derivatives can be exploited. To ease the description of the different substitution patterns around the borazine core, the nomenclature depicted in Figure 1.2 will be used throughout this manuscript. Being the central core of the molecule composed of a substituted  $B_3N_3$  motif, each nitrogen and boron atom can bear different functional groups that, depending on their chemical nature, can form an ‘inner’ and an ‘outer shell’, with the latter decorating the peripheral rim of the molecule. In accordance with this general scheme, a labelling nomenclature is proposed as  $(ACD)B_3N_3(EFG)$ , where A, C, D and E, F, and G are the boron and nitrogen substituents, respectively. B was kept as the boron atom label for clarity. Whenever the substituents are the same, the letter with higher grade in the alphabet will be used to describe the substitution pattern (*e.g.*,  $A_3B_3N_3E_3$  when the substituents on the B and N atoms are the same, either with  $A = E$  or  $A \neq E$ ).

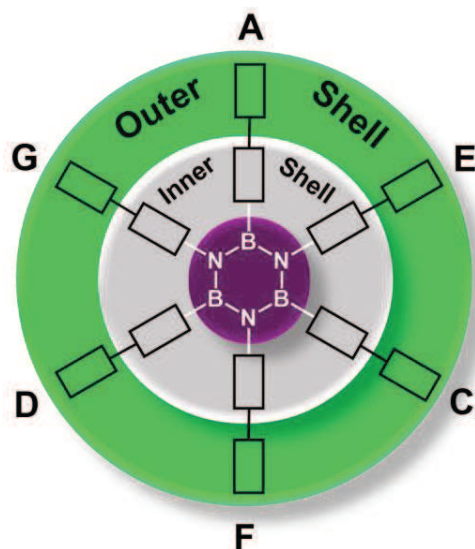


**Figure 1.2** - General representation of a borazine derivative, displaying the different substitution regions along with the labelling, as will be used in this manuscript.

## 1.2 Synthesis of the Borazine Core

As shown in Figure 1.3, the borazine core can be prepared following two cyclisation approaches: either *via* a  $[1+1'+1+1'+1+1']$  hexamerisation route from a mixture of the selected borane (*i.e.*, hydro or halide) and amine precursors, or through a  $[2+2+2]$  trimerisation strategy using a pre-formed imino or aminoborane derivative. Depending on the borane chemical nature, different reactions have been used: thermal or metal-catalysed dehydrogenation with boron hydrides, or condensation reactions with  $BX_3$ .

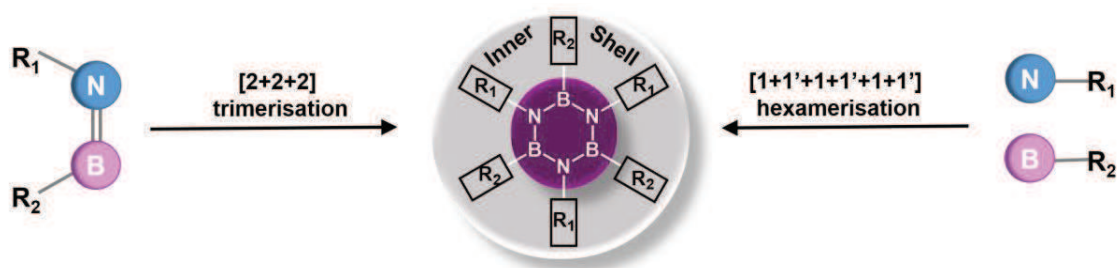
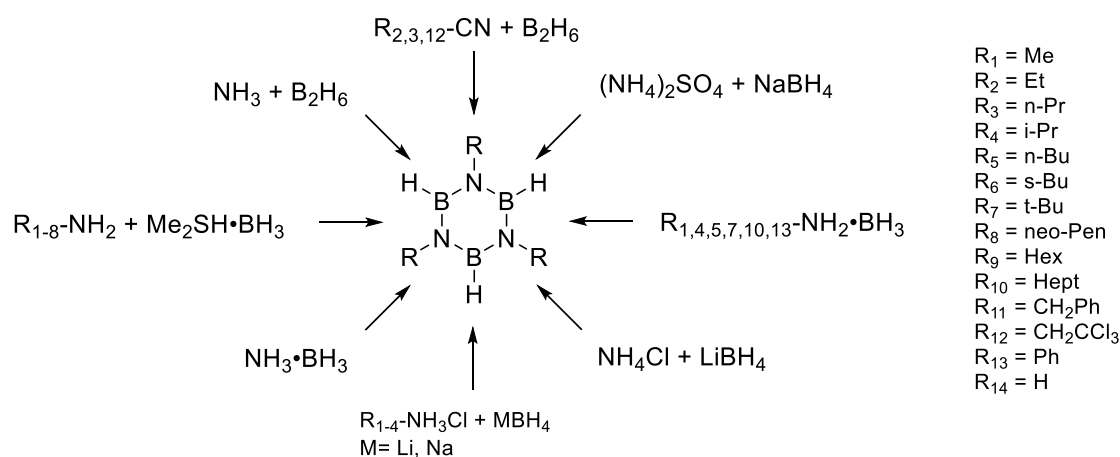


**Figure 1.3** - Synthetic strategies toward the synthesis of the borazine core, with  $R_1 = R_2$  or  $R_1 \neq R_2$  being an aryl, alkyl or hydrogen substituent.

### 1.2.1 [1+1'+1+1'+1+1'] Hexamerisation via Dehydrogenation Reactions

Historically, the thermal dehydrogenation of ammonia-borane complexes, firstly described by Stock and Pohland, was the very first method used to prepare borazine **1-1** ( $\text{H}_3\text{B}_3\text{N}_3\text{H}_3$ ).<sup>[1]</sup> The reaction firstly comprises the formation of a  $\text{NH}_3 \cdot \text{BH}_3$  adduct that, upon thermal dehydrogenation at 200 °C, undergoes formation of  $\text{H}_3\text{B}_3\text{N}_3\text{H}_3$ . In spite of the required high temperatures and the anhydrous conditions, this seminal protocol inspired further synthetic developments and exploitations, like for  $\text{H}_2$  storage applications. Following this method, other procedures were further developed (Scheme 1.2), which employed higher pressure (11 atm),<sup>[58]</sup> lower temperatures (140–160 °C),<sup>[59,60]</sup> or different precursors as a mixture of  $\text{NH}_4\text{Cl}$  and  $\text{LiBH}_4$ <sup>[61]</sup> or  $(\text{NH}_4)_2\text{SO}_4$  and  $\text{NaBH}_4$ .<sup>[55]</sup>



**Scheme 1.2** - Different protocols and precursors used for the thermal dehydrogenation of amino-borane complexes.

In a similar venue, both *N*-substituted alkyl- and aryl-borazines could also be synthesised (Scheme 1.2). Treatment of a *t*- $\text{BuNH}_2 \cdot \text{BH}_3$  adduct in a sealed tube at 360 °C for 5 h gives tri-*N*-*tert*-butylborazine ( $\text{H}_6\text{B}_3\text{N}_3t\text{-Bu}_3$ ) in nearly quantitative yield,<sup>[62]</sup> as well as aromatic amino-borane adducts lead to tri-*N*-arylborazines.<sup>[60]</sup> Notably, tri-*N*-methylcyclotriborazane ( $\text{H}_3\text{B}_3\text{N}_3\text{H}_3\text{Me}_3$ ) could be selectively obtained from  $\text{MeNH}_2 \cdot \text{BH}_3$  at 120 °C, that could be further converted into the corresponding tri-*N*-methylborazine ( $\text{H}_3\text{B}_3\text{N}_3\text{Me}_3$ ) at 200 °C.<sup>[60]</sup>

Analogously, alkylammonium chlorides were used to prepare tri-*N*-ethyl-, tri-*N*-propyl-, and tri-*N*-isopropylborazine in high yields (94%, 92%, and 84%, respectively).<sup>[63,64]</sup>

Nitriles precursors were also found to be a valid alternative to amines.<sup>[15]</sup> For instance, tri-*N*-methyl, tri-*N*-ethyl, and *N*-(2,2,2-trichloroethyl)borazine were obtained with 50–60% yield by heating at 85 °C in dimethoxyethane solutions of the corresponding alkylnitriles and  $\text{B}_2\text{H}_6$ .<sup>[15,65]</sup>

Remarkably, the nitrile-borane adducts decomposed at room temperature in few days to give *N*-alkylborazines with comparable yields.

In a different work,  $\text{Me}_2\text{S}\cdot\text{BH}_3$  was also proposed as boron source for borazines.<sup>[66]</sup> Several alkylamines were used to form borane adducts in solution that, after evaporation and heating at 120 °C, were transformed into a mixture of *N*-alkylcycloborazanes ( $\text{H}_6\text{B}_3\text{N}_3\text{H}_3\text{Alk}_3$ ) and *N*-alkylborazines ( $\text{H}_3\text{B}_3\text{N}_3\text{Alk}_3$ ). By further eliminating  $\text{H}_2$  at 200 °C, *N*-alkylcycloborazanes were converted into the corresponding *N*-alkylborazines with yields between 73% and 85%, with the dehydrogenation rates depending on the steric demand of the *N*-substituents. *In situ* preparation protocols of the borane derivative, *e.g.*  $\text{MeNH}_2\cdot\text{BH}_3$  from  $\text{NaBH}_4$  in the presence of  $\text{BF}_3\cdot\text{Et}_2\text{O}$  and  $\text{MeNH}_2$  in THF, also quantitatively yielded the corresponding methylborazine.<sup>[66]</sup>

In the last years, metal catalysed processes have also been used for preparing borazine by the dehydrogenation reaction. For example, using  $[\text{Rh}(1,5\text{-cod})(\mu\text{-Cl})_2]$  as catalyst, Manners and co-workers prepared borazines from  $\text{NH}_3\cdot\text{BH}_3$  or  $\text{CH}_3\text{NH}_2\cdot\text{BH}_3$  at lower temperatures (45 °C).<sup>[67]</sup> Kinetic studies showed that the rate-determining step for both substrates is the loss of the last  $\text{H}_2$  molecule, which has been demonstrated to be fast only at high temperature.<sup>[60]</sup> Tri-*N*-phenylborazine ( $\text{H}_3\text{B}_3\text{N}_3\text{Ph}_3$ ) could be obtained from  $\text{PhNH}_2\cdot\text{BH}_3$  in 56% yield after 16 h at 25 °C with the same rhodium complex. The higher tendency towards dehydrogenation of the tri-*N*-phenylcycloborazane with respect to the tris-*N*-methyl and to the all-hydrogen analogues is rationalised by the steric hindrance of the *N*-substituents. In other words, the greater the steric hindrance is, the faster the dehydrogenation reaction. Several  $\text{Cr}^{\text{IV}}$ ,  $\text{Mo}^{\text{III}}$ , and  $\text{W}^{\text{IV}}$  complexes were studied as catalysts, with the  $\text{Cr}^{\text{IV}}$  complexes displaying the highest dehydrogenation activities with  $\text{NH}_3\cdot\text{BH}_3$  or *t*-BuNH<sub>2</sub>·BH<sub>3</sub>.<sup>[68]</sup>

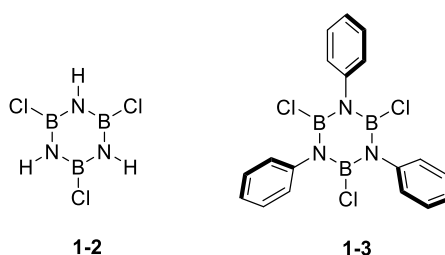
Hexacarbonyl complexes of such metals ( $\text{Cr}^0$ ,  $\text{Mo}^0$ ,  $\text{W}^0$ ) were also employed for the synthesis of *N*-alkylborazines from alkylamine-borane complexes.<sup>[68]</sup> The catalyst and the boron-nitrogen precursors were dissolved in benzene and irradiated for 8 h with a Hg lamp, then left in the dark at room temperature for further 24 h. Similarly to the previously discussed works, the best results were obtained using  $\text{Cr}^0$  complexes.<sup>[69]</sup>  $\text{MeNH}_2\cdot\text{BH}_3$  and  $\text{EtNH}_2\cdot\text{BH}_3$  gave comparable transformations in very high yields, whereas *t*-BuNH<sub>2</sub>·BH<sub>3</sub> yielded tri-*N-tert*-butylborazine in low yield. Moderate dehydrogenation yields (53%) were also obtained using nickel nanoparticles as catalysts in tetraglyme at 80 °C.<sup>[70,71]</sup>

The last example of borazine formation *via* dehydrogenation is by Lewis acid-catalysed reaction.<sup>[72]</sup> Indeed, by reacting  $(\text{NH}_4)_2\text{SO}_4$  with  $\text{NaBH}_4$  in tetraglyme in the presence of a catalytic amount of  $\text{AlCl}_3$ , borazine **1-1** was formed in 67% yield (recovered by vacuum distillation), while in the absence of the catalyst only 30% yield was obtained.

## 1.2.2 [1+1'+1+1'+1+1'] Hexamerisation via Condensation Reactions

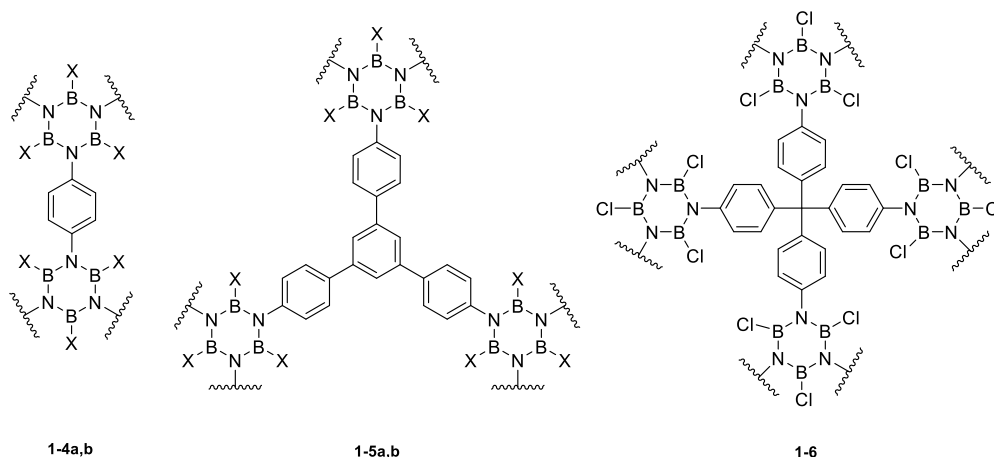
In 1955, a new methodology for the synthesis of cyclic condensed boron-nitrogen systems has been described using boron halides ( $BX_3$ ) as precursors. Reacting  $BCl_3$  with  $NH_4Cl$  at high temperatures, tri-*B*-chloro-borazine **1-2** (Scheme 1.3) could be synthesised in good yields,<sup>[73]</sup> and the structure was confirmed by X-ray diffraction.

Similarly, *B,B',B''*-trichloro-*N,N',N''*-tri(phenyl)borazine **1-3** can be prepared from  $BCl_3$  and aniline in anhydrous toluene heating under reflux (110.6 °C).<sup>[74]</sup> This product could be used for further functionalisation at the boron sites by nucleophilic substitution reactions (see Subsection 1.3.3 and Section 1.4).



**Scheme 1.3** - Molecular structures of trichloro-borazine derivatives **1-2** and **1-3**.

Besides aniline, different aryl amines have been used to prepare a large numbers of *N*-substituted borazines polymers (Scheme 1.4). For instance, by reacting *para*-phenylenediamine,<sup>[75]</sup> 1-3-5-tris-(4-aminophenyl)benzene,<sup>[75]</sup> or tetra-(4-aminophenyl)methane<sup>[76]</sup> with  $BCl_3$  or  $BBr_3$ , different amorphous polymers (**1-4**, **1-5**, and **1-6**) could be prepared for gas storage applications (see also Section 1.5).



**Scheme 1.4** - Linear and branched borazino-linked polymers prepared with aryl di, tri and tetraamines.<sup>[75–77]</sup> **1-4a** X = Cl, **1-4b** X = Br, **1-5a** X = Cl, **1-5b** X = Br.

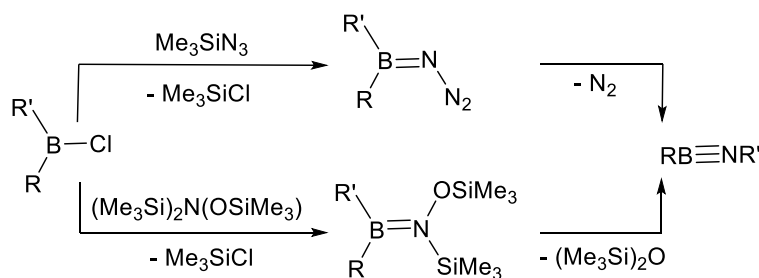
### 1.2.3 [2+2+2] Trimerisation Reaction

As alternative to the hexamerisation approach, borazine derivatives can be prepared by trimerisation of already prepared boron-nitrogen precursors, as proposed firstly by Paetzold and co-workers, later rediscovered by Liu and co-workers, and finally used by Bettinger and co-workers.

#### 1.2.3.a Via Formation of Iminoboranes as Precursors

Paetzold has based his investigations on the study of dialkyliminoboranes ( $R-B=NR'$ ), as the boron-nitrogen analogues to alkynes.<sup>[78]</sup> From these iminoboranes, depending on the steric hindrance of the alkyl groups and on the presence or not of catalyst, stable borazine derivatives could be synthesised.

The synthesis of this precursor starts from dialkylchloroborane, which can be transformed into azidoboranes or borane derivatives. Upon thermolysis of those intermediates, elimination of  $N_2$  or  $(Me_3Si)_2O$ , respectively, and by the migration of one of the alkyl groups from the boron to the nitrogen atom, the corresponding iminoboranes could be obtained (Scheme 1.5).<sup>[79]</sup>



**Scheme 1.5** - Formation of iminoborane precursors.<sup>[79]</sup>

As happens with alkynes, iminoboranes are thermodynamically unstable towards cyclooligomerisation or polymerisation reactions, and they just can be isolated under moist conditions by making the oligomerisation unfavourable (low temperature, high dilution, or/and in the presence of bulky alkyl groups).

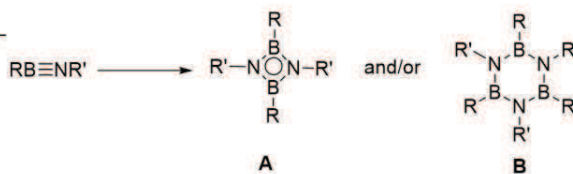
Cyclomerisation of these iminoborane derivatives can lead to the formation of a borazine cycle (cyclotrimerisation) or to the formation of a four-membered ring (*via* cyclodimerisation). During the process, linear B-N-structures can be also obtained.<sup>[78]</sup> Therefore, thermal oligomerisation yields four-membered rings (**A**) when the alkyl groups are big enough (*i.e.*  $R = R' = \textit{tert}$ -butyl), and otherwise, six-membered rings (borazines **B**) are obtained (*i.e.*  $R = R' = \text{Me}$ ) (Table 1.1).<sup>[79]</sup>

**Table 1.1** - Products obtained from the thermal stabilisation of  $RB=NR'$ .<sup>[79]</sup>

Entry	R/R'	Product
1	Me/Me	Borazine <b>B</b>
2	Me/ <sup>t</sup> Bu	Borazine <b>B</b>
3	Et/Et	Borazine <b>B</b>
4	Et/ <sup>t</sup> Bu	Borazine <b>B</b>
5	Pr/Pr	Borazine <b>B</b>
6	Pr/ <sup>t</sup> Bu	Borazine <b>B</b>
7	<sup>i</sup> Pr/ <sup>i</sup> Pr	Borazine <b>B</b>
8	Bu/ <sup>t</sup> Bu	Borazine <b>B</b>
9	<sup>i</sup> Bu/ <sup>i</sup> Bu	Borazine <b>B</b>
10	<sup>s</sup> Bu/ <sup>s</sup> Bu	Borazine <b>B</b> and Cycle <b>A</b>

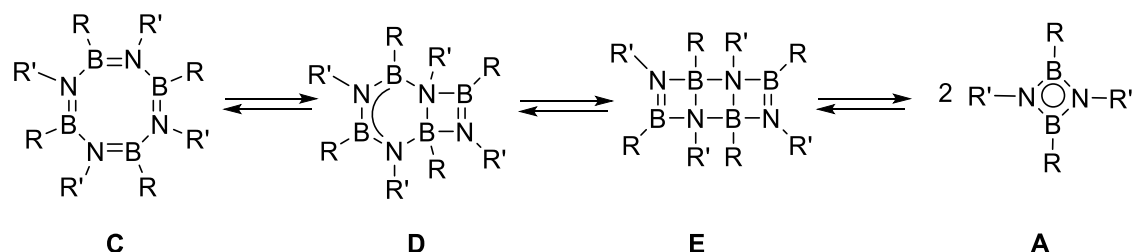
  

Entry	R/R'	Product
11	<sup>t</sup> Bu/ <sup>i</sup> Pr	Cycle <b>A</b>
12	<sup>t</sup> Bu/ <sup>t</sup> Bu	Cycle <b>A</b>
13	<sup>t</sup> Bu/Ph	Cycle <b>A</b>
14	<sup>t</sup> Bu/Mes	Cycle <b>A</b>
15	<sup>t</sup> Bu/SiMe <sub>3</sub>	Cycle <b>A</b>



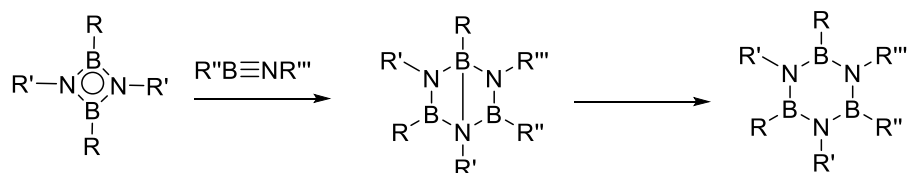
The presence of a catalyst can drastically change the result. Some of these iminoboranes, such as  $RB=NtBu$  ( $R = Et, Pr, iPr, Bu$ ) can yield cyclodimer **A**, instead of borazine **B**, upon stabilisation in the presence of catalytic amounts of the isonitrile  $C=NtBu$ .<sup>[78]</sup>

This catalyst can also govern the cyclotetramerisation of  $MeB=NtBu$  **1-7** to give the corresponding eight-membered ring (**C**). Paetzold and co-workers have postulated a mechanistic proposal for the formation of this cycle. Firstly, catalysed cyclodimerisation of the iminoborane precursor yields a four-membered ring, which can later dimerise at room temperature toward the formation of the eight-membered cycle. This results as a reversible equilibrium for two particular sets ( $R/R' = Me/tBu$  **1-7** and  $iPr/iPr$  **1-8**) and has been followed kinetically and thermodynamically by NMR methods. The cyclotetramer predominates at room temperature, while the four-membered ring predominates at higher temperatures (70-100 °C). The cyclotetramer is more favourable in energy, presumably because of a lower ring tension, but it is obviously disfavoured in entropy. Paetzold hypothesised the possible interconversion mechanism between these two species, as shown in Scheme 1.6:

**Scheme 1.6** - Possible mechanism for the interconversion between eight and four-membered rings.<sup>[78]</sup>

To postulate this mechanism, it was assumed the BN-analogues of bicyclo[4,2,0]octa-2,4,7-triene (**D**) and the Diels-Alder adduct of two molecules of the cyclodimer (**E**) to be the intermediates in this equilibration process. The all-carbon analogue, cyclooctatetraene,  $C_8H_8$ , is known to be in equilibrium with a small amount of bicyclo-[4,2,0]octatriene. In addition, cyclobutadiene gives irreversibly the Diels-Alder dimer. Nevertheless, this complete reversibility (as shown in Scheme 1.6) is unknown for the all-carbon analogues.<sup>[78]</sup>

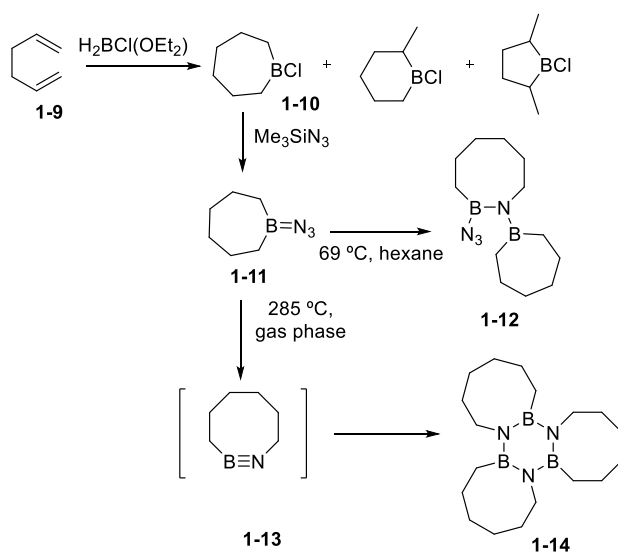
Besides, interconversion between four-membered rings (**A**) and six-membered rings (borazine type **B**) can be observed, upon addition of an external iminoborane. In particular, a four-membered ring undergoes [4+2] cycloaddition reaction when  $RB=NtBu$  is added. Therefore, [4+2] cycloaddition reaction is faster than the [2+2] cyclodimerisation of the iminoborane itself. The mechanistic proposal entails the formation of an intermediate, known as Dewar-borazine. (Scheme 1.7).<sup>[78]</sup>



**Scheme 1.7** - Interconversion between four-membered B-N-cycle (**1-a**) and six-membered borazine ring (**1-b**).<sup>[78]</sup>

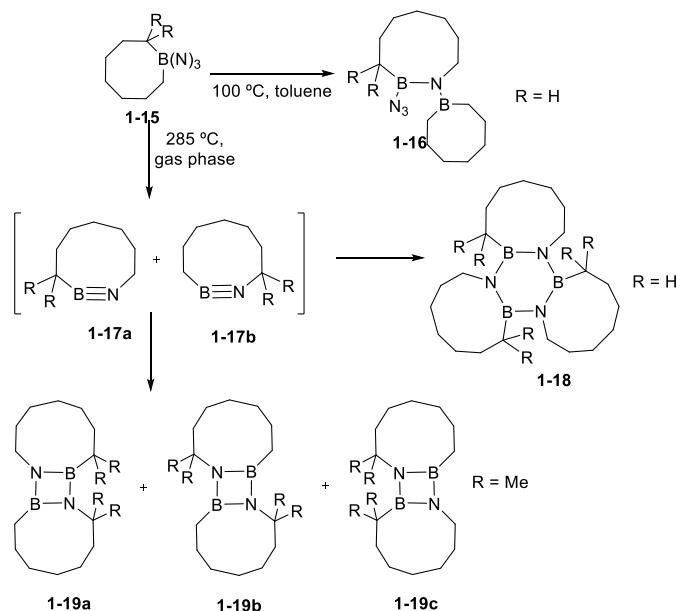
The generalisation of this [4+2] cycloaddition reaction might allow the synthesis of borazine derivatives with a mixed set of ligands. Note that an interconversion of four-membered rings into thermodynamically more favourable six-membered rings has been never observed in the absence of iminoboranes, apparently because of a high activation barrier.

More recently, the same group has published the synthesis of four-membered rings or six-membered rings using cyclic iminoboranes as precursors.<sup>[79]</sup> Starting by the hydroboration of 1,5-hexadiene **1-9** with  $H_2BCl(OEt_2)$ , chloroborane derivatives have been synthesised. The main product **1-10** can be separated from the others isomers thanks to its easy ring-opening polymerisation at 20-80 °C. Afterwards, the polymeric form gives pure compound **1-10** upon depolymerisation at 160 °C. The azidation of **1-10** gives monomeric **1-11**, that can yield **1-12** in boiling hexane by the azidoboration of iminoborane **1-11**. Conversely, in the gas phase at 285 °C, borazine **1-14** could be synthesised (Scheme 1.8).



**Scheme 1.8** - Formation of borazine **1-14** via cyclic iminoboranes in the gas phase.<sup>[79]</sup>

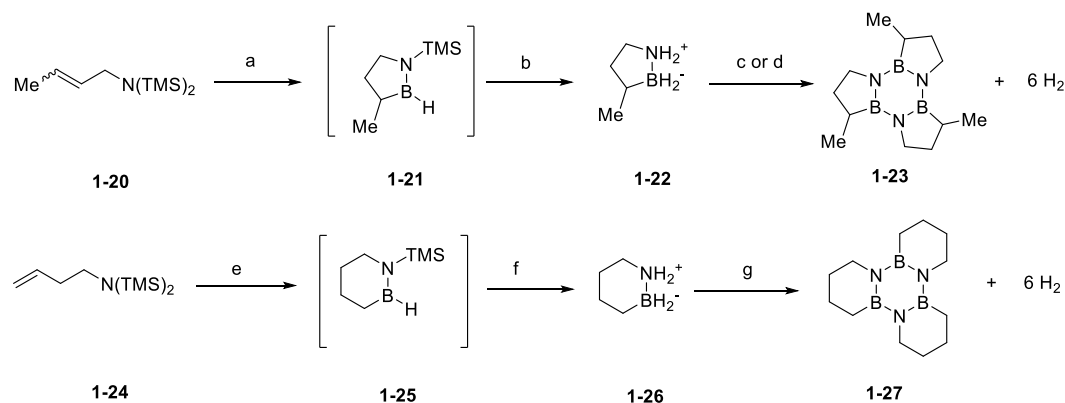
The role of the steric hindrance in the formation of the possible cycles was clearly demonstrated in the next example. Using 1-azidoboracyclooctanes **1-15** as precursors, four-membered or six-membered rings can be obtained. Cyclic iminoboranes are formed as described before, but it can evolve to borazine **1-18** just in the cases with no substituents close to the iminoboranes groups, otherwise four-membered rings are formed (Scheme 1.9).



**Scheme 1.9** - Selective formation of four-membered ring or six-membered ring, depending on the substituents on the cyclic iminoboranes.<sup>[79]</sup>

### 1.2.3.b Via Formation of Aminoboranes as Precursors

Starting from aminoboranes 1,2-BN-cyclopentane<sup>[71]</sup> **1-22** and 1,2-BN-cyclohexane<sup>[80]</sup> **1-26**, Liu and co-workers were able to prepare borazines **1-23** and **1-27** (Scheme 1.10) in quantitative yields *via* fast thermal or catalytic dehydrogenation using cheap metal halides (*e.g.* FeCl<sub>2</sub>) under very mild reaction conditions. Starting with commercially available compounds **1-20** and **1-24**, and by cyclisation with BH<sub>3</sub>·NEt<sub>3</sub> at high temperatures, intermediates **1-21** and **1-25** are obtained, which lead to the desired aminoboranes in the presence of KH firstly, and later HF·pyr. This allowed a controlled release of H<sub>2</sub> at temperatures below or at the proton exchange membrane fuel cell waste-heat temperature of 80°C. The reaction conditions are such that this chemical process can be considered as a suitable candidate for liquid-phase H<sub>2</sub> storage material (see also Subsection 1.5.3).



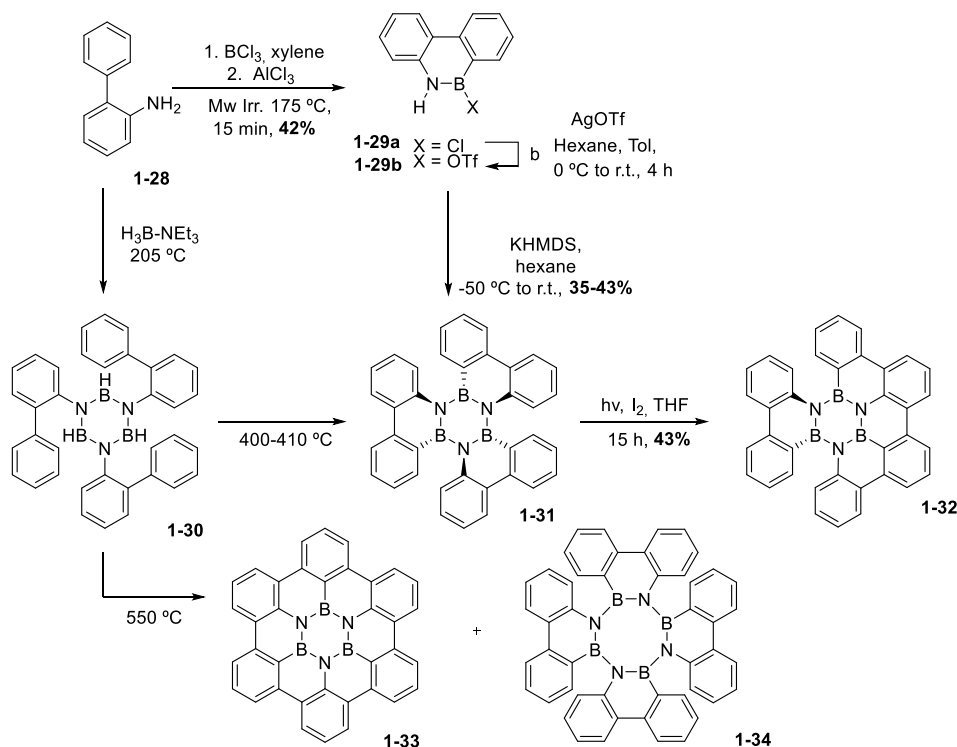
**Scheme 1.10** - Formation of borazine derivatives **1-23** and **1-27** by trimerisation from cyclic amino-boranes.<sup>[71,80]</sup> (a) BH<sub>3</sub>·Et<sub>3</sub>N, 160 °C, 48 h; (b) 1) KH, THF, r.t., 12 h; 2) HF·pyr, r.t., 2 h, 51%; (c) FeCl<sub>2</sub> (5 mol%), 80 °C, 20 min, quant.; (d) 150 °C, 1 h, 98%; (e) BH<sub>3</sub>·THF, 90 °C, 12 h; (f) 1) KH, THF, r.t., 12 h; 2) HF·pyr, r.t., 1 h, 94%; (g) toluene, 150 °C, 1 h, quant.

### 1.2.3.c Via Trimerisation from a BN- Phenanthrene Derivative

In a parallel study, Bettinger and co-workers developed a trimerisation protocol to prepare borazine **1-31**, in which three 9,10-BN-phenanthrene moieties are linked in a borazine core (Scheme 1.6). In a first venue, intermediate **1-29a** was prepared by microwave-assisted reaction of 2-aminobiphenyl **1-28** with BCl<sub>3</sub> in the presence of AlCl<sub>3</sub>.<sup>[51]</sup> Either through direct transformation or *via* the triflate derivative (**1-29b**), base-induced elimination reaction gave borazine **1-31** through cycloaddition-type reactions involving a BN-aryne intermediate.<sup>[81]</sup> Further irradiation of cyclotrimer **1-31** under a Hg lamp in the presence of I<sub>2</sub> afforded borazine **1-32** in 43% yield by ring-closure reaction (Scheme 1.11).<sup>[82]</sup>

Alternatively, cyclotrimer **1-31** could be also obtained by the thermolysis of borazine **1-30**, the latter being prepared from 2-aminophenyl **1-28** and Et<sub>3</sub>N·BH<sub>3</sub> at 205 °C. Through pyrolysis at 550 °C, the same group reported very recently about the identification by mass-spectrometry of an

unprecedented BN-doped coronene, borazinocoronene derivative **1-33** (Scheme 1.11) as a minority product in the reaction (yield 3-5%), and cyclotetramer **1-34** as major product.<sup>[83]</sup>



Scheme 1.11 - Formation of borazines **1-32** and **1-33**.<sup>[81,82]</sup>

## 1.3 Reactivity of the Borazine Core

### 1.3.1 General Considerations about the Chemical Stability and Reactivity of the $\text{B}_3\text{N}_3$ Core

Borazine derivatives are known to be very reactive towards nucleophiles, which undergo addition to the electrophilic boron atoms favouring the opening of the cycle and inducing the degradation of the borazine cycle. This usually gives a mixture of the corresponding amine and the boronic/boric acid. Notable examples include water, alcohols,<sup>[71]</sup> pyrazole and urea.<sup>[84,85]</sup> For instance, borazine **1-1** ( $\text{H}_3\text{B}_3\text{N}_3\text{H}_3$ ) rapidly decomposes to boric acid, ammonia and  $\text{H}_2$  in the presence of ambient humidity. This has been one of the major deterrents toward a more widespread synthetic development of BN-doped aromatic hydrocarbons and their exploitation.

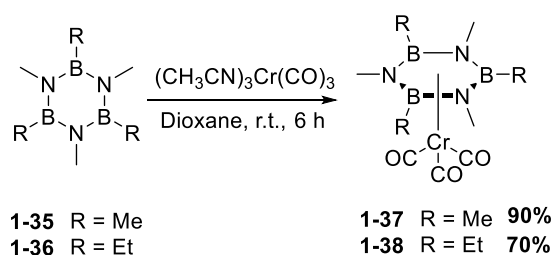
Three main approaches have been developed to significantly prevent the hydrolytic decomposition of borazines: *i*) the insertion of bulky substituents in proximity to the boron centres, *ii*) the introduction of electron-donating substituents on the nitrogen centres, and *iii*) the introduction

of electronegative groups in the proximity of the boron sites to prevent the attack of nucleophiles by electrostatic repulsion. For instance, the presence of electron-donating substituents on the nitrogen centres enhances the aromatic character of the BN core by allowing a better electron delocalisation from the nitrogen to the boron atoms, thus strengthening the B-N double bond character.<sup>[86]</sup> This in turn increases the cycle's stability toward hydrolysis, and more in general the reactivity toward any nucleophile addition.<sup>[87,88]</sup> The opposite is true for electron-withdrawing substituents on the boron atoms, which also enhance the cycle's stability.<sup>[89]</sup>

On the other hand, the presence of sterically-hindered substituents on the nitrogen<sup>[87]</sup> or boron atoms<sup>[90]</sup> can slow down the hydrolysis, with 2,6-xylyl,<sup>[16]</sup> 2-mesityl,<sup>[90]</sup> and 9-anthryl<sup>[91]</sup> groups displaying the greater effect. X-ray crystal structure analyses of these compounds clearly show that the boron atoms are sterically protected by the *ortho*-substituents.

Besides nucleophiles, oxidants are also able to decompose the borazine ring, however no experimental data on the products obtained has been published so far, except the description of intractable mixtures.

Similarly to benzene, the weakly aromatic borazine ring is also able to complex metals, forming half-sandwiched “piano-stool” complexes with Cr<sup>0</sup> (Scheme 1.12).<sup>[92]</sup> Hexa-alkylborazines form R<sub>3</sub>B<sub>3</sub>N<sub>3</sub>R<sub>3</sub>·Cr(CO)<sub>3</sub> at room temperature, which can be crystallised and characterised as η<sup>6</sup> complexes.<sup>[93]</sup> However, the weaker interaction holding the borazine core to the metal can lead to the protodeborylation of the phenyl substituents, decomposing the borazine core and yielding C<sub>6</sub>H<sub>6</sub>·Cr(CO)<sub>3</sub> as the main product.<sup>[94]</sup> Complexation with Li is also possible, giving rise to multiple binding motifs (η<sup>1</sup>, η<sup>2</sup> or η<sup>3</sup> complexes) depending on the reagents and equivalents used.<sup>[95]</sup>

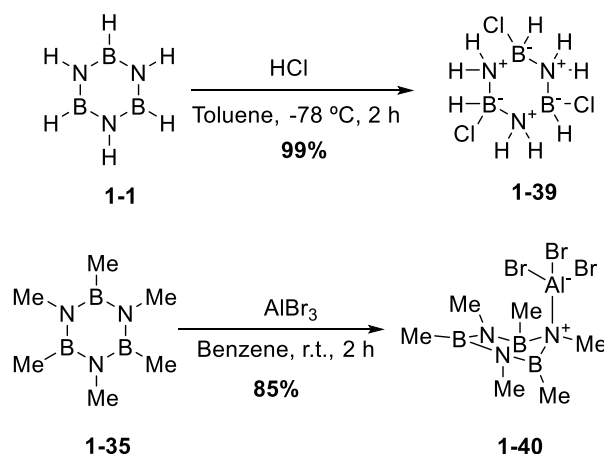


**Scheme 1.12** - Formation of borazine-chromium complexes **1-37** and **1-38**.<sup>[93]</sup>

### 1.3.2. Electrophilic Addition Reactions at the Borazine Core

Borazine rings readily undergo addition of hydric acids, such as HCl and HBr at -78 °C, yielding molecular derivatives featuring a broken aromaticity and thus a non-planar conformation of the central ring.<sup>[96–98]</sup> The reaction takes place on each B-N bond, breaking the partial double bond character, ultimately forcing the borazine core to adopt a chair-like conformation. For instance, addition of HCl to H<sub>3</sub>B<sub>3</sub>N<sub>3</sub>H<sub>3</sub> **1-1** at low temperature in the absence of water, forms adduct

$\text{H}_3\text{B}_3\text{N}_3\text{H}_3 \cdot 3\text{HX}$  **1-39** in quantitative yields (Scheme 1.13). Heating to 130 °C dissociates the complex back to the former  $\text{H}_3\text{B}_3\text{N}_3\text{H}_3$  **1-1** condensing HCl, thus favouring the formation of the weakly aromatic borazine core. The separation of a monoprotonated borazinium ion  $\text{H}_3\text{B}_3\text{N}_3\text{H}_4^+$  proved to be very difficult with direct HX addition, but it could be achieved with sterically-hindered conjugated base, like  $\text{AlX}_3\text{Z}^-$ . For instance, non-planar borazinium ion **1-40** could be prepared upon addition of  $\text{AlBr}_3$  to borazine **1-35** (Scheme 1.13).<sup>[99,100]</sup>

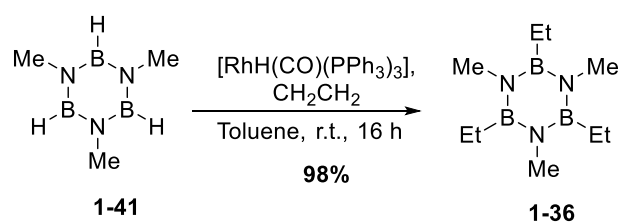


**Scheme 1.13** - Electrophilic addition of HCl to borazine **1-1**<sup>[99]</sup> and  $\text{AlBr}_3$  to borazine **1-35**.

Theoretical modelling investigations have been also performed to study the reactivity of the borazine core toward electrophilic substitution reactions and to explore the aromatic character of the BN ring compared to benzene.<sup>[5]</sup> Although the results did not show any magnetic anisotropy, the significant calculated energies for the resonance stabilisation (9.6 kcal/mol for  $\text{H}_3\text{B}_3\text{N}_3\text{H}_3$  **1-1**, compared to 21.9 kcal/mol for benzene)<sup>[5]</sup> as well as for the protonation suggest that the borazine core is weakly aromatic, thus displaying a similar chemical behaviour to that of benzene.<sup>[101]</sup>

### 1.3.3. Exchange Reactions at the Boron Sites

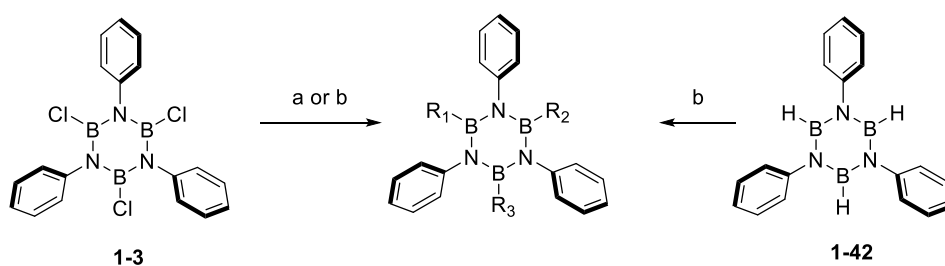
The first halogenation exchange reactions at the boron sites were reported by T. Schaeffer *et al.* and later revisited by Niedenzu *et al.* who prepared at room temperature *B*-mono and *B*-dihalogeno borazines in moderate moderate yields (25-35%) by treating molecule **1-1** with  $\text{BCl}_3$  and  $\text{BBr}_3$ .<sup>[59,102]</sup> Alternatively, halogenation with HCl, HBr,<sup>[14]</sup> or with  $\text{Br}_2$ ,<sup>[103]</sup> also affords *B*-substituted mono-, di- and tri-haloborazines. In addition,  $\text{H}_3\text{B}_3\text{N}_3\text{E}_3$  derivatives can be functionalised by hydroboration of alkenes using a rhodium catalyst,<sup>[66]</sup> allowing the isolation of mono-, bi- and tri-*B*-alkylborazine derivatives in 70-98% yield (Scheme 1.14).



**Scheme 1.14** - Hydroboration of ethylene by  $\text{H}_3\text{B}_3\text{N}_3\text{Me}_3$  **1-41**, catalysed by a Rh complex.<sup>[66]</sup>

However, the most common synthetic approach to functionalise a borazine core is based on the substitution reaction at the boron site of a borazine with *organolithium* or *organomagnesium* reagents. Since the reports in 1958 by Groszos and Stafiej,<sup>[104]</sup> the alkylation or arylation of hydroborazines with  $\text{RLi}/\text{ArLi}$  or  $\text{RMgBr}/\text{ArMgBr}$  has become one of the most versatile approaches to add substituents on the borazine core. In particular, following the  $\text{BCl}_3$ -based synthetic methodology, for which a tri-*B*-chloroborazine intermediate is formed in the presence of an amine, substituents at the boron centres can be added through substitution reactions upon addition of the relevant organometallic species.

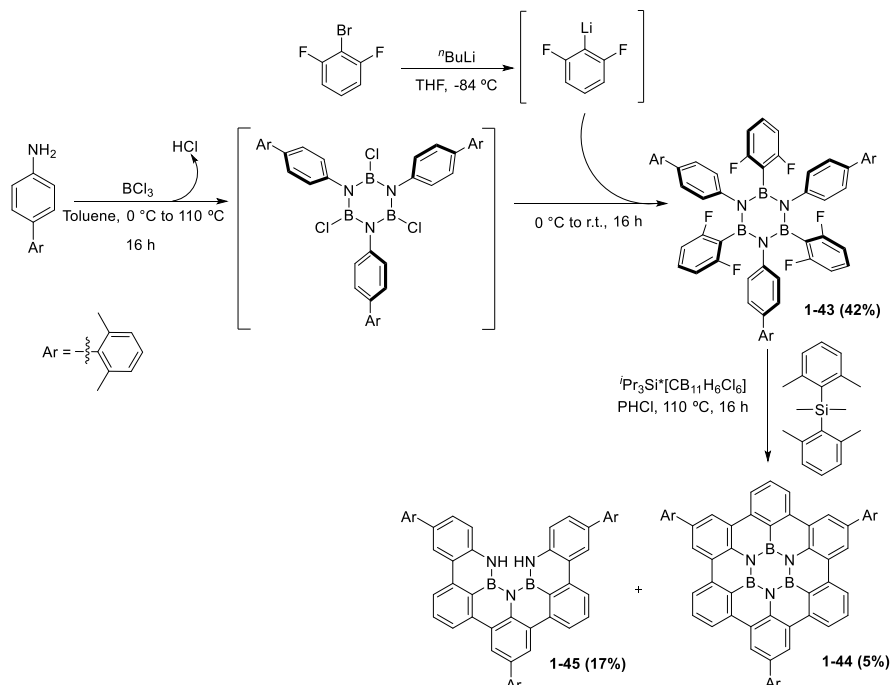
For instance, tri-*B*-chloroborazine **1-3** undergoes substitution reactions in the presence of an alkyl- or aryl Grignard or *organolithium* reagent into *B*-alkyl or *B*-aryl substituted derivatives (Scheme 1.15). Depending on the stoichiometry and the addition sequence, different *B*-substituted derivatives, *i.e.*,  $\text{A}_3$ -,  $\text{A}_2\text{C}$ -, or  $\text{ACD}$ -, could be obtained (Scheme 1.15). Alternatively, borazine **1-42** can be also used as effective substrates to give *B*-alkyl derivatives in the presence of a Grignard reagent.<sup>[90,91,104–108]</sup>



**Scheme 1.15** - Synthetic approaches toward the preparation of *B*-substituted borazines using organometallic reagents. (a) Sequential additions of  $\text{R}_1\text{Li}$ ,  $\text{R}_2\text{Li}$ ,  $\text{R}_3\text{Li}$  in THF; (b) Sequential additions of  $\text{R}_1\text{MgBr}$ ,  $\text{R}_2\text{MgBr}$ ,  $\text{R}_3\text{MgBr}$  in  $\text{Et}_2\text{O}$ .  $\text{R}_1 = \text{R}_2 = \text{R}_3$ ,  $\text{R}_1 = \text{R}_2 \neq \text{R}_3$ , or  $\text{R}_1 \neq \text{R}_2 \neq \text{R}_3$ .

Following this strategy, our group has recently presented the first rational synthesis of a BN-doped coronene derivative in which the central benzene atoms was replaced by a borazine ring. In particular, borazine derivative **1-43** has been synthesised using 4-xylyl aniline as amino precursor, and a difluoro *aryl lithium* for the substitution reaction.<sup>[109]</sup> This molecule yields hexa-*peri*-hexabenzoborazinocoronene derivative **1-44** (5%) upon six C-C ring-closure steps through an intramolecular Friedel-Crafts-type reaction, in the presence of  $[\text{iPr}_3\text{Si}\cdots\text{CB}_{11}\text{Cl}_6]$  and  $\text{Me}_2\text{SiMes}_2$  at

110 °C in PhCl. Together with derivative **1-44**, partially fused BN-derivative **1-45** was obtained as major product (17% yield) (Scheme 1.16). This suggests that the ring-closure occurs stepwise, the last closure being potentially the rate-determining step.



**Scheme 1.16** - Synthetic path for preparing xyllyl-substituted **1-44**.<sup>[109]</sup>

The identity of **1-44** was unambiguously determined by X-ray diffraction analysis, which confirms the nearly flat shape of the structure, similar to the all-carbon analogue (Figure 1.4). Finally, UV/Vis absorption, emission and electrochemical investigations show that the introduction of this central BN-core generates a dramatic widening of the HOMO-LUMO gap and an enhancement of the blue-shifted emissive properties with respect to the full-carbon analogous.

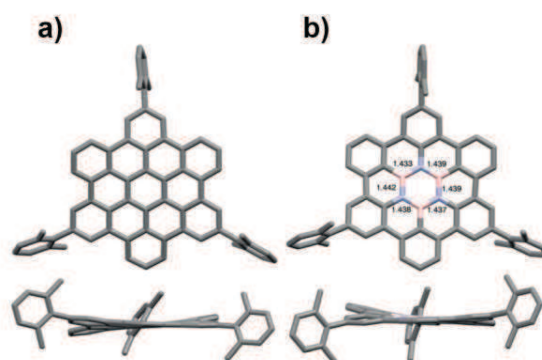


**Figure 1.4** – Horizontal (top) and side (bottom) view of the X-ray crystal structures of molecule **1-44** and of the full-carbon analogous.<sup>[109]</sup>

## 1.4 Building an ‘Outer Shell’: Peripheral Functionalisation of the ‘Inner Shell’

In this Section, different strategies undertaken to create an ‘outer shell’ of substituted borazines by functionalisation of the ‘inner shell’ are described (Figure 1.5).

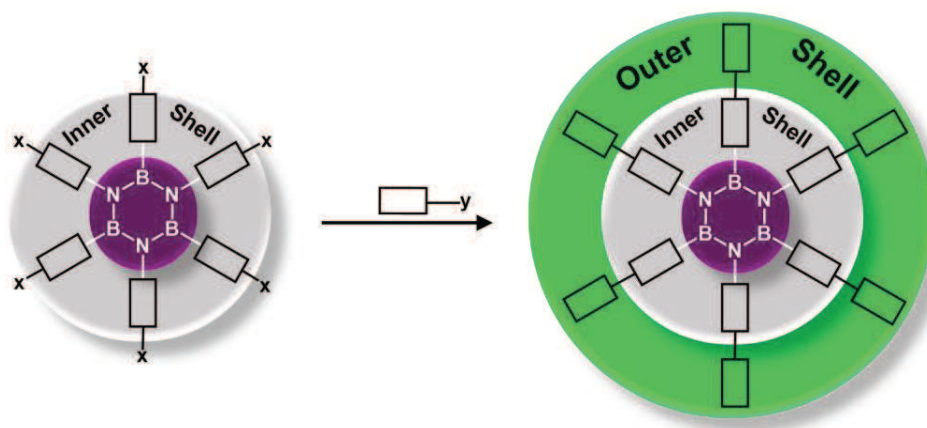
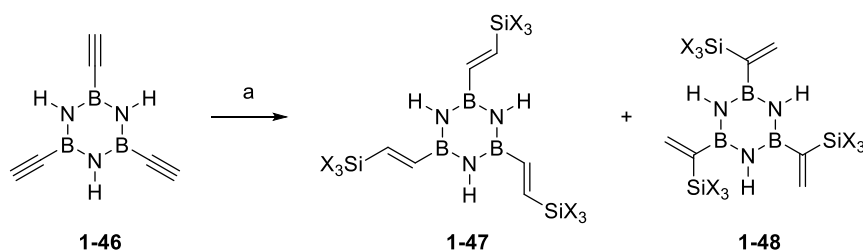


**Figure 1.5** - Formation of the borazine ‘Outer shell’, with X and Y being the reactive functional groups.

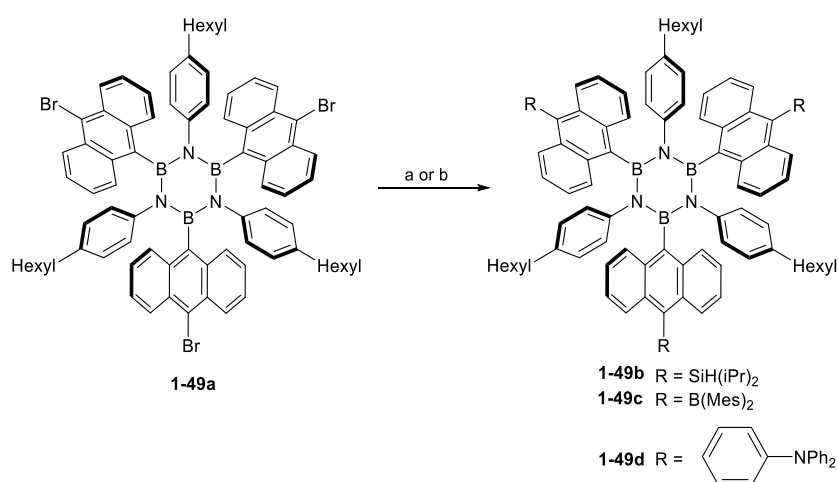
In 2003, Grützmacher and co-workers reported the functionalisation of tri-*B*-ethynylborazine **1-46** through a platinum-catalysed hydrosilylation reaction.<sup>[110]</sup> Indeed, using  $\text{HSiCl}_3$  or  $\text{HSi(OR')}_3$  as reagents in the presence of a catalytic amount of Pt/C in toluene at 120 °C, trivinylborazines **1-47** and **1-48** could be easily obtained (Scheme 1.17). Notably, the addition of the silane on the triple bond proceeded with *cis*-stereoselectivity, thus affording the  $\beta$ -*trans* isomers as major products. The addition of trichlorosilane  $\text{HSiCl}_3$  afforded isomer **1-47** in 80% of yield; alkoxysilanes gave rise to a complex mixture of regioisomers. It should be noted that the hydrolysis of the  $\text{RSiCl}_3$  is more rapid than the one occurring at the core, thus revealing to be compatible for the preparation of amorphous silica gel.



**Scheme 1.17** - Pt-catalysed hydrosilylation of tri-ethynylborazine **1-46**.<sup>[110]</sup> (a)  $\text{HSiX}_3$ , Pt/C (1 wt%), toluene, 120 °C, 48 h, X = Cl, **1-47** (80%), X = OMe, OEt, O<sup>i</sup>Pr, **1-47** (60%) + **1-48** in mixture with other isomers (40%).

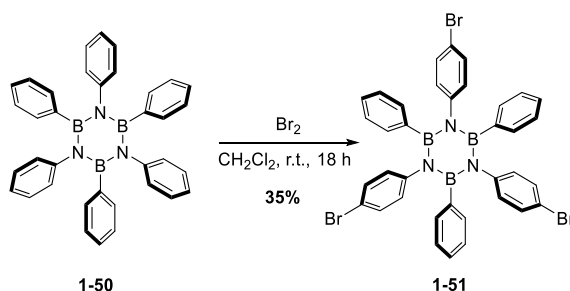
In a later work by Yamaguchi and co-workers, the synthesis and functionalisation of 10-bromo-anthryl-bearing borazine **1-49a** has been described.<sup>[91]</sup> The anthryl hydrogen atom sitting atop the boron centers shields the electrophilic centers from nucleophile additions, thus allowing the use of a large variety of organometallic reagents (Scheme 1.18).

Consequently, the treatment of **1-49a** with *t*-BuLi in THF at -78 °C followed by the addition of TIPSCl or Mes<sub>2</sub>BF led to tri-(diisopropylsilyl) **1-49b** and tri-(dimesitylboryl) **1-49c** derivatives in 45 and 34% yields, respectively, leaving intact the central borazine core. In addition, Negishi cross-coupling reaction between tri-bromo derivative **1-49a** with *p*-bromo(di-phenylamino) benzene gave tri-phenylamine-bound derivative **1-49d** in 24% yield,<sup>[92]</sup> the latter revealing to be a very good emitter.



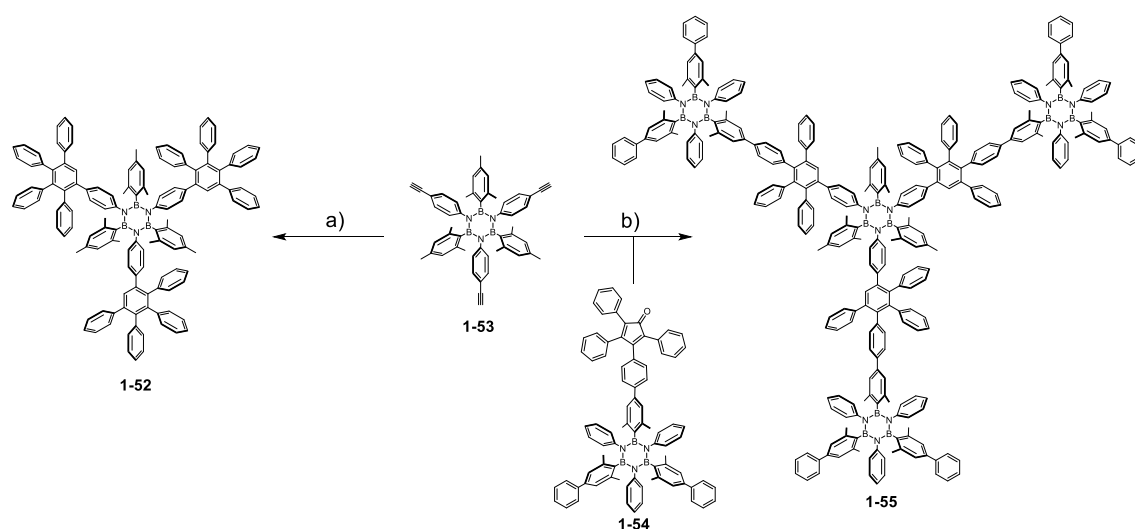
**Scheme 1.18** - Functionalisation strategies of trianthrylborazine **1-49a**.<sup>[91]</sup> (a) 1) *t*-BuLi, THF, -78 °C, 2) H(*i*-Pr)<sub>2</sub>SiCl or Mes<sub>2</sub>BF, r.t., 20 h, R = SiH(*i*-Pr)<sub>2</sub>, **1-49b** (45%), R = B(Mes)<sub>2</sub>, **1-49c** (34%); (b) 1) *t*-BuLi, THF, -78 °C 2) ZnCl<sub>2</sub>(tmen), 0 °C, 3) Ph<sub>2</sub>NPhBr, [Pd(PPh<sub>3</sub>)<sub>4</sub>], THF, r.t., 24 h, **1-49d** (24%).

In a recent work, Bettinger and co-workers reported the electrophilic aromatic bromination of hexaphenylborazine Ph<sub>3</sub>B<sub>3</sub>N<sub>3</sub>Ph<sub>3</sub> **1-50**, to yield selectively borazine **1-51** in 35% as the major product.<sup>[111]</sup> Only decomposition of the borazine core could be observed when tri-*N*-phenylborazine H<sub>3</sub>B<sub>3</sub>NPh<sub>3</sub> **1-42** was reacted with Br<sub>2</sub>, further demonstrating the crucial role of the *B*-substituents on the chemical reactivity of the derivative (Scheme 1.19).



**Scheme 1.19** - Bromination of arylborazine **1-50**.<sup>[111]</sup>

Finally, in a novel work presented by our group, decarbonylative [4+2] Diels-Alder cycloaddition reaction between ethynyl and tetraphenylcyclopentadienone derivatives has proved to be an efficient tool for the construction of borazine-doped polyphenylenes.<sup>[112]</sup> This new family of BN-polyphenylenes, featuring different doping dosages and orientations, has been achieved by the preparation of two different molecular modules: a core and a branching unit. For instance, borazine derivative **1-52** can be synthesised by [4+2] cycloaddition reaction between borazine derivative **1-53**, decorated with three triple bonds, and tetraphenylcyclopentadienone (CPD). Besides, if the tetracyclopentadienone is previously introduced in another borazine derivative (*i.e.* molecule **1-54**), by Suzuki cross-coupling reaction between an organoboron derivative of tetraphenylcyclopentadienone and a borazine exposing a suitable aryl halide, three-branched BN-doped polyphenylenes derivative **1-55** can be formed (Scheme 1.20).

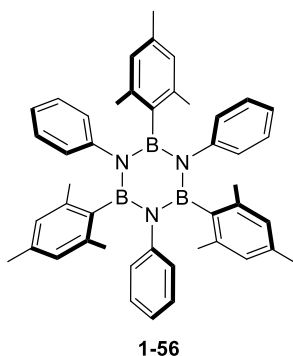


**Scheme 1.20** - Synthesis of borazine doped frameworks **1-52** and **1-55**: (a) tetraphenylcyclopentadienone (CPD), Ph<sub>2</sub>O, 180 °C, 2 h, 56%; (b) **1-54**, Ph<sub>2</sub>O, 180 °C, 18 h, 55%.<sup>[112]</sup>

## 1.5 A Reactivity Chart for Bis-Substituted Borazines: Compatible Reagents and Conditions

When selecting the strategy toward the functionalisation of either the ‘inner’ or ‘outer shell’ of a borazine derivative, it is of high importance to consider the reactivity, chemical compatibility and stability of the BN-core toward the different reagents and reaction conditions. It is now apparent to the reader that the borazine ring itself is very sensitive to nucleophiles, however if properly functionalised with sterically hindered groups, such as mesityl moieties at the boron sites of the BN-ring, namely the most extended example in literature, the BN-core becomes chemically inert.<sup>[90]</sup>

In an effort to assess the effect of a wide variety of standard types of reagents and reactions conditions on sterically bis-protected borazine rings, some of the results obtained in our group or taken from the literature are reported in Table 1.2.<sup>[57]</sup> Even though the reported reagents and experimental conditions are very limited if compared to the numerous synthetic tools nowadays available to organic chemists, Table 1.2 gathers the work developed in our group during the last years of activities in the field. Therefore, Table 1.2 may help those approaching the topic to further expand the organic chemical space of this kind of compounds. In particular, three levels of reactivity have been described and are reported as following: *i*) “S” stands for ‘stable’ and indicates that under the reported conditions, the borazine core remains intact; *ii*) “D” stands for ‘degradation’ and indicates the complete degradation of the borazine core under the given reaction conditions; and *iii*) “SD” stands for ‘slow degradation’ and indicates that the degradation of the borazine derivatives occurs after a prolonged reaction time ( $\geq 8$  h). This study was particularly focused on the reactivity of molecule **1-56** (Scheme 1.21), as well as on similar borazine derivatives decorated also with *ortho*-methyl groups for the steric protection of the core, but also containing functional groups in *para*-position of the *B*- or *N*-aryl rings. The tested reaction conditions were mainly targeted to protection–deprotection conditions of several typical protecting groups (*e.g.* silyl or benzyl), metal-catalysed cross-couplings, cycloadditions, oxidations, or acid–base reactions.



**Scheme 1.21** – Molecular structure of borazine **1-56**.

**Table 1.2** - Experimental conditions tested on bis *ortho*-protected hexaarylborazine derivatives.

	Reagents	Reactivity
<b>Organometallics</b>	RLi	S
	RMgX	S
	RZnX	S
	Pd-catalysed reactions	S
<b>Oxidants</b>	Aniline, NaI, <sup>t</sup> BuOCl, MeCN, r.t.	D
	tri-fluorobenzaldehyde, MeCN, r.t.	S
	Dimethoxyphenol, <sup>t</sup> BuONO, BF <sub>3</sub> ·OEt <sub>2</sub> , CH <sub>2</sub> Cl <sub>2</sub> , 0 °C-r.t.	D
	MAD <sup>a</sup> , nitrosobenzene, MeCN, r.t.	D
	Nitrosobenzene, KOH, DMF, 150 °C	D
	Aniline, CuBr, Py, 65 °C	D
	O <sub>3</sub> , Me <sub>2</sub> S, CH <sub>2</sub> Cl <sub>2</sub> , -85 °C	D
	m-CPBA, CH <sub>2</sub> Cl <sub>2</sub> , r.t.	SD
	FeCl <sub>3</sub> , MeNO <sub>2</sub> , 90 °C	S
	FeCl <sub>3</sub> , MeNO <sub>2</sub> , TFA, r.t.	S
	CAN <sup>b</sup> , CH <sub>2</sub> Cl <sub>2</sub> or THF, r.t.	S
<b>Reductants</b>	NaBH <sub>4</sub> , CHCl <sub>3</sub> , r.t.	S
	Fe, CH <sub>2</sub> Cl <sub>2</sub> , r.t.	S
	H <sub>2</sub> , Pd/C	S
<b>Bases</b>	TBAF, THF, r.t.	S
	NaOH aq, MeOH, THF, r.t.	S
	K <sub>2</sub> CO <sub>3</sub> , THF, MeOH, r.t.	S
<b>Electrophiles</b>	BnBr, NaH, DMF, r.t.	S
	Tf <sub>2</sub> O, pyridine, r.t.	S
	Me <sub>2</sub> NSO <sub>2</sub> Cl, DBU, MeCN, r.t.	S
<b>Irradiation</b>	I <sub>2</sub> , hv, cyclohexane or THF, r.t.	D
	I <sub>2</sub> , hv, toluene/heptane, r.t.	D
<b>Pericyclic reactions</b>	CPD, Ph <sub>2</sub> O, 180 °C	S

<sup>a</sup>MAD: methylaluminum bis(2,6-di-*tert*-butyl-4-methylphenoxide). <sup>b</sup>CAN: cerium ammonium nitrate.

The table has been divided following family reactions. As it was already explained along this manuscript, the best method to functionalise borazine cores is the use of organometallics, and of course, any decomposition is observed when using them.

As it can be seen in Table 1.2, borazine is sensitive to most of the oxidising agents that were tested, as degradation of the borazine core was observed within short times. The electron of the nitrogen atoms, poorly delocalised in the borazine ring, are not sterically protected by any bulky group. Consequently, in the presence of an oxidant, the borazine derivative can lose those electrons, leading to the decomposition of the ring. Some oxidants are yet compatible with this molecule, as shown with iron trichloride and CAN.

Being the boron atom sterically protected by the methyl groups, any addition to the electrophilic boron atoms can take place. Hence, the borazine core is stable in the presence of all tested reductants, bases and electrophiles, making those reagents a good tool for the formation of the ‘outer borazine shell’. Irradiation produces decomposition of the borazine core for this particular example, even though other examples has been reported in literature to be stable.<sup>[82]</sup> Finally, pericyclic reactions have demonstrated to be compatible with the stability of the borazine core. In particular, [4+2] cycloaddition reaction has been successfully performed, in spite of the required high temperatures. This showed that the formation of borazine’s ‘outer shell’ can be achieved with a large variety of synthetic strategies.<sup>[112]</sup>

## 1.6 Materials and Applications

As depicted in the Figure 1.6, borazine and its derivatives can find applications not only as precursors for optoelectronic organic materials but also as molecular materials for gas storage or supramolecular systems. In the following subsections, an overview of the main achievements in the field will be described. The applications related to the preparation of coatings,<sup>[113–115]</sup> ceramics,<sup>[116,117]</sup> 2D<sup>[118–120]</sup> and 3D<sup>[121]</sup> crystalline boron nitrides, and BN nanomeshes<sup>[122]</sup> have already been discussed in the past, and the interested reader is addressed to the topical reviews<sup>[123]</sup> or the literature in the field.

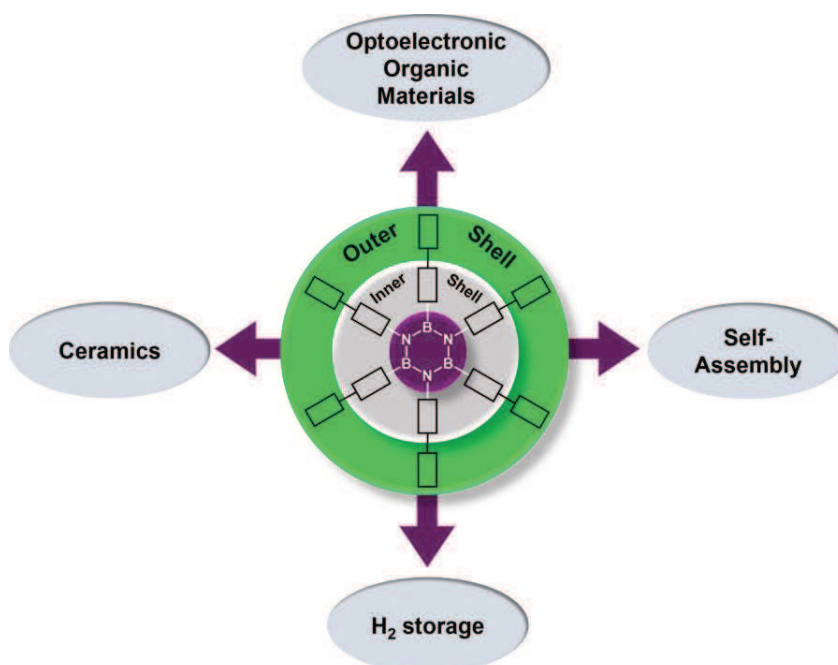


**Figure 1.6** - Schematic presentation of applications involving borazine and its derivatives.

### 1.5.1 Materials for Optoelectronic Device

To achieve emission in the higher energy gap region, namely in the normal and deep UV regions, chemists have designed molecules that, relying on the idea of ‘broken conjugation’,<sup>[43]</sup> display short conjugation length thus featuring high-energy HOMO-LUMO gaps falling in the ultraviolet energy region. Owing to the polarity of the B-N bond, an efficient way to decrease the conjugation length of an organic aromatic hydrocarbons emitter would be to dope all-carbon scaffolding with boron-nitrogen units.<sup>[43,90]</sup>

In this respect, with their high molecular bandgap (4 eV),<sup>[20,124]</sup> borazine-based UV-emitters represent valuable scaffolds to be inserted in active layers of organic light emitting devices (OLEDs) for the emission in the UV or deep UV. In a collaborative endeavour with the group of Cacialli, our group has recently reported the use of a borazine-based UV-emitter as active layer in a light-emitting electrochemical cell (LEC).<sup>[90]</sup> In solution, the spectra profiles of the Mes<sub>3</sub>B<sub>3</sub>N<sub>3</sub>Ph<sub>3</sub> **1-56** show photoluminescence quantum yields ( $\Phi_{em}$ ) between 6.6% and 7.7%, displaying little dependence on the solvent used. On the contrary, in the solid state, the emission profile changes in a dramatic depending on the obtained polymorph (Figure 1.7, left). When borazine **1-56** was used to form the emissive layer of LEC, weak UV-emission was observed at high voltages. In particular, charge injection into the LEC is observed with a strong nonlinear dependence of the current density  $J$  on the applied voltage  $V$ . Current densities of  $> 100 \text{ mA cm}^{-2}$  were achieved at high voltage ( $\sim 15 \text{ V}$ ), whereas a change of slope in the  $J/V$  characteristics suggests that a bipolar injection mechanism is present at  $\sim 5 \text{ V}$ . Similar results were obtained for the corresponding LEDs giving a promising EL quantum efficiency values of  $\sim 10^{-4} \%$  that, although rather weak, are the first of its kind and give hope to use borazine as suitable molecular scaffolds for UV-devices.

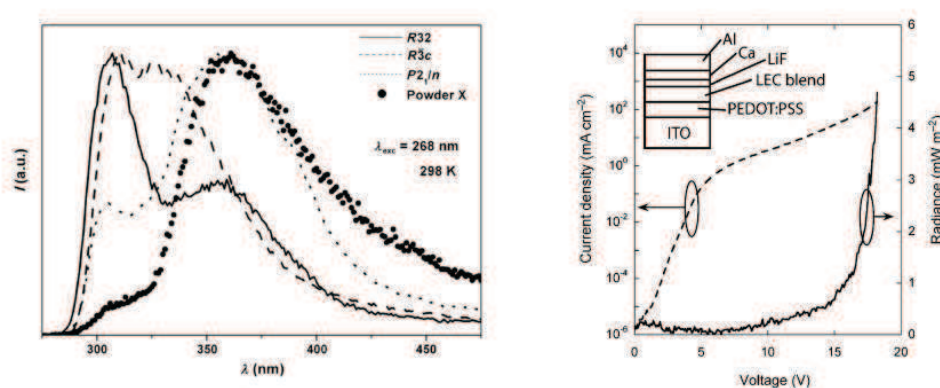
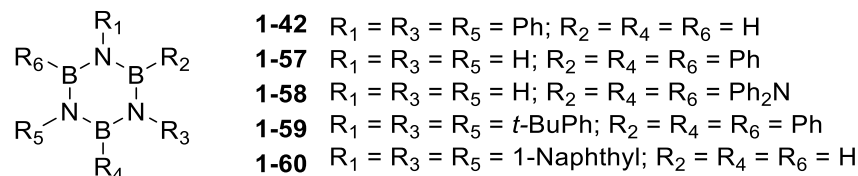


**Figure 1.7** - Left: normalised emission spectra of different polymorphs formed by borazine **1-56**: space group R3<sub>2</sub> (solid line), R3<sub>c</sub> (dashed line), P2<sub>1</sub>/n (dotted line), and ground powder (full circle). Right: current and radiance versus light characteristics of an LEC incorporating an active layer of borazine emitter **1-56**, blended with PEO as ion transporter and LiOTf as mobile ions. The device was fabricated with vertical structure ITO/PEDOT:PSS(80 nm)/active layer/LiF (6 nm)/Ca (30 nm)/Al (150 nm).

Through the introduction of different substituents in the borazine ‘inner shell’, it has been demonstrated the ability to tune the physical properties of such organic materials.<sup>[20]</sup> Five borazine derivatives **1-42**, **1-57**, **1-58**, **1-59** and **1-60** have been prepared (Scheme 1.22), and revealed to be suitable dopants owing to their promising values of hole and electron mobilities ( $\mu_h = 10^{-6}$ - $10^{-4}$  cm<sup>2</sup> V<sup>-1</sup> s<sup>-1</sup> and  $\mu_e = 10^{-6}$ - $10^{-3}$  cm<sup>2</sup> V<sup>-1</sup> s<sup>-1</sup> respectively).



**Scheme 1.22** - Structure of borazine derivatives **1-42**, **1-57**, **1-58**, **1-59** and **1-60**.<sup>[20]</sup>

OLED devices fabricated with borazine derivative **1-59** as hole transporting materials gave yellow EL emission characteristic of Alq<sub>3</sub> (tri-(8-hydroxyquinoline)); and a maximum luminance of 290 cd m<sup>-2</sup> at 11 V, with the maximum luminance of 6200 cd m<sup>-2</sup> at 21 V. The ability of the device to maintain high luminance at high voltages could be due in part to the high thermal stability of borazine compounds.

### 1.5.2 Self-Assembled Architectures at the Solid State and on Surfaces

The rapid development of molecule-based technologies has created a new impetus for studying the interaction and supramolecular assemblies of functional molecular units on surfaces, essential if one wants to fully understand the physical and structural nature of organic interfaces with metal electrodes.<sup>[125–128]</sup> Understanding and controlling the assembly of borazine molecular layers will provide the conceptual basis to engineer functional borazine-based supramolecular materials.<sup>[129–132]</sup>

In 2013, Kervyn *et al.* reported the first bottom-up preparation of borazine-based supramolecular architectures on metal surfaces.<sup>[133]</sup> Borazines **1-56** (Mes<sub>3</sub>B<sub>3</sub>N<sub>3</sub>Ph<sub>3</sub>) and **1-61** (Scheme 1.23) assembled in very different architectures on Cu(111) surfaces, as revealed by low-temperature (LT) scanning tunnelling microscopy (STM) measurements. While molecule **1-56** self-organizes into large islands forming full monolayers most likely held by van der Waals (vdW) interactions, A<sub>2</sub>C-type borazine **1-61** bearing a hydroxyl group ((Ph)<sub>2</sub>(OH)B<sub>3</sub>N<sub>3</sub>Ph<sub>3</sub>) undergoes exclusive “magic” clustering forming architectures composed of 7, 10, 11, 12 and 13 molecules (Figure 1.8). These findings are rationalised as a delicate interplay of short-range vdW attractions between neighbouring molecules and long-range Coulomb repulsions between deprotonated charged molecules.

**Figure 1.8** - Left: STM images for borazine **1-56** on Cu(111), deposited at 300 K, imaged at 77 K. (a) Large area of the Cu(111) surface. (b) and (c) Expanded views of the molecular islands, (d) Calculated structure superimposed on the imaged. Right: STM images of borazine **1-61** on Cu(111). (a) Isolated molecular cluster, highlighting the regular 7-mers. (b) Expanded view of Cu(111) step edge, revealing two enantiomers of an irregular cluster, (c) Expanded view of two 90° rotated regular 7-mers. (d) Calculated molecular model superimposed onto 7-mer.<sup>[133]</sup>

**Scheme 1.23** - Chemical formula of borazine derivatives **1-61** and **1-62**.

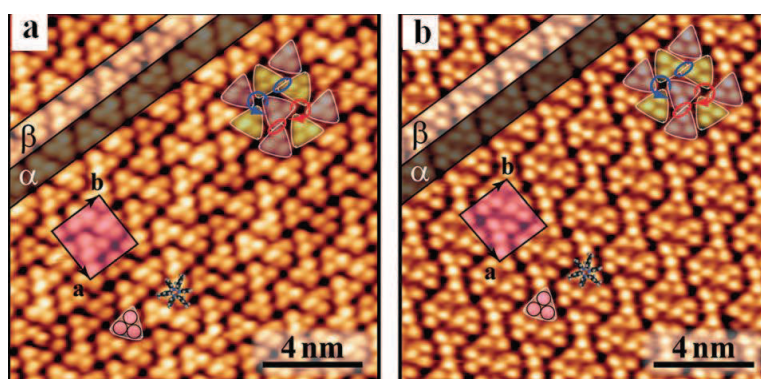


**Figure 1.1** - STM high resolution images of parallel supramolecular stripes constituting the general assembly of borazine **1-56** deposited on (a) Au(111) and (b) Cu(111) surfaces held at 300 K. The images were acquired at 77 K.<sup>[134]</sup>

In contrast, derivative **1-62** arranged into porous motifs. The porosity of the network was revealed to strongly depend on the nature of the metal substrate and the affinity of the outer rim with the surface (Figure 1.10).

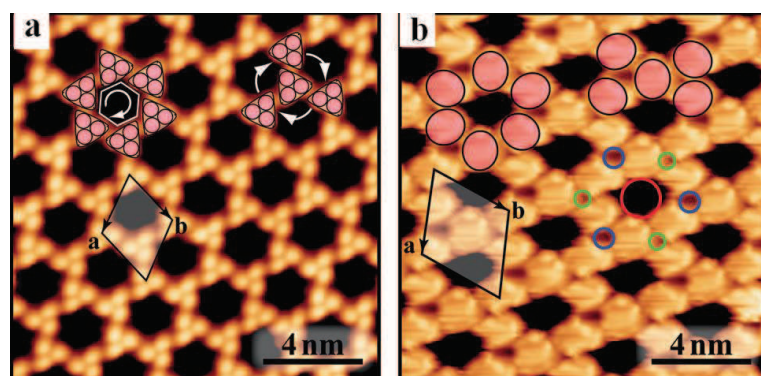


**Figure 1.10** - STM high resolution images of the porous network of borazine **1-62** deposited at r.t. on (a) Au(111) and (b) Cu(111). The images were acquired at 77 K.<sup>[134]</sup>

MD simulations rationalized the behaviour in terms of the structural differences of the peripheral substituents between the two structures. Consequently, it can be reasonably concluded that the B-N core does not influence the molecular ability to adsorb, self-assemble, or interact on different surfaces. In particular, the protruding phenyl-4-phenylethynyl substituents of molecule **1-62** act as intermolecular spacers, thus driving the formation of a porous network. Moreover, their flexibility allows a stronger interaction with the substrate which, in the case of the more reactive Cu(111) surface, causes a higher porosity (Figure 1.11).

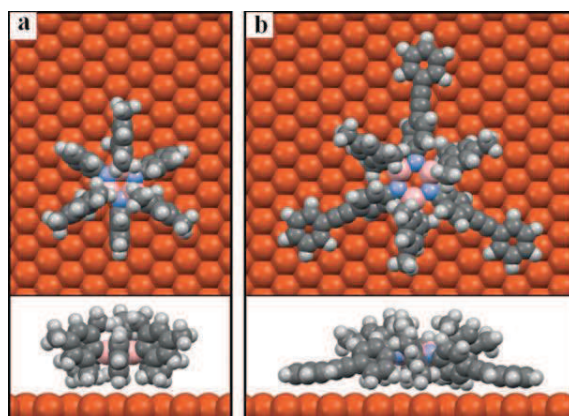


**Figure 1.11** - Calculated minimum energy adsorption configuration of (a) borazines **1-55** and (b) **1-61** on a Cu(111) surface. The steric hindrance between the Ph- and Mes- substituents results in the effective decoupling of the central borazine core from the surface for both molecules.<sup>[134]</sup>

The presence of different substituents in the borazine ‘inner shell’ can affect not only the self-assembly of the borazine on the solid surface but also in crystal packing. For instance, borazine bundles could be formed in the solid state (Figure 1.12).<sup>[91]</sup> On the basis of their  $C_3$ -symmetric gear-shaped molecular structures, tri-anthryl borazine **1-63** formed characteristic two-dimensional honeycomb-like networks, which consist of offset face-to-face intermolecular  $\pi$ -stacking of anthracene moieties (Figure 1.12). As such, these structures might be suitable for achieving high carrier transport in optoelectronic devices. In terms of fluorescence quantum yield, a 2-fold improvement was observed between anthracene alone ( $\Phi_f = 0.27$ ) and bundled molecule **1-63** ( $\Phi_f = 0.63$ ). This bundle effect can be rationalized by considering the rigidity of the bundled structure, which prevents conformationally-induced non-radiative decays of the excited states.

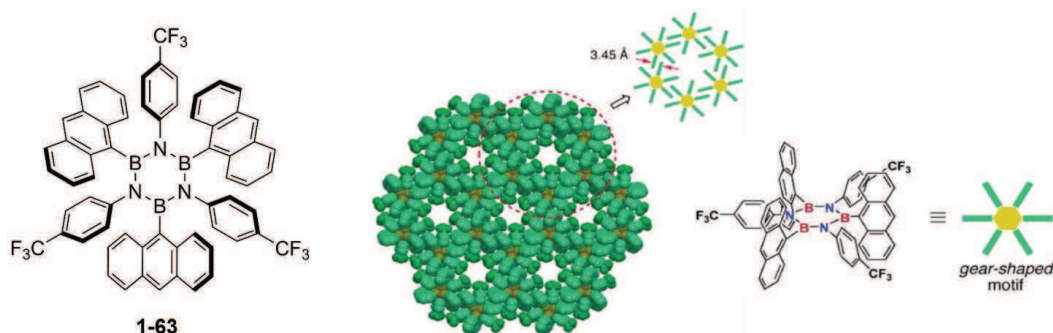
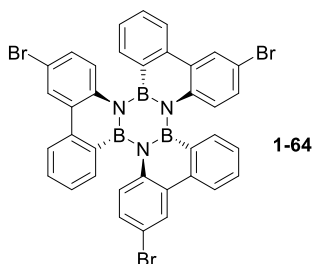


**Figure 1.12** - Chemical structure of borazine derivative **1-63** and its windmill arrangement at the solid state.<sup>[91]</sup>

In 2015, Sánchez-Sánchez *et al.* reported the surface-assisted polymerisation of borazine **1-64** (Scheme 1.24) on Ag(111) surfaces. By means of a stepwise thermal methodology, interlinked BN-HBC networks could be prepared on a Ag(111) surface under ultra-high vacuum (UHV) conditions (Figure 1.7).<sup>[135]</sup> In particular, thermal deposition of **1-64** on Ag(111) led to the formation

of non-covalent flower-like assemblies at 425 K (Figure 1.13, a). When temperature is raised to 475 K, phenyl-phenyl type cross-coupling reaction catalysed by Ag atoms occurred at the C-Br functionalities (Figure 1.13, b), forming covalently assembled networks. Complete cyclodehydrogenation of partially planarised molecule **1-64** could be achieved at 575 K (Figure 1.13, c), ultimately leading to the formation of the covalently-linked borazinocoronene network.



Scheme 1.24 - Chemical structure of borazine derivative **1-64**.

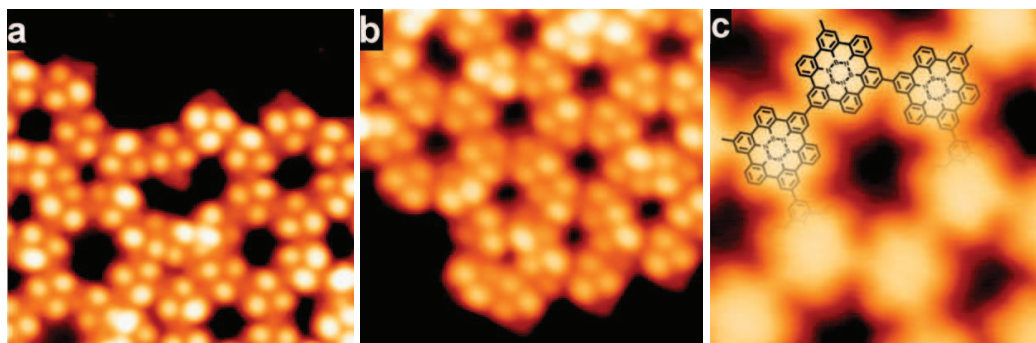


Figure 1.13 – (a) STM image of borazine **1-64** after deposition and annealing to 425 K. (b) Covalent network after polymerization at 475 K and (c) High resolution STM of the planar network after fully cyclodehydrogenation at 575 K. [135]

Together with the first self-assembly studies on surfaces, this represents the first step toward the implementation of the BN-doped hybrid carbon materials and the assessment of their real electronic properties and potentials applications in molecular devices.

### 1.5.3 Materials for H<sub>2</sub> Storage

One of the biggest technological challenges of modern societies is the development of cleaner energy sources that can mitigate the current dependence on fossil fuels. Over the last decades, H<sub>2</sub> has appeared as a long-term sustainable solution able to meet our future energy demands.<sup>[136,137]</sup> However, the safe and economical storage of hydrogen remains one of the biggest problem for its implementation.<sup>[138]</sup>

A possible way to solve this problem is the physical storage of H<sub>2</sub> inside porous materials or as chemical product to be released upon need by a sustainable chemical reaction, as for example

the dehydrocoupling of amine-boranes adducts (see also Subsection 1.2.3).<sup>[139–144]</sup> The synthesis of porous organic polymers with predefined porosity displaying high surface areas has attracted considerable attention due to their great potentials for gas storage and separation as well.<sup>[145]</sup> The synthesis and performance (Table 1.3) of five polymers containing borazine cores as polar molecular modules in order to improve H<sub>2</sub> absorption have been recently described (Scheme 1.4).<sup>[146]</sup> The Brunauer-Emmett-Teller (BET) surface areas were higher for the Cl-decorated borazine polymers than the Br-decorated borazine polymers.

**Table 1.3** - Porous properties of BLPs. <sup>a</sup> Calculated by Langmuir and BET methods. <sup>b</sup> Calculated from nitrogen adsorption at P/P<sub>0</sub> = 0.9.

Polymer	SA <sub>BET</sub> (m <sup>2</sup> /g) <sup>a</sup>	P <sub>vol</sub> (cm <sup>3</sup> /g) <sup>b</sup>	H <sub>2</sub> 77 K (wt%)
4a (Cl)	1364	0.746	1.00
4b (Br)	503	0.303	0.68
5a (Cl)	1174	0.649	1.30
5b (Br)	849	0.571	0.98
6 (Cl)	1569	0.853	1.75

This trend in the surface area might be surprising at a first glance, as material **1-5a** should exhibit higher surface area than that of **1-4a**. However, these polymers do not conform to such expectations due to their amorphous nature. Regarding the volume, the calculated results at P/P<sub>0</sub> = 0.9 showed a strong dependence on the halide as the chlorinated polymers always give rise to higher pore volumes than those of their brominated analogues. This is due to the smaller atomic size of the Cl atom with respect to that of Br.

## 1.7 Outline of the dissertation

The intention of this Chapter was to explore the history of borazine and its derivatives, describing the recent developments in their organic synthesis and functionalisation, as well as their use in material applications. In this doctoral work, our research activities were directed toward the investigation of the effect of different substituents on the formation of the borazine ring and its functionalisation at the boron site. Accordingly, the work presented here is divided into two main Chapters, as schematically represented in Figure 1.14.

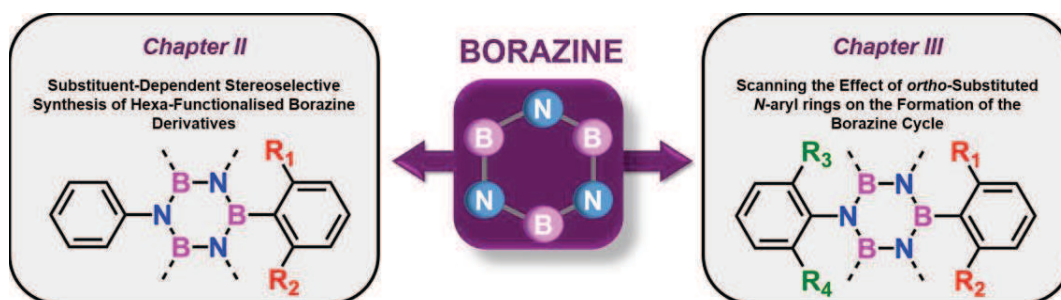


Figure 1.14 – Schematic representation of the outline of this doctoral dissertation.

*Chapter II* deals with the study of the effect of *ortho*-substituents on the *B*-aryl moieties during the addition/elimination process for the functionalisation at the boron site. More specifically, following a  $[1+1'+1+1'+1+1']$  hexamerisation route toward the formation of the borazine core (using an amino precursor and boron trichloride), the latter can be further functionalised by the addition of a nucleophile, which will lead to the formation of stable borazine derivatives. Accordingly, the synthesis of multiple borazine moieties has been performed, using only one type of amino-precursor (aniline) and different organometallic derivatives during the functionalisation step. These organometallic moieties consist of aryl groups that contain one or two *ortho*-substituents, which allows for a partial- or full-protection of the borazine core, respectively. In the first case, the control of the stereoselectivity of the process in a reaction in which two different isomers (*cc* and *ct*) can be formed, will be the main focus of this study. Finally, the chemical compatibility and the stability of the novel class of partially-protected borazine moieties developed along this doctoral thesis will be also discussed.

On the other hand, *Chapter III* addresses the investigation of the effect of *ortho*-substituents in the *N*-aryl moieties during the formation of the borazine cycle and its functionalisation. For this purpose, the formation of the BN-core will be performed by reaction of different amino precursors with boron trichloride. Later functionalisation at the boron site can lead to the formation of stable final molecules, depending on the nature of those amino precursors.

## 1.8 References

- [1] E. P. A. Stock, *Berichte Dtsch. Chem. Ges. B Ser.* **1926**, 59, 2210.
- [2] Jeffrey, J. A. G. A., Ruble, J. R., McMullan, R. K., Pople, *Proc. R. Soc. Math. Phys. Eng. Sci.* **1987**, 414, 47.
- [3] W. Harshbarger, G. H. Lee, R. F. Porter, S. H. Bauer, *Inorg. Chem.* **1969**, 8, 1683.
- [4] H. Bock, W. Fuss, *Angew. Chemie Int. Ed. English* **1971**, 10, 182.
- [5] B. Kiran, A. K. Phukan, E. D. Jemmis, *Inorg. Chem.* **2001**, 40, 3615.
- [6] R. Islas, E. Chamorro, J. Robles, T. Heine, J. C. Santos, G. Merino, *Struct. Chem.* **2007**, 18, 833.
- [7] D. J. Grant, D. A. Dixon, *J. Phys. Chem.* **2006**, 110, 12955.
- [8] S. J. Blanksby, G. B. Ellison, *Acc. Chem. Res.* **2003**, 36, 255.
- [9] L. R. Thorne, R. D. Suenram, F. J. Lovas, *J. Chem. Phys.* **1983**, 78, 167.
- [10] A. Kaldor, *J. Chem. Phys.* **1971**, 55, 4641.
- [11] D. C. Frost, F. G. Herring, C. A. McDowell, I. A. Stenhouse, *Chem. Phys. Lett.* **1970**, 5, 291.
- [12] J. R. Platt, H. B. Klevens, G. W. Schaeffer, *J. Chem. Phys.* **1947**, 15, 598.
- [13] J. A. Tossell, J. H. Moore, K. McMillan, C. K. Subramaniam, M. A. Coplan, *J. Am. Chem. Soc.* **1992**, 114, 1114.
- [14] R. I. Wagner, J. L. Bradford, I. Ross, *Inorg. Chem.* **1962**, 1, 93.
- [15] A. J. Leffler, *Inorg. Chem.* **1964**, 3, 145.
- [16] K. Nagasawa, *Inorg. Chem.* **1966**, 5, 442.
- [17] C. K. Narula, R. Schaeffer, A. Datye, R. T. Paine, *Inorg. Chem.* **1989**, 28, 4053.
- [18] L. Maya, *Appl. Organomet. Chem.* **1996**, 10, 175.
- [19] K. Moon, D. Min, D. Kim, *J. Ind. Eng. Chem.* **1997**, 3, 288.
- [20] I. H. T. Sham, C.-C. Kwok, C.-M. Che, N. Zhu, *Chem. Commun.* **2005**, 2, 3547.
- [21] Jishan Wu, Wojciech Pisula, K. Müllen, *Chem. Rev.* **2007**, 107, 718.
- [22] M. Fujita, K. Wakabayashi, K. Nakada, K. Kusakabe, *J. Phys. Soc. Japan* **1996**, 65, 1920.
- [23] J. Liu, B.-W. Li, Y.-Z. Tan, A. Giannakopoulos, C. Sanchez-Sanchez, D. Beljonne, P. Ruffieux, R. Fasel, X. Feng, K. Müllen, *J. Am. Chem. Soc.* **2015**, 137, 6097.
- [24] A. Narita, X. Feng, K. Müllen, *Chem. Rec.* **2015**, 15, 295.
- [25] J. Cai, P. Ruffieux, R. Jaafar, M. Bieri, T. Braun, S. Blankenburg, M. Muoth, A. P. Seitsonen, M. Saleh, X. Feng, et al., *Nature* **2010**, 466, 470.
- [26] C. Chen, J. Z. Wu, K. T. Lam, G. Hong, M. Gong, B. Zhang, Y. Lu, A. L. Antaris, S. Diao, J. Guo, et al., *Adv. Mater.* **2015**, 27, 303.

- [27] T. H. Vo, M. Shekhirev, D. A. Kunkel, M. D. Morton, E. Berglund, L. Kong, P. M. Wilson, P. A. Dowben, A. Enders, A. Sinitskii, *Nat. Commun.* **2014**, 5, 3189.
- [28] D. V. Kosynkin, A. L. Higginbotham, A. Sinitskii, J. R. Lomeda, A. Dimiev, B. K. Price, J. M. Tour, *Nature* **2009**, 458, 872.
- [29] K. S. Novoselov, A. K. Geim, S. V. Morozov, D. Jiang, Y. Zhang, S. V. Dubonos, I. V. Grigorieva, A. A. Firsov, *Science* **2004**, 306, 666.
- [30] F. Schwierz, *Nat. Nanotechnol.* **2010**, 5, 487.
- [31] S. Park, R. S. Ruoff, *Nat. Nanotechnol.* **2009**, 4, 217.
- [32] C. Bronner, S. Stremlau, M. Gille, F. Brauße, A. Haase, S. Hecht, P. Tegeder, *Angew. Chem. Int. Ed.* **2013**, 52, 4422.
- [33] H.-W. Liang, X. Zhuang, S. Brüller, X. Feng, K. Müllen, *Nat. Commun.* **2014**, 5, 4973.
- [34] N. S. Makarov, S. Mukhopadhyay, K. Yesudas, J.-L. Brédas, J. W. Perry, A. Pron, M. Kivala, K. Müllen, *J. Phys. Chem. A* **2012**, 116, 3781.
- [35] R. R. Cloke, T. Marangoni, G. D. Nguyen, T. Joshi, D. J. Rizzo, C. Bronner, T. Cao, S. G. Louie, M. F. Crommie, F. R. Fischer, *J. Am. Chem. Soc.* **2015**, 137, 8872.
- [36] Z. Liu, T. B. Marder, *Angew. Chem. Int. Ed.* **2008**, 47, 242.
- [37] K. Watanabe, T. Taniguchi, T. Niiyama, K. Miya, M. Taniguchi, *Nat. Photonics* **2009**, 3, 591.
- [38] K. Watanabe, T. Taniguchi, H. Kanda, *Nat. Mater.* **2004**, 3, 404.
- [39] D. Golberg, Y. Bando, Y. Huang, T. Terao, M. Mitome, C. Tang, C. Zhi, *ACS Nano* **2010**, 4, 2979.
- [40] C. Zhi, Y. Bando, T. Terao, C. Tang, H. Kuwahara, D. Golberg, *Adv. Funct. Mater.* **2009**, 19, 1857.
- [41] M. Côté, P. D. Haynes, C. Molteni, *Phys. Rev. B* **2001**, 63, 125207.
- [42] M. Kawaguchi, T. Kawashima, T. Nakajima, *Chem. Mater.* **1996**, 8, 1197.
- [43] L. Ci, L. Song, C. Jin, D. Jariwala, D. Wu, Y. Li, A. Srivastava, Z. F. Wang, K. Storr, L. Balicas, et al., *Nat. Mater.* **2010**, 9, 430.
- [44] A. Kazemi, X. He, S. Alaie, J. Ghasemi, N. M. Dawson, F. Cavallo, T. G. Habteyes, S. R. J. Brueck, S. Krishna, *Sci. Rep.* **2015**, 5, 11463.
- [45] C. Huang, C. Chen, M. Zhang, L. Lin, X. Ye, S. Lin, M. Antonietti, X. Wang, *Nat. Commun.* **2015**, 6, 7698.
- [46] M. J. S. Dewar, P. A. Marr, *J. Am. Chem. Soc.* **1962**, 84, 3782.
- [47] P. G. Campbell, A. J. V. Marwitz, S.-Y. Liu, *Angew. Chem. Int. Ed.* **2012**, 51, 6074.
- [48] S. S. Chissick, M. J. S. Dewar, P. M. Maitlis, *Tetrahedron Lett.* **1960**, 23, 8.
- [49] M. J. D. Bosdet, W. E. Piers, T. S. Sorensen, M. Parvez, *Angew. Chem. Int. Ed.* **2007**, 46,

- 4940.
- [50] M. J. S. Dewar, V. P. Kubba, R. Pettit, *J. Chem. Soc.* **1958**, 3073.
  - [51] M. J. D. Bosdet, C. A. Jaska, W. E. Piers, T. S. Sorensen, M. Parvez, *Org. Lett.* **2007**, 9, 1395.
  - [52] M. J. S. Dewar, R. Dietz, *J. Chem. Soc.* **1959**, 2728.
  - [53] P. Paetzold, C. Stanesco, J. R. Stubenrauch, M. Bienmüller, U. Englert, *Z. Anorg. Allg. Chem.* **2004**, 630, 2632.
  - [54] X. Fang, H. Yang, J. W. Kampf, M. M. Banaszak Holl, A. J. Ashe, *Organometallics* **2006**, 25, 513.
  - [55] G. A. Molander, S. R. Wisniewski, *J. Org. Chem.* **2014**, 79, 6663.
  - [56] S. R. Wisniewski, C. L. Guenther, O. A. Argintaru, G. A. Molander, *J. Org. Chem.* **2014**, 79, 365.
  - [57] D. Bonifazi, F. Fasano, M. M. Lorenzo-Garcia, D. Marinelli, H. Oubaha, J. Tasseroul, *Chem. Commun.* **2015**, 51, 15222.
  - [58] H. I. Schlesinger, D. M. Ritter, A. B. Burg, *J. Am. Chem. Soc.* **1938**, 60, 1296.
  - [59] G. W. Schaeffer, R. Schaeffer, H. I. Schlesinger, *J. Am. Chem. Soc.* **1951**, 73, 1612.
  - [60] E. Framery, M. Vaultier, *Heteroat. Chem.* **2000**, 11, 218.
  - [61] T. Wideman, L. Sneddon, *Inorg. Chem.* **1995**, 34, 1002.
  - [62] A. Meller, E. Schaschel, *Inorg. Nucl. Chem. Lett* **1966**, 2, 41.
  - [63] G. W. Schaeffer, E. R. Anderson, *J. Am. Chem. Soc.* **1949**, 71, 2143.
  - [64] W. V. Hough, G. W. Schaeffer, M. Dzurus, A. C. Stewart, *J. Am. Chem. Soc.* **1955**, 77, 864.
  - [65] H. J. Emeléus, *J. Chem. Soc* **1960**, 2614.
  - [66] Y. Yamamoto, K. Miyamoto, J. Umeda, Y. Nakatani, T. Yamamoto, N. Miyaura, *J. Organomet. Chem.* **2006**, 691, 4909.
  - [67] C. A. Jaska, K. Temple, A. J. Lough, I. Manners, *J. Am. Chem. Soc.* **2003**, 125, 9424.
  - [68] D. García-Vivó, E. Huergo, M. A. Ruiz, R. Travieso-Puente, *Eur. J. Inorg. Chem.* **2013**, 2013, 4998.
  - [69] Y. Kawano, M. Uruichi, M. Shimoi, S. Taki, T. Kawaguchi, T. Kakizawa, H. Ogino, *J. Am. Chem. Soc.* **2009**, 131, 14946.
  - [70] S.-K. Kim, H. Cho, M. J. Kim, H.-J. Lee, J. Park, Y.-B. Lee, H. C. Kim, C. W. Yoon, S. W. Nam, S. O. Kang, *J. Mater. Chem. A* **2013**, 1, 1976.
  - [71] W. Luo, P. G. Campbell, L. N. Zakharov, S. Y. Liu, *J. Am. Chem. Soc.* **2011**, 133, 19326.
  - [72] J. S. Li, C. R. Zhang, B. Li, F. Cao, S. Q. Wang, *Eur. J. Inorg. Chem.* **2010**, 5, 1763.
  - [73] A. W. Laubencayer, C. A. Brown, *J. Am. Chem. Soc.* **1955**, 77, 3699.

- [74] J. H. Smalley, S. F. Stafiej, *J. Am. Chem. Soc.* **1959**, *81*, 582.
- [75] T. E. Reich, K. T. Jackson, S. Li, P. Jena, H. M. El-Kaderi, *J. Mater. Chem.* **2011**, *21*, 10629.
- [76] K. T. Jackson, M. G. Rabbani, T. E. Reich, H. M. El-Kaderi, *Polym. Chem.* **2011**, *2*, 2775.
- [77] T. E. Reich, S. Behera, K. T. Jackson, P. Jena, H. M. El-Kaderi, *J. Mater. Chem.* **2012**, *22*, 13524.
- [78] P. Paetzold, *Phosphorus. Sulfur. Silicon Relat. Elem.* **1994**, *93*, 39.
- [79] J. Münster, P. Paetzold, E. Schröder, H. Schwan, T. von Bunnigsen-Mackiewicz, *Zeitschrift für Anorg. und Allg. Chemie* **2004**, *630*, 2641.
- [80] W. Luo, L. N. Zakharov, S.-Y. Liu, *J. Am. Chem. Soc.* **2011**, *133*, 13006.
- [81] S. Biswas, M. Müller, C. Tönshoff, K. Eichele, C. Maichle-Mössmer, A. Ruff, B. Speiser, H. F. Bettinger, *Eur. J. Org. Chem.* **2012**, *2012*, 4634.
- [82] M. Müller, S. Behnle, C. Maichle-Mössmer, H. F. Bettinger, *Chem. Commun.* **2014**, *50*, 7821.
- [83] M. Krieg, F. Reicherter, P. Haiss, M. Ströbele, K. Eichele, M. J. Treanor, R. Schaub, H. F. Bettinger, *Angew. Chem. Int. Ed.* **2015**, *54*, 8284.
- [84] J. Bielawski, M. K. Das, E. Hanecker, K. Niedenzu, H. Noeth, *Inorg. Chem.* **1986**, *25*, 4623.
- [85] M. K. Das, A. L. DeGraffenreid, K. D. Edwards, L. Komorowski, J. F. Mariategui, B. W. Miller, M. T. Mojesky, K. Niedenzu, *Inorg. Chem.* **1988**, *27*, 3085.
- [86] H. Newsom, W. English, A. McCloskey, *J. Am. Chem. Soc.* **1961**, *83*, 4134.
- [87] I. B. Atkinson, D. C. Blundell, D. B. Clapp, *J. Inorg. Nucl. Chem.* **1972**, *34*, 3037.
- [88] A. G. Massey, A. J. Park, *J. Organomet. Chem.* **1964**, *2*, 461.
- [89] H. Watanabe, T. Totani, T. Yoshizaki, *Inorg. Chem.* **1965**, *4*, 657.
- [90] S. Kervyn, O. Fenwick, F. Di Stasio, Y. S. Shin, J. Wouters, G. Accorsi, S. Osella, D. Beljonne, F. Cacialli, D. Bonifazi, *Chem. - A Eur. J.* **2013**, *19*, 7771.
- [91] Atsushi Wakamiya, and Toshihisa Ide, S. Yamaguchi, *J. Am. Chem. Soc.* **2005**, *127*, 14859.
- [92] E. O. Fischer, K. Öfele, *Chem. Ber.* **1957**, *90*, 2532.
- [93] H. Werner, R. Prinz, E. Deckelmann, *Chem. Ber.* **1969**, *102*, 95.
- [94] M. A. Beckett, R. J. Gilmore, K. Idrees, *J. Organomet. Chem.* **1993**, *455*, 47.
- [95] H. Nöth, A. Troll, *Eur. J. Inorg. Chem.* **2005**, *2005*, 3524.
- [96] A. Stock, E. Wiberg, H. Martini, *Berichte der Dtsch. Chem. Gesellschaft (A B Ser.)* **1930**, *63*, 2927.
- [97] E. Wiberg, A. Bolz, *Berichte der Dtsch. Chem. Gesellschaft (A B Ser.)* **1940**, *73*, 209.

- [98] A. W. Laubengayer, O. T. Beachley, R. F. Porter, *Inorg. Chem.* **1965**, *4*, 578.
- [99] K. Anton, H. Fußstetter, H. Nöth, *Chem. Ber.* **1981**, *114*, 2723.
- [100] B. Gemünd, B. Günther, H. Nöth, *ARKIVOC* **2008**, *136*, 152.
- [101] R. Carion, V. Liégeois, B. Champagne, D. Bonifazi, S. Pelloni, P. Lazzeretti, *J. Phys. Chem. Lett.* **2010**, *1*, 1563.
- [102] J. Bai, K. Niedenzu, J. Serwatowska, J. Serwatowski, *Inorg. Chem.* **1991**, *30*, 4631.
- [103] R. F. Riley, C. J. Schack, *Inorg. Chem.* **1964**, *3*, 1651.
- [104] S. J. Groszos, S. F. Stafiej, *J. Am. Chem. Soc.* **1958**, *80*, 1357.
- [105] D. T. Haworth, L. F. Hohnstedt, *J. Am. Chem. Soc.* **1960**, *82*, 3860.
- [106] G. E. Ryschkewitsch, J. J. Harris, H. H. Sisler, *J. Am. Chem. Soc.* **1958**, *80*, 4515.
- [107] L. A. Melcher, J. L. Adcock, J. J. Lagowski, *Inorg. Chem.* **1972**, *11*, 1247.
- [108] L. A. Jackson, C. W. Allen, *J. Chem. Soc. Dalt. Trans.* **1989**, 2423.
- [109] J. Dosso, J. Tasseroul, F. Fasano, D. Marinelli, N. Biot, A. Fermi, D. Bonifazi, *Angew. Chem. Ed.* **2017**, DOI 10.1002/anie.201700907.
- [110] J. Haberecht, A. Krummland, F. Breher, B. Gebhardt, H. Rüegger, R. Nesper, H. Grützmacher, *Dalt. Trans.* **2003**, 2126.
- [111] M. Müller, C. Maichle-Mössmer, P. Sirsch, H. F. Bettinger, *Chempluschem* **2013**, *78*, 988.
- [112] D. Marinelli, F. Fasano, B. Najjari, N. Demitri, D. Bonifazi, *J. Am. Chem. Soc.* **2017**, DOI 10.1021/jacs.7b01477.
- [113] D. Cornu, P. Miele, B. Toury, B. Bonnetot, H. Mongeot, J. Bouix, *J. Mater. Chem.* **1999**, *9*, 2605.
- [114] J.-G. Kho, K.-T. Moon, J.-H. Kim, D.-P. Kim, *J. Am. Ceram. Soc.* **2004**, *83*, 2681.
- [115] M. J. Meziani, W.-L. Song, P. Wang, F. Lu, Z. Hou, A. Anderson, H. Maimaiti, Y.-P. Sun, *ChemPhysChem* **2015**, *16*, 1339.
- [116] K. Su, E. E. Remsen, G. A. Zank, L. G. Sneddon, *Chem. Mater.* **1993**, *5*, 547.
- [117] Q. D. Nghiem, J.-K. Jeon, L.-Y. Hong, D.-P. Kim, *J. Organomet. Chem.* **2003**, *688*, 27.
- [118] J. I. Urgel, M. Schwarz, M. Garnica, D. Stassen, D. Bonifazi, D. Ecija, J. V. Barth, W. Auwärter, *J. Am. Chem. Soc.* **2015**, *137*, 2420.
- [119] P. Dibandjo, F. Chassagneux, L. Bois, C. Sigala, P. Miele, *J. Mater. Chem.* **2005**, *15*, 1917.
- [120] S. Xie, O. M. Istrate, P. May, S. Barwich, A. P. Bell, U. Khan, J. N. Coleman, *Nanoscale* **2015**, *7*, 4443.
- [121] P. Dibandjo, F. Chassagneux, L. Bois, C. Sigala, P. Miele, *Microporous Mesoporous Mater.* **2006**, *92*, 286.
- [122] M. Corso, W. Auwärter, M. Muntwiler, A. Tamai, T. Greber, J. Osterwalder, *Science* **2004**, *303*, 217.

- [123] B. Jaschke, U. Klingebiel, R. Riedel, N. Doslik, R. Gadow, *Appl. Organomet. Chem.* **2000**, *14*, 671.
- [124] S. Kervyn, T. Nakanishi, J. Aimi, A. Saeki, S. Seki, B. Champagne, D. Bonifazi, *Chem. Lett.* **2012**, *41*, 1210.
- [125] S. R. Forrest, *Nature* **2004**, *428*, 911.
- [126] A. R. M. and, J. M. J. Fréchet, *Chem. Rev.* **2007**, *104*, 1066.
- [127] A. Facchetti, *Chem. Mater.* **2011**, *23*, 733.
- [128] A. Della Pia, M. Riello, A. Floris, D. Stassen, T. S. Jones, D. Bonifazi, A. De Vita, G. Costantini, *ACS Nano* **2014**, *8*, 12356.
- [129] D. Bonifazi, S. Mohnani, A. Llanes-Pallas, *Chem. - A Eur. J.* **2009**, *15*, 7004.
- [130] J. V. Barth, G. Costantini, K. Kern, *Nature* **2005**, *437*, 671.
- [131] J. A. A. W. Elemans, S. Lei, S. De Feyter, *Angew. Chem. Int. Ed.* **2009**, *48*, 7298.
- [132] R. Otero, J. M. Gallego, A. de Parga, N. Martín, R. Miranda, *Adv. Mater.* **2011**, *23*, 5148.
- [133] S. Kervyn, N. Kalashnyk, M. Riello, B. Moreton, J. Tasseroul, J. Wouters, T. S. Jones, A. De Vita, G. Costantini, D. Bonifazi, *Angew. Chem. Int. Ed.* **2013**, *52*, 7410.
- [134] N. Kalashnyk, P. Ganesh Nagaswaran, S. Kervyn, M. Riello, B. Moreton, T. S. Jones, A. De Vita, D. Bonifazi, G. Costantini, *Chem. - A Eur. J.* **2014**, *20*, 11856.
- [135] C. Sánchez-Sánchez, S. Brüller, H. Sachdev, K. Müllen, M. Krieg, H. F. Bettinger, A. Nicolai, V. Meunier, L. Talirz, R. Fasel, et al., *ACS Nano* **2015**, *9*, 9228.
- [136] W. E. Winsche, K. C. Hoffman, F. J. Salzano, *Science* **1973**, *180*, 1325.
- [137] L. Schlappbach, A. Züttel, *Nature* **2001**, *414*, 353.
- [138] M. Hirscher, *Handbook of Hydrogen Storage: New Materials for Future Energy Storage*, Wiley-VCH: Weinheim, **2009**.
- [139] A. Staubitz, A. Presa Soto, I. Manners, *Angew. Chem. Int. Ed.* **2008**, *47*, 6212.
- [140] C. W. Hamilton, R. T. Baker, A. Staubitz, I. Manners, *Chem. Soc. Rev.* **2009**, *38*, 279.
- [141] A. Staubitz, A. P. M. Robertson, I. Manners, *Chem. Rev.* **2010**, *110*, 4079.
- [142] M. E. Sloan, A. Staubitz, T. J. Clark, C. A. Russell, G. C. Lloyd-Jones, I. Manners, *J. Am. Chem. Soc.* **2010**, *132*, 3831.
- [143] A. Staubitz, M. E. Sloan, A. P. M. Robertson, A. Friedrich, S. Schneider, P. J. Gates, J. S. auf der Günne, I. Manners, *J. Am. Chem. Soc.* **2010**, *132*, 13332.
- [144] H. Helten, A. P. M. Robertson, A. Staubitz, J. R. Vance, M. F. Haddow, I. Manners, *Chem. - A Eur. J.* **2012**, *18*, 4665.
- [145] N. B. McKeown, P. M. Budd, *Macromolecules* **2010**, *43*, 5163.
- [146] M. G. Rabbani, T. E. Reich, R. M. Kassab, K. T. Jackson, H. M. El-Kaderi, *Chem. Commun.* **2012**, *48*, 1141.



## CHAPTER 2

# Substituent-Dependent Stereoselective Synthesis of Hexa-Functionalised Borazine Derivatives

In this Chapter, the study of the effect of different during the functionalisation step, namely, the nucleophilic substitution in the borazine ring of *B,B',B''*-tri(chloro)-*N,N',N''*-tri(aryl)-borazines, is described. *Chapter 2* is divided into four main sections: *i)* *Section 2.1* consists of a brief introduction on the reactivity of the borazine ring, focused on the nucleophilic substitution reaction with *organometallic* reagents; *ii)* *Section 2.2* introduces the research project; *iii)* the results obtained during this investigation are described and discussed in *Section 2.3* and *iv)* some conclusions are summarised in *Section 2.4*.

More specifically, *Section 2.3* addresses first the effect of the substituents in bis-protected borazine derivatives, in terms of synthesis and stability. Later, the effect of substituents on the stereoselectivity of the process has been studied in a novel class of mono-protected borazine derivatives, in which two different isomers can be obtained. Moreover, a tentative mechanistic proposal is given to justify the effect of the *ortho*-substituents in the stereoselectivity of different borazine derivatives. At last, the reactivity of the borazine core against different nucleophiles as well as the stability and chemical reactivity of mono-protected borazine derivatives is fully discussed.

The X-Ray analyses presented in this Chapter were either performed by *Dr. Nicola Demitri* (*Electra-Sincrotrone, Basovizza, Trieste, Italy*) or by *Davide Marinelli and Nicolas Biot* (*Cardiff University, Cardiff, United Kingdom*). Theoretical calculations were carried out by *Dr. Simone Velari* (*University of Trieste, Trieste, Italy*) and *Nicolas Biot*. Finally, *Francesco Fasano and Jacopo Dosso* (*Cardiff University, Cardiff, United Kingdom*) are kindly acknowledged for their collaboration in this project.

## 2.1. Introduction

During the process developed toward the formation of hexa-substituted borazine derivatives, nucleophilic substitution reaction occurs at the boron site of the borazine ring. In fact, the formation of *B,B',B''*-tri(chloro)*N,N',N''*-tri(aryl)borazine ring initially takes place by the reaction of an aniline moiety and boron trichloride.

The borazine ring is described by the same type of bonding model as benzene, namely a  $\sigma$ -skeleton of  $sp^2$ -hybrid orbitals and a set of delocalised  $\pi$ -orbitals.<sup>[1]</sup> However, the orbitals are not symmetrical in borazine. Indeed, the more electronegative nitrogen atoms have larger coefficients for the bonding molecular orbitals, while the less electronegative boron atoms have a larger contribution for the antibonding molecular orbitals (Figure 2.1). Such an uneven distribution of the  $\pi$ -electron density reduces the ring  $\pi$ -bonding, and renders the borazine less aromatic than benzene. This difference is reflected in the chemistry of borazine, which can undergo addition reactions. In particular, the electrophilic boron atoms of the borazine ring are the perfect candidates for nucleophilic substitution when in the presence of a nucleophile.

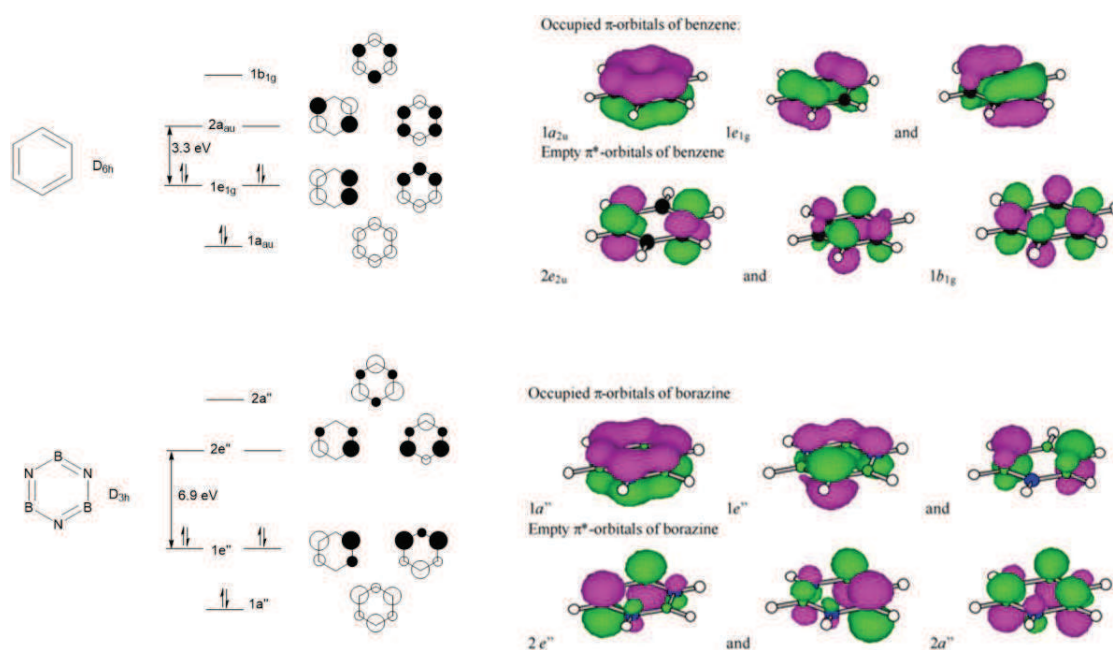


Figure 2.1 – Comparison between the molecular orbitals of benzene and those of borazine.

Organometallic compounds are powerful nucleophiles able to react with the boron site of the borazine ring. More specifically, due to the electropositive metal atom, the carbon–metal  $\sigma$ -bond of organometallic compounds is highly polarised toward the carbon atom, resulting in a carbon-

based nucleophilic group able to react with the electrophilic boron atom of the borazine. This leads to a newly-formed carbon-boron bond.

All the requirements for a successful nucleophilic substitution reaction at the borazine ring are known to be satisfied in the presence of a good electrophile, an excellent nucleophile (as the abovementioned organometallic species) and a leaving group (such as the chloride atom in *B,B',B''*-tri(chloro)-*N,N',N''*-tri(aryl) borazines). Nevertheless, the effect of different substituents in the reaction has not yet been determined. This reaction can either consists of *i) addition-elimination*, *ii) elimination-addition* or *iii) an  $S_N2$  concerted mechanism*. Because of geometric reasons, the last option can easily be discarded. Indeed, the concerted  $S_N2$  reaction would involve an attack of the nucleophile at  $180^\circ$  respect to the B-Cl bond. Due to the planar trigonal geometry of boron, the B-Cl bond is in the plane of the borazine ring. This means that the nucleophile would need to appear inside of the borazine ring to react in a  $S_N2$  mechanism, which is not realistic. On the other hand, the other two possibilities are sensible in terms of geometry. However, addition of the nucleophile is most likely to occur before the elimination of the leaving group. Indeed, boron atoms are good Lewis acids and have the tendency to undergo addition reactions in the presence of a base such as organometallics compounds. This involves the formation of intermediate '*ate complexes*', namely tetrahedral salts also referred to as borates.

Therefore, along this Chapter, the addition-elimination process for the nucleophilic substitution in the borazine rings will be fully discussed. More specifically, the effect of different substituents on the stereoselectivity of the reaction will be addressed, which will also help elucidating the steps of the addition/elimination mechanism.

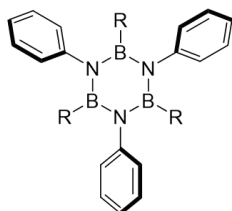
## 2.2. Research Aim

The conception of this doctoral project was motivated by both the study of the functionalisation of the borazine core, namely the nucleophilic substitution reaction at the boron site of the borazine ring, and by the possibility to control the stereoselectivity of the process when using different functional groups at the *ortho*-positions of the aryl moieties bonded to the boron atoms.

The protocol for the synthesis of hexa-functionalised borazines has already been described. Starting from *B,B',B''*-tri(chloro)-*N,N',N''*-tri(aryl)borazine, obtained by the reaction of different aniline species with boron trichloride in toluene under refluxing conditions for 16 h, several *B,B',B''*-tri(aryl)-*N,N',N''*-tri(aryl)borazine derivatives can be synthesised upon addition of organometallic derivatives (*organolithium* or *organomagnesium*) to the mixture. This methodology has been introduced by Groszos and Stafiej in 1958<sup>[2]</sup> for the production of a series of *B*-alkyl and *B*-aryl borazine species (Table 2.1). Since that work, different examples of borazine derivatives obtained *via* nucleophilic substitution reaction have been reported in the literature.<sup>[3][4][5]</sup>

**Table 2.1** – Different borazine species obtained *via* exchange reaction at the boron site, described in 1958 by Groszos and Stafiej.<sup>[2]</sup>

Entry	R	Yield (%)
1	CH <sub>3</sub>	77
2	C <sub>2</sub> H <sub>5</sub>	68
3	<i>n</i> -C <sub>3</sub> H <sub>7</sub>	84
4	<i>i</i> -C <sub>3</sub> H <sub>7</sub>	20
5	<i>n</i> -C <sub>4</sub> H <sub>9</sub>	70
6	<i>i</i> -C <sub>4</sub> H <sub>9</sub>	67



As it has already been mentioned, one of the main shortcoming of borazine species is their reactivity toward nucleophiles by addition onto the electrophilic boron atoms, leading to the opening of the cycle and the degradation of the borazine ring. This results in a high sensitivity of borazines to H<sub>2</sub>O. Additionally, it is known that the insertion of bulky substituents in the proximity of the boron sites prevents the attack of nucleophiles; therefore, it prevents the decomposition of the borazine cycle.

The effect of the substituents has been measured in the cyclohexane system, and it is defined as A-Values. More specifically, A-Values are numerical values used in the determination of the most stable orientation of substituents in a molecule, as well as a general representation of steric bulk. A-values are derived from energy measurements of a mono-substituted cyclohexane ring.

Substituents on a cyclohexane ring prefer to reside in the equatorial position to the axial. The difference in Gibbs free energy ( $\Delta G$ ) between the higher energy conformation (axial substitution) and the lower energy conformation (equatorial substitution) is the A-value for that particular substituent. Besides, the utility of A-values can be generalised for use outside of cyclohexane conformations, helping to predict the steric effect of a substituent in a system. In general, the larger the A-value is for a substituent, the larger the steric effect is for that substituent. For instance, methyl has an A-value of 1.74 kcal/mol while *tert*-butyl has an A-value of 4.7-4.9 kcal/mol. Because the A-value of *tert*-butyl is higher, *tert*-butyl has a larger steric effect than methyl.

Herein, the effect of the insertion of different substituents on the *ortho*-position of the *B*-aryl groups of hexa-functionalised borazine derivatives will be addressed. The study will be divided in two different categories, depending on the number of substituents inserted on *B*-aryl rings. On one hand, when the three *B*-aryl moieties contain substituents in both *ortho*-positions, bis-substituted borazine derivatives are obtained. On the other hand, when the three *B*-aryl moieties contain substituents in only one *ortho*-position, mono-substituted borazines are formed. Besides, the substituents can be directly attached to the *B*-aryl moieties (short-range substituents, SRoS) or they can be connected through a spacer (long-range substituents, LRoS) (Figure 2.2).

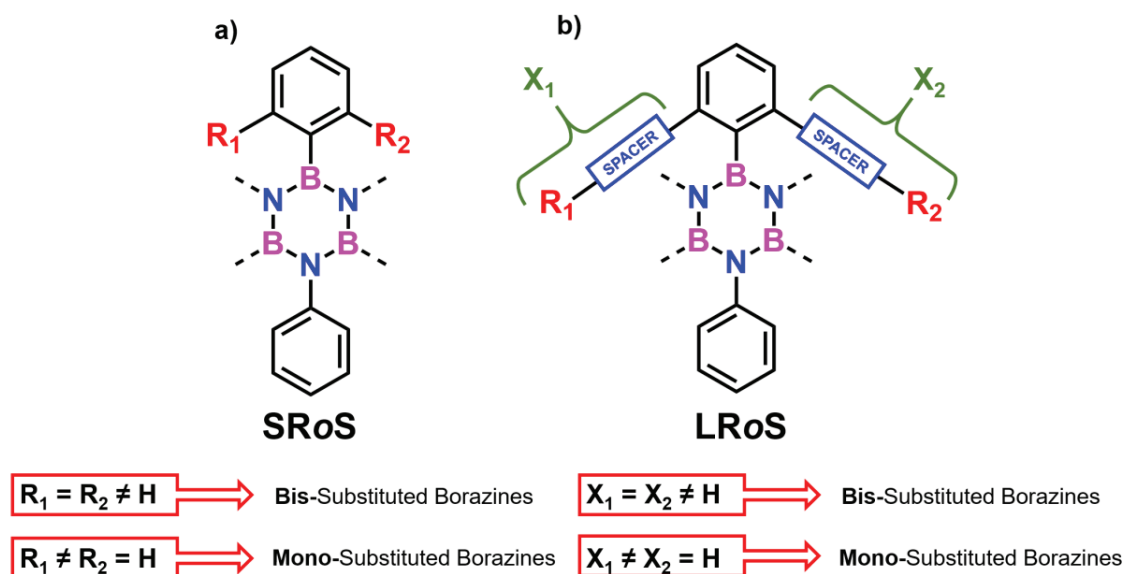


**Figure 2.2** – (a) Short-range *ortho*-substituents (SRoS) in the *B*-aryl moieties; (b) Long-range *ortho*-substituents (LRoS) in the *B*-aryl moieties, for bis-substituted and mono-substituted borazine derivatives.

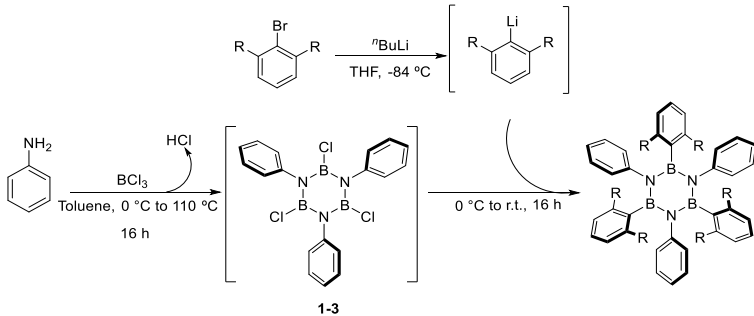
## 2.3. Results and Discussion

The study is divided depending on the number and nature of the substituents. Firstly, the synthesis and characterisation of bis-substituted borazine derivatives decorated with short- and long-range *ortho*-substituents in the *B*-aryl moieties will be addressed. Later, the same study will be developed for mono-substituted borazine moieties decorated with short- and long-range *ortho*-substituents. Finally, a mechanistic proposal is presented, in order to explain the influence of the substituents in the stereoselectivity of the reaction.

### 2.3.1. Study of the Steric Protection using Bis-*B-ortho*-Substituted Groups

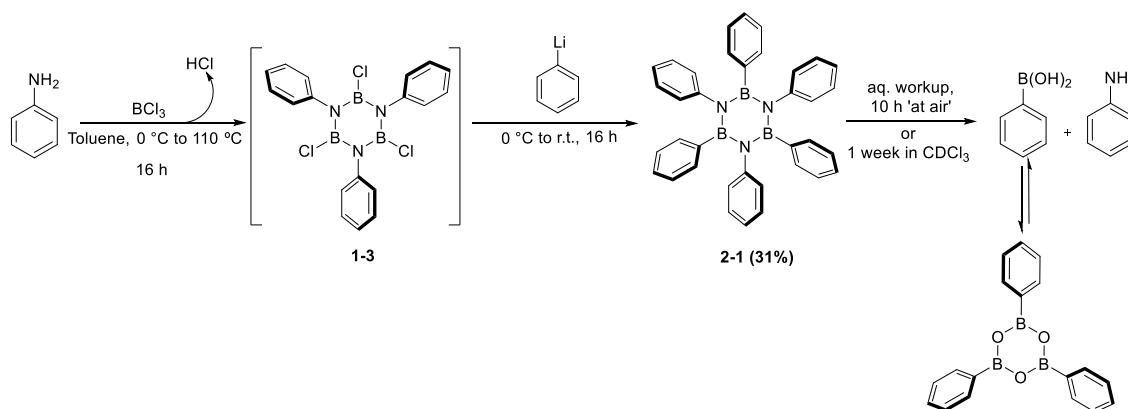
In this Subsection, the results obtained during the investigation developed to evaluate the steric effect of different R substituents on bis-*B*-substituted aryl rings are analysed. For this purpose, the synthesis of different borazine derivatives have been carried out. Reaction of aniline with BCl<sub>3</sub> under refluxing conditions for 16 h, leads to the formation of **1-3**, which can be later functionalised by addition of a bis-*ortho*-substituted *ArLi* (Table 2.2). Some data have been taken from literature.

**Table 2.2** - Synthesis of bis-protected borazine derivatives.



Entry	Precursor for the Ad/E			Outcome
	Reagent	R	A-value (kcal mol <sup>-1</sup> )	
1	PhLi	H	0	<b>2-1</b> : 31
2	1,3-difluoro-2-bromobenzene	F	0.25-0.42	<b>2-2</b> : 65
3	1,3-dimethoxy-2-bromobenzene	OMe	0.55-0.75	<b>2-3</b> : 81
4	2-bromomesitylene	CH <sub>3</sub>	1.74	<b>2-4</b> : 75
5	1,3-diisopropyl-2-bromobenzene	<i>i</i> Pr	2.21	--
6	1,3-di-tert-butyl-2-bromobenzene	<i>t</i> Bu	4.7-4.9	--
7	1,3-di((trimethylsilyl)ethynyl)-2-bromobenzene	≡—TMS	0.41-0.52 (≡) 2.5 (TMS)	--

To start, hexaphenylborazine **2-1**<sup>[6]</sup> (Table 2.2, entry 1), in which the R group is an hydrogen atoms (A-value = 0 kcal/mol), is highly unstable upon exposure to air. It is therefore difficult to be isolated as it degrades into boronic acid (in equilibrium with its anhydride form) and aniline in the presence of H<sub>2</sub>O, or even in solution using non anhydrous solvent for a long time (Scheme 2.1).



**Scheme 2.1** – Synthesis of hexaphenylborazine **2-1** and subsequent degradation into phenylboronic acid, in equilibrium with triphenylboroxine.<sup>[6]</sup>

Suitable crystals for X-ray diffraction analysis has been obtained by slow evaporation of a chloroform solution.<sup>[6]</sup> The crystal structure reveals that there is indeed no steric protection around the boron atoms by the *ortho*-hydrogen atoms of the *B*-phenyl groups, consistent with the observation of low stability of this derivative toward moisture (Figure 2.3).

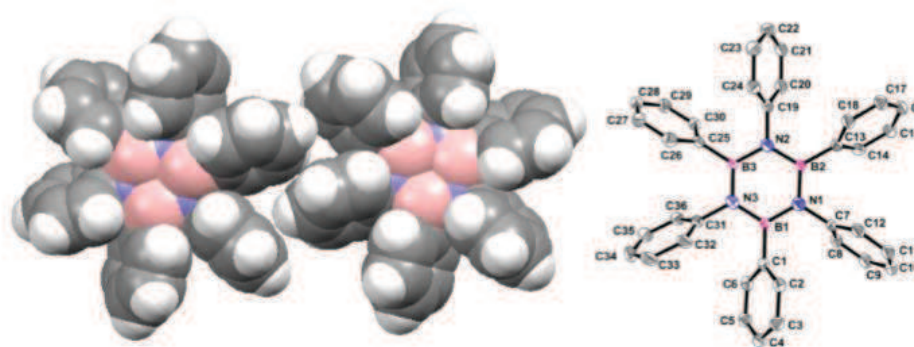


**Figure 2.3** - Spacefill (left) and ORTEP (right, hydrogen were omitted for the sake of clarity) representation of the crystal structure of hexaphenylborazine **2-1**.<sup>[6]</sup> The spacefill representation reveals the two possible turns of **2-1**, having a propeller shape. Space group Pna21. Colour code: grey: C, pink: B, white: H and blue: N.<sup>[6]</sup>

As already mentioned, the insertion of bulky groups (SR*o*S or LR*o*S) close to the boron atoms provides a steric protection against hydrolysis. The effect of the insertion of short-range substituents will be firstly addressed. In this context, our group has recently presented borazine derivative **2-2**, decorated with electro-withdrawing groups, in particular, fluorides (Table 2.2,

entry 2). The crystal structure of borazine **2-2** was recorded from single crystals obtained by slow diffusion of MeOH in CH<sub>2</sub>Cl<sub>2</sub>. As it can be observed in Figure 2.4, the boron atoms are not totally covered by the introduction of this steric protection. In fact, fluoride has a very low A-value (0.25-0.42 kcal/mol).

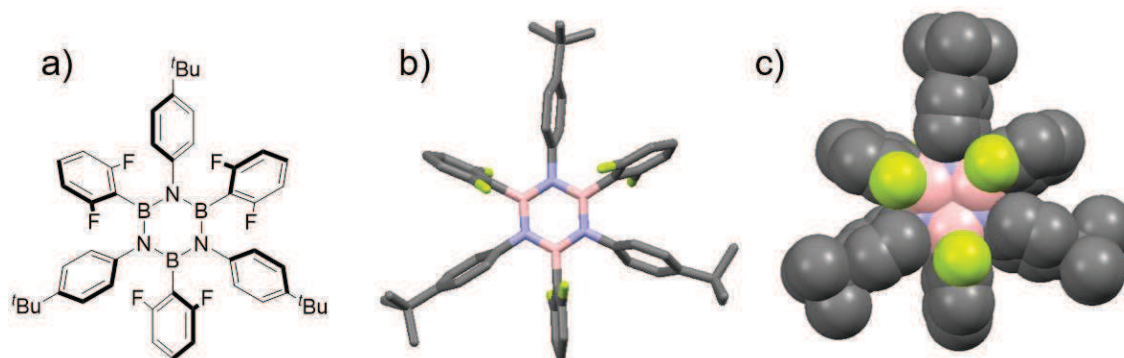


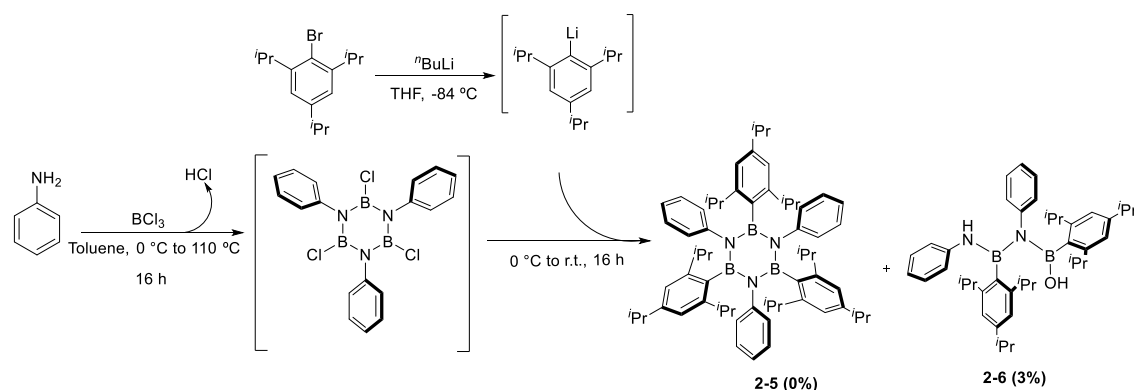
**Figure 2.4** - Crystal structure of borazine derivative **2-2**; (a) molecular structure; (b) crystal structure represented in *capped sticks*; (c) crystal structure represented in *spacefill*. Space group: P21-c. The crystal was grown by slow diffusion of methanol in CH<sub>2</sub>Cl<sub>2</sub>. Colour code: grey: C, pink: B, blue: N, and green: F. Hydrogen were omitted for the sake of clarity.

In this case, the stability of molecule **2-2** is justified by the partial negative charge of the fluoride atoms (electronegativity in Pauling scale: 4.0), which provides a fluorophobic pocket that prevents the addition of any nucleophile to the boron sites (electrostatic repulsion). Besides, it is known that one of the approaches to prevent the hydrolysis of the ring is the insertion of electron-withdrawing substituents on the boron atoms.<sup>[10]</sup> Those groups enhance the aromaticity of the BN-cycle by allowing a better delocalisation of the electrons from the nitrogen atoms to the boron atoms, thus strengthening the B-N double bond character and increasing the stability.

Borazine derivative **2-3** has been also successfully obtained and the molecular shows to be stable under moisture (Table 2.2, entry 3). This molecule was unambiguously confirmed by NMR (<sup>11</sup>B-NMR revealed a broad peak at 35.94 ppm) and high-resolution mass spectroscopy analysis (Figure 2.5). The measured peak ( $m/z = 717.2853$ ) corresponds to the molecular mass of borazine **2-3**, [M]<sup>+</sup>, and matches with the calculated one ( $m/z = 717.3373$ ) for C<sub>42</sub>H<sub>42</sub>B<sub>3</sub>N<sub>3</sub>O<sub>6</sub>.



With the aim of further exploring the effect of other groups with larger steric effect, namely higher A-values, on the borazine' reaction, the study was carried out using 1,3,5-triisopropyl-2-bromobenzene ( $R = i\text{Pr}$ , A-value = 2.21 kcal/mol) for the halogen-lithium exchange, and the further functionalisation of the borazine ring at the boron site (Table 2.2, entry 5). However, when using  $i\text{Pr}$  groups, expected borazine **2-5** is not formed. Upon purification, borazene **2-6** was found in a very low yield, and 48% of starting material aniline was recovered (Scheme 2.2).



**Scheme 2.2** - Failed reaction towards the synthesis of hexa-functionalised borazine derivative **2-5**, using isopropyl moieties for the steric protection. However, molecule **2-6** was obtained in a very low yield.

This result suggests that the none of the three boron atoms of the borazine ring can be substituted by such bulky aryl groups, and the unsubstituted cycle  $B,B',B''$ -tri(chloro)- $N,N',N''$ -tri(phenyl)borazine **1-3** decomposes during the aqueous workup. In addition, suitable crystals of obtained borazene **2-6** were obtained by slow evaporation of  $\text{CHCl}_3$  that allowed to unambiguously asses its chemical identity (Figure 2.7).<sup>[6]</sup>

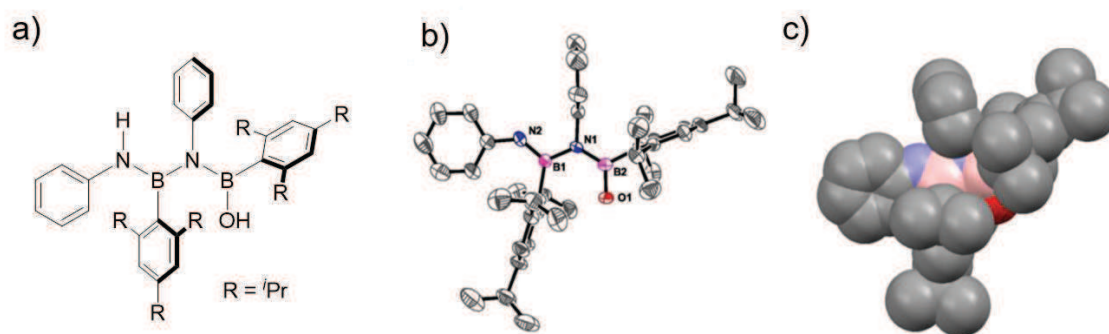
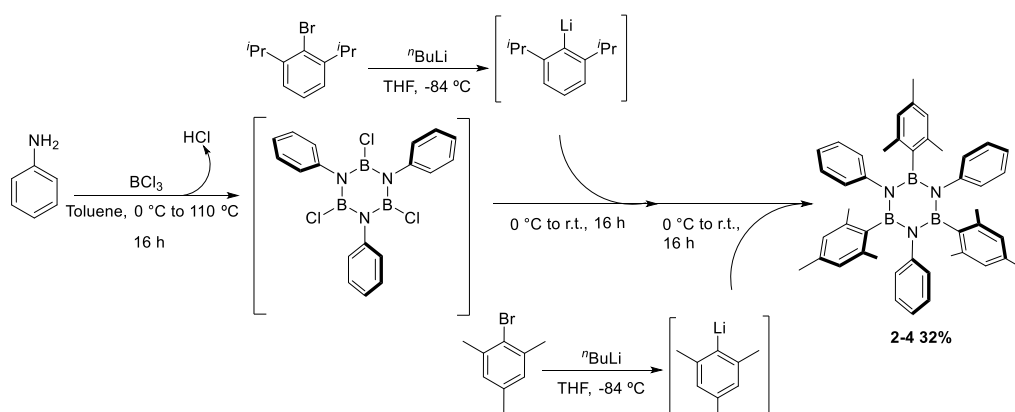


**Figure 2.7** - Crystal structure of borazene **2-6**, obtained by slow evaporation in  $\text{CHCl}_3$ . (a) molecular structure; (b) ORTEP representation; (c) crystal structure represented in *spacefill*. Space group: P-1. Colour code: grey: C, pink: B, blue: N, red: O. Hydrogen were omitted for the sake of clarity.

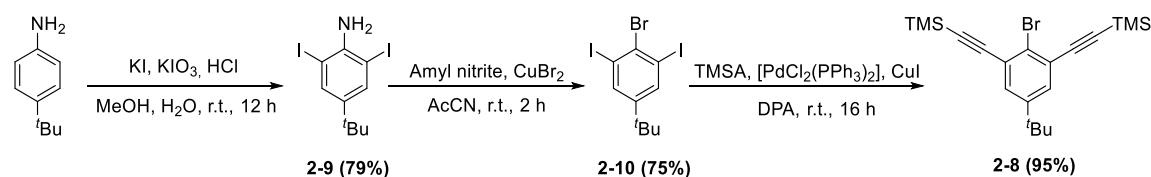
To understand this chemical behaviour, it was envisaged to further investigate this reaction by addition of a second *ArLi* reagent, less hindered than the one with isopropyl groups, which could lead to the formation of a stable borazine derivative in which the boron atoms are differently substituted (Scheme 2.3). More specifically, the *ArLi* derived from 1,3-diisopropyl-2-bromobenzene was first added to the reaction mixture. After 16 hours, the less hindered *MesLi* (R = Me, A-value = 1.75 kcal/mol) was added as the second *ArLi* reagent in the reaction mixture. However, the only borazine derivative found upon purification was borazine **2-4** in 32% yield, but no traces of borazine derivative containing any diisopropyl-substituted *B*-aryl moieties was identified (Scheme 2.3). Hence, the bulkiness of the isopropyl groups prevents the attack to the borazine ring, and just *MesLi* can react with it.



**Scheme 2.3** - Failed reaction towards the synthesis of hexa-functionalised borazine, using isopropyl and methyl moieties as protecting groups. Only borazine **2-4** has been obtained.

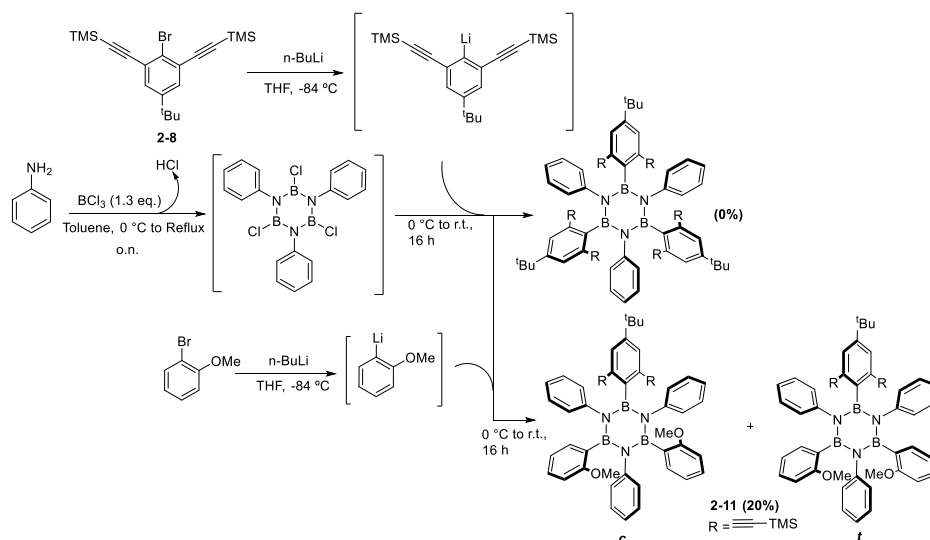
The reaction was also tested using a bis *ortho-tert*-butyl aryl moiety for the functionalisation at the boron site (*tert*-butyl, A-value = 4.7-4.9 kcal/mol). As before, the presence of groups with higher A-values in the *ArLi* prevents the synthesis of expected borazine **2-7** (Table 2.2, entry 6).

Finally, the reaction has been tested using a long-range substituent. Specifically, the reaction was attempted using 1,3-di((trimethylsilyl)ethynyl)-2-bromobenzene **2-8** as precursor (Table 2.2, entry 7) (A-value of the acetylene = 0.41-0.52 kcal/mol; A-value of TMS = 2.5 kcal/mol). For this purpose, the preparation of compound **2-8** has been achieved. Commercially available 4-*tert*-butylaniline was iodinated with KI and  $\text{KIO}_3$  under acidic conditions, yielding compound **2-9** as a red oil.<sup>[11]</sup> Afterwards, amino derivative **2-9** was treated with amyl nitrite to obtain the corresponding *diazonium* salt, which was subsequently reacted with  $\text{CuBr}_2$  to produce molecule **2-10** as a white solid.<sup>[12]</sup> A Sonogashira cross-coupling reaction was then exploited for the synthesis of compound **2-8**. More specifically, **2-10** was reacted with TMSA in the presence of  $[\text{PdCl}_2(\text{PPh}_3)_2]$  as catalysts and CuI as co-catalyst, yielding compound **2-8** (Scheme 2.4) in 95% yield.<sup>[13]</sup>



**Scheme 2.4** - Synthetic pathway undertaken for the synthesis of molecule **2-8**.

The reaction toward the formation of the borazine derivative was attempted but formation of the final borazine was not observed. This hypothetical borazine derivative would contain six acetylene TMS groups around the borazine cycle. The huge steric hindrance that would exist between them (TMS A-value = 2.5 kcal/mol) seems to prevent the synthesis. Also in this case, trial to add a second *ArLi* reagent (*MesLi*, R = Me) has been attempted, but the expected combined product was not identified and just borazine **2-4** was formed (36%). In a last attempt, and taking the risk of obtaining an unstable borazine derivative, the reaction was tried with an even less hindered second *ArLi* reagent (mono *ortho*-substituted *ArLi*, derived from 2-bromoanisole, R = OMe, A-value = 0.55-0.75 kcal/mol). If this aryl moiety is linked to a boron atom, that boron atom would be just partially protected by a mono *ortho*-substituted aryl derivative, and the stability of the final compound would decrease. With this approach, borazine **2-11** was successfully obtained, and proved to be stable against moisture (Scheme **2.5**). Therefore, it was confirmed that just one equivalent of the *ArLi* that contains the acetylene TMS (even if working in excess of it) can react with one equivalent of *B,B',B''*-tri(chloro)-*N,N',N''*-tri(phenyl)borazine **1-3**. The other two boron atoms thus become not accessible for the hindered reagents and just the less hindered *ArLi* derivatives (as *o*-OMePhLi) can approach the reaction centre. Besides, <sup>1</sup>H-NMR confirmed the formation of the two possible isomers (isomer *c* and *t*). Isomer *c* defines the structure in which the two methoxy groups are pointing in the same direction, while in isomer *t*, one methoxy group is located above and the other below the borazine plane. The ratio between them could not be determined due to the vicinity of the peaks of both methoxy and TMS groups in the <sup>1</sup>H-NMR (Figure **2.8**). Additionally, AP-HRMS of molecule **2-11** confirmed the peak at 868.4288 whose isotopic pattern is consistent with [M+Na]<sup>+</sup> (*m/z* = 868.6400 calculated for C<sub>52</sub>H<sub>58</sub>B<sub>3</sub>N<sub>3</sub>NaO<sub>2</sub>Si<sub>2</sub>).



**Scheme 2.5** - Synthetic strategy followed for the synthesis of molecule **2-11**.

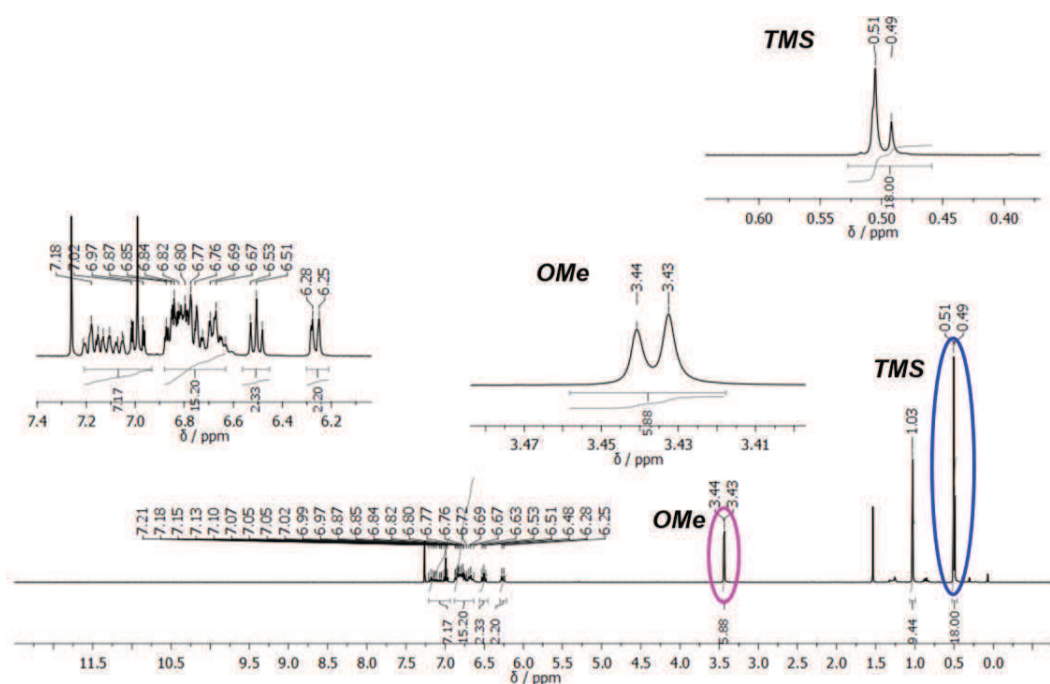


**Figure 2.8** -  $400\text{ MHz } ^1\text{H-NMR}$  of molecule **2-11** in  $\text{CDCl}_3$  (Solvent residual peak:  $7.26\text{ ppm}$ ), where two different peaks are observed for the protons corresponding to the methoxy groups and to the (triisopropylsilyl) acetylene groups.

Molecule **2-11** constitutes the first example of a borazine derivative in which two out of the three boron atoms are just partially protected, showing that this partial protection is enough to prevent decomposition of the borazine ring.

### 2.3.2. Study of the Steric Protection using Mono-*Ortho*-Substituted groups

As a consequence of the synthesis of molecule **2-11**, the study at this stage will be driven toward the investigation of the effect of the substituents in the stereoselectivity of the process. For that purpose, a novel family of borazine derivatives will be presented. In this new class, the substituents that provide the steric protection are introduced in only one of the two *ortho*-positions of the *B*-aryl moieties. Therefore, two different isomers can be produced (isomer *cc* and isomer *ct*), depending on the position of the substituents, in respect to the borazine plane. Note that isomer *cc* is obtained when the three *ortho*-substituents of the *B*-aryl moieties are all pointing in the same direction, while isomer *ct* corresponds to two *ortho*-groups pointing in one direction, while the third one is pointing in the opposite one.

Stability is a second particularly important feature to take into account during this research, considering that borazines decorated with only three *ortho*-substituents (one per boron atom) were designed in this project (Figure 2.9). The influence of the steric effect of those *ortho*-substituents in regard to the protection of the borazine core will therefore be screened by using diverse groups. For this reason, the analysis in this case will be done from LRoS to SRoS, and in the second case, from substituents with larger steric effect to those with lower.

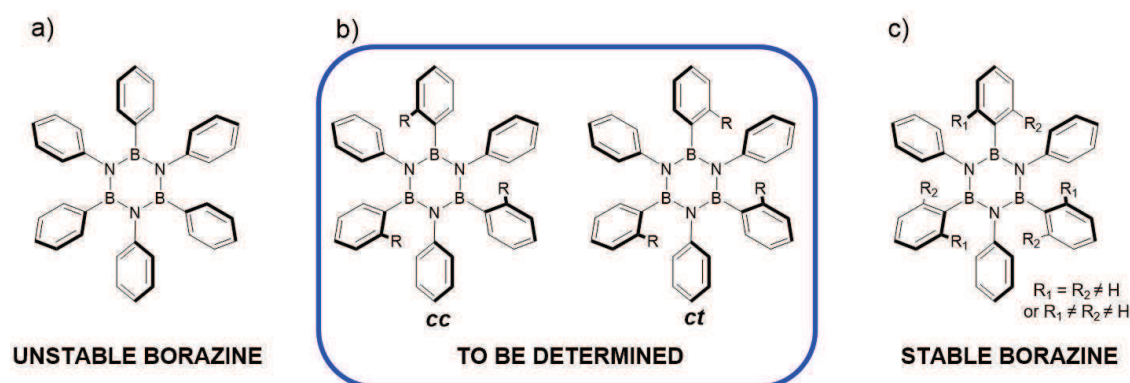
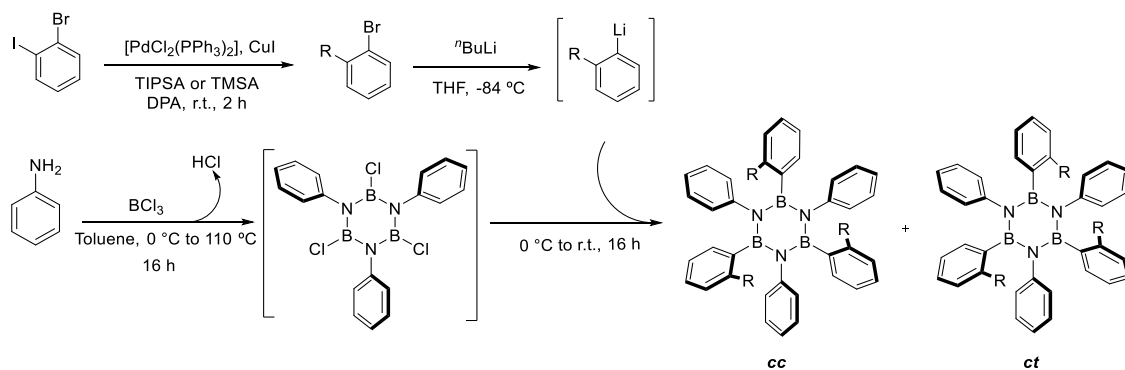


**Figure 2.9** - Representation of the three possible kind of aryl substituted borazine derivatives. (a) Highly unstable borazine **2-1**, (b) partial protected borazine, isomer *cc* and *ct*; and (c) stable borazine derivatives.

#### 2.3.2.a Syntheses of Borazine Derivatives containing Long-Range *ortho*-Substituents (Silyl Protected acetylene moieties)

The first borazine derivatives to be synthesised contain (triisopropylsilyl) or (trimethylsilyl) acetylene as substituents in one *ortho*-position of the *B*-aryl groups. For their preparation, derivative **2-12** (99%) and derivative **2-13** (quant.) were synthesised by Sonogashira cross-coupling reaction from 2-iodobromobenzene with (triisopropylsilyl) acetylene or (trimethylsilyl) acetylene at room temperature during two hours, using  $[PdCl_2(PPh_3)_2]$  as catalyst and CuI as co-catalyst.<sup>[14]</sup> The

reaction toward the synthesis of these hexa-functionalised borazines, using molecule **2-12** or **2-13** for the halogen-lithium exchange (*n*-BuLi was used as lithium source)<sup>[15]</sup> successfully led to the formation of desired borazines **2-14** (37%) and **2-15** (63%), respectively (Scheme 2.6).



Entry	Precursor for the Ad / E		Outcome
	R	Reagent	Yield (%)
1	≡—TIPS	<b>2-12</b>	Borazine <b>2-14</b> : 40
2	≡—TMS	<b>2-13</b>	Borazine <b>2-15</b> : 63

**Scheme 2.6** - Preparation of borazines **2-14** and **2-15**.

Compound **2-14** was analysed by <sup>1</sup>H-NMR (Figure 2.10). The presence of two peaks in the aliphatic region, at 1-1.5 ppm, which correspond to the hydrogen atoms of the (triisopropylsilyl) acetylene moieties are attributed to the formation of isomer *ct*. In fact, the peak at 1.34 ppm integrates for 21 protons, while the other at 1.24 ppm corresponds to 42 protons, integrating to the expected total of 63 protons. The aromatic region does not help to elucidate the obtained isomer.

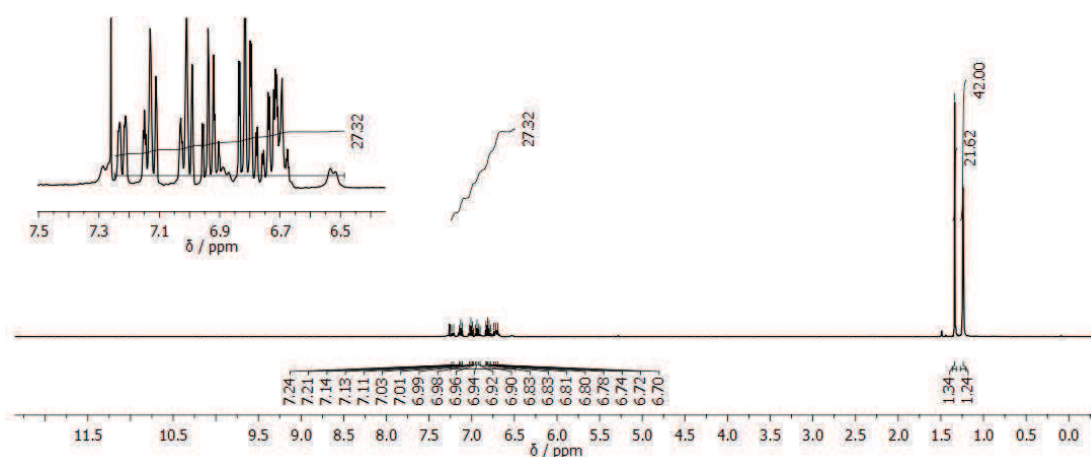


**Figure 2.10** - 400 MHz  $^1\text{H}$ -NMR of molecule **2-14** in  $\text{CDCl}_3$  (Solvent residual peak: 7.26 ppm), where two different peaks are observed for the protons corresponding to the tri(isopropyl)silyl acetylene: at 1.33 ppm the signal integrates for 21 protons, and the second signal at 1.23 ppm for 42 protons.

Nevertheless, the chemical identity of molecule **2-14** was unambiguously confirmed by X-Ray diffraction analysis. Molecule **2-14** was crystallised by slow diffusion of MeOH in  $\text{CH}_2\text{Cl}_2$ . As already predicted by  $^1\text{H}$ -NMR studies, isomer *ct* was found, where two of the (triisopropylsilyl) acetylene groups are on the same side, and the third one is on the opposite with respect to the borazine ring (Figure 2.11).

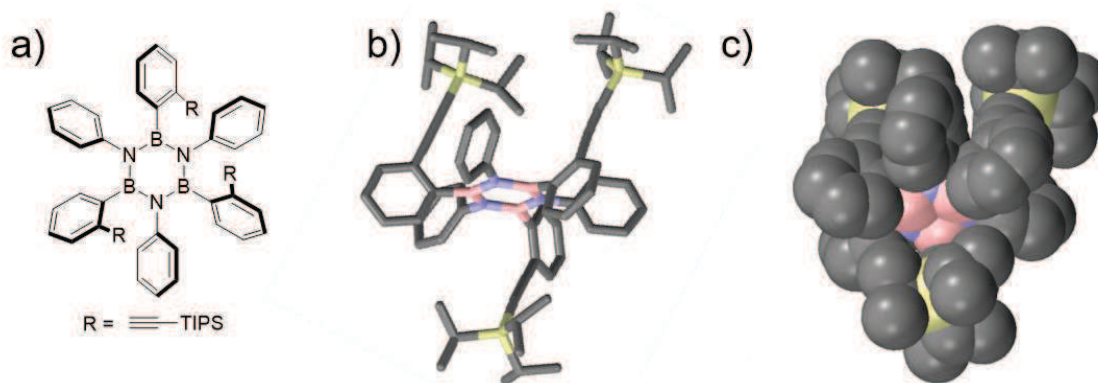


**Figure 2.11** - Crystal structure of borazine derivative **2-14**; (a) molecular structure; (b) crystal structure represented in *capped sticks*; (c) crystal structure represented in *spacefill*. Space group: P -1. The crystal was grown by slow diffusion of MeOH in  $\text{CH}_2\text{Cl}_2$ . Colour code: grey: C, pink: B, blue: N and yellow: Si. Hydrogen atoms were omitted for the sake of clarity.

Similarly, borazine **2-15** was also analysed by  $^1\text{H}$ -NMR. Conversely, in this case, three different NMR resonances were found for the TMS groups in the aliphatic region, which were associated to the formation of both isomers *cc* and *ct*. The analysis of the integral ratio between the three different peaks defines the composition of the mixture as *cc:ct* 2:1 (Figure 2.12).

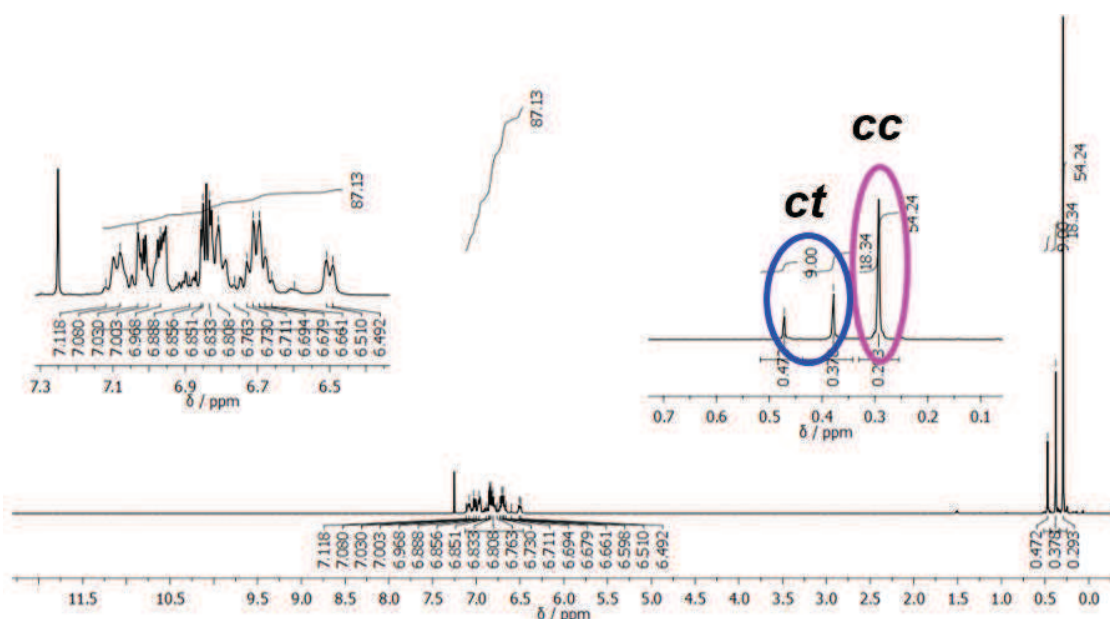


**Figure 2.12** -  $^1\text{H}$ -NMR spectrum of molecule **2-15** in  $\text{CDCl}_3$  (residual peak: 7.26 ppm), where three different peaks are observed for the protons of the tri(methyl)silyl acetylene. Firstly, at 0.472 ppm a peak that integrates for 9 protons, secondly, a peak at 0.378 ppm for 18 protons and finally at 0.293 ppm that integrates for 54 protons, confirming the presence of isomer **cc** and isomer **ct**.

Furthermore, it was also noticed that isomerisation from isomer **cc** to isomer **ct** occurs in solution upon heating up to 60 °C. Taking in consideration this phenomenon, the reaction was repeated but temperature was kept at maximum 15 °C during the functionalisation reaction and workup. This afforded desired borazine **2-15** in a 89:11 **cc:ct** mixture.

Both isomers of molecule **2-15** were confirmed by X-ray diffraction analysis. In particular, suitable crystals of isomer **2-15cc** were prepared by slow diffusion of  $^i\text{PrOH}$  in acetone from a solution of borazine enriched in isomer **cc** (**cc:ct** 89:11). The temperature was kept below 4 °C during the crystallisation step to avoid further isomerisation. Secondly, suitable crystals of the **ct** were also obtained by slow diffusion of  $\text{MeOH}$  in  $\text{CH}_2\text{Cl}_2$  from a solution of borazine enriched in isomer **ct** (**cc:ct** 5:95) at room temperature (Figure 2.13 and 2.14).

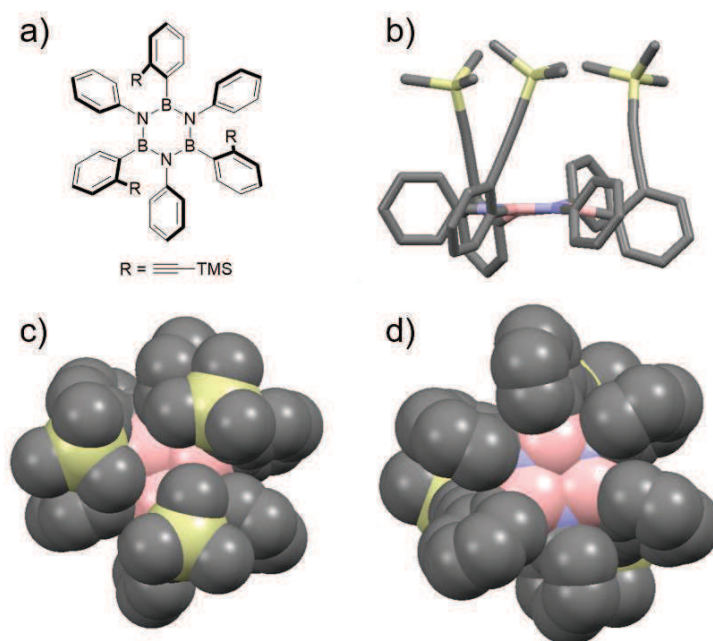


**Figure 2.13** - Crystal structure of borazine derivative **2-15** (isomer *cc*); (a) molecular structure; (b) crystal structure represented in *capped sticks*; (c) crystal structure represented in *spacefill* view from the top, (d) crystal structure represented in *spacefill* view from the bottom. Space group:  $P 2_1$ . The crystal was grown by slow diffusion of  $i$ PrOH in acetone. Colour code: grey: C, pink: B, yellow: Si and blue: N. Hydrogen was omitted for the sake of clarity.

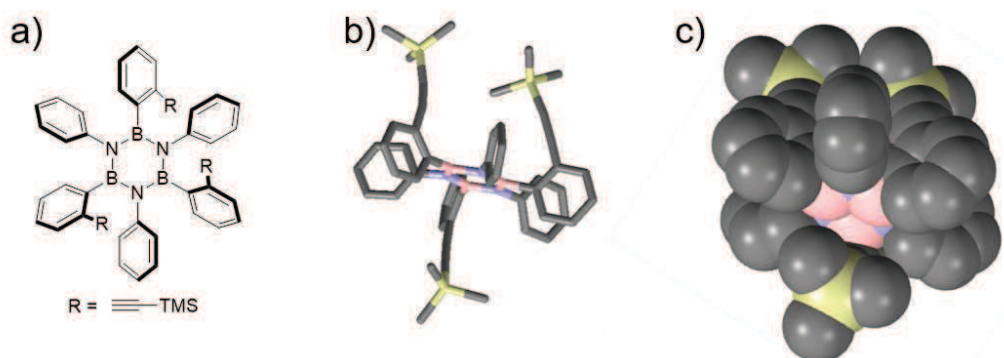
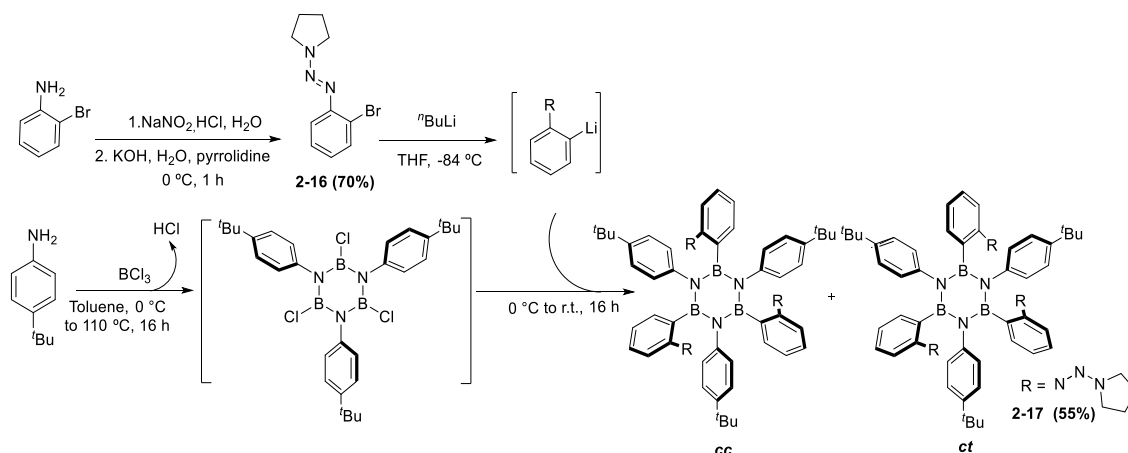


**Figure 2.14** - Crystal structure of borazine derivative **2-15** (isomer *ct*); (a) molecular structure; (b) crystal structure represented in *capped sticks*; (c) crystal structure represented in *spacefill*. Space group:  $P n a 2_1$ . The crystal was grown by slow diffusion of MeOH in  $CH_2Cl_2$ . Colour code: grey: C, pink: B, yellow: Si and blue: N. Hydrogen was omitted for the sake of clarity.

These two examples (borazines **2-14** and **2-15**) constitute the first syntheses of borazines derivatives in which the borazines cores are just partially protected. Notably, no decomposition has been observed during aqueous workup.

### 2.3.2.b Synthesis of Borazine 2-17 using a Triazene Moiety for the Steric Protection

The second part of the investigation consisted of the synthesis of borazine **2-17** decorated with an encumbered triazene derivative (A-value of this triazene derivative is unknown, as example of a similar structure:  $\text{N}=\text{CHCH}(\text{CH}_3)_2$ , A-value = 0.75 kcal/mol). For that purpose, molecule **2-16** was prepared from a solution of 2-bromoaniline in concentrated hydrochloric acid at 0 °C. Afterwards, a solution of  $\text{NaNO}_2$  in cold water was added dropwise. Once the diazonium salt was formed, a solution of pyrrolidine in KOH was added, and target molecule **2-16** was obtained in 70% yield after filtration.<sup>[16]</sup> Borazine **2-17** was later obtained as a white solid in 55% yield (Scheme 2.7).



Scheme 2.7 - Preparation of borazine **2-17**.

The complexity of the  $^1\text{H}$ -NMR did not allow elucidating a fully structure description of the isomers obtained. Nonetheless, isomer *cc* was unambiguously determined by X-Ray diffraction. Single crystals of desired molecule **2-17** were obtained by slow diffusion of MeOH in  $\text{CH}_2\text{Cl}_2$ . As observed in Figure 2.15, the three triazene groups are located on the same side of the borazine ring. Even with no bulky group located on one side of the BN-ring, borazine **2-17** shows a good stability, and does not decompose in the presence of  $\text{H}_2\text{O}$ .

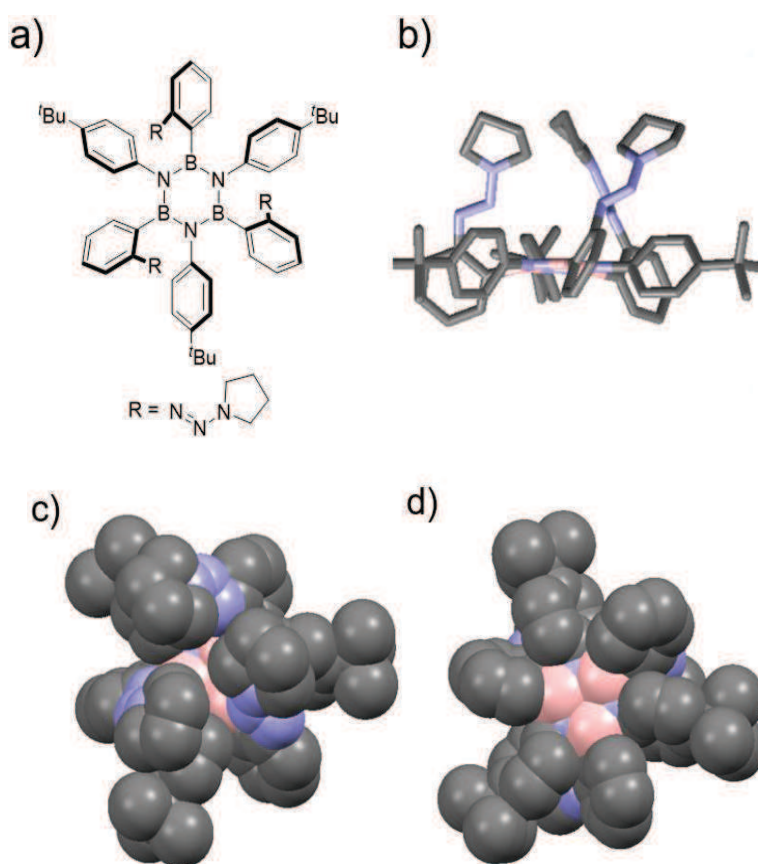


**Figure 2.15** - Crystal structure of borazine derivative **2-17**; (a) molecular structure; (b) crystal structure represented in *capped sticks*; (c) crystal structure represented in *spacefill* (view from the top); (d) crystal structure represented in *spacefill* (view from the bottom). Space group:  $P 2_1/c$ . The crystal was grown by slow diffusion of MeOH in  $\text{CH}_2\text{Cl}_2$ . Colour code: grey: C, pink: B and blue: N. Hydrogen was omitted for a sake of clarity.

### 2.3.2.c Study of the Isomerisation Process in Borazine **2-15** from *cc* to *ct*

The isomerisation process of borazine derivative **2-15** from isomer *cc* to isomer *ct* has been studied in detail. Note that isomerisation has not been observed for the other two borazine derivatives **2-14** and **2-17**.

#### 2.3.2.c.1 Variable Temperature Analysis

As previously mentioned, when the reaction toward the synthesis of molecule **2-15** and the subsequent workup is carried out at a temperature below 15 °C it is possible to obtain the molecule with a ratio of isomers of *cc:ct* 89:11. However, upon raising the temperature, borazine **2-15** undergo isomerisation and the ratio of isomers changes from *cc:ct* 89:11 to *cc:ct* 5:95.

With the aim of investigating the process, variable temperature experiment was developed. During this experiment, acquisition was taken every five minutes at specific preset temperatures. Figure **2.16** describes an overlay of all  $^1\text{H}$ -NMR spectra recorded at different temperatures during

the study, and zoomed on the region of interest, namely, in the aliphatic part of the spectra where the signals of the trimethylsilyl groups appear. Figure 2.17 displays a graphic representation of the percentage of isomer *cc* during the experience. Both figures will be used to explain the process.

Starting from a mixture of borazine *cc:ct* 89:11 and applying a temperature cycle set up from 25 °C to 60 °C, and from 60 °C to 25 °C, conversion of isomer *cc* into isomer *ct* was observed and the final composition of the mixture was then *cc:ct* 5:95. More specifically, a first <sup>1</sup>H-NMR spectrum was acquired at 25 °C (t = 0 min). It is highlighted by the blue line in Figure 2.16 and thus corresponds to a *cc:ct* 89:11 mixture. Subsequently, the temperature was linearly increased until 50 °C, and <sup>1</sup>H-NMR spectrum was acquired every 5 minutes, corresponding to a temperature increase of 5 °C (Figure 2.17). At 50 °C (t = 25 min), the overall ratio between isomers had changed from *cc:ct* 89:11 (T = 25 °C, t = 0 min) to *cc:ct* 72:28 (T = 50 °C, t = 25 min). When looking closely at the evolution of the isomers ratio in function of time (Figure 2.17), a more abrupt isomerisation occurred between the temperature range of 45-50 °C. In particular, the isomer ratio was observed to change from *cc:ct* 82:18 (T = 45 °C, t = 20 min) to *cc:ct* 72:28 (T = 50 °C, t = 25 min). This indicates that the higher the temperature is, the faster the isomerisation process occurs. This is the reason why the temperature was maintained constant at 50 °C for an additional 155 minutes (to reach a final t = 180 min), after which the ratio between the isomers was calculated to be *cc:ct* 9:91. The temperature was finally increased up to 60 °C, at which the isomers ratio was *cc:ct* 5:95 (Figure 2.17). In order to determine whether the isomerisation is a reversible process, the temperature was brought back to room temperature and a final acquisition was performed at 25 °C. The isomers ratio remained at 5:95, indicating that no inverse isomerisation had occurred. The final mixture is thus composed by a mixture of isomers at *cc:ct* 5:95 (Figure 2.16, magenta line), suggesting that isomer *ct* is the most stable one.

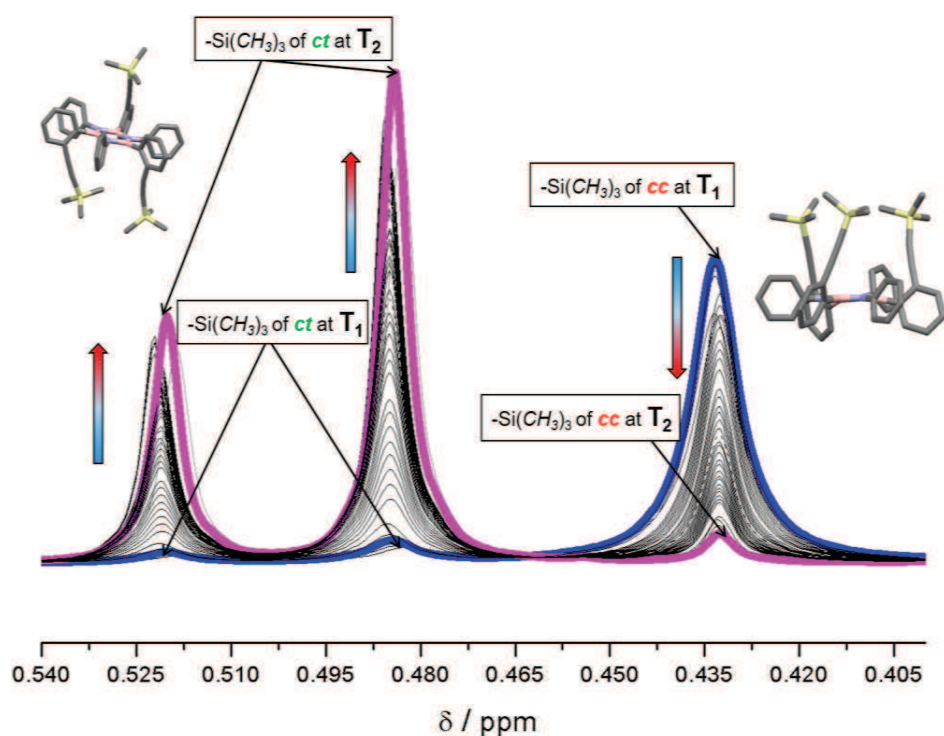


**Figure 2.16** - VT  $^1\text{H}$ -NMR studies of molecule **2-15** in  $\text{C}_6\text{D}_6$ , zoomed in the aliphatic area of the spectra, specifically around 0.4-0.54 ppm where three different peaks are observed corresponding to the protons of the (trimethylsilyl) acetylene. At 0.435 ppm, there is a signal assigned to isomer *cc*. At 0.485 ppm and 0.525 ppm the peaks are attributed to isomer *ct*.  $T_1$  (blue line) corresponds to the initial temperature ( $T_1 = 25^\circ\text{C}$ ), and  $T_2$  (magenta line) to the final one, after the variable temperature experience ( $T_2 = 25^\circ\text{C}$ ). The maximum temperature reached during the process was  $60^\circ\text{C}$ .

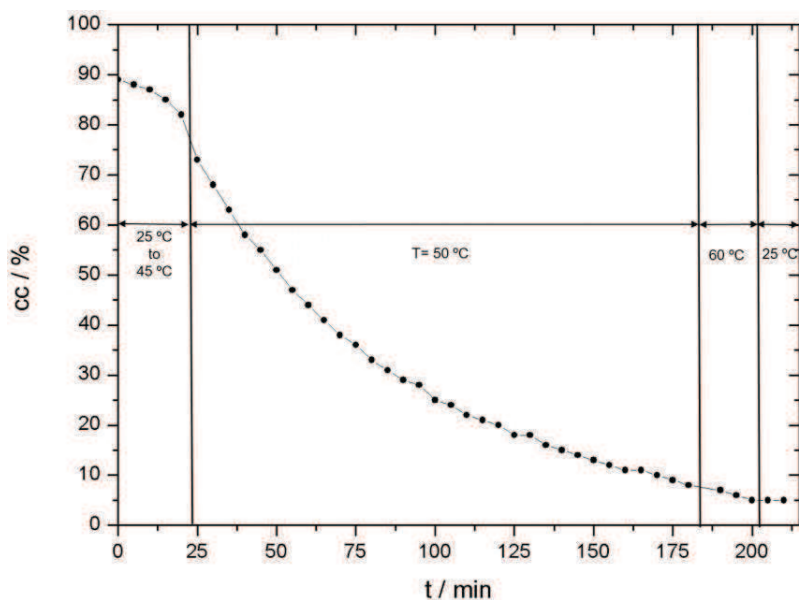


**Figure 2.17** - Graphic representation of the percentage of isomer *cc* in borazine derivative **2-15** during the experiment. First, the studies were developed at different temperatures, from  $25^\circ\text{C}$  to  $45^\circ\text{C}$ . Afterwards, the temperature was stabilised at  $50^\circ\text{C}$ . Then, the process was developed at  $60^\circ\text{C}$ , and finally the cooling down ramp to come back to room temperature is represented.

To confirm it, the variation on the heat of formation between both isomers has been theoretically calculated. In line with the previous experimental observations, the results show that isomer *ct* is more stable than *cc* isomer. In particular, calculations for the geometric optimisations in gas phase revealed that *ct* isomer is 0.11 eV (10.63 kJ/mol) more stable than *cc* isomer. DFT calculations were performed with the plane-wave pseudopotential package QUANTUM ESPRESSO using a GGA-PBE ultrasoft pseudopotentials.

### 2.3.2.c.2 Calculation of $k$ and $\Delta G^\ddagger$ at 50 °C

The rate constant ( $k$ ) of the isomerisation reaction can experimentally be obtained following a first order equation, where  $k$  depends on the concentration of only one reagent. In our case,  $\ln [A]_t/[A]_0$  vs time is represented for a temperature of 50 °C (Figure 2.18). The slope of the graphic then corresponds to the rate constant of the process ( $k$ ), as shown in Equation 1:

$$\ln [A]_t = \ln[A]_0 - k \cdot t \quad (\text{eq. 1})$$

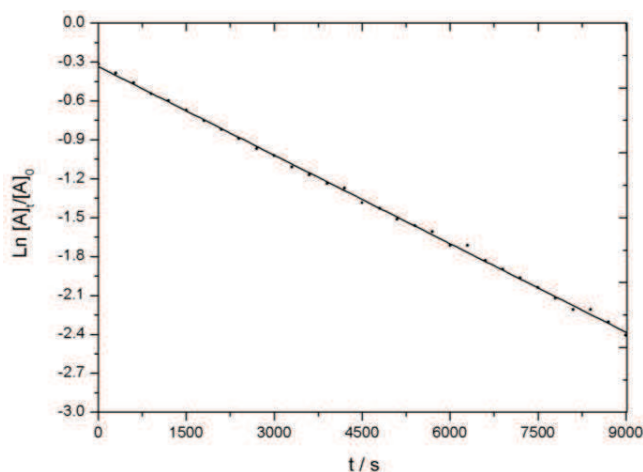


**Figure 2.18** - Graphic where  $\ln [A]_t$  vs  $t$  is represented for the calculation of  $k$  at  $T = 50$  °C.

Therefore, the isomerisation process at 50 °C occurs according to the following equation:

$$\ln [A]_t = -0.3357 - 0.0002 \cdot t$$

From which the rate constant ( $k$ ) can be obtained:

$$k = 0.0002 \text{ s}^{-1}$$

On the other hand, Gibbs energy of activation ( $\Delta G^\ddagger$ ) can be also calculated *via* Eyring equation, which describes the variation of the rate of a chemical reaction in function of the temperature (equation 2):

$$k = \frac{k_B \cdot T}{h} \cdot e^{\frac{-\Delta G^\ddagger}{R \cdot T}} \quad (\text{eq. 2})$$

where,  $k_B$  is the Boltzmann constant ( $1.381 \cdot 10^{-23} \text{ J} \cdot \text{K}^{-1}$ ),  $T$  is the absolute temperature in Kelvin (K),  $h$  is the Planck constant ( $6.626 \cdot 10^{-34} \text{ J} \cdot \text{s}$ ),  $\Delta G^\ddagger$  is the Gibbs energy of activation, and  $R$  is the universal gas constant ( $8.3145 \text{ J} \cdot \text{mol}^{-1} \text{ K}^{-1}$ ).

As the rate constant is known, as well as all the other constants, the Gibbs energy of activation at 50 °C ( $\Delta G^\ddagger$ ) can be calculated as:

$$\Delta G^\ddagger = 102 \text{ kJ} \cdot \text{mol}^{-1}$$

To summarise, Figure 2.19 represents the graphic for the calculated energies ( $\Delta G$  has been theoretically calculated and  $\Delta G^\ddagger$  has been experimentally calculated) of the isomerisation process at 50 °C.

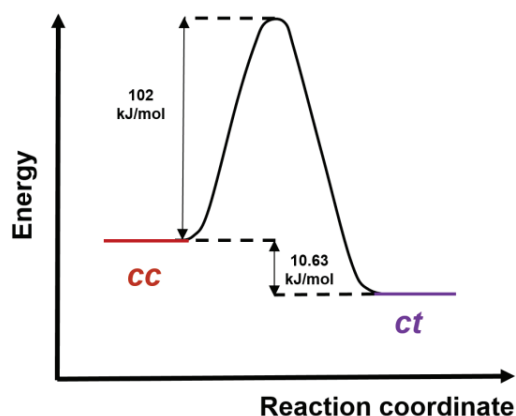


**Figure 2.19** - Graphic representation of heat change of formation of isomer *cc* and isomer *ct* (theoretically calculated) and the Gibbs energy of activation at 50 °C (experimentally calculated). Energy vs reaction coordinate.

### 2.3.2.c.3 Study of the Isomerisation Process

To the best of our knowledge, two processes could explain the isomerisation observed in borazine **2-15**, namely, fast ring-opening-closure or rotation around the  $\sigma$ -bond between the boron atom of the borazine ring and the carbon of the aryl moiety that contains the (trimethylsilyl) acetylene group in *ortho*-position (Figure 2.20). In order to elucidate which of these two phenomena takes place, different tests have been developed.

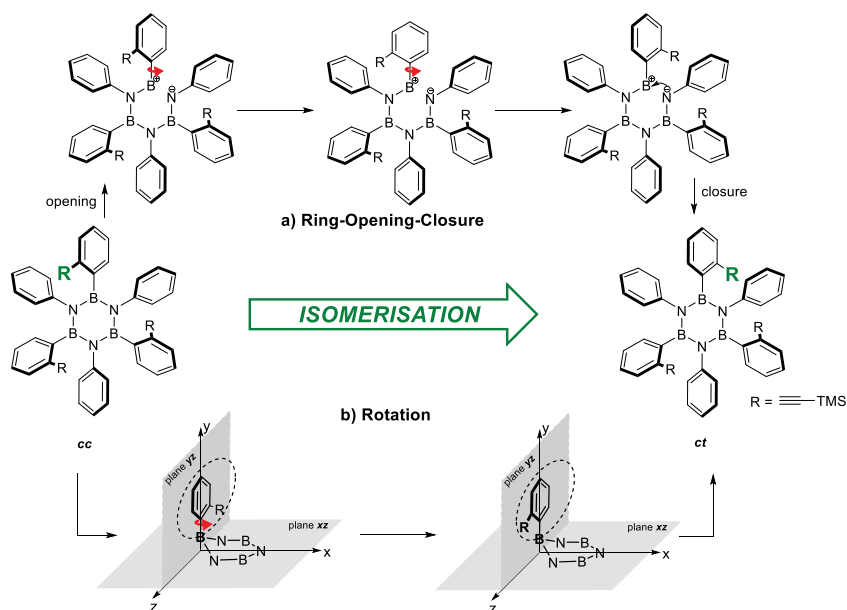
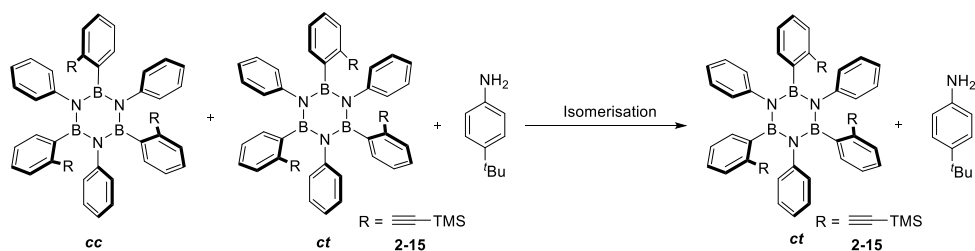


**Figure 2.20** - Study of the isomerisation process, (a) ring-opening-closure route; (b) rotation around  $\sigma$ -bond between the boron atom and the aryl moiety.

- **Study of the ring-opening route:**

To start with, borazine **2-15** was subjected to VT  $^1\text{H}$ -NMR experiments in toluene- $d_8$  and in the presence of either 4-*tert*-butylaniline or 2,4,6-(trimethylphenyl) boronic acid. In the case of isomerisation *via* the fast ring-opening route, upon addition of 4-*tert*-butylaniline in the NMR tube containing the solution of borazine **2-15** and heating, reaction between 4-*tert*-butylaniline and the ‘opened-borazine’, resulting in the formation of a new B-N bond with 4-*tert*-butylaniline, would be expected (Scheme 2.8). However, this was not observed and only isomerisation occurred, affording 95% of isomer *ct* from an original *cc*:*ct* 2:1 mixture. 4-*tert*-butylaniline was also recovered after the heating cycle.



**Scheme 2.8** - Fast ring-opening-closure isomerisation test using 4-*tert*-butylaniline as external agent.

Following the same strategy, 2,4,6-trimethylphenylboronic acid was added to the NMR tube containing the solution of borazine **2-15**. However, neither in this case, formation of a new B-N bond with the external boronic acid has been detected.

These two tests show that the isomerisation process does not occur *via* fast ring-opening-closure reaction.

- **Study of the possible rotation around the  $\sigma$ -bond:**

Instead, the isomerisation can occur *via* rotation around the formal  $\sigma$ -bond between the boron atom of the borazine ring and the  $sp^2$ -carbon of the *B*-aryl moiety that contains the (trimethylsilyl) acetylene group in *ortho*-position. In order to confirm this, introduction of additional short-range *ortho*-substituents (SRoS) on the *B*-aryl groups or on the *N*-aryl moieties of the borazine derivatives was carried out (Figure 2.21). Indeed, by increasing the steric hindrance around the borazine ring, the rotational energy barrier of rotations around the single bonds should raise, preventing the interconversion of one isomer into the other, thereby preventing isomerisation to take place.

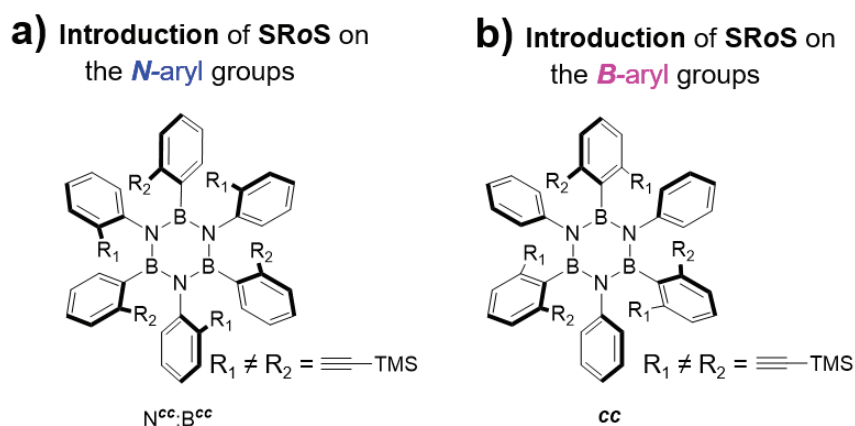
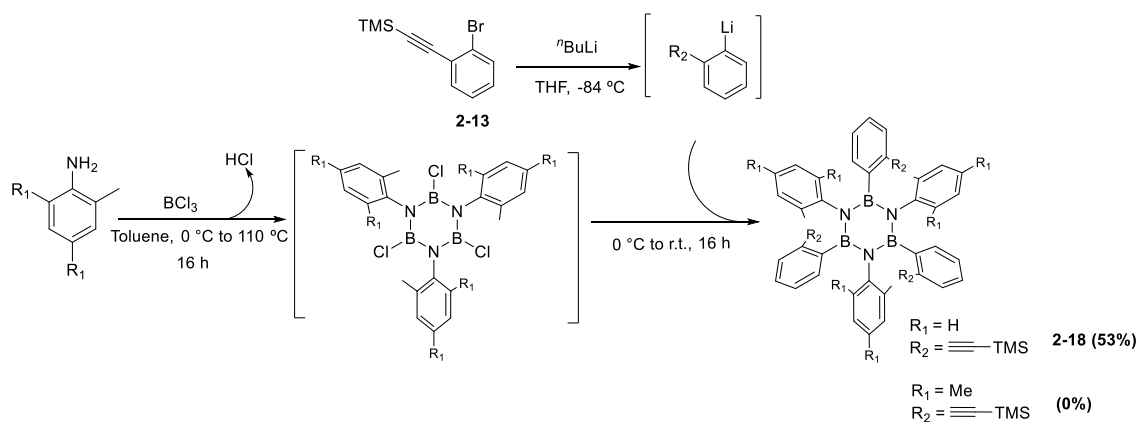


**Figure 2.21** – Schematic representation of the target tests, when introducing short-range *ortho*-substituents on the (a) *N*-aryl groups, or (b) *B*-aryl groups.

In this context, the two different sets of experiments were performed and classified according to the ring on which the new groups were introduced.

In the first set, *ortho*-substituted aniline derivatives were reacted with the *ArLi* reagent derived from **2-13** to introduce additional substituents on the *ortho*-positions of the *N*-aryl groups of the resulting borazine. More specifically, the reaction was respectively carried out with bis *ortho*-substituted 2,4,6-trimethylaniline, and with mono *ortho*-substituted 2-methylaniline. While the reaction with 2,4,6-trimethylaniline did not provide the desired borazine derivative, reaction with

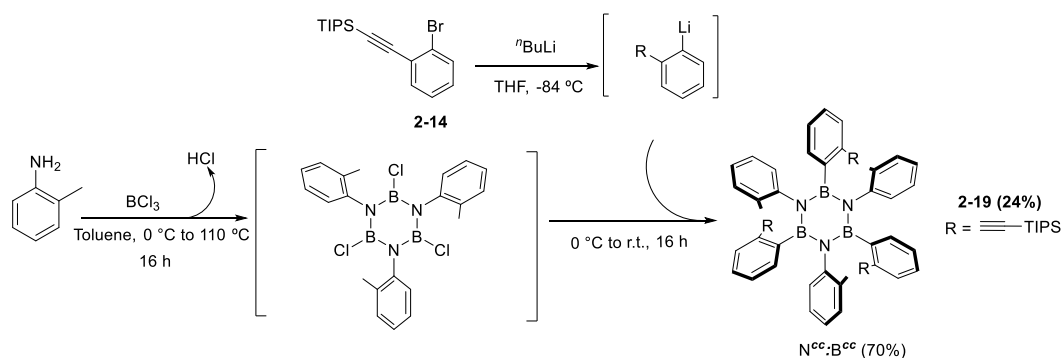
2-methylaniline can give rise to eight different isomers of desired borazine **2-18**, owing to the combinations of the two mono *ortho*-aryl moieties (Scheme 2.9).



**Scheme 2.9** – Introduction of SRoS on the *N*-aryl moieties. Synthesis of borazine derivative **2-18**.

Because the mixture of **2-18** was not enriched in any isomer, further VT-NMR experiments were not performed. They would indeed not have helped understanding the mechanism of isomerisation. Note that a full study with *ortho*-substituted aniline moieties will be addressed in Chapter 3.

In the same context, the introduction of SRoS on the *N*-aryl rings has been also explored using **2-12** for the halogen-lithium exchange. When the reaction was carried out with aniline, only isomer *ct* was observed (**2-14**). However, when introduction of a methyl group on the *N*-aryl ring, 70% of isomer  $\text{N}^{\text{cc}}:\text{B}^{\text{cc}}$  was obtained (molecule **2-19**, Figure 2.21), and no further isomerisation was observed even if the sample is heated (Scheme 2.10). This suggests that borazine **2-14** is initially formed as isomer *cc*, but it directly isomerises to isomer *ct* at room temperature, as it probably has a lower rotational energy barrier than **2-15**. Therefore, we can confirm that by increasing the steric hindrance of the *ortho*-positions, the rotational energy barrier allowing for rotations around the single bonds raises, preventing from the interconversion of one isomer into the other (Figure 2.21).



**Scheme 2.10** – Introduction of SRoS on the N-aryl moieties. Synthesis of borazine derivative **2-19**.

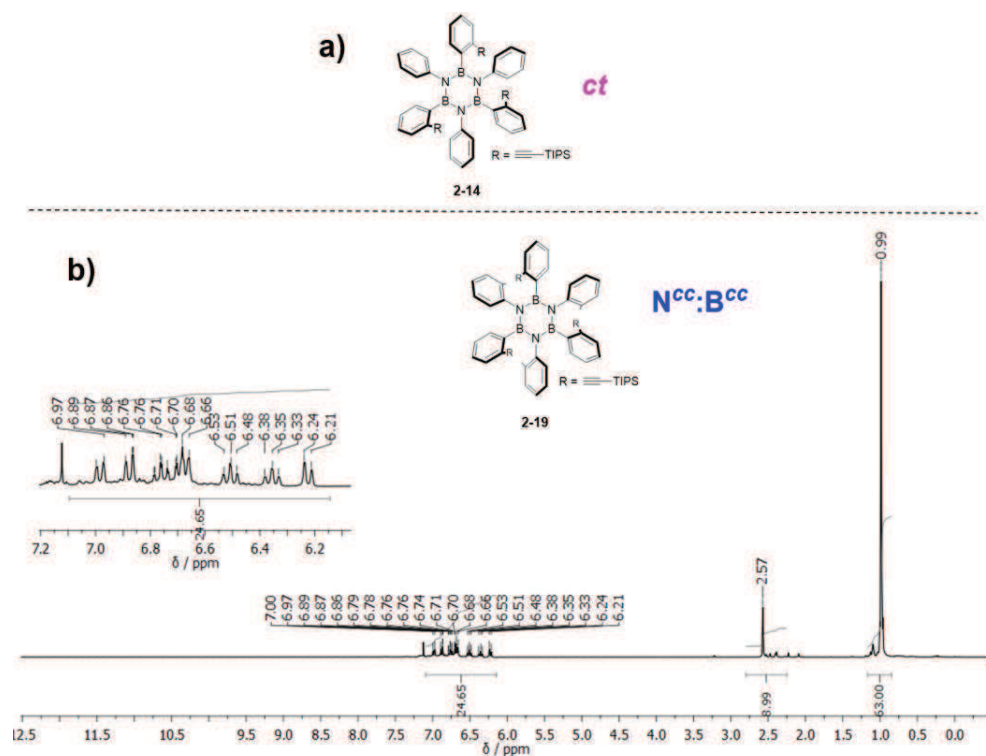
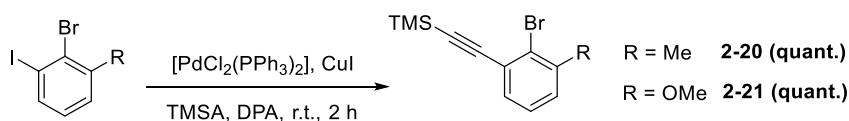


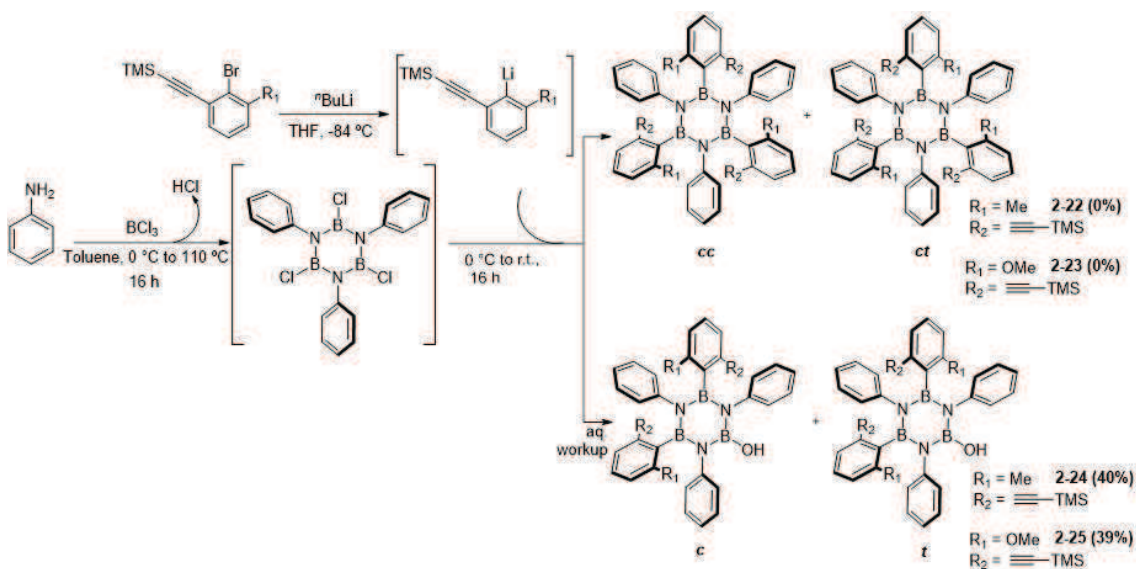
**Figure 2.21** – (a) Molecule **2-14**; (b) introduction of SRoS on the N-aryl moieties, molecule **2-19**.  $^1\text{H-NMR}$  in  $\text{CDCl}_3$  (residual peak: 7.26 ppm) of borazine derivative **2-19**  $\text{N}^{\text{cc}}:\text{B}^{\text{cc}}$  (70%).

In the second set of experiments, the additional substituents on the *ortho*-positions of the aryl groups of the resulting borazines were brought through the *ArLi* reagent (asymmetrical *ArLi* derivatives, where  $\text{R}_1 \neq \text{R}_2 \neq \text{H}$ ). For this purpose, 3-(trimethylsilyl)-acetylene-2-bromotoluene<sup>[19]</sup> **2-20** and 3-(trimethylsilyl)-acetylene-2-bromoanisole **2-21** have been quantitatively prepared by Sonogashira cross-coupling reaction of 3-iodo-2-bromotoluene or 3-iodo-2-bromoanisole with (trimethylsilyl) acetylene at room temperature during two hours, using  $[\text{PdCl}_2(\text{PPh}_3)_2]$  as catalyst and  $\text{CuI}$  as co-catalyst (Scheme 2.11).



**Scheme 2.11** – Preparation of compounds **2-20** and **2-21** by Sonogashira cross-coupling reaction.

For the synthesis of the target borazines **2-22** and **2-23**, aniline reacts overnight with  $\text{BCl}_3$  under refluxing conditions. Addition of the corresponding nucleophile derived from compound **2-20** or compound **2-21**, respectively, would lead to the formation of the expected borazines (isomers *cc* and/or *ct*) (Scheme 2.12). However, in both cases, the expected borazine was not formed, and just borazine **2-24** and **2-25** were obtained (isomer *t*).



**Scheme 2.12** – Failed attempt toward the synthesis of borazine **2-22** and **2-23**. However, borazines **2-24** and **2-25** were obtained.

The identification of each borazine was corroborated by  $^{11}\text{B}$ -NMR analysis, in which two peaks, instead of one, were detected. For instance, for borazine **2-24**, one peak was observed at 35.98 ppm, corresponding to the expected chemical shift for the boron atom of a borazine substituted by the aryl groups, and a second peak at 25.72 ppm, suggesting the presence of a B-O bond (Figure 2.22).<sup>[4]</sup>

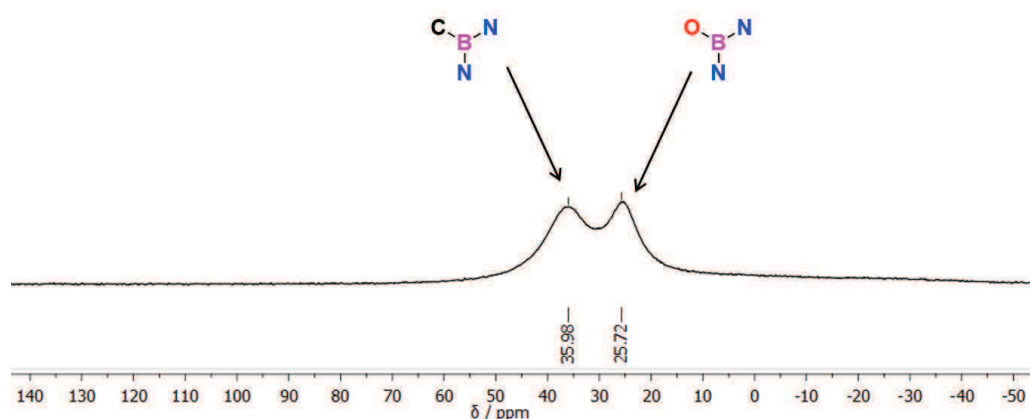


**Figure 2.22** – 128 MHz  $^{11}\text{B}$ -NMR of molecule **2-24** in  $\text{CDCl}_3$ , where two peaks are observed. The first one at 35.98 ppm is typical for borazine derivatives, while the second one at 25.72 ppm corresponds to a boron linked to an oxygen.

Suitable crystals of **2-24** and **2-25** for X-Ray diffraction analysis were obtained by slow diffusion of MeOH in  $\text{CHCl}_3$  and depicted in Figure 2.23 and Figure 2.24. Identification of isomer **t** was achieved thanks to X-Ray analysis. Thus, for borazine **2-24**, the (trimethylsilyl) acetylene and methyl groups in the *ortho*-positions of the aryl substituents are distributed in an opposite way, respectively. Namely, there are one (trimethylsilyl) acetylene of one *B*-aryl substituent, and one methyl corresponding to the other *B*-aryl group pointing in the same direction, while the complementary groups are pointing in the opposite direction. The same was observed for borazine **2-25**.

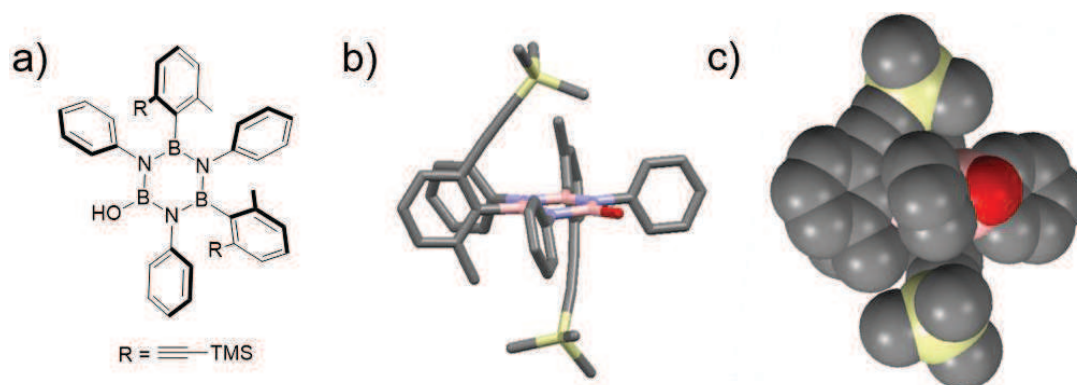


**Figure 2.23** – Crystal structure of borazine derivative **2-24**; (a) molecular structure; (b) crystal structure represented in *capped sticks*; (c) crystal structure represented in *spacefill*. Space group:  $P - 1$ . The crystal was grown by slow diffusion of MeOH in  $\text{CDCl}_3$ . Colour code: grey: C, pink: B, yellow: Si, red: O, and blue: N. Hydrogen was omitted for the sake of clarity.

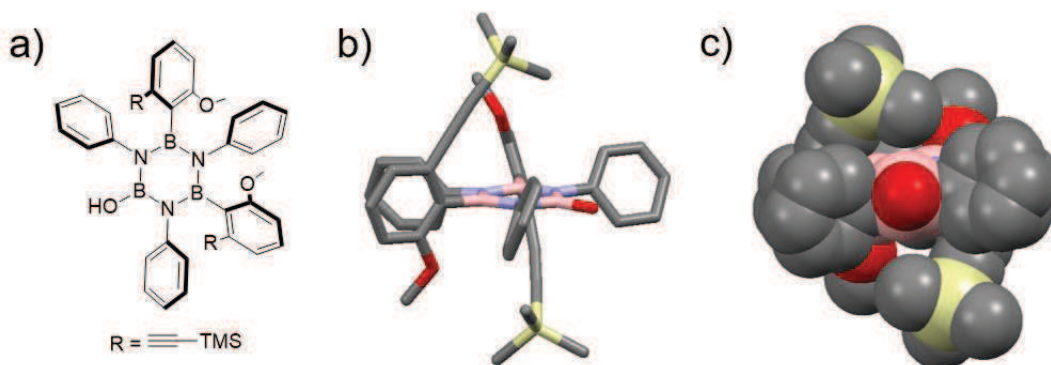


**Figure 2.24** – Crystal structure of borazine derivative **2-25**; (a) molecular structure; (b) crystal structure represented in *capped sticks*; (c) crystal structure represented in *spacefill*. Space group: P 1. The crystal was grown by slow diffusion of MeOH in CDCl<sub>3</sub>. Colour code: grey: C, pink: B, yellow: Si, red: O, and blue: N. Hydrogen was omitted for the sake of clarity.

VT <sup>1</sup>H-NMR of borazines **2-24** and **2-25** in benzene-*d*<sub>6</sub> were also performed. However, no change was observed upon temperature increase, even after 1 hour. The molecules are thus not subjected to any isomerisation process. VT <sup>1</sup>H-NMR spectrum of molecule **2-24** is depicted in Figure 2.25. This is in accordance with the previous result obtained with borazine **2-15**, namely once the most stable isomer *t* (or *ct*) is obtained, isomerisation toward isomer *c* (or *cc*) no longer takes place.

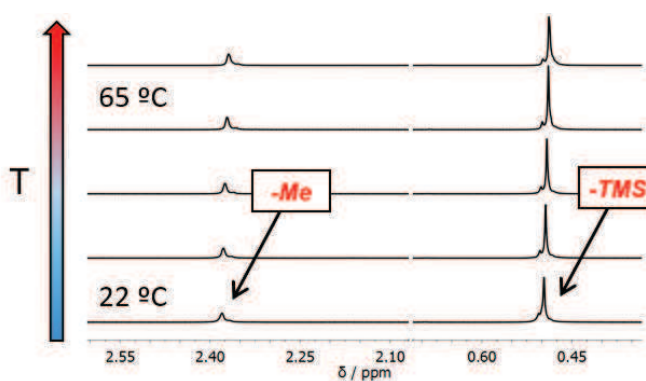
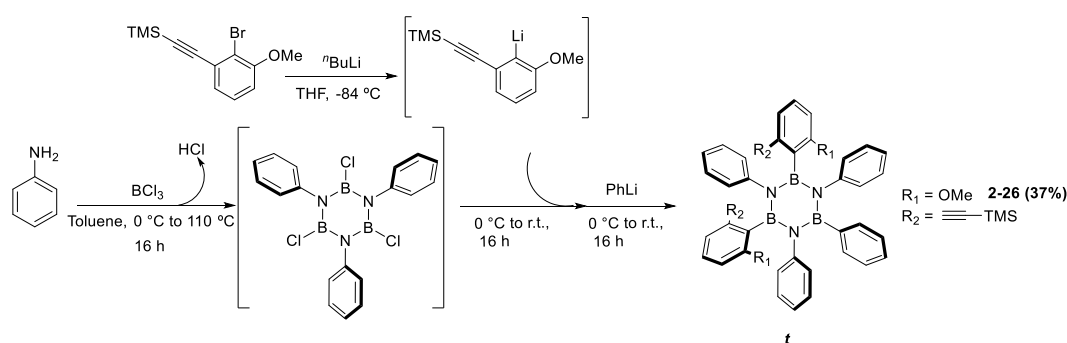


**Figure 2.25** – Variable temperature <sup>1</sup>H-NMR of molecule **2-24** in C<sub>6</sub>D<sub>6</sub>, zoomed in the aliphatic area of the spectra, specifically around 2.6-2.10 and 0.70-0.35 ppm. In the first region it can be observed the peak corresponding to the methyl groups, and in the second one, the one corresponding to trimethylsilyl. When increasing the temperature, from 22 °C to 65 °C and again back to 22 °C, any variation can be observed.

These experiments have demonstrated that *B*-aryl moieties containing one short-range *ortho*-substituent (*e.g.* Me, A-value = 1.74 kcal/mol, or OMe, 0.55-0.75 kcal/mol) and one long-range *ortho*-substituent ((trimethylsilyl) acetylene) cannot be used to obtain final borazine derivatives in which the three boron atoms are equally substituted. During the addition/elimination

process, just two nucleophiles are able to react with two boron sites of the borazine core, and the third boron atom remains bonded to the chlorine. Later, during the aqueous workup step, H<sub>2</sub>O acts as nucleophile and addition/elimination process occurs at that boron atom, leading to the formation of both borazines **2-24** and **2-25**. Therefore, this set cannot help to confirm whether isomerisation occurs *via* rotation.

In order to determine whether the entrance of less hindered groups is feasible, quenching of the reaction with different nucleophiles was achieved. The test showed that when using *PhLi*, the attack on the third boron atom is possible, leading to 37% of the isomer *t* of borazine **2-26** (Scheme 2.13). The presence of only one isomer was confirmed by <sup>1</sup>H-NMR spectroscopy (Figure 2.26).



Scheme 2.13 – Synthesis of borazine **2-26**.

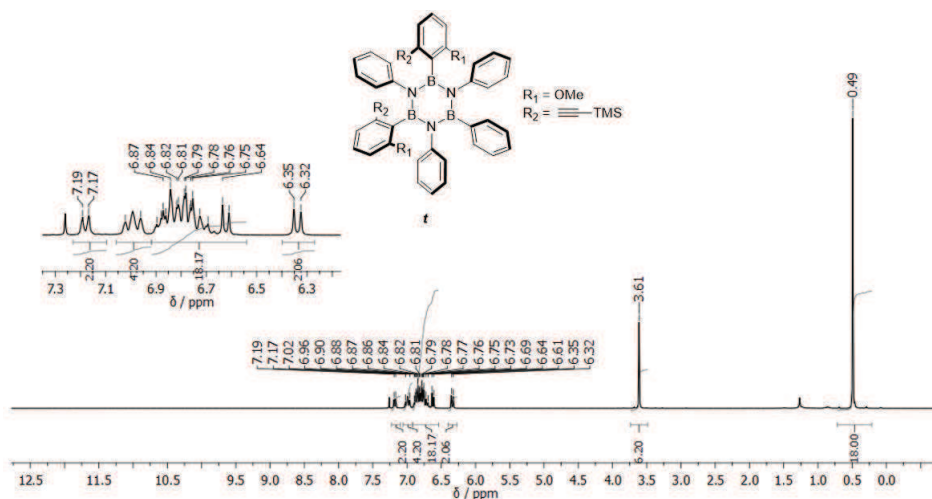


Figure 2.26 <sup>1</sup>H-NMR in CDCl<sub>3</sub> (residual peak: 7.26 ppm) of borazine derivative **2-26**.

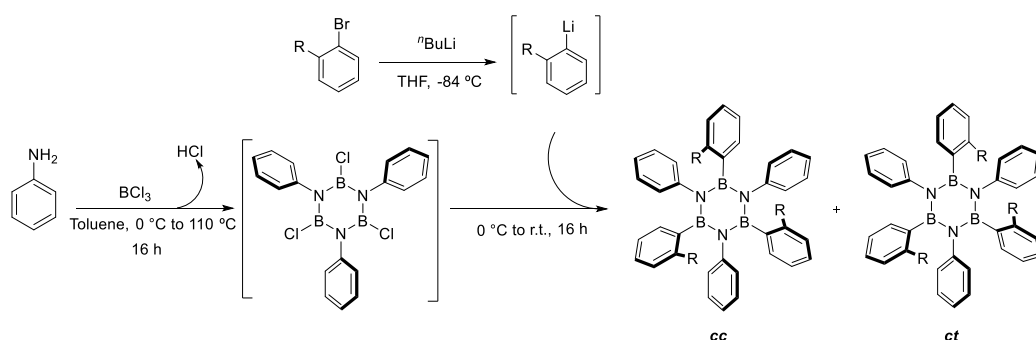
In conclusion, the studies developed for the elucidation of the mechanism through which isomerisation takes place, helped confirming that isomerisation does not occur *via* fast ring opening-closure. Therefore, and thanks to the result obtained with similar derivative **2-19**, it can be confirmed that the process occurs *via* rotation around the  $\sigma$ -bond between the boron atom of the borazine ring

and the  $sp^2$ -carbon of the *B*-aryl moiety that contains the (trimethylsilyl) acetylene group in *ortho*-position.

### 2.3.2.d Syntheses of Borazine Derivatives containing Short-Range *ortho*-Substituents

The fourth part of the project toward the study of the effect of a substituent in the stereoselectivity of the process was carried out with *ortho*-substituents that have a lower steric effect ( $R = \text{Me}$ ,  $\text{CF}_3$ , and  $\text{NMe}_2$ ) in comparison to those already discussed. For this purpose, synthesis of borazine **2-27**, **2-28**, and **2-29** has been achieved with respectively 2-bromotoluene, 2-bromo-trifluoromethylbenzene and 2-bromo-*N,N*-dimethylaniline as precursors for the formation of the desired *ArLi* derivatives (using *n*-BuLi for the exchange).<sup>[20,21]</sup> For the synthesis of those borazine derivatives, the same methodology previously described was followed. All target molecules were formed with success in yields ranging from 69 to 47%. These new borazine derivatives show to be stable against moisture. In the three cases, and in contrast with the previous results, both isomers *cc* and *cc* were obtained in a ratio *cc:cc* 1:3. The identification of both isomers was determined by  $^1\text{H}$ -NMR in which three different peaks were found in the aliphatic part of the spectrum, and the integral relation between them allowed to calculate the ratio obtained (in the case of the  $\text{CF}_3$  with  $^{19}\text{F}$ -NMR) (Table 2.3).

**Table 2.3** – Synthesis of mono-protected borazine derivatives, using short-range *ortho*-substituents.



Entry	Precursor for the Ad / E			Outcome
	<i>R</i>	Reagent	A-value (kcal/mol)	Yield (%)
1	<b>Me</b>	2-bromotoluene	1.74	Borazine <b>2-27</b> : 69
2	<b>CF<sub>3</sub></b>	2-bromotrifluoromethylbenzene	2.4-2.5	Borazine <b>2-28</b> : 51
3	<b>NMe<sub>2</sub></b>	2-bromo- <i>N,N</i> -dimethylaniline	$\text{N}^+\text{H}(\text{Me})_2$ 2.4	Borazine <b>2-29</b> : 47

VT  $^1\text{H}$ -NMR experiments with borazine derivatives **2-27** and **2-29** were also developed to see if any interconversion or isomerisation takes place between the isomers. However, after heating up to 75 °C, no variation in the integration of the peaks was observed, indicating that no isomerisation had occurred when increasing the temperature (Figure 2.27).

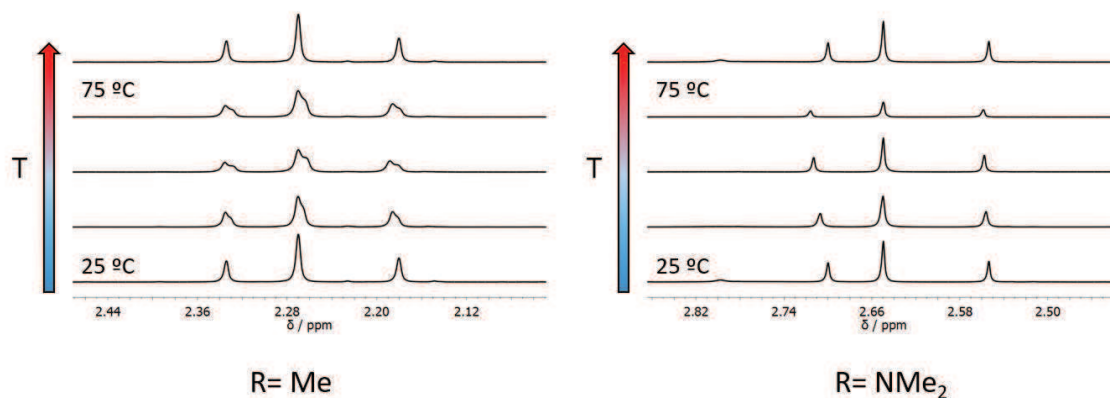
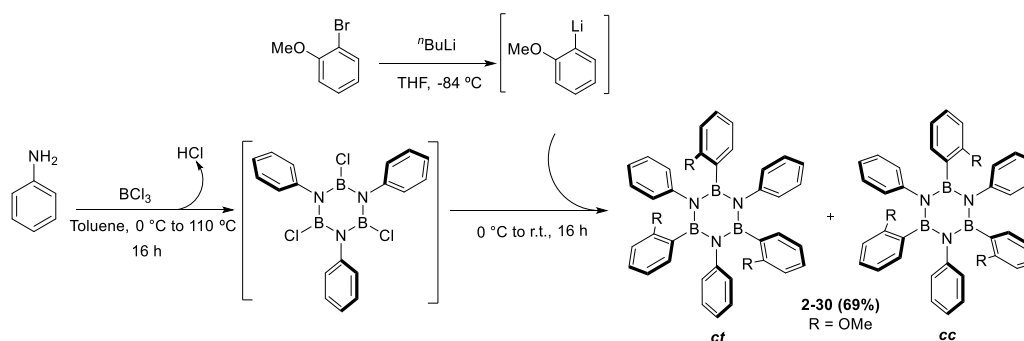


**Figure 2.27** – Variable temperature  $^1\text{H}$ -NMR of molecules **2-27** and **2-29** in  $\text{C}_6\text{D}_6$ , zoomed in the aliphatic area of the spectra. When increasing the temperature, from 25 °C to 75 °C and again back to, 25 °C, any variation can be observed, confirming no isomerisation.

2-Bromoanisole, which contains a methoxy group in the *ortho*-position (OMe A-value = 0.55-0.75 kcal/mol), was used as a fourth precursor for the halogen-lithium exchange.<sup>[22]</sup> Borazine **2-30** was successfully obtained (Scheme 2.14), and showed to be stable in the presence of water during the short times required for the workup. Both isomers *cc* and *ct* were also formed. However, the ratio between them was not consistent with the precedent result. In this case, the ratio obtained was measured as *cc:ct* 1:5.



**Scheme 2.14** – Synthesis of borazine **2-30**.

Also in this case, variable temperature  $^1\text{H}$ -NMR studies of molecule **2-30** in benzene- $d_6$  have been carried out and similarly, no isomerisation has been observed upon raising the temperature to 75 °C, as shown in Figure 2.28.

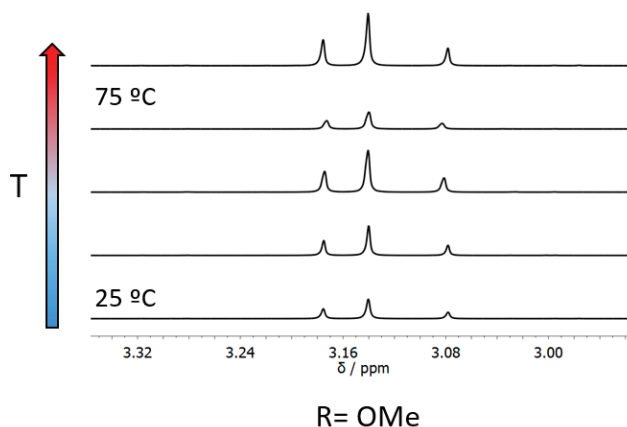


**Figure 2.28** – Variable temperature  $^1\text{H}$ -NMR of molecule **2-30** in  $\text{C}_6\text{D}_6$ , zoomed in the aliphatic area of the spectrum. When increasing the temperature, from 25 °C to 75 °C and again back to 25 °C, any variation can be observed and not isomerisation process takes place.

In this case, the steric effect of the methoxy groups is lower if compared with the previous examples (OMe, A-value = 0.55-0.75 kcal/mol), and this is clearly reflected on the stability of molecule **2-30**. After 5 days, decomposition toward the formation of the corresponding boronic acid and aniline is observed when the borazine is stored under argon atmosphere at room temperature, while previous borazines are stable under similar conditions. In Figure **2.29** is depicted the  $^1\text{H}$ -NMR of molecule **2-30** in  $\text{CDCl}_3$  at different times, and compared to the  $^1\text{H}$ -NMR of the corresponding boronic acid **2-31**. After workup by extraction with water, and subsequent purification just the peaks corresponding to the target borazine are observed. However when time passes, borazine **2-30** starts to decompose, as shown in Figure **2.29**, where not only peaks of borazine are observed, but also those which correspond to boronic acid **2-31**. It is important to remark that the integral relation between the aliphatic peaks did not change when decomposition starts (*cc:ct* 1:5). This suggests that both isomers *cc* and *ct* are equally unstable and both can undergo hydrolysis at the same time under the same conditions.

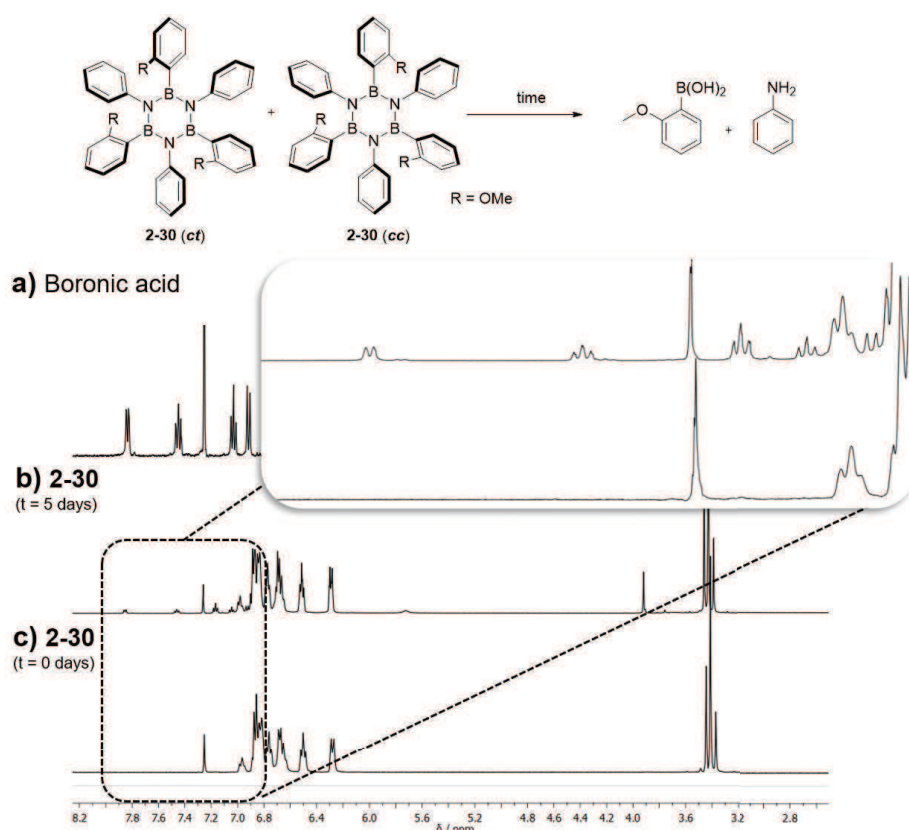


**Figure 2.29** – 400 MHz <sup>1</sup>H-NMR of molecule **2-30** in CDCl<sub>3</sub> (solvent residual peak: 7.26 ppm), at different times, (a) corresponds to the <sup>1</sup>H-NMR of the corresponding boronic acid **2-31** (b) shows borazine **2-30** after 5 days, where decomposition toward boronic acid can be observed, and (c) shows borazine **2-30** directly after purification.

As previously mentioned, the ratio between isomers in this case was different, *cc:ct* 1:5 instead of 1:3. Therefore, the next step was to clarify the reasons that could drive to this ratio. Firstly, in order to test if it was due to any kind of coordination between the lithium atoms and the oxygen atoms of the methoxy groups in the *ortho*-positions, external agents that could cancel that coordination were added. For example, HMPA (hexamethylphosphoramide) has been added to the reaction. HMPA can selectively solvate cations (as Li<sup>+</sup>), generating more "naked" anions, which could help during the reaction. Nevertheless, no variation in the final ratio has been detected. Metal exchange was also studied to observe its effect during the reaction. For that reason, a potassium salt was added to the reaction mixture, but no change has been observed. As *B,B',B''*-tri(chloro)*N,N',N''*-tri(phenyl)borazine **1-3** is insoluble in toluene, different groups in the *para*-position of the aniline could help in terms of solubility, and ease the reaction. For that, the aniline precursor has been slightly modified, using 4-*tert*-butylaniline or 4-chloroaniline. However, same ratio between isomers has been obtained. The solvent used during the formation of the *ArLi* has been also tested but no modification in the ratio between isomers has been observed (Table 2.4).

In light of these results, it was concluded that the observed ratio was not linked to any external agent and was therefore due to the steric effect of the substituent.

**Table 2.4** - Summarised conditions tested for the reaction towards the formation of borazine **2-30**.

Entry	Reagents		Conditions		Outcome	
	Precursor for the Ad / E	Aniline moiety	Solvent	External agent	Ratio <i>cc/ct</i>	Yield (%)
1	<b>2-bromo anisole</b>	Aniline	Toluene /THF	--	1:5	69
2		Aniline	Toluene /THF	HMPA	1:5	5
3		4-tert-butyl-aniline	Toluene /THF	--	1:5	72
4		4-tert-butyl-aniline	Toluene /THF	HMPA	1:5	4
5		4-tert-butyl-aniline	Toluene /THF	TMEDA	1:5	--
6		4-tert-butyl-aniline	Toluene /Et <sub>2</sub> O	--	1:5	74
7		4-tert-butyl-aniline	Toluene /Et <sub>2</sub> O	HMPA	1:5	4
8		4-tert-butyl-aniline	Toluene /Et <sub>2</sub> O	tBuOK	1:5	54
9		4-tert-butyl-aniline	Toluene /THF	tBuOK	1:5	55
10		4-chloro-aniline	Toluene /THF	--	1:5	67

In addition, when using 4-*tert*-butylaniline (**2-32**) as amino precursor, it was possible to grow suitable crystals of the molecule corresponding to isomer *ct*, by slow diffusion of MeOH in CH<sub>2</sub>Cl<sub>2</sub> and confirm its structure by X-Ray analysis (Figure **2.30**). Even if the mixture of both isomers (*cc:ct* 1:5) was submitted to crystallise, just single crystals of isomer *ct* were found in the vial, as well as some white powder, which corresponds to the remaining mixture.

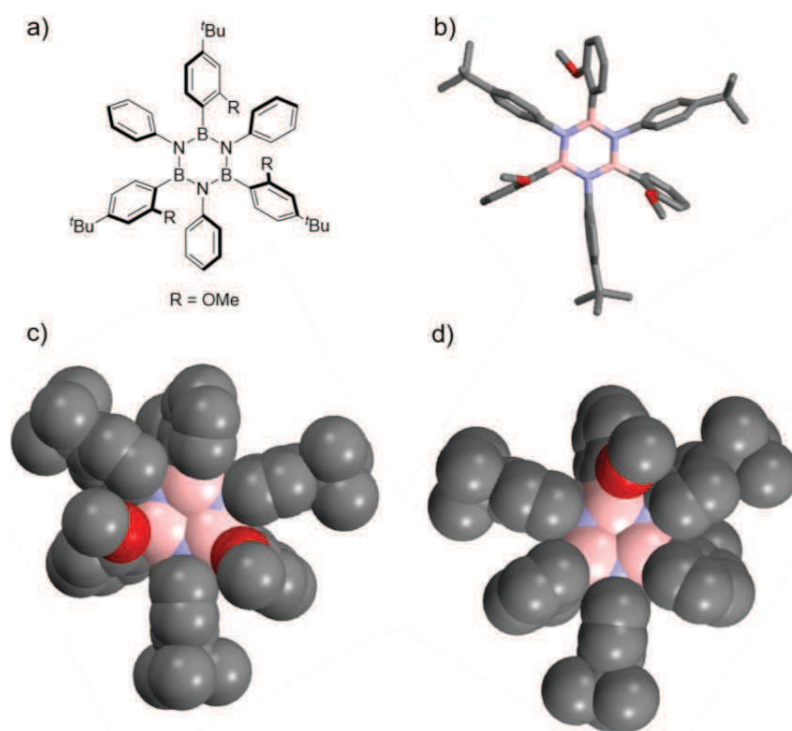
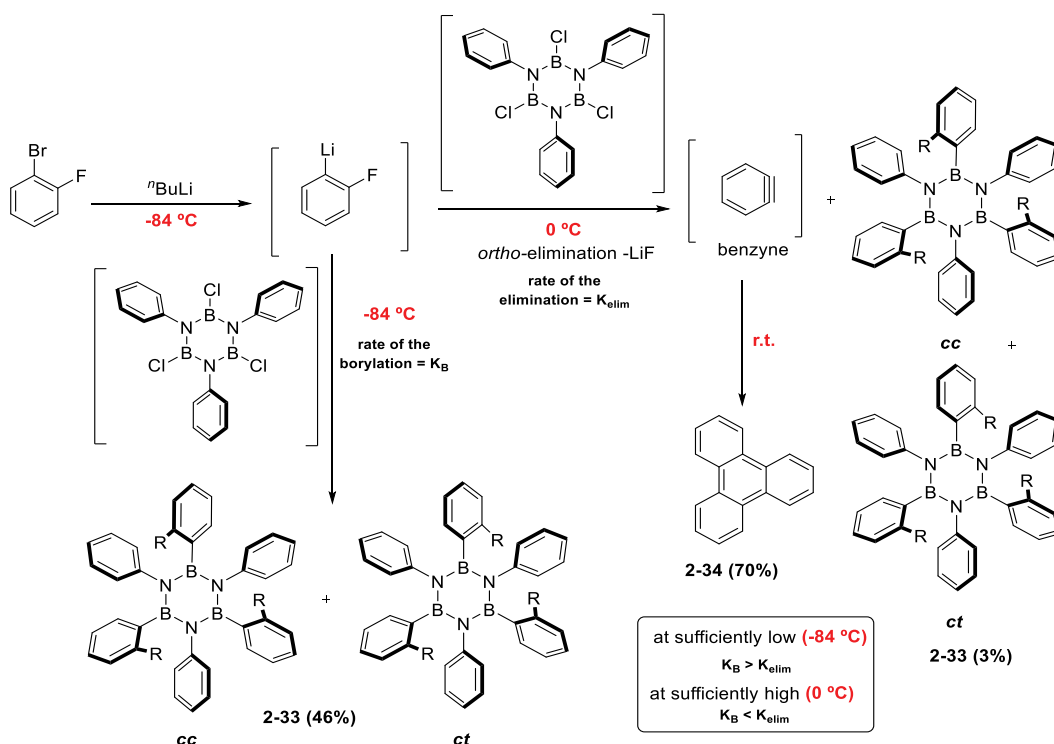


**Figure 2.30** – Crystal structure of borazine derivative **2-32** (isomer *ct*); (a) molecular structure; (b) crystal structure represented in *capped sticks*; (c) crystal structure represented in *spacefill*, front view; and (d) crystal structure represented in *spacefill*, back view. Space group: P 21/c. The crystal was grown by slow diffusion of MeOH in CH<sub>2</sub>Cl<sub>2</sub>. Colour code: grey: C, pink: B, yellow: Si, red: O and blue: N. Hydrogen was omitted for the sake of clarity.

Still in the context aiming at the determination of the substituents' effect during the addition/elimination step at the borazine ring *via* the use of short groups, a borazine derivative decorated with fluorine atoms for the steric protection has been synthesised. This protection would be the smallest introduced up to now (F, A-value = 0.25-0.42 kcal/mol). For this purpose and following the standard procedure, 2-fluorobromobenzene was used, and after reaction with *n*-BuLi at -84 °C during 5 min, *B,B',B''*-tri(chloro)*N,N',N''*-tri(phenyl)borazine **1-3** was cannulated at 0 °C. The resulting yield of this reaction was very low (**2-33**, ~3%) if compared with other borazine derivatives, for which yields higher than 45% were obtained. Instead of the desired reaction, a competitive secondary reaction actually takes place. Indeed, *ortho*-elimination of lithium fluoride generates the highly reactive benzyne intermediate,<sup>[23]</sup> capable of forming triphenylene **2-34** (70%), as the major product of the reaction (Scheme **2.15**). Nonetheless, if the reaction is undertaken at lower temperatures, the rate of the borylation is higher than the *ortho*-elimination of LiF, as described by Lei and co-workers.<sup>[24]</sup> In particular, when the cannulation takes place at -84 °C, followed by 3 h at that temperature, 3 h at 0 °C and 16 h at r.t., the yield of the reaction increases up to 46%.



**Scheme 2.15** – Synthesis of borazine **2-33**. Competition reactions that can take place with 2-lithiumfluorobenzene, under different condition reactions.

As it was observed for borazine **2-30**, the ratio between isomers of **2-33** is *cc:ct* 1:5 in both syntheses. Borazine **2-33** could also undergo aqueous workup without observing any hydrolysis. Yet, if stored in solution for long times (1 week), it fully decomposes.

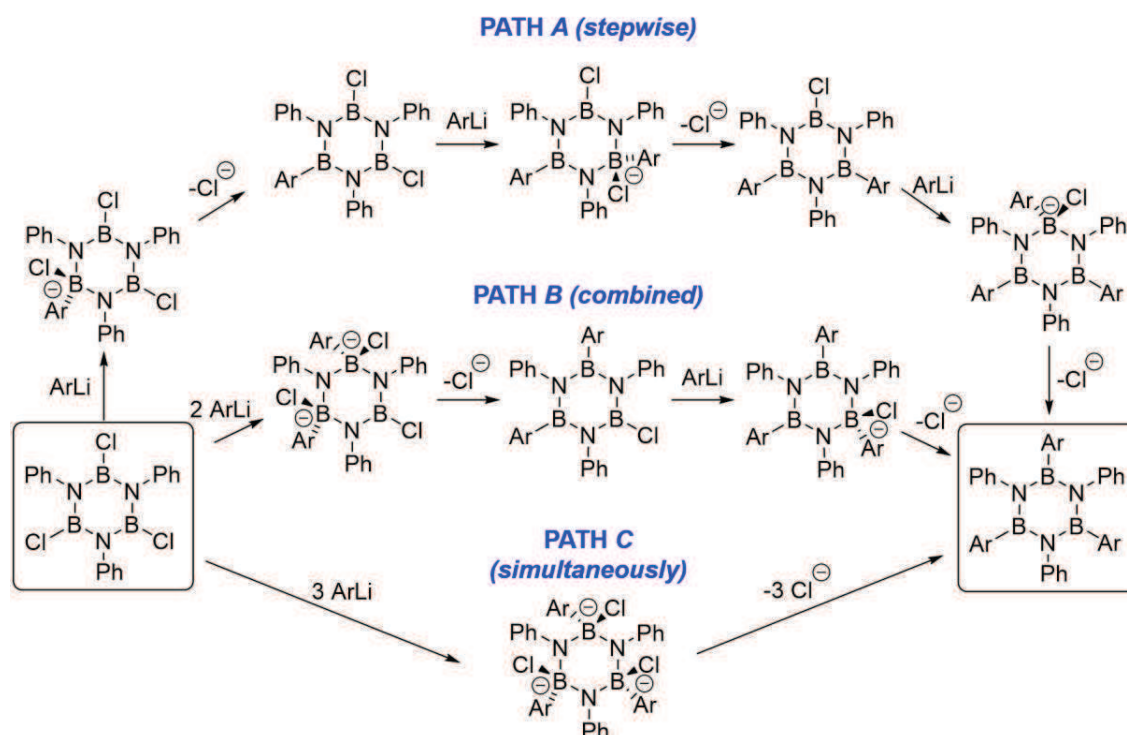
### 2.3.4 Study of the Effect of the *ortho*-Substituent in the Stereoselectivity of the Process

As described in the previous subsections, the ratio obtained for the two possible isomers depends on the nature of the R group, moving from molecules where just one isomer is obtained, to other examples where the ratio between the isomers can vary from *cc:ct* 1:3 to 1:5. Herein, the possible parameters that govern the process and lead to the formation of isomer *cc* or isomer *ct* are presented, and further explained in each particular case.

As known, during the nucleophilic substitution, a new bond is created while another one is broken. The new bond will be formed between the  $sp^2$ -carbon atom bonded to the electropositive lithium atom of the nucleophile and the electrophilic boron atom of the borazine ring. The orbitals involved in the process are the Highest Occupied Molecular Orbital (HOMO) of the nucleophile,

the Li-C  $\sigma$ -bond polarised toward the carbon atom; and the Lowest Unoccupied Molecular Orbital (LUMO) of the electrophile, the  $p$ -orbital of the boron atom, perpendicular to the borazine cycle. During the process, the boron centre changes its hybridisation. At the initial stage, the boron centre presents  $sp^2$  hybridisation (planar trigonal geometry), with a  $p$  vacant orbital. After the addition of the nucleophile, an 'ate complex' is formed in which the boron atom has a tetrahedral  $sp^3$  hybridisation and the borazine ring losses its planarity. Finally, with the elimination of the chloride, the boron atom recovers its initial trigonal  $sp^2$  hybridisation and the borazine cycle its planarity.

During the functionalisation, three addition/elimination reactions can occur (i) stepwise (Path A), (ii) following a route where two Ad/E reactions occur first, followed by the last one (Path B), or (iii) the three additions simultaneously, followed by the three eliminations (Path C) (Scheme 2.16).



**Scheme 2.16** – Three possible routes for the addition-elimination process at the borazine ring.

When addition occurs, the boron atom is negatively charged, due to the formation of the 'ate complex'. In the cases where two or three additions take place at the same time, the intermediate would be double or triple charged. In addition, for Path B or C, three or four molecules have to participate at the same time in the same reaction, which could complicate these routes. For all these reasons, the stepwise route (Path A) seems to be the most plausible and the reaction will be described following this postulate, even though there is no any experimental confirmation.

### 2.3.4.a Proposed explanation for the stereoselective process

For the explanation of how the presence of a substituent can affect the addition/elimination process, the Cartesian coordinate system will be used, which will help to clearly understand where the molecules are located at each moment. The following discussion was made possible to the performing of theoretical calculations. Geometry optimisation and saddle geometry optimisation were performed using *Gaussian 09 RHF/6-31G\* with d01 revision*.

- Addition of the first organolithium derivative:

The model represented in Figure 2.31 will be used as reference in order to simplify the discussion. At the beginning, borazine *B,B',B''*-tri(chloro)-*N,N',N''*-tri(phenyl)borazine **1-3** is situated on the *xz*-plane (Figure 2.31.a). The nucleophile (*ArLi* derivative) approaches the borazine core from the top. When the addition at the boron site occurs, the aryl moiety of the nucleophile stands along the *yz*-plane (Figure 2.31.b). The boron atom of the borazine ring that has been attacked is bonded at this stage, to the two adjacent nitrogen atoms of the ring, the chlorine (in an equatorial manner) and the new aryl moiety (with an axial geometry). Therefore, four bonds in total. Thus, the hybridisation in the atom is not anymore  $sp^2$ , but is  $sp^3$ , and the borazine ring loses its planarity and aromaticity, having now a different conformation. In this conformation, the boron atom attacked is located above the *xz*-plane (in **bold font**), while the two adjacent nitrogen atoms has also changed their hybridisation (from  $sp^2$  to  $sp^3$ ), and consequently the *N*-phenyl groups are below than before the attack. The changes in the hybridisation are reflected on the bond-distances between the atoms. The other three atoms that make up the borazine cycle do not change their hybridisation and position.

The new aryl group then rotates around the B-C bond (from the *yz*-plane to the *xy*-plane) to have the correct predisposition needed for the recovery of the aromaticity, while allowing the elimination of chlorine. From this point, two different behaviours can be encountered, based on the position that will occupy the R group, as shown in Figure 2.31.b. If the aryl ring rotates clockwise, the R group will be located far away from the top of the borazine cycle, leading to an *exo* conformation (Figure 2.31.c). On the other hand, if the aryl ring rotates counter-clockwise, the R moiety will be located on top of the borazine cycle, leading to an *endo* conformation (Figure 2.31.d). This *endo* intermediate induces a stronger steric hindrance, and should be considered in each case, depending on the R group. For the release of the chlorine, the new aryl group moves from the axial-position to the equatorial one, while the chlorine moves from the equatorial to the axial one, below the ring. Finally, elimination of this axial chlorine comes up with the recovery of the aromaticity, while the boron atom regains its initial hybridisation ( $sp^2$ ). As a result, the new aryl moiety is perpendicular (*yz*-plane) to the borazine ring (*xz*-plane). In the *exo* case, the R group will end up on

the opposite side of the attack (Figure 2.31.e), while for the *endo* intermediate, the R group will be located on the same side of the attack (Figure 2.31.f).

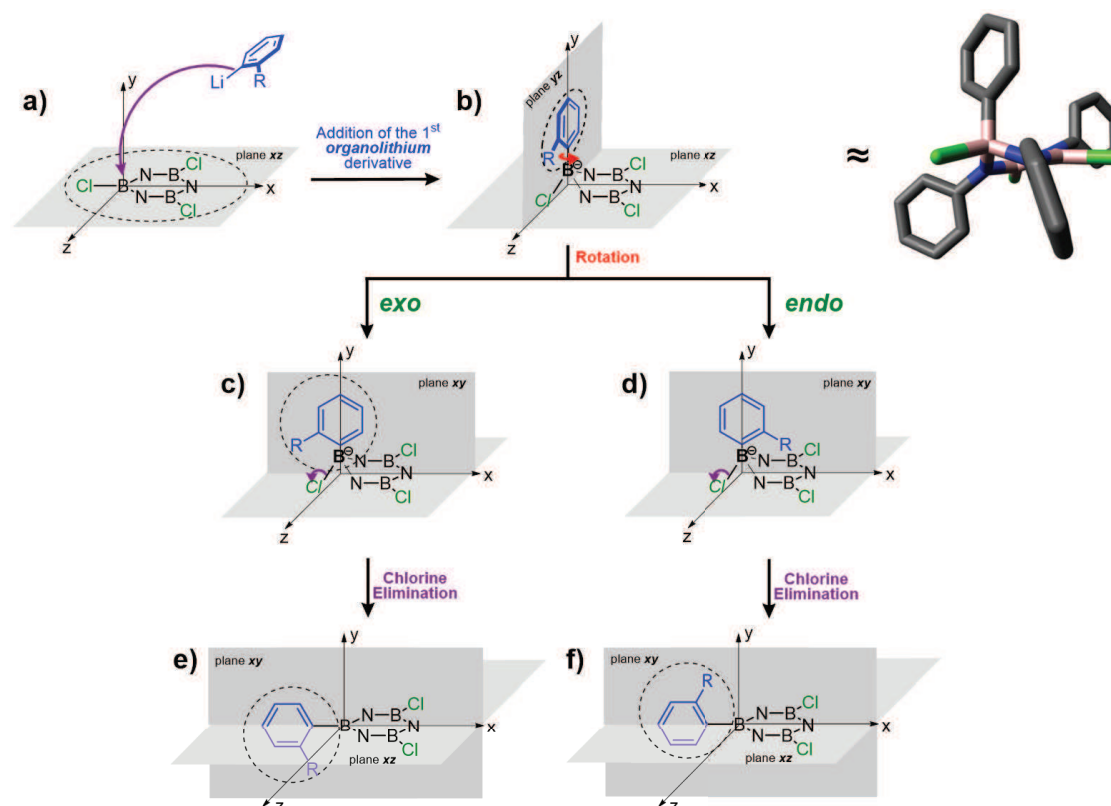


**Figure 2.31** - Proposed mechanism for the addition of the first *organolithium* derivative to B,B',B''-tri(chloro)-N,N',N''-tri(phenyl)borazine 1-3, where R is a general *ortho*-substituent on the aryl group bonded to the boron atoms of the borazine ring. The *N*-aryl groups were omitted for the sake of clarity. In the borazine core, the atoms written in **bold** font are on top on the *xz*-plane, while those written in *italics* font are situated below the *xz*-plane. Saddle point geometry optimisation of the (b) intermediate is included (in which R = H), performed at *RHF/6-31G(d,p)* level of theory. Colour code: grey: C, pink: B, blue: N, green: Cl.

- Addition of the second *ArLi* derivative:

The second *ArLi* derivative can approach the borazine core from the same side where is located the previous R substituent (addition *syn*) or from the opposite side (addition *anti*), as shown in Figure 2.32.

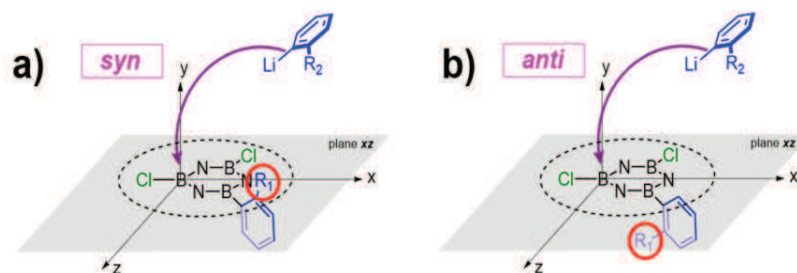


**Figure 2.32** - (a) *Syn* addition of the second nucleophile; (b) *anti* addition of the second nucleophile.

*Anti*-addition. This term defines the process that occurs when the second *organolithium* derivative approaches the borazine core from the opposite side of the previous R substituent (named  $\text{R}_1$  at this stage) and is depicted in Figure 2.33. The postulates that apply for the addition of the first *ArLi* derivative can be assumed for this second one. However, in this case, the formation of two isomers is possible because of the presence of two R groups on the final compound. In the *exo* case, the  $\text{R}_2$  group ends up on the opposite side of the attack, hence on the same one where is located the  $\text{R}_1$  group (Figure 2.33.e), leading to the formation of isomer *c* (for *cis*). Whereas, for the *endo* intermediate, the  $\text{R}_2$  group is located on the same side of the attack and on the opposite side in respect to the  $\text{R}_1$  group, obtaining isomer *t* (for *trans*) (Figure 2.33.f).

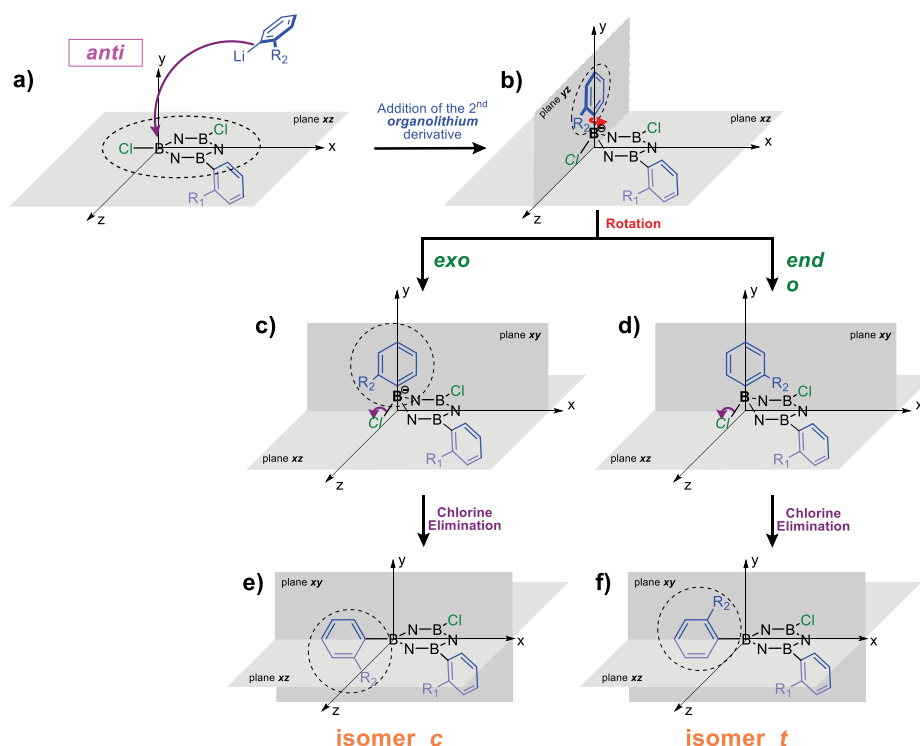


**Figure 2.33** - Proposed mechanism for the *anti*-addition (as referred to the position of  $\text{R}_1$ ) of the second *organolithium* derivative. Both  $\text{R}_1$  and  $\text{R}_2$  are general *ortho*-substituent on the aryl group bonded to the boron atoms of the borazine ring. The *N*-aryl groups were omitted for the sake of clarity. In the borazine core, the atoms written in **bold** font are on top on the  $xz$ -plane, while those written in *italic* font are situated below the  $xz$ -plane.

*Syn*-addition. This term defines the process that occurs when the second *ArLi* derivative approaches the borazine core from the same side of the previous R substituent (named R<sub>1</sub> at this stage) which entails a stronger steric hindrance than the precedent one (Figure 2.34). In the *exo* case, the R<sub>2</sub> group ends up on the opposite side of the attack and of the R<sub>1</sub> group (Figure 2.34.e), leading to the formation of isomer *t*. On the other hand, for the *endo* intermediate, the R<sub>2</sub> group will be located on the same side of both the attack and the R<sub>1</sub> group, obtaining isomer *c* (Figure 2.34.f).

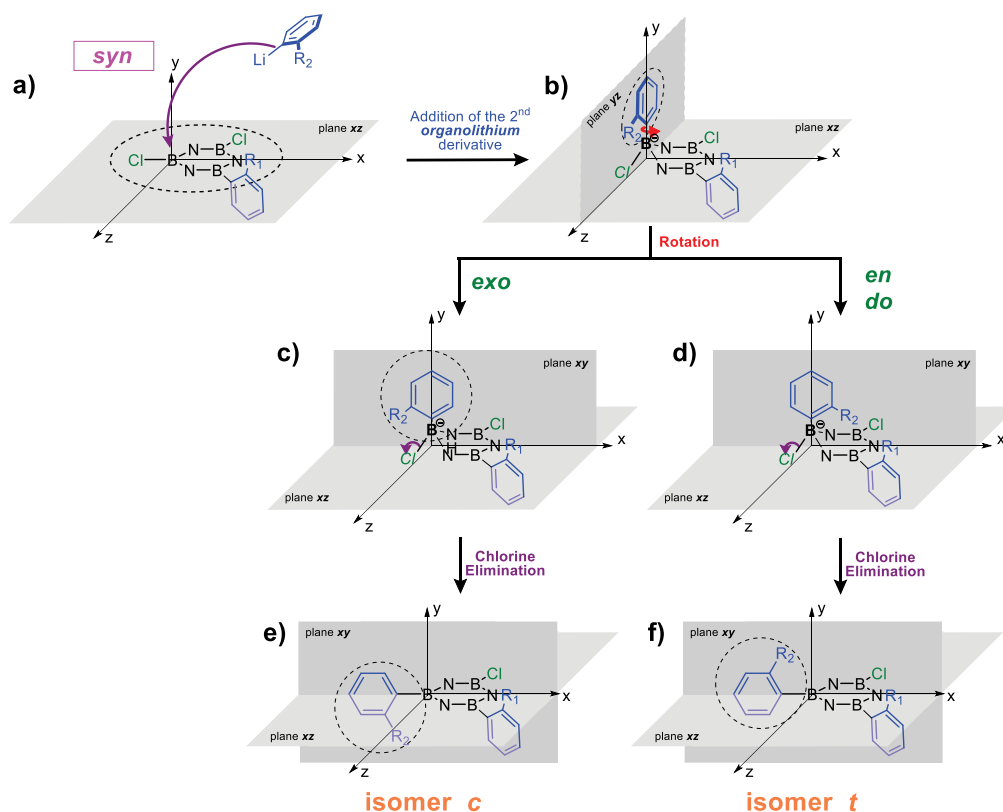


**Figure 2.34** - Proposed mechanism for the *syn* addition (as referred to the position of R<sub>1</sub>) of the second *organolithium* derivative. Both R<sub>1</sub> and R<sub>2</sub> are general *ortho*-substituent on the aryl group bonded to the boron atoms of the borazine ring. The *N*-aryl groups were omitted for the sake of clarity. In the borazine core, the atoms written in **bold** font are on top on the *xz*-plane, while those written in *italics* font are situated below the *xz*-plane.

- Addition of the third *ArLi* derivative:

From the previous steps, four intermediates have been obtained (two corresponding to isomer *c* and two corresponding to isomer *t*). The addition of the third *ArLi* derivative can be again *anti* or *syn* (as referred to the position of R<sub>1</sub>) and the R<sub>3</sub> group can rotate in *exo* or *endo*. Therefore, and following the nomenclature *cc* and *ct*, used in this Chapter, there are sixteen possibilities, and the **statistical distribution** of the isomers corresponds to *cc:ct* 4:12 (= 1:3) (Figure 2.35).



According to the theory described before, the *cc:ct* ratio would always be 1:3 if the reaction was following a purely statistical distribution. However, as the steric effect of the R groups changes as a function of its structure, this statistical ratio can fluctuate as it has been previously detailed in the previous Subsections. In order to clarify these experimental observations, the next Subsections will address each of the cases.

### 2.3.5.b LROS: triazene, acetylene TMS, acetylene TIPS

In the case of using a triazene derivative (**2-17**), isomer *cc* was found as product after the reaction. Figure 2.36 shows the proposed route for the formation of this isomer *cc*.

Addition of the first equivalent of the *ArLi* derivative to the borazine core takes place, and during the rotation, the *exo* approach is favoured due to the strong steric effect that would entail the other approach. The second equivalent can approach the core in *anti* or *syn* in respect to R<sub>1</sub>. The *anti*-attack is preferred due to the impediment generated on the side where is located R<sub>1</sub>. The favoured rotation is again the *exo* one, leading to the formation of isomer *c*. The third *ArLi* derivative is added following the *anti-exo* route as before. Following this explanation, isomer *cc* would be formed, in agreement to the experimental observation (Figure 2.36). A similar description could be applied for the case of acetylene TMS, in which formation of isomer *cc* is observed after the reaction. In addition, isomerisation is observed when this borazine derivative **2-15** is subjected to higher temperatures. However, borazine **2-14** (where R is an acetylene TIPS moiety) was observed as isomer *ct*. Presumably, during the reaction, isomer *cc* is formed and due to the high steric hindrance between the groups, it directly isomerises to the most stable isomer *ct*. TIPS having a higher steric effect than TMS, isomer *cc* becomes less stable. Thus, the isomerisation occurs faster and at lower temperatures than the one for molecule **2-15**, hence, the isomer *cc* could not be isolated.

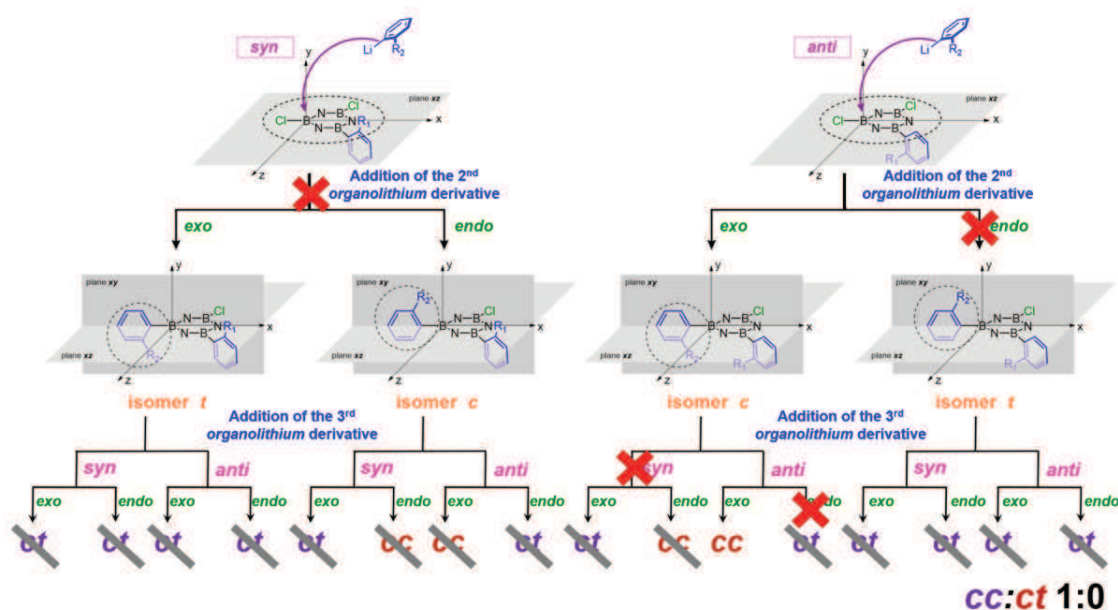


**Figure 2.36** – Proposed route for the formation of isomer *cc* when using mono-*ortho* long-range substituents in the aryl moieties bonded to the boron atoms. The *N*-aryl groups were omitted for the sake of clarity.

### 2.3.4.c SROs: Me

When the R group is a methyl moiety, the observed ratio between the isomers is *cc:ct* 1:3. Even if this ratio is the same as that observed *via* the statistical distribution, due to the steric hindrance generated by the presence of the methyl (A-value = 1.74 kcal/mol); some of the routes are cancelled. All the routes are considered for the first and second addition, and it is during the third one that some of them are prohibited. For instance, with isomer *c*, the third *syn* attack is restricted, as that side already contains two hindered methyl groups. For the isomer *t*, with the addition of the third equivalent, the *endo* rotation is favoured (Figure 2.37).

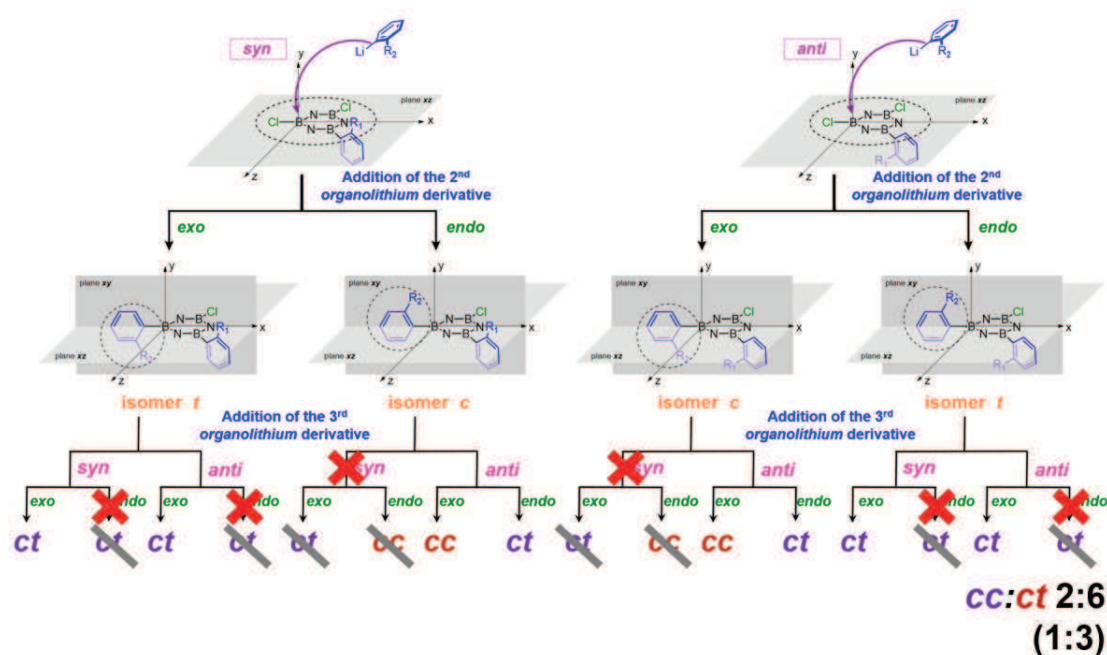


**Figure 2.37** – Proposed route for the formation of isomers *cc:ct* 1:3 when using mono-*ortho* short-range substituents (as methyl) in the aryl moieties bonded to the boron atoms. The *N*-aryl groups were omitted for the sake of clarity.

#### 2.3.4.d SROs: OMe

When the R group is a methoxy moiety (A-value = 0.55-0.75 kcal/mol, lower than for methyl groups) the ratio between the isomers is *cc:ct* 1:5. All the routes are considered for the first and second addition, and it is during the third one that some of them are prohibited. When isomer *c* is formed, the third addition preferably goes from the other side in respect to *R*<sub>1</sub> and *R*<sub>2</sub>. Following this premise, the ratio obtained is in accordance to the one experimentally observed (Figure 2.38).

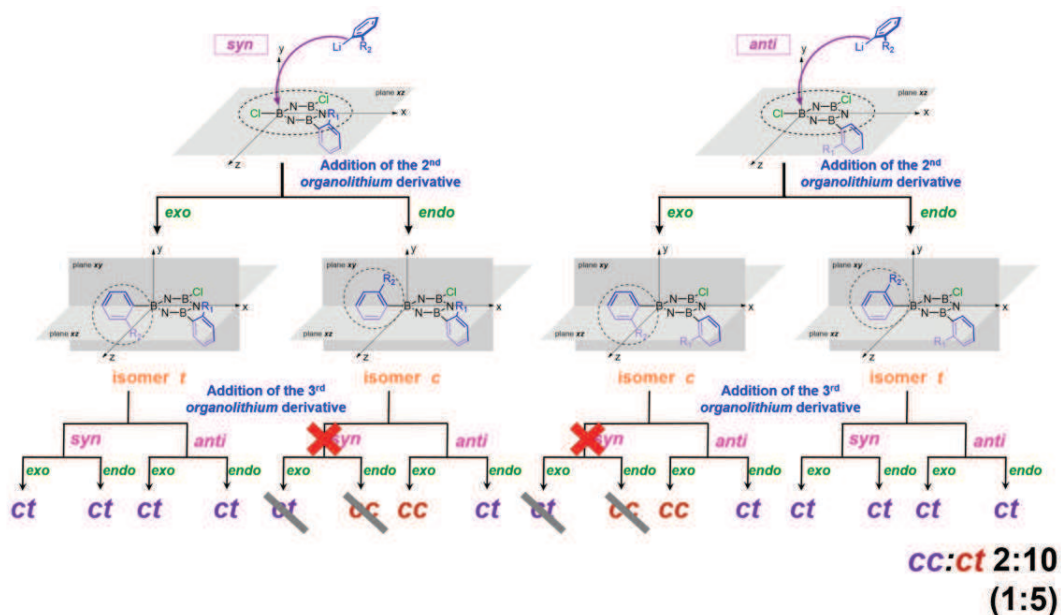


**Figure 2.38** – Proposed route for the formation of isomers *cc:ct* 1:5 when using mono-*ortho* short-range substituents (as methoxy) in the aryl moieties bonded to the boron atoms. The *N*-aryl groups were omitted for the sake of clarity.

#### 2.3.4.e SROs: Me, and LROs: acetylene TMS

Moreover, when using *ArLi* derivatives that contain both short- and long-range substituents (**2-20** and **2-21**) and molecules **2-24** and **2-25** are formed (where just two equivalents of *ArLi* derivatives are able to react with the borazine core) as isomer *t*, the mechanistic routes that can lead to the formation of this isomer are represented in Figure 2.39. In the figure, *R*<sub>1</sub> refers to the long-range substituent (acetylene TMS) and *R*<sub>2</sub> to the short-range one (Me or OMe). The terms *syn* or *anti* refer to the position of *R*<sub>1</sub>.

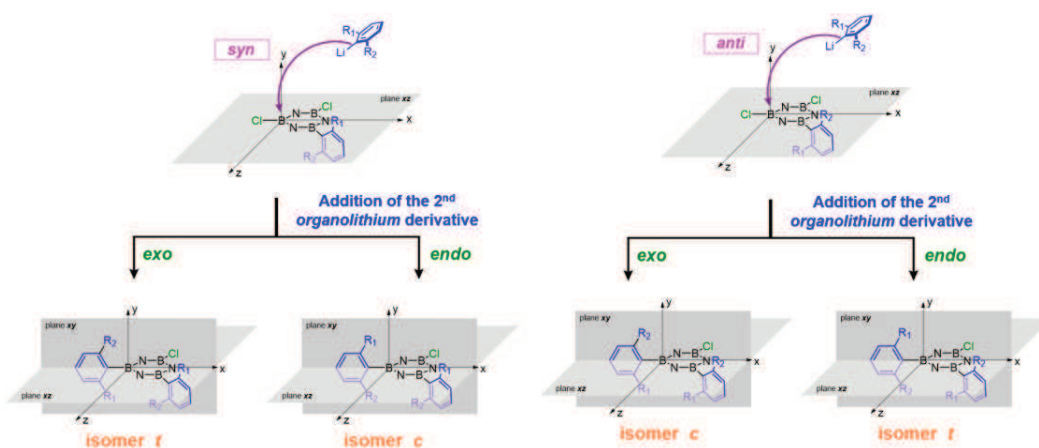


**Figure 2.39** – Statistical distribution of the possible isomers; *c:t* 1:1, where *R*<sub>1</sub> is a long range substituent, while *R*<sub>2</sub> is a short range one, both *ortho*-substituents in the aryl group bonded to the boron atoms of the borazine ring. The *N*-aryl groups were omitted for the sake of clarity.

In this case, both options have to be considered. Concretely, the formation of isomer *t* can be due to *syn-exo* route or to an *anti-endo* one, while isomer *c* is formed by either *syn-endo* route or *anti-exo*. Based on the previous results, long-range groups prefer the *anti-exo* route. On the other hand, short-range substituents can follow all the routes, thus all the possibilities should be considered for them. However, it is difficult to predict which side of the borazine ring would be the elected one during the second attack. In addition, isomer *c* could isomerise to isomer *t*, as previously observed in other examples.

In consequence, two different and opposed conclusions can be postulate. Either (i) short-range substituents are able to better protect from the attack than long range substituents; therefore, the attack is produced in *syn* (followed by an *exo* rotation) and isomer *t* is formed; either (ii) long-range substituents better protect from successive attacks, so the attack takes places in *anti* (followed by and *exo* rotation) and isomer *c* is formed. Then, by isomerisation, isomer *t* could be formed. As both postulates lead to the formation of same isomer, no conclusion can be taken.

### 2.3.5 Reactivity of the Borazine Core against Different Nucleophiles

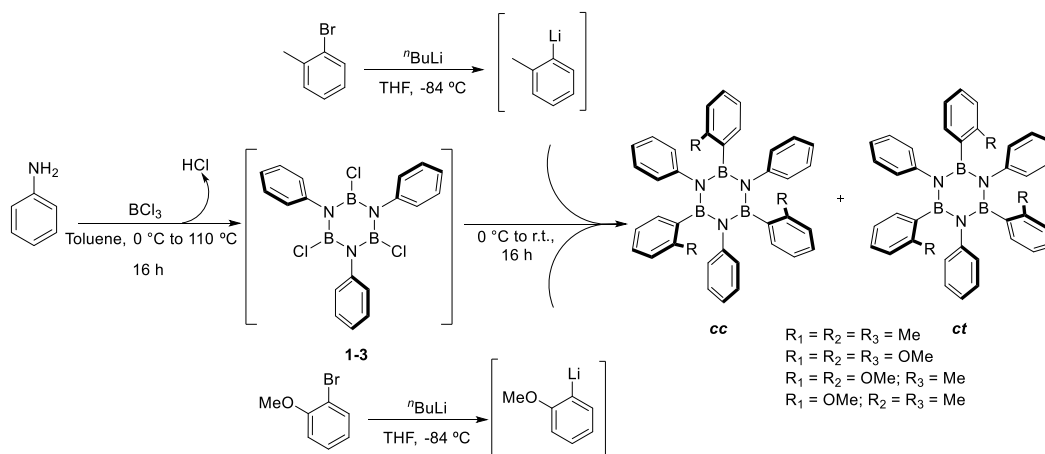
This Subsection presents some aspects of the addition/elimination step, which had not been previously considered. In particular, comparative studies have been developed in order to address i) the effect of the nucleophilicity of the *organolithium* derivative used during the addition/elimination reaction; and ii) the effect of the steric hindrance of the *organolithium* derivative during the reaction.

#### 2.3.5.a Comparative Study of the Process in Terms of Nucleophilicity of the *ArLi* Reagent

The first part was based on the study of how the nucleophilicity of the *organolithium* derivative used during the addition/elimination reaction can influence the formation of the final borazine derivative. For this purpose, two different precursors for the halogen-lithium exchange have been used, both containing short-ranges mono *ortho*-substituents. In particular, 2-bromoanisole and 2-bromotoluene, respectively displaying a methoxy and a methyl group, have been selected. Due to a mesomeric effect (+M), the methoxy group present in 2-bromoanisole is expected to improve the nucleophilicity of the *organolithium* reagent respect to *PhLi*. The methyl group, by inductive effect (+I), is also an activating agent which should enhance the nucleophilicity of the corresponding *ArLi* reagent in comparison with *PhLi*. However, the effect of the methyl group

should be weaker compared to that of the methoxy group.

The experiment set up to confirm our hypothesis consisted of adding in the same reaction mixture both *organolithium* derivatives to the already prepared intermediate *B,B',B''*-trichloro-*N,N',N''*-triphenyl-borazine **1-3** at 0 °C, and monitoring which borazine species was favourably formed. In addition of the respective isomers, four different borazine species may be obtained by the combination of the two *organolithium* derivatives, as shown in Scheme 2.16.



**Scheme 2.16** - Synthetic strategy followed for the nucleophilicity test.

Following reaction, the borazine mixture was purified by precipitation with MeOH. Unfortunately, due to the poor separation observed by TLC, as well as the low solubility of the borazine containing methoxy groups, the different borazine products could not be isolated. However, as shown in Figure 2.40, <sup>1</sup>H-NMR allowed identifying the percentage of each substituent in the final mixture, thanks to the different chemical shifts of the respective functional groups (around 3.5 ppm for methoxy moieties and around 2 ppm for methyl ones). Therefore, the final mixture was calculated to contain 74% of methoxy moieties (3.51-3.38 ppm, highlighted in magenta) and 26% of methyl moieties (2.21-2.14 ppm, highlighted in blue). Our hypothesis was thus confirmed as the experiment showed that under the same conditions, *organolithium* derivatives containing –OMe are more reactive toward molecule **1-3** than those with –Me groups.

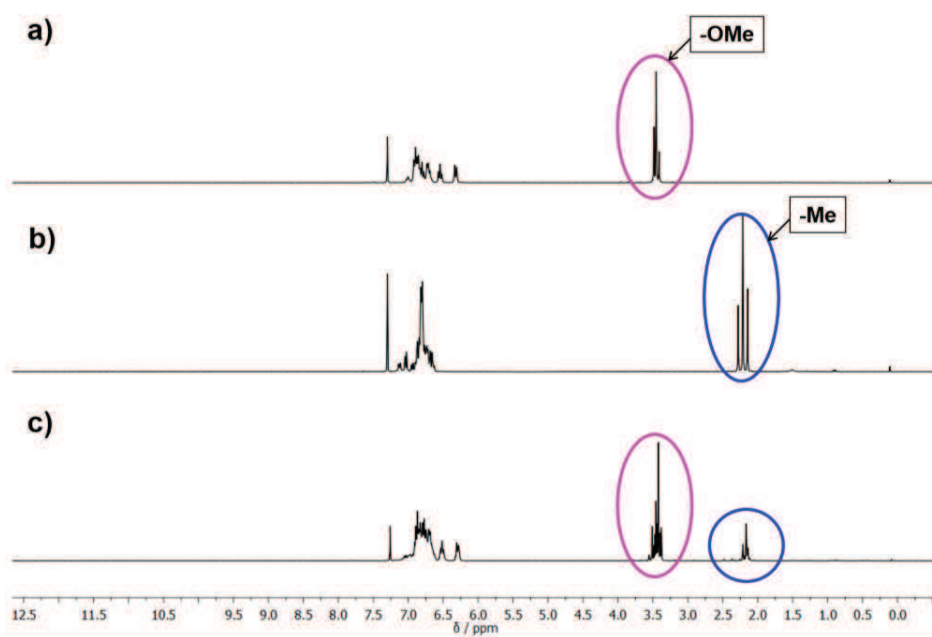
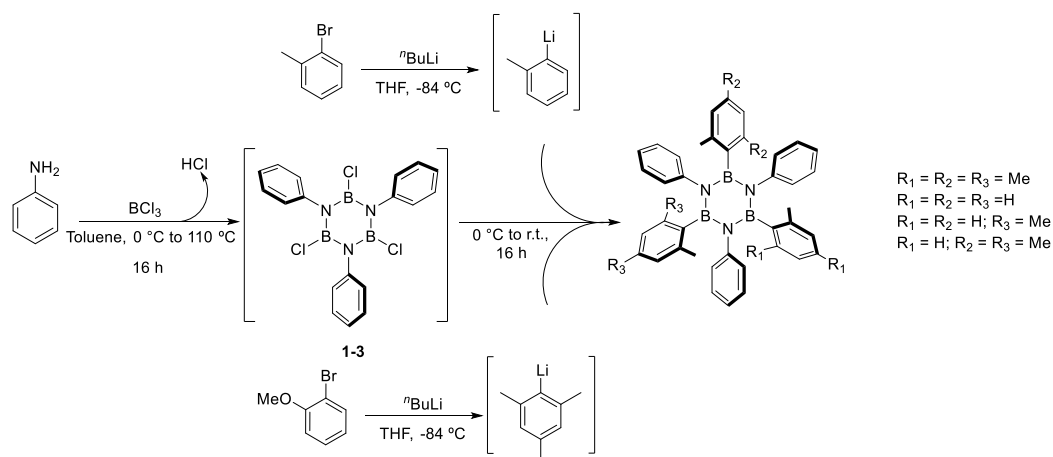


**Figure 2.40** - 300 MHz  $^1\text{H}$ -NMR in  $\text{CDCl}_3$  (solvent residual peak: 7.26 ppm) of (a) borazine **2-30**, (b) borazine **2-27**, and (c) the mixture obtained during the nucleophilicity test reaction.

### 2.3.5.b Comparative Study of the Process in Terms of the Steric Hindrance of the *ArLi* Reagent

The second investigation aimed at the evaluation of the effect of the steric hindrance of the *ArLi* species used for the formation of the borazine. To this end, 2-bromotoluene and 2-bromomesitylene were used as precursors for the halogen-lithium exchange. Both reagents contain methyl groups in *ortho*-position; the first one only contains one methyl, while the second contains methyl groups in the *ortho*-positions and is thereby more hindered (Scheme 2.17).



**Scheme 2.17** - Synthetic strategy followed for the steric hindrance test.

After purification by precipitation with MeOH, due to a lack of polarity difference between the formed products, separation of the resulting borazine derivatives was not successful. Therefore, and as previously achieved during the nucleophilicity test, the composition of the final mixture was determined by  $^1\text{H}$ -NMR studies. The mono-methyl specie was shown to be present in a 94% ratio of the final mixture, while the bis-methyl was only constituting 6% of the crude, confirming the fundamental role of the steric hindrance of the nucleophile during the addition reaction. Note that the calculation was performed thanks to the different chemical shifts of the mesityl moieties in the aromatic region (6.34-6.31 ppm) and its relation with the peaks of the methyl protons (2.36-1.98 ppm) (Figure 2.41).

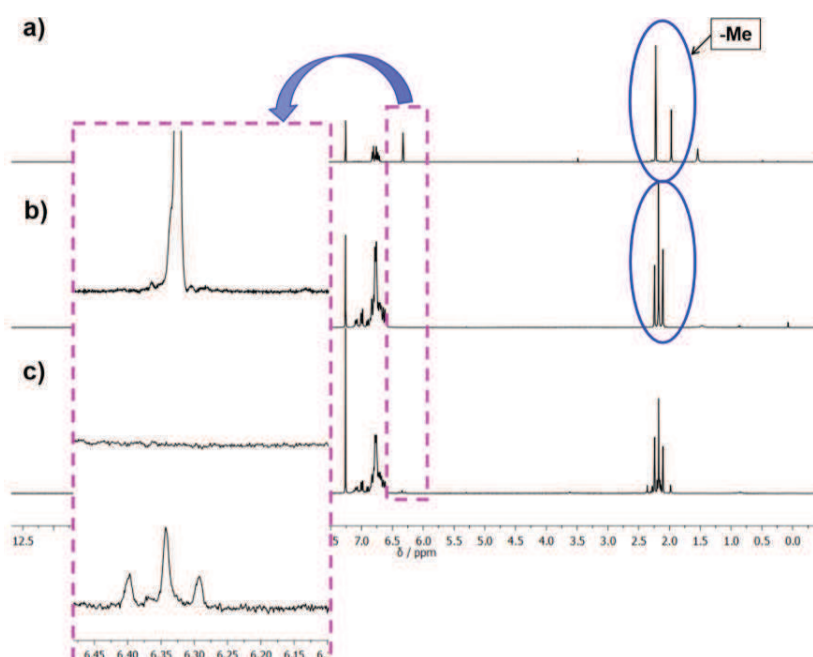


**Figure 2.41** - 300 MHz  $^1\text{H}$ -NMR in  $\text{CDCl}_3$  (solvent residual peak: 7.26 ppm) of (a) borazine **2-4**, (b) borazine **2-27**, and (c) the mixture obtained during the steric hindrance test reaction. Inset: zoom at 6.35 ppm.

## 2.3.6 Mono-Protected Borazine Derivatives: Stability and Chemical Tools for the Formation of an ‘Outer Shell’

### 2.3.6.a Stability of the Borazine Core

As previously mentioned, unprotected borazine derivatives are highly sensitive to moisture. However, when mono *ortho*-protected, although the steric protection around the boron centres is reduced when compared to fully-protected cores, stability of the borazines is already improved. As presented in the previous Subsections, all the mono-protected borazine derivatives were stable toward moisture and aqueous workups were performed without observing degradation, at least

during short times. The stability of these molecules could be explained following the same model previously used for the addition/elimination reactions. More specifically, once that mono-protected borazine is formed, one could expect the decomposition of the BN-ring by addition of nucleophiles (such as  $\text{H}_2\text{O}$ ) to the boron sites from the opposite side to the substituent. This addition would involve the formation of an 'ate complex' in which the *B*-aryl moiety is stands along the *xy*-plane with the substituent on the top of the borazine cycle; which entails a huge steric hindrance between them. This prevents or at least decreases the decomposition of the system (Figure 2.42). For this reason, the larger the steric effect of the substituents is, the higher is the stability of the BN-core.

Borazine derivatives sterically protected with acetylene TIPS, acetylene TMS, triazene, or methyl do not decompose along the time, and they can be stored for long times under nitrogen at low temperatures or at room temperatures for shorter times (one month). However, stability decreases when using fluorine or methoxy groups (lower A-values), and partial decomposition is observed after one week stored under nitrogen at room temperature. Also in solution, degradation is observed after one week.

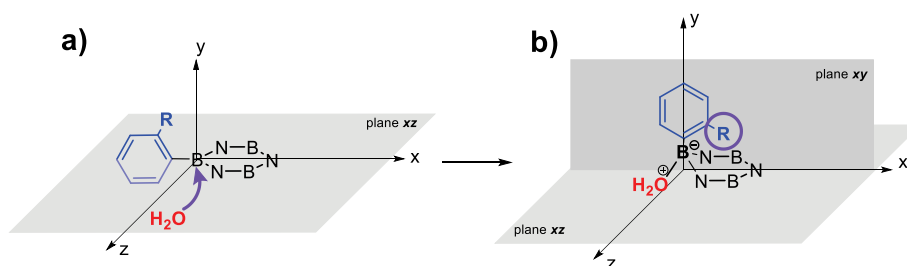


**Figure 2.42** - Decomposition of mono-protected borazine derivatives by addition of  $\text{H}_2\text{O}$ , which acts as a nucleophile. Only substituents in one boron atom are shown, the others are not represented for the sake of clarity.

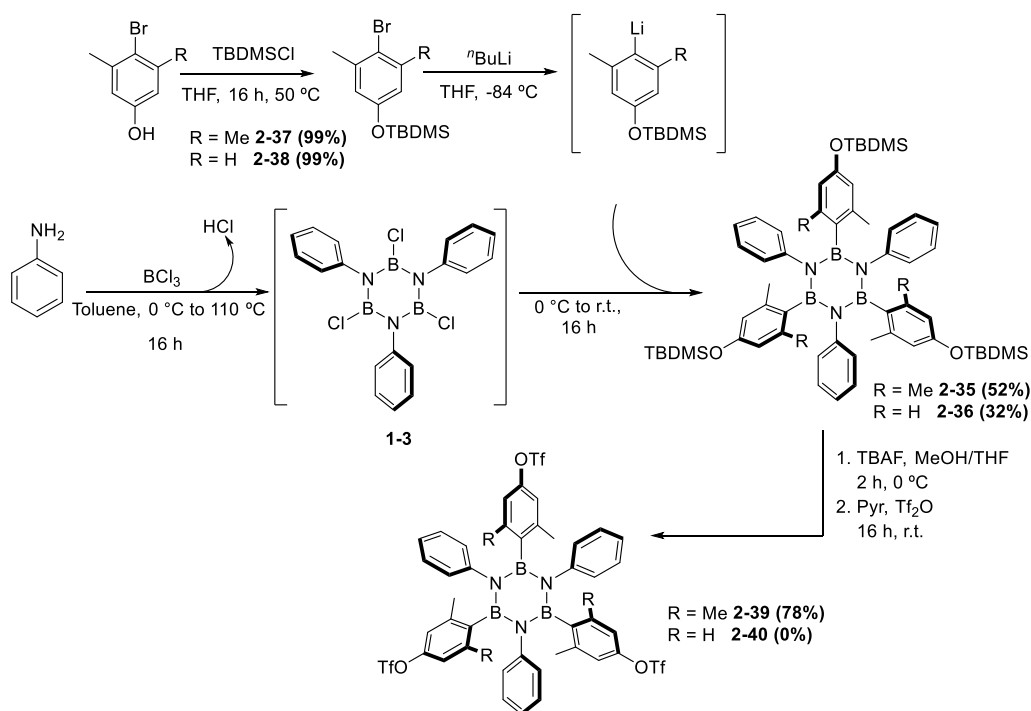
### 2.3.6.b Chemical Tools for the Formation of the 'Outer Shell'

In this Subsection, different tested reaction conditions are presented, such as to give an overall view of the main properties of these novel class of mono-protected borazines (Table 2.5). As previously described in Chapter 1 for bis-protected borazine derivatives, the levels of reactivity are reported as 'S' for stable, 'SD' for slow degradation (reaction times  $\geq 8$  h) and 'D' for complete degradation or decomposition. The conditions which had already been tested on bis-protected borazine derivatives and which showed complete degradation of the borazine core were not used for this study, considering the even lower stability of partially-protected borazines compared to the bis-protected species. Note that nucleophiles, reductants and strong bases can attack the boron atoms, while electrophiles, oxidants and strong acids can attack the nitrogen atoms. The other factor to take in consideration is the thermal stability of the BN-cycle.

Table 2.5 – Experimental conditions tested on mono *ortho*-protected borazine derivatives.

Reagents	Reactivity
<b>Organometallics</b>	RLi S
	RMgX S
	Pd-catalysed reactions SD (Me)
	S (iPr)
<b>Oxidants</b>	FeCl <sub>3</sub> , MeNO <sub>2</sub> , 90 °C SD (OMe, Me)
	FeCl <sub>3</sub> , MeNO <sub>2</sub> , TFA, r.t. SD (OMe, Me)
<b>Bases</b>	TBAF, THF, r.t. S (acetylene)
	NaOH aq, MeOH, THF, r.t. S (Me, iPr)
	K <sub>2</sub> CO <sub>3</sub> , THF, MeOH, r.t. S (acetylene)
<b>Electrophiles</b>	Tf <sub>2</sub> O, pyridine, r.t. D (Me)
	BF <sub>3</sub> ·OEt <sub>2</sub> D (triazene)
<b>Pericyclic reactions</b>	CPD, Ph <sub>2</sub> O, 180 °C S (acetylene, OMe)

Palladium-catalysed reactions, in particular, Suzuki-Miyaura cross-coupling reaction has been reported to lead to successful formations of the ‘outer shell’ of fully-protected borazine derivatives. However, in the case of partially-protected borazine moieties, a certain decomposition of the borazine ring was observed upon prolonged reaction times ( $\geq 8$  h). Similar observation was made with mild oxidizing agents. Indeed, on the contrary of fully-protected species, partially-protected borazine derivatives slowly decomposed in the presence of mild oxidizing agents, such as iron trichloride. On the other hand, the use of bases for the deprotection of acetylene moieties in the *ortho*-position of *B*-aryl rings has shown to be an efficient method to modify the ‘inner shell’ in which the borazine core remains stable. Besides, borazine derivatives decorated with –OTBDMS groups (*tert*-butyl-dimethylsilyl ether) at the *para*-position of the *B*-aryl rings can easily be synthesised (borazines **2-35** and **2-36**) using the corresponding mono- or bis- *ortho*-substituted *ArLi* derivative (molecules **2-37** and **2-38**), as shown in Scheme **2.18**.



**Scheme 2.18** - Synthesis of molecules **2-35** and **2-36**. Further transformation of **2-35** into **2-39**.

Crystal structure of borazine derivatives, **2-35** and **2-36** were obtained. Molecule **2-35** was obtained by slow diffusion of MeOH in CH<sub>2</sub>Cl<sub>2</sub> (Figure 2.42), while borazine **2-36** (isomer *ct*) was obtained by slow diffusion of MeOH in CHCl<sub>3</sub> (Figure 2.43).

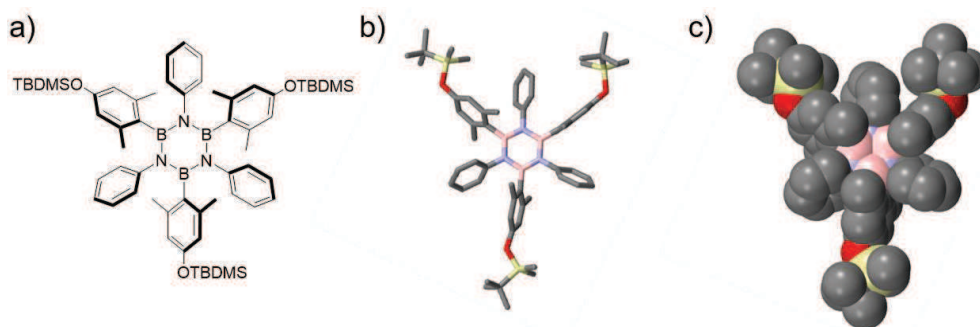


**Figure 2.42** - Crystal structure of borazine derivative **2-35**; (a) molecular structure; (b) crystal structure represented in *capped sticks*; (c) crystal structure represented in *spacefill*. Space group: P21-c. The crystal was grown by slow diffusion of MeOH in CH<sub>2</sub>Cl<sub>2</sub>. Colour code: grey: C, pink: B, blue: N, yellow: Si, and red: O. Hydrogen were omitted for the sake of clarity.

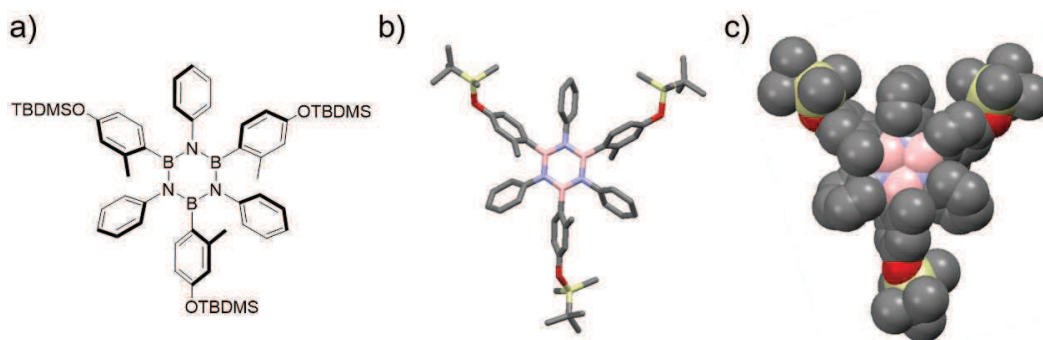


**Figure 2.43** - Crystal structure of borazine derivative **2-36**; (a) molecular structure; (b) crystal structure represented in *capped sticks*; (c) crystal structure represented in *spacefill*. Space group: P21-c. The crystal was grown by slow diffusion of MeOH in  $\text{CHCl}_3$ . Colour code: grey: C, pink: B, blue: N, yellow: Si, and red: O. Hydrogen were omitted for the sake of clarity.

Transformation of **2-35** into a suitable electrophilic partner, with an excellent leaving group (trifluoromethanesulfonate group, -OTf) was successfully undertaken leading to fully-protected borazine derivative **2-39**. However, when applying the same reaction conditions to partially-protected borazine **2-36**, total degradation of the borazine core was observed. The reaction entails a deprotection reaction with TBAF, to form the corresponding hydroxy-derivative. Subsequent esterification with  $\text{TF}_2\text{O}$  in pyridine would end up with the formation of the tri-triflate derivative (Scheme 2.18, molecules **2-39** and **2-40**). Presumably, during the second step, the presence of a nucleophile like the pyridine can attack the boron atom of the partially-protected borazines. This addition involves the ring-opening of the borazine core. The degradation of the core produces the liberation of aniline, which can after react with  $\text{TF}_2\text{O}$ , to form the amino-derivative **2-41**. Suitable crystals for X-ray diffraction analysis of derivative **2-41** were obtained by slow diffusion of EtOH in  $\text{CH}_2\text{Cl}_2$  (Figure 2.43).

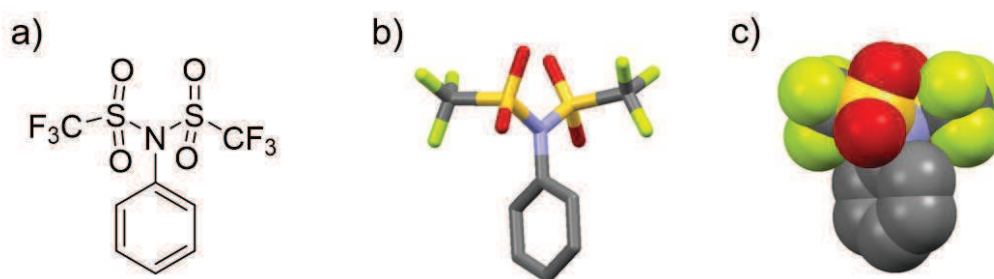
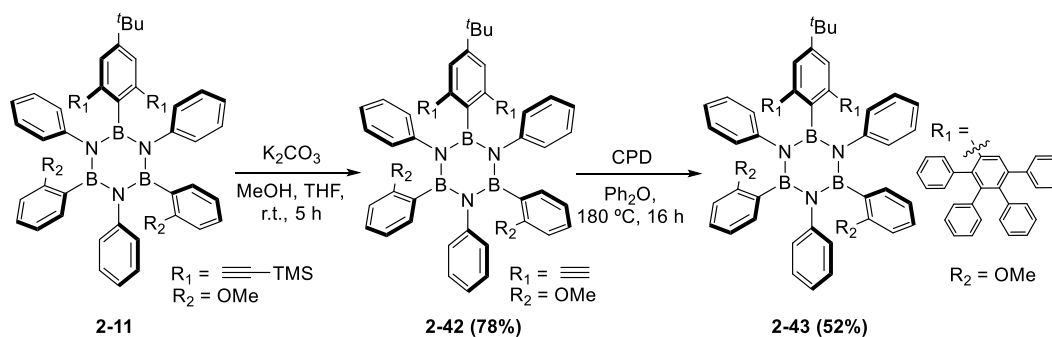


**Figure 2.43** - Crystal structure of borazine derivative **2-41**; (a) molecular structure; (b) crystal structure represented in *capped sticks*; (c) crystal structure represented in *spacefill*. Space group: P21/n. The crystal was grown by slow diffusion of methanol in acetone. Colour code: grey: C, blue: N, red: O, yellow: S and green: F. Hydrogen were omitted for the sake of clarity.

## 2.3.6.c Toward extended BNC-hybrids

Finally, cycloaddition reactions were evaluated. As the reaction was proven successful in previous studies in our labs and has already been described in literature (see Chapter 1), particular focus was given to the [4+2] cycloaddition reaction for the functionalisation at the *ortho*-position of *B*-aryl rings. Namely, the triple bond which acts as steric protection, also plays the role of dienophile for the [4+2] cycloaddition reaction. For example in borazine **2-11**, cleavage of the TMS group with  $K_2CO_3$  yields borazine **2-42** (78%). This *bis*-acetylene dienophile was then submitted to [4+2] cycloaddition reaction with tetraphenylcyclopenta-2,4-dienone (CPD) in  $Ph_2O$  at 180 °C for 16 h, yielding borazine derivative **2-43** (52%) as a white solid (Scheme 2.19).



**Scheme 2.19** - Synthetic methodology for the synthesis of molecule **2-43**, through decarbonylative [4+2] Diels-Alder cycloaddition reaction.

The molecular structure of this cycloadduct was unambiguously identified by NMR spectroscopy and mass spectrometry through the detection of the peak corresponding to the molecular ion  $[M+H]^+$ , as well as those corresponding to  $[M+Na]^+$  and  $[M+K]^+$ . HRMS-ES mass spectrogram for molecule **2-43** ( $C_{102}H_{83}B_3N_3O_2^+$ , calc.: 1414.6803, found: 1414.6837) is displayed in Figure 2.44.

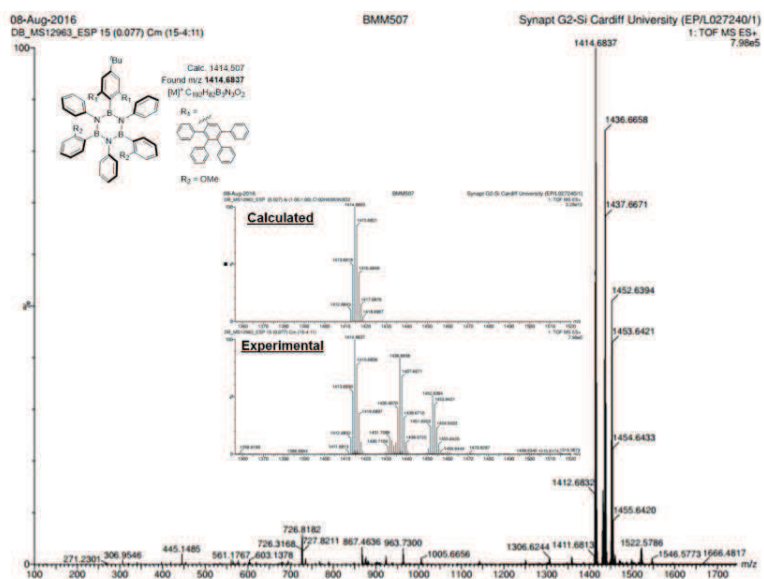


**Figure 2.44-** HRMS-ES mass analysis of **2-43**. Insets: zoomed calculated (above) and experimental (below) spectra.

Last but not least, the cycloaddition reaction was studied with three free acetylene groups around the borazine core (borazine derivative **2-44**, obtained after deprotection of the TMS group using potassium carbonate). As a result of the high steric hindrance of the final product, not only the desired derivative was successfully formed (achieved with three cycloaddition reactions), but the product which only underwent two cycloaddition reactions and still presented one acetylene free was also found (Scheme **2.20**). This has been confirmed by HRMS-ES (molecular **2-45**, obtained after three cycloadditions:  $[M+H]^+ C_{126}H_{91}B_3N_3$ , calc.: 1678.7537, found: 1678.7604; and molecular **2-46**, obtained after two cycloaddition reactions:  $[M+H]^+ C_{98}H_{71}B_3N_3$  calc.: 1322.57 found: 1322.5977). Separation by GC allows the purification of them (Figure **2.45**).

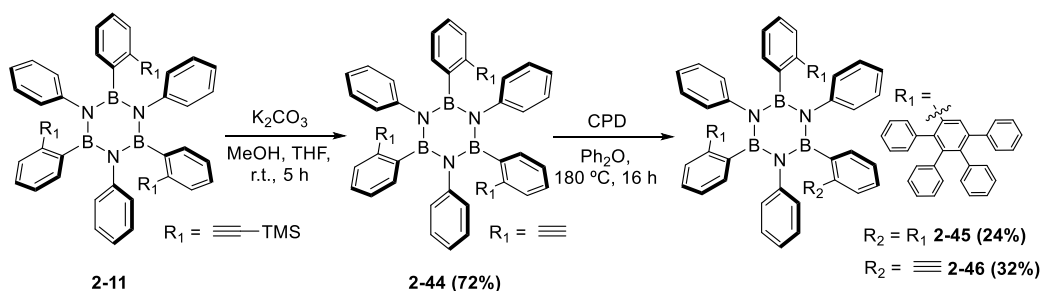


**Figure 2.20** - Synthetic methodology for the synthesis of molecule **4-13**, by through decarbonylative [4+2] Diels-Alder cycloaddition reaction.

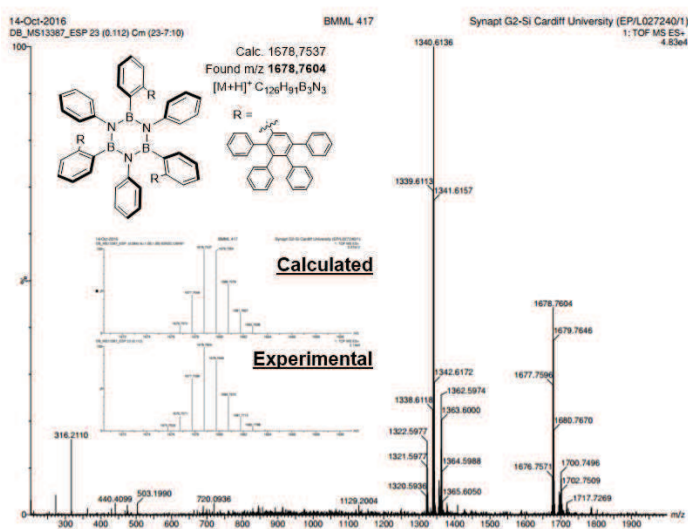


**Figure 2.45** - HRMS-ES mass analysis of both molecules **2-45** and **2-46**. Insets: zoomed calculated (above) and experimental (below) spectra.

## 2.4 Conclusions and Perspectives

The work presented in this Chapter corresponds to the study of the effect of the substituents during the addition/elimination reaction at the boron site of a BN-cycle for the synthesis of hexa-functionalised borazine derivatives. This investigation has been achieved thanks to the study of substituents which display diverse steric effects, that have been introduced in the *ortho*-position of the *B*-aryl groups of the BN-ring. These substituents allow us to stereoselectivity control the synthesis of these borazine derivatives. Moreover, it has been proof the stability of this novel class of borazine derivatives toward hydrolysis.

Firstly, the synthesis and characterisation of molecules bearing two short-range *ortho*-substituents in each *B*-aryl moiety have been presented, moving from unstable borazine **2-1** ( $R = H$ ) to stable molecules which bear fluorine, methoxy or methyl groups (A-values from 0.75 to 1.74 kcal/mol). Moreover, if substituents with larger steric effects are used (*i.e.*  $tPr$ , or  $tBu$ , A-value = 2.21 and 4.7-4.9 kcal/mol, respectively), the desired borazine derivatives could not be produced. The same protocol has been applied for the study of bis protected-borazine derivatives, using long-range substituents (*i.e.* acetylene TMS, A-value acetylene = 0.41-0.52, A-value TMS = 2.5 kcal/mol). However, only one equivalent of the nucleophile that contains that group is accessible for the attack to one boron site of the BN-core, and the formation of the final borazine is achieved by addition of *ArLi* derivatives with lower steric effect (Figure 2.46).

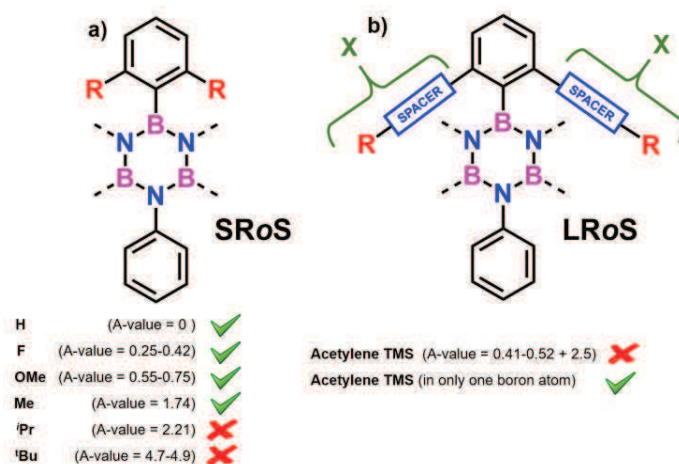


**Figure 2.46** – Summarised results for the synthesis of bis protected-borazine derivatives.

Secondly, a novel class of borazine derivatives has herein been introduced, in which the boron atoms are just partially protected. This partial protection has been exploited using multiple experimental instances from long-range substituents (acetylene TIPS, acetylene TMS and a triazene derivative) to short-range ones (Me,  $CF_3$  and  $NMe_2$ , or OMe and F). The design, synthesis and

characterisation of those molecules have been accomplished. This family has shown to be stable against moisture in most of the cases. In addition, a complete study for the isomerisation process of molecule **2-15** has been developed (Figure 2.47).

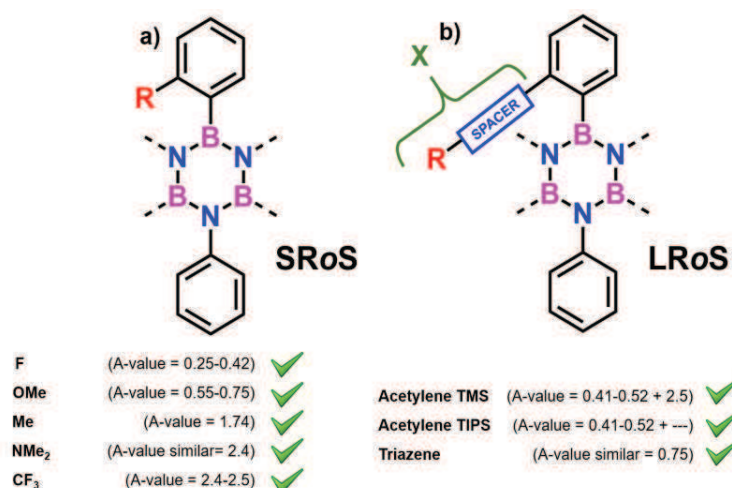


**Figure 2.47** – Summarised results for the synthesis of mono protected-borazine derivatives.

During the investigation with mono-protected borazine derivatives, a novel sub-class of bis protected borazine has been designed, in which the *B*-aryl moieties contain short- and long-range substituents. With this methodology, just two boron sites can be accessible to those groups, and the third one is just accessible for smaller groups (such as H<sub>2</sub>O or *PhLi*). In addition, the insertion of short-range groups in the *N*-aryl moieties has been presented, but this family of borazines will be fully discussed in *Chapter 3*.

Moreover, the substituent's effect on the stereoselectivity of the process has been fully explained in Subsection 4, in which the addition/elimination steps are presented. Firstly, it was possible to demonstrate the statistical distribution of the isomers *cc:ct*, which corresponds to 4:12 (1:3) when three equivalents of *ArLi* derivatives react with the borazine core. After, and depending on the nature of the *ortho*-substituent, some of the possible routes could be cancelled out, leading to the different ratios experimentally obtained.

In the last Subsections, the reactivity of the borazine core against different nucleophiles as well as the stability and chemical reactivity on mono-protected borazine derivatives is fully discussed.

## 2.5 References

- [1] R. T. Boéré, “1. The Group 13 Elements,” **n.d.**
- [2] S. J. Groszos, S. F. Stafiej, *J. Am. Chem. Soc.* **1958**, *80*, 1357.
- [3] A. Wakamiya, T. Ide, S. Yamaguchi, *J. Am. Chem. Soc.* **2005**, *127*, 14859.
- [4] S. Kervyn, N. Kalashnyk, M. Riello, B. Moreton, J. Tasseroul, J. Wouters, T. S. Jones, A. De Vita, G. Costantini, D. Bonifazi, *Angew. Chem. Int. Ed.* **2013**, *52*, 7410.
- [5] K. T. Jackson, T. E. Reich, H. M. El-Kaderi, *Chem. Commun.* **2012**, *48*, 8823.
- [6] Simon Kervyn, *Synthesis, Physical Properties and Supramolecular Organization of Boron-Doped Supramolecular Materials*, **2013**.
- [7] S. Kervyn, O. Fenwick, F. Di Stasio, Y. S. Shin, J. Wouters, G. Accorsi, S. Osella, D. Beljonne, F. Cacialli, D. Bonifazi, *Chem. - A Eur. J.* **2013**, *19*, 7771.
- [8] B. Neuwald, L. Caporaso, L. Cavallo, S. Mecking, *J. Am. Chem. Soc.* **2013**, *135*, 1026.
- [9] W. Uhl, J. Bohnemann, B. Kappelt, K. Malessa, M. Rohling, J. Tannert, M. Layh, A. Hepp, *Zeitschrift für Naturforsch. B* **2014**, *69*, 1333.
- [10] H. Watanabe, T. Totani, T. Yoshizaki, *Inorg. Chem.* **1965**, *4*, 657.
- [11] M. Khan, A. Akther, M. Alam, *Synlett* **2014**, *25*, 831.
- [12] Y. Hirano, S. Kojima, Y. Yamamoto, *J. Org. Chem.* **2011**, *76*, 2123.
- [13] S. H. Chanteau, J. M. Tour, *J. Org. Chem.* **2003**, *68*, 8750.
- [14] T. Dumsla, B. Yang, A. Maghsoumi, G. Velpula, C. Castiglioni, S. De Feyter, M. Tommasini, A. Narita, X. Feng, K. Mullen, *J. Am. Chem. Soc.* **2016**, *138*, 4726.
- [15] P. N. W. Baxter, R. Dali-Youcef, *J. Org. Chem.* **2005**, *70*, 4935.
- [16] W. M. W. Margaret L. Gross, David H. Blank, *J. Org. Chem.* **1993**, *58*, 2104.
- [17] A. S. K. Hashmi, J. Hofmann, S. Shi, A. Schütz, M. Rudolph, C. Lothschütz, M. Wietek, M. Bührle, *Chem. - A Eur. J.* **2013**, *19*, 382.
- [18] H. Kinoshita, N. Hirai, K. Miura, *J. Org. Chem.* **2014**, *79*, 8171.
- [19] J. K. Jan Storch, Jan Cermak, *Tetrahedron Lett.* **2007**, *48*, 6814.
- [20] P. P. Deshpande, B. A. Ellsworth, F. G. Buono, A. Pullockaran, J. Singh, T. P. Kissick, M.-H. Huang, H. Lobinger, T. Denzel, R. H. Mueller, *J. Org. Chem.* **2007**, *72*, 9746.

- [21] S.-I. Murahashi, *Org. Synth.* **1984**, 62, 39.
- [22] D. C. Babbini, V. M. Iluc, *Organometallics* **2015**, 34, 3141.
- [23] R. W., Hoffmann, *Dehydrobenzene and Cycloalkanes* **1967**.
- [24] J. A. Newby, D. W. Blaylock, P. M. Witt, R. M. Turner, P. L. Heider, B. H. Harji, D. L. Browne, S. V Ley, *Org. Process Res. Dev.* **2014**, 18, 1221.

## CHAPTER 3

# Scanning the Effect of *ortho*-Substituted *N*-aryl rings on the Formation of the Borazine Ring

This Chapter addresses the study of the first step of the reaction toward the formation of stable borazine derivatives, that is to say, the formation of the BN-core, by using different amino precursor sources. *Chapter 3* is divided into four main sections: *i*) *Section 3.1* includes a journey along the literature already reported for the reaction with those amino species; *ii*) *Section 3.2* introduces the research project; *iii*) *Section 3.3* deals with the discussion of the results obtained during this investigation, emphasising the study of the stereoselectivity of the reaction when possible; and finally *iv*) *Section 3.4* summarises the main conclusion that can be extracted from this work.

More specifically, *Section 3.3* describes the study of the reaction between different mono or bis short-range and mono long-range *ortho*-substituted anilines and boron trichloride. During the addition/elimination step, different *ortho*-substituted *ArLi* reagents have been tested, including short- and long-range groups.

This work has been fully performed at the *University of Cardiff, Cardiff, United Kingdom*.

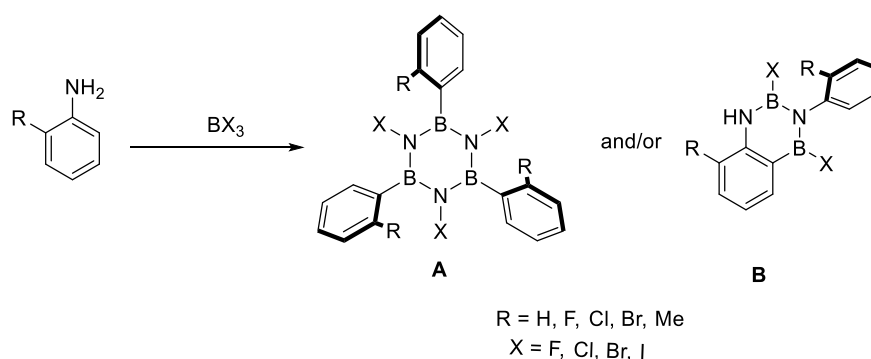
The X-Ray analysis presented in this Chapter were performed by *Nicolas Biot* and *Davide Marinelli*. Furthermore, *Nicolas* and *Francesco Fasano* are kindly acknowledged for the fruitful discussions and collaboration.

## 3.1 Introduction

### 3.1.1 Mono-*ortho*-substituted Aniline Moieties

The reaction of primary aromatic amines containing substituents in one out of the two *ortho*-positions of the ring (*i.e.* R = H, F, Cl, Br, or Me) with boron trihalides (X = F, Cl, Br and I) has been well investigated by the group of Prof. Frange.<sup>[1]</sup> Those reactions lead to the formation of not only the expected borazine ring (molecule type **A**), but also the formation of a new six-membered heterocycle (molecule type **B**), which is composed by two boron atoms, two nitrogen atoms and two carbon atoms (Scheme 3.1).

The formation of heterocycle **A** or heterocycle **B** depends, firstly, on the boron trihalide chosen for the reaction. With boron trifluoride, BF<sub>3</sub>, formation of borazine **A** is observed, whereas boron triiodide, BI<sub>3</sub>, favours the evolution towards heterocycle **B**. The obtained results can be explained taking in consideration the hardness of the halogen in the boron trihalide moieties. The hardness of the halide favours the formation of the borazine core, while the softness favours the formation of heterocycle **B**. Boron trifluoride, BF<sub>3</sub>, is a hard Lewis acid that favours the formation of boron-nitrogen bonds, while boron triiodide, BI<sub>3</sub>, is a soft Lewis acid that favours the boron-carbon bond, driving to the formation of heterocycle **B**. Moreover, aniline is considered as an ambidextrous reagent, where the hard centre is placed in the nitrogen atom, and the soft centre is located in the *ortho*-carbon.



**Scheme 3.1** – Schematic representation for the formation of the two possible heterocycles; borazine derivatives **A** or heterocycles type **B**, that can be obtained from the reaction of *ortho*-substituted anilines and boron trihalides.<sup>[1]</sup>

In addition, a point worth noting is the effect of different substituents on the aniline ring on the reaction. For instance, with 2-methylaniline, 2-bromoaniline, 3-chloro-2-methylaniline or 4-chloro-2-methylaniline, borazine **A** is formed when using BF<sub>3</sub> or BCl<sub>3</sub>, while heterocycle **B** is obtained when the boron trihalides are BBr<sub>3</sub> or BI<sub>3</sub>. Namely, the presence of those substituents in

the aniline ring does not preclude the formation of borazine rings, and the formation of the final product (**A** or **B**) depends only on the boron trihalide used. However, there is an exception, when using 5-bromo-2-methylaniline, borazine **A** is obtained in all cases, regardless of the boron trihalide employed ( $X = \text{F, Cl, Br, or I}$ ). This is easily understandable for steric reasons, where the bulky substituent in the fifth position inhibits the cyclisation in position six of the aniline ring towards the formation of heterocycle **B** for steric reasons.

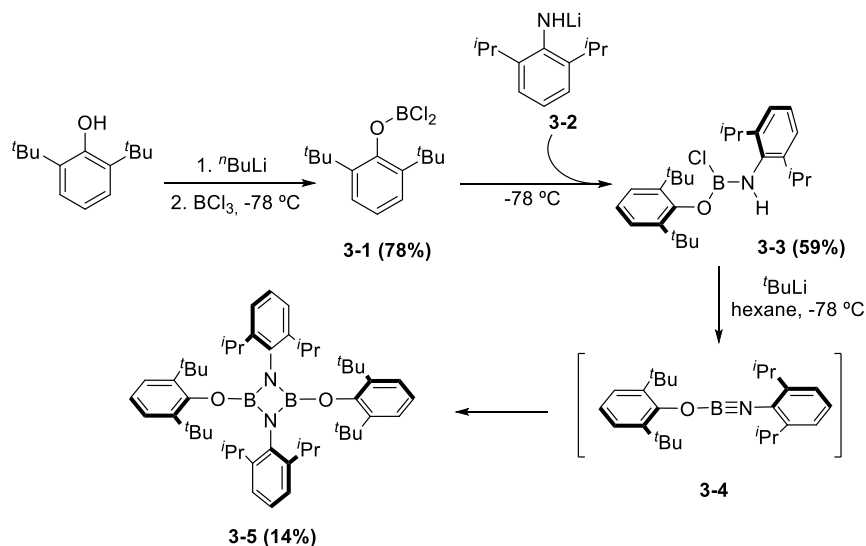
Once the conditions to get the borazine ring are clear (suitable boron trihalide, and *ortho*-substituted aniline,  $R = \text{H, Me}$ ), the next point to take in consideration is the stereoselectivity of the reaction.<sup>[2]</sup> The fact that aromatic rings in hexa-functionalised borazine moieties are placed almost perpendicular to the plane of the borazine ring is well supported; and along *Chapter II*, where different crystal structures have been presented, it has been fully confirmed. Moreover, the perpendicularity is also confirmed for *B,B',B''*-trichloro-*N,N',N''*-triphenyl-borazine **1-3**, thanks to the crystal structure (specific data: 77-87° for the angle between the phenyl substituents and the borazine cycle).<sup>[3]</sup> Therefore, as a clear consequence of such conformation for the substituents, if aniline contains any *ortho*-substituent, two isomers can be obtained (*cc* and *ct*, as discussed in the case of mono *ortho*-substituted *B*-aryl in *Chapter II*).

In 1985, the group of Prof. Frange reported preliminary studies of this family of compounds, using 2-methylaniline as amino precursor for the formation of the borazine ring, in which Cl, Br or Me groups were located at the boron place.<sup>[2]</sup> Unfortunately, the spectroscopy techniques were not sophisticated enough to clearly determine the ratio of isomers obtained and <sup>1</sup>H-NMR or <sup>13</sup>C-NMR did not yield useful information. Furthermore, those borazine derivatives were not stable towards hydrolysis, complicating once again the study.

### 3.1.2 Bis-*ortho*-substituted Aniline Moieties

With respect to the reaction between bis *ortho*-substituted aniline moieties and boron trichloride, not much information can be found in literature. In any case, the group of Meller has reported the synthesis of boron-nitrogen heterocycles containing 2,6-di-*tert*-butylaniline, 2,6-di-*iso*-propylaniline or 2,4,6-trimethylaniline.<sup>[4]</sup> In particular, a four membered ring is presented. The synthesis does not include the direct reaction between the aniline and BCl<sub>3</sub>, but it represents the best approach toward the synthesis of B-N heterocycles using as amino precursor a bis hindered aniline moiety. Firstly, hindered phenol reacted with boron trichloride to give the corresponding organyloxy(dihalo)borane **3-1**. Afterwards, compound **3-1** was coupled with lithiated amine **3-2**. This reaction led to amino(halo)(organyloxy)borane **3-3**, which was submitted to a dehydrohalogenation in the presence of <sup>t</sup>BuLi for the final step (Scheme **3.2**). The intermediate

obtained is iminoborane **3-4**. As it has been presented in *Chapter I*, iminoboranes can easily evolve to borazine derivatives or to four-membered heterocycles. In this case, no borazine is formed due to the steric requirements of the substituents in the vicinity of the B=N. Conversely, heterocycle **3-5** was obtained in moderate yield (14%) and was fully characterised, showing the characteristic peak at 25 ppm in the  $^{11}\text{B}$ -NMR analysis.



**Scheme 3.2** – Synthesis of molecule **3-5** via formation of hindered iminoborane **3-4**.<sup>[4]</sup>

### 3.2 Research Aim

In this third Chapter, the attention is focused on the study the effect of substituents during the formation of the borazine ring. For this purpose, the reaction has been realised using different *ortho*-substituted aniline moieties as amino precursors. These *N*-substituents can be located in just one *ortho*-position of the aniline, thus, two isomers can be obtained during the formation of the cycle (isomer *cc* or isomer *ct*), or in both *ortho*-positions of the *N*-aryl. Besides, the substituents can be directly attached to the *N*-ring (short-range *ortho*-substituents, SRoS) or through a spacer (long-range *ortho*-substituents, LRoS) (Figure 3.1).

During the first step of the reaction toward the formation of the borazine, the obtained intermediates, *B,B',B''*-tri(chloro)-*N,N,N''*-tri(aryl)borazines are not stable and decompose in the presence of moisture. For that reason, the second step (functionalisation at the boron site) has to be carried out to complete the formation of the stable products.

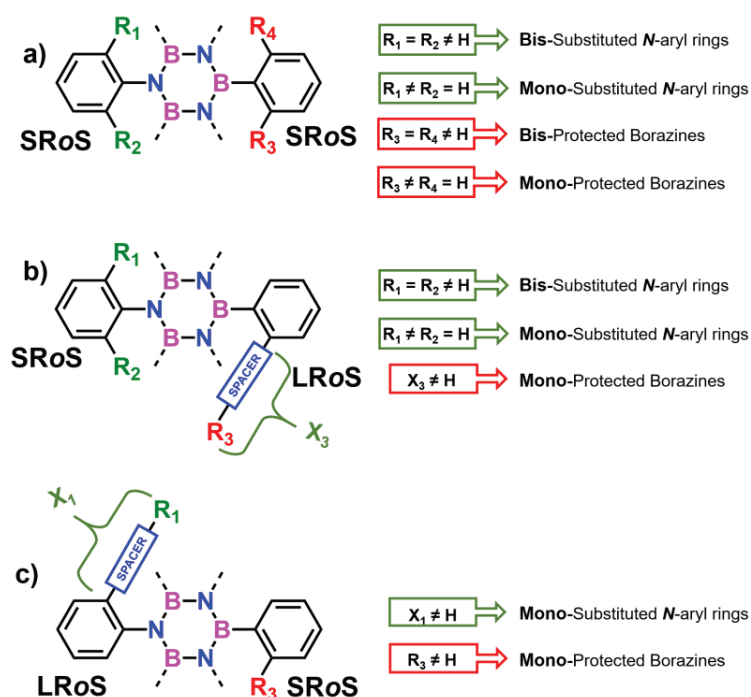


**Figure 3.1** – Schematic representation of the study developed for the construction of the borazine ring.

### 3.3 Results and Discussion

The discussion will be divided in three different parts; (i) initially, the work developed with non-substituted aniline precursors will be presented; then, (ii) the results obtained with mono-substituted aniline moieties are discussed; and finally (iii) bis-substituted aniline precursors are examined during the reaction toward the formation of the BN-core.

#### 3.3.1 Formation of the BN-core from Aniline as Amino Precursor

In order to understand the effect of the substituents in the *ortho*-position of the aniline, the process was firstly investigated with aniline. As already presented, by the reaction of aniline with boron trichloride for 16 h at 110 °C, *B,B',B''*-trichloro-*N,N',N''*-triphenyl-borazine **1-3** is formed. After cooling down the reaction mixture to room temperature, *B,B',B''*-trichloro-*N,N',N''*-triphenyl-borazine **1-3** can be easily separated from the reaction mixture by precipitation as a white crystalline solid. This unstable white solid was dried under reduced pressure. In addition to the already reported crystallography data,<sup>[3]</sup> it was possible to characterise this compound by NMR spectroscopy (<sup>1</sup>H, <sup>11</sup>B, <sup>13</sup>C-NMR) using anhydrous methylene chloride-*d*<sub>2</sub>. In particular, <sup>11</sup>B-NMR analysis shows the presence of only one peak at 31.57 ppm. The corresponding spectra are shown in Figure 3.3, as well as those obtained for the starting aniline for comparison (Figure 3.2).

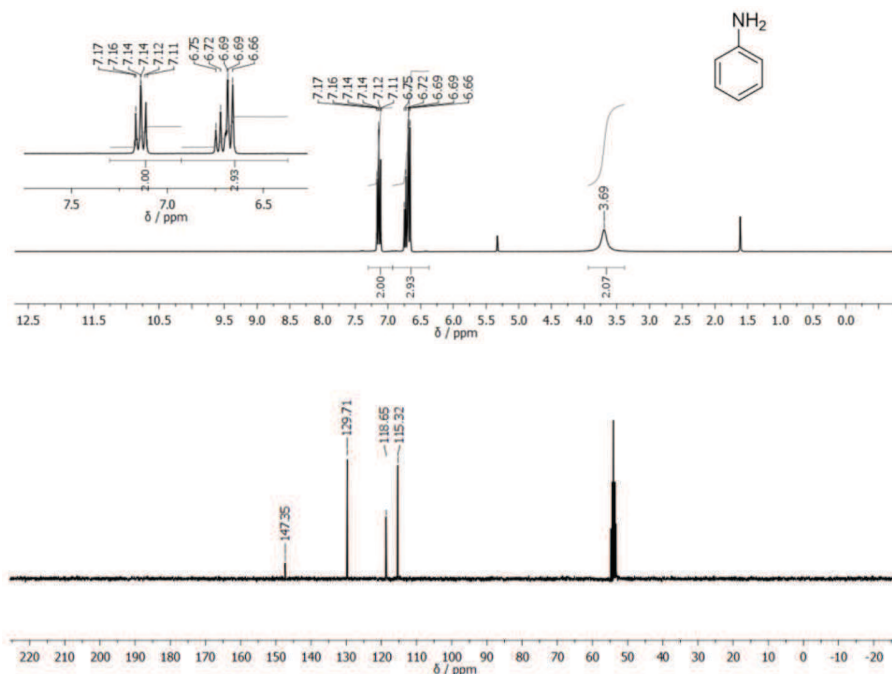


**Figure 3.2** – 300 MHz <sup>1</sup>H-NMR (top) and 75 MHz <sup>13</sup>C-NMR (bottom) in methylene chloride-*d*<sub>2</sub> (solvent residual peak <sup>1</sup>H-NMR: 5.32 ppm; water 1.52 ppm; <sup>13</sup>C-NMR: 53.84 ppm) of starting material aniline.

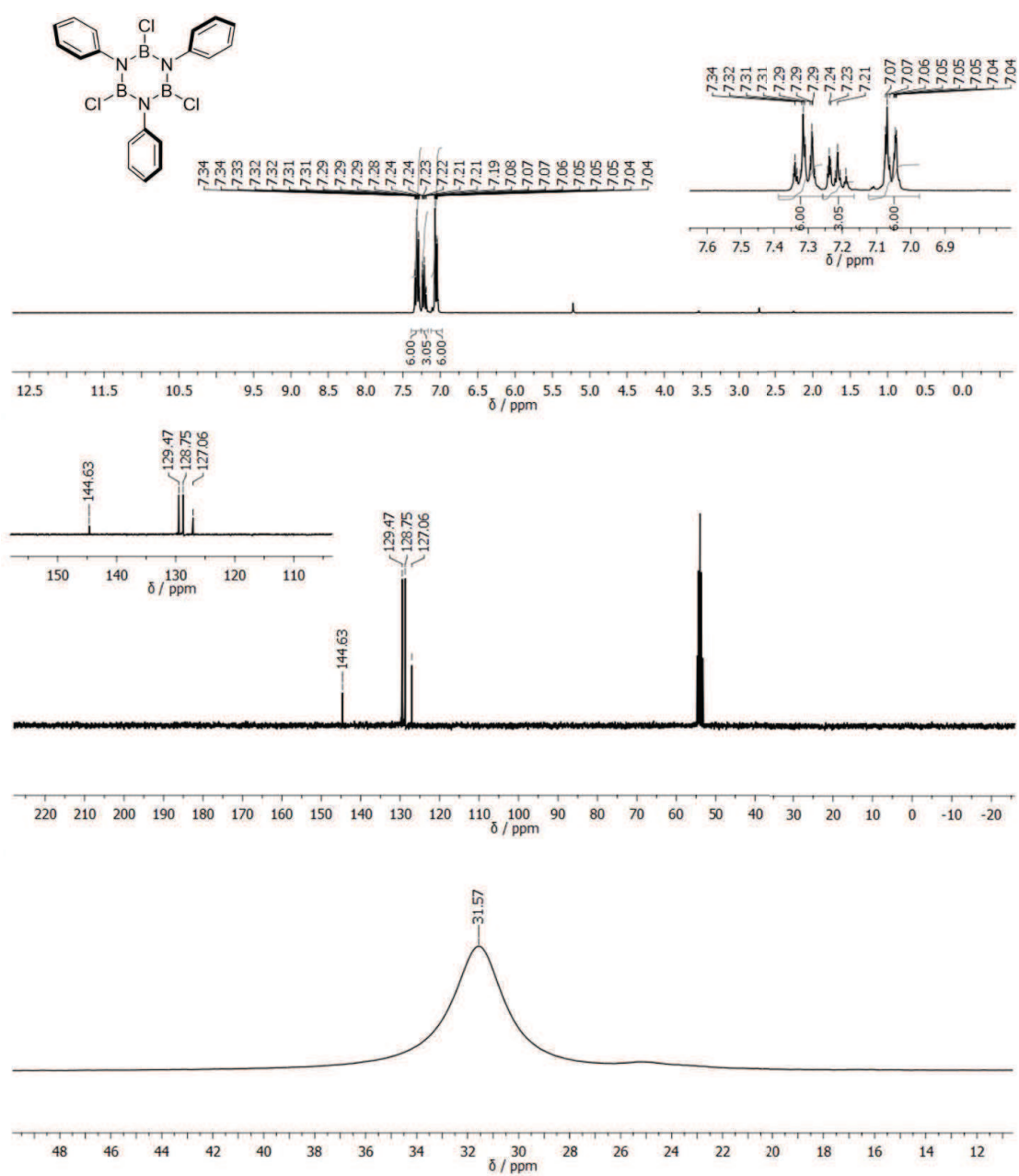


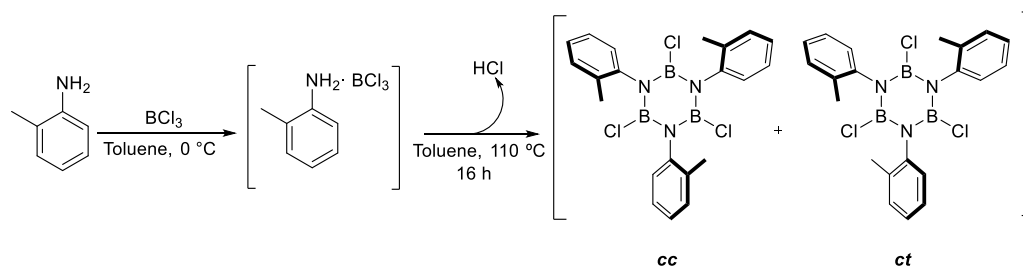
**Figure 3.3** – 300 MHz  $^1\text{H}$ -NMR (top), 75 MHz  $^{13}\text{C}$ -NMR (centre), and 128 MHz  $^{11}\text{B}$ -NMR (bottom) in methylene chloride- $d_2$  (solvent residual peak  $^1\text{H}$ -NMR: 5.32 ppm,  $^{13}\text{C}$ -NMR: 53.84 ppm) of *B,B',B''*-trichloro-*N,N,N'*-triphenylborazine **1-3**.

### 3.3.2 Formation of the BN-core from mono-substituted Anilines as Amino Precursor

Similarly to the protocol followed for the study of the formation of the initial borazine cycle with aniline, this subsection addresses the synthesis of borazine derivatives obtained from mono-substituted anilines. Those reactions could lead to the formation of different isomers, which will be address thereafter. Those *ortho*-substituents are of two types; (i) short-range substituents (*e.g.* Me); or (ii) long-range substituents (*e.g.* acetylene TIPS).

#### 3.3.2.a Formation of the BN-core from 2-methylaniline

The reaction toward the formation of the borazine core using 2-methylaniline (Me, A-value = 1.74 kcal/mol) as amino precursor, has been followed by NMR spectroscopy, in particular by  $^{11}\text{B}$ -NMR. The experiment set up to study the reaction consisted of adding anhydrous 2-methylaniline and dry toluene to a *Schlenk* flask under  $\text{N}_2$  atmosphere. The mixture was then cooled down to 0 °C, and  $\text{BCl}_3$  added to it (Scheme 3.3). At this step, one aliquot was taken, dried under vacuum and submitted to  $^{11}\text{B}$ -NMR analysis, revealing a peak at 6.86 ppm on the spectrum. The remaining reaction mixture was then heated up to 110 °C for 16 h (Scheme 3.3). Afterwards, and after cooling down the reaction mixture to room temperature under  $\text{N}_2$  atmosphere, a second aliquot was analysed after drying under vacuum.



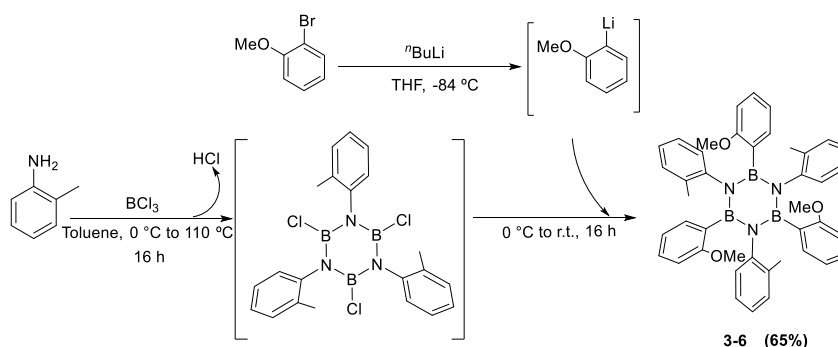
**Scheme 3.3** – Formation of the borazine core, using 2-methylaniline as amino precursor.

$^{11}\text{B}$ -NMR spectrum shows the presence of two peaks, one at 6.58 ppm, and a second one at 32.26 ppm. Complete  $^1\text{H}$ , and  $^{13}\text{C}$ -NMR investigations have been also performed, but due to the formation of not only two isomers, but also other by-products, no useful information could be extracted from them. The presence of the second peak appeared around 32 ppm after heating, in the same region of the one corresponding to the *B,B',B''*-trichloro-*N,N',N''*-triphenyl-borazine **1-3** (31.57 ppm in  $\text{CD}_2\text{Cl}_2$ ), can be initially attributed to the formation of *B,B',B''*-trichloro-*N,N',N''*-tri[2-(methyl)phenyl]-borazine. As already mentioned, this specie is not stable, and decomposes

under ambient conditions. For this reason, the study was completed by addition/elimination reaction at the boron sites. The chosen aryl moieties for the functionalisation of the borazine core at the boron site are presented in the next subsections.

### 3.3.2.a.1 Functionalisation with mono short-range *ortho*-substituted aryl species

The attention can be firstly focused in the investigation developed using a short-range *ortho*-substituted *ArLi* derived from 2-bromoanisole (*A*-value = 0.55-0.75 kcal/mol), in which borazine **3-6** was successfully obtained in 65% (Scheme 3.4).



Scheme 3.4 – Synthesis of molecule **3-6**.

The reaction was monitored by <sup>11</sup>B-NMR. In the <sup>11</sup>B-NMR spectra collection shown below (Figure 3.4), the different states of the reaction have been analysed in CDCl<sub>3</sub> at r.t. Primarily, the spectrum corresponding to BCl<sub>3</sub>, is reported as reference showing a peak at 46.58 ppm (41.9 ppm in literature)<sup>[5]</sup> (Figure 3.4, *a*). Spectra (*b*) and (*c*) correspond to the data collected during the first step of the reaction, before and after heating. A peak around 6.50 ppm is detected and can be attributed to the formation of the adduct between the BCl<sub>3</sub> and the aniline (BCl<sub>3</sub>·NH<sub>2</sub>Ar). Multiple examples of similar adducts are described in the literature, such as 10.2 ppm for BCl<sub>3</sub>·NMe<sub>3</sub> (CDCl<sub>3</sub>),<sup>[6]</sup> 10 ppm for BCl<sub>3</sub>·NEt<sub>3</sub>,<sup>[7]</sup> or 8 ppm for BCl<sub>3</sub>·Py.<sup>[7]</sup> As already mentioned, the peak around 32 ppm in spectrum (*c*), is attributed to the formation of the BN-core. Lastly, spectrum (*d*) corresponds to purified final *B,B',B''*-tri[2-(methoxy)phenyl]-*N,N',N''*-tri[2-(methyl)phenyl]-borazine **3-6**, obtained after the addition of the *ArLi* derivative to the reaction mixture, which shows a broad peak around 36 ppm. The formation of final borazine **3-6** was fully confirmed by <sup>1</sup>H, <sup>11</sup>B, <sup>13</sup>C-NMR spectroscopy, as well as by ESI-HRMS spectrometry. HRMS shows the detection of a peak at 670.3657 for [M+H]<sup>+</sup> (C<sub>42</sub>H<sub>43</sub>B<sub>3</sub>N<sub>3</sub>O<sub>3</sub> calc. 670.3604). As expected, molecule **3-6** is stable under ambient conditions, and aqueous workup could be applied without observing decomposition.

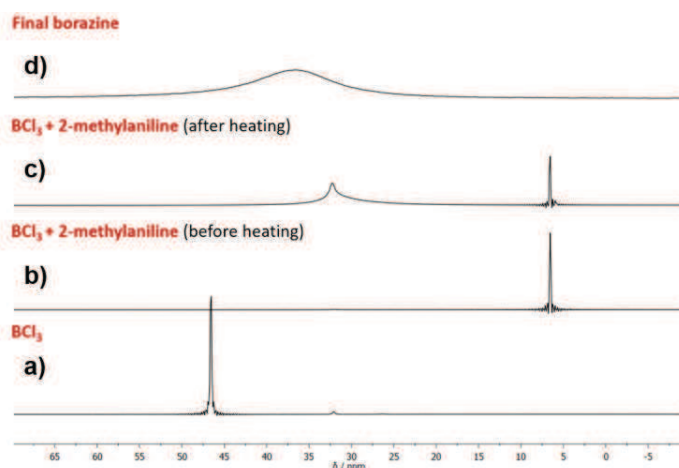
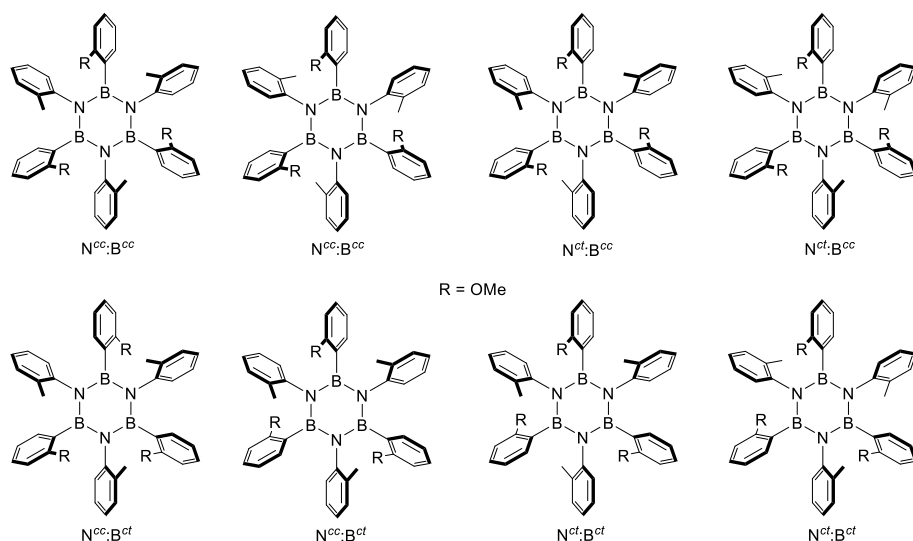


**Figure 3.4** – 128 MHz  $^{11}\text{B}$ -NMR spectra collection of the study developed with 2-methylaniline in  $\text{CDCl}_3$ ; (a)  $\text{BCl}_3$ ; (b) reaction mixture before and (c) after heating; (d) purified borazine  $B,B',B''$ -tri(2-(methoxy)phenyl) $N,N',N''$ -tri(2-(methyl)phenyl)borazine **3-6**.

Moreover,  $^1\text{H}$ -NMR analysis of molecule **3-6** in  $\text{CDCl}_3$  shows the presence of different isomers. In fact,  $^1\text{H}$ -NMR spectrum consists of two peculiar regions for the methoxy, around 3.5 ppm and for the methyl groups, around 2.2 ppm, which are both formed by a bunch of peaks (Figure 3.5). When using mono *ortho*-substituted aniline moieties, two different isomers can be theoretically obtained during the first step of the reaction (formation of the BN-ring), as it has been mentioned before. Furthermore, if the employed *ArLi* derivative is also a mono short-range *ortho*-substituted aryl moiety, the number of final isomers that could be obtained is not anymore two (*cc* or *ct*), but the result of the combination of the two mono species, thus, eight different isomers (Scheme 3.5).



**Scheme 3.5** – Possible isomers of molecule **3-6**.

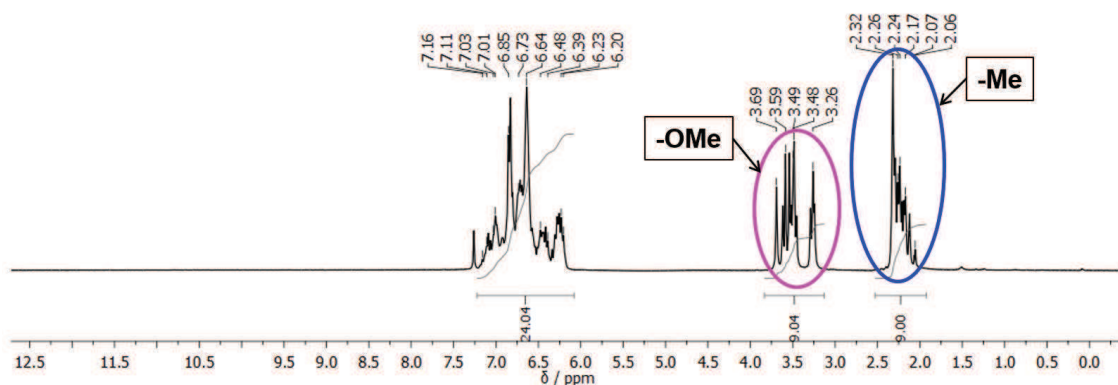


**Figure 3.5** – 300 MHz  $^1\text{H}$ -NMR of borazine **3-6** in  $\text{CDCl}_3$  (solvent residual peak  $^1\text{H}$ -NMR: 7.26 ppm).

Encouraged by the good results obtained with a mono short-range *ortho*-substituted aryl moiety (borazine derivative **3-6**, 65%), the synthetic versatility of the initial BN-cycle was further investigated, using different nucleophiles that can be added in order to get stable final borazine derivatives. Accordingly, a series of examples developed using different nucleophiles for the addition/elimination step is presented (bis short-range *ortho*-substituted *ArLi* derivatives, and mono long-range *ortho*-substituted ones).

### 3.3.2.a.2 Functionalisation with bis short-range *ortho*-substituted aryl species

The functionalisation at the boron sites of *B,B',B''*-trichloro-*N,N',N''*-tri[2-(methyl)phenyl]-borazine was developed using a bis short-range *ortho*-substituted *ArLi*, derived from 2,6-dimethoxybromobenzene (OMe A-value = 0.55-0.75 kcal/mol). Borazine **3-7** was successfully synthesised in 39% using the standard protocol (Scheme 3.6). The molecular identity of the compound was unambiguously confirmed by  $^1\text{H}$ ,  $^{13}\text{C}$  and  $^{11}\text{B}$ -NMR spectroscopy and HRMS spectrometry. In particular,  $^{11}\text{B}$ -NMR spectrum showed two distinct peaks at 37.33 and 24.92 ppm, attributed to two different substituted boron atoms (Figure 3.6). As discussed in Chapter 2, boron atoms linked to hydroxyl groups (-OH) show a peak around 25 ppm, while boron atoms of borazine cycles, bonded to an aryl moieties have a characteristic peak around 36 ppm, which confirms the formation of hydroxyl derivative **3-7**.

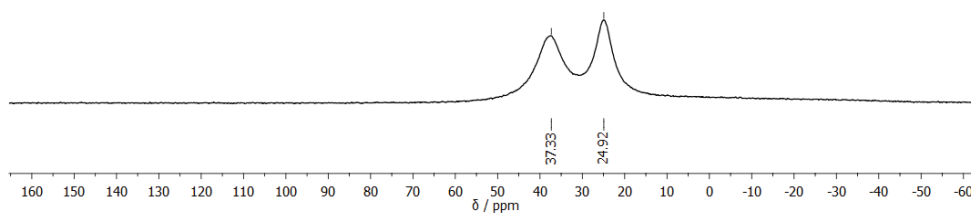
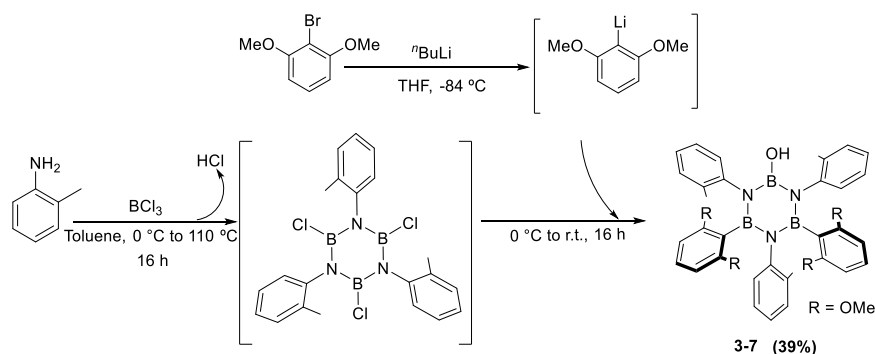


**Figure 3.6** – 128 MHz  $^{11}\text{B}$ -NMR of molecule **3-7** in  $\text{CDCl}_3$ .

In fact, only two equivalents of *ArLi* reacted with the *B,B',B''*-trichloro-*N,N',N''*-tri[2-(methyl)phenyl]-borazine. The third boron atom, presumably due to steric reasons, remained bonded to chlorine, which was subsequently replaced by hydroxyl group after addition of H<sub>2</sub>O, yielding molecule **3-7** (Scheme 3.6). No formation of fully substituted borazine at boron sites was detected.



Scheme 3.6 – Synthesis of molecule **3-7**.

Moreover, <sup>1</sup>H-NMR analysis (Figure 3.7) reveals that molecule **3-7** is composed by a mixture of the three possible isomers, one isomer *cc*, and two isomers *ct* (Scheme 3.7).

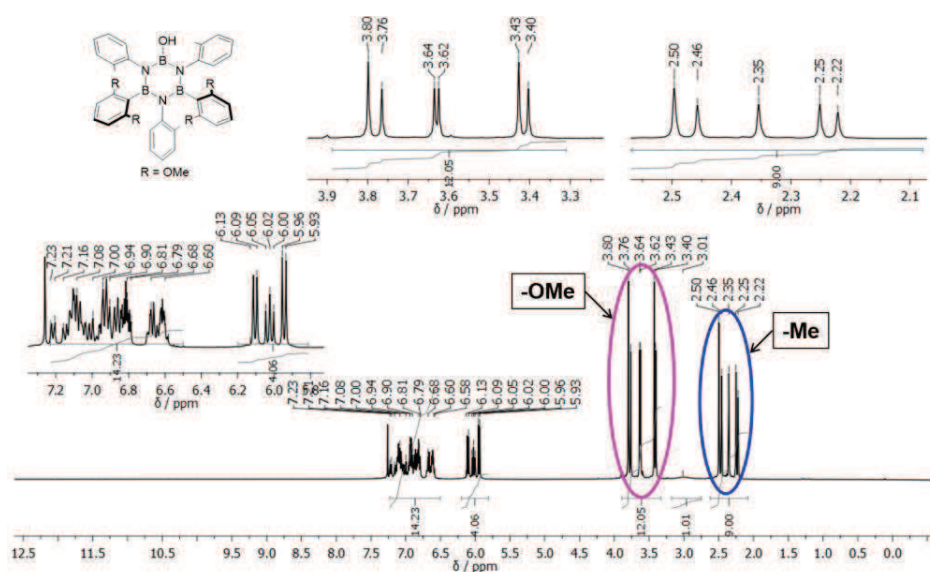
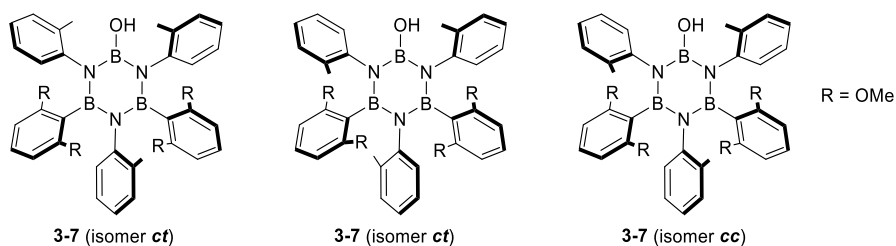
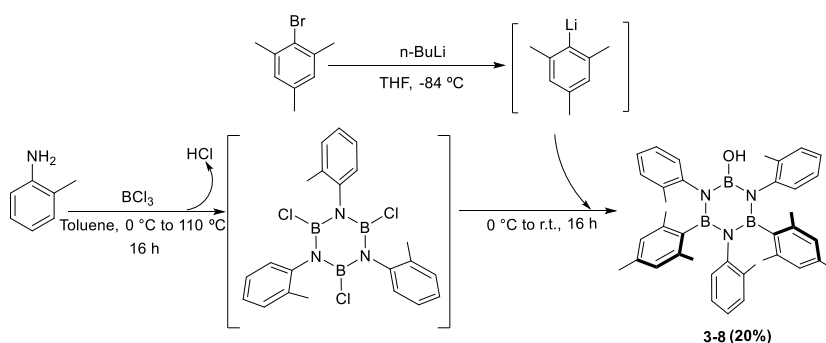


Figure 3.7 – 400 MHz <sup>1</sup>H-NMR molecule **3-7** in CDCl<sub>3</sub> (solvent residual peak: 7.26 ppm).



Scheme 3.7 – Possible isomers of molecule **3-7**.

The functionalisation of *B,B',B''*-trichloro-*N,N',N''*-tri[2-(methyl)phenyl]-borazine was further explored using a bis *ortho*-substituted aryl compound containing groups with larger steric effect with respect to the methoxy, such as methyl moieties (A-value = 1.74 kcal/mol). In particular, molecule **3-8** was obtained by reaction of 2-methylaniline with  $\text{BCl}_3$  and subsequent functionalisation with *MesLi*, in 20% yield (Scheme 3.8). The molecular identity was unambiguously confirmed by  $^1\text{H}$ ,  $^{13}\text{C}$  and  $^{11}\text{B}$ -NMR spectroscopy and HRMS spectrometry. The HRMS spectrum shows a peak corresponding to the molecular mass  $m/z$  at 603.3807 ( $[\text{M}]$ ;  $\text{C}_{39}\text{H}_{44}\text{B}_3\text{N}_3\text{O}_3$ , calc.: 603.3782). In this case,  $^1\text{H}$ -NMR analysis clearly shows the prevalence of one isomer (*cc*) with respect to the others (*ct*). In fact, additional weak peaks in intensity are visible in the aliphatic region of the spectrum, and they can be attributed to the minor formation of *ct* isomers (Figure 3.8). The preponderant formation of isomer *cc* in molecule **3-8** suggests that the main reactive specie of the intermediate *B,B',B''*-trichloro-*N,N',N''*-tri[2-(methyl)phenyl]-borazine is isomer *cc*.



**Scheme 3.8** – Synthesis of molecule **3-8**.

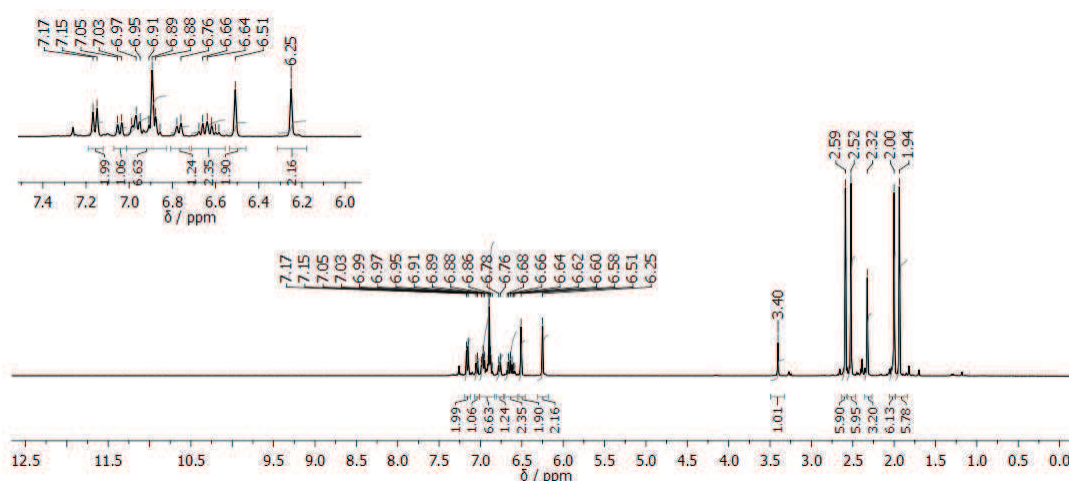


**Figure 3.8** – 300 MHz  $^1\text{H}$ -NMR spectrum of molecule **3-8** in  $\text{CDCl}_3$  (solvent residual peak: 7.26 ppm).

Suitable crystals of **3-8** for preliminary X-Ray diffraction analysis were grown by slow diffusion of MeOH in CH<sub>2</sub>Cl<sub>2</sub>. The X-Ray structure confirmed the presence of isomer *cc*, where the three methyl groups of the *N*-aryl rings are pointing in the same direction (Figure 3.9).

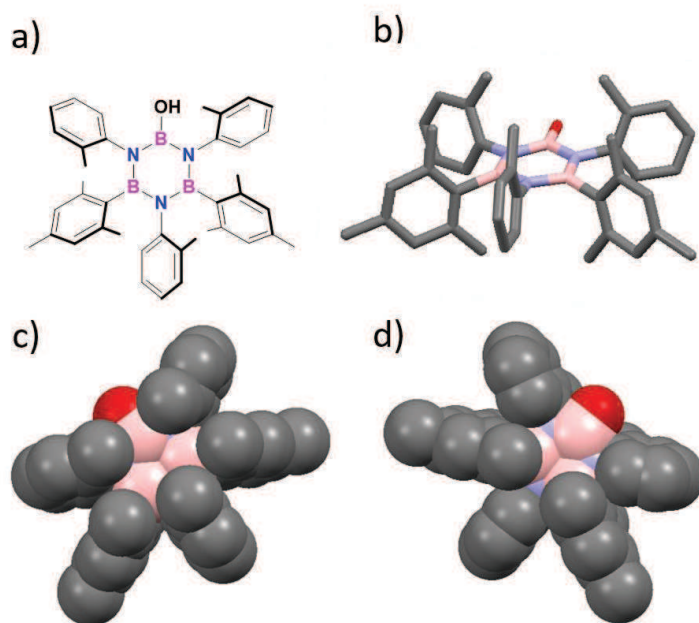
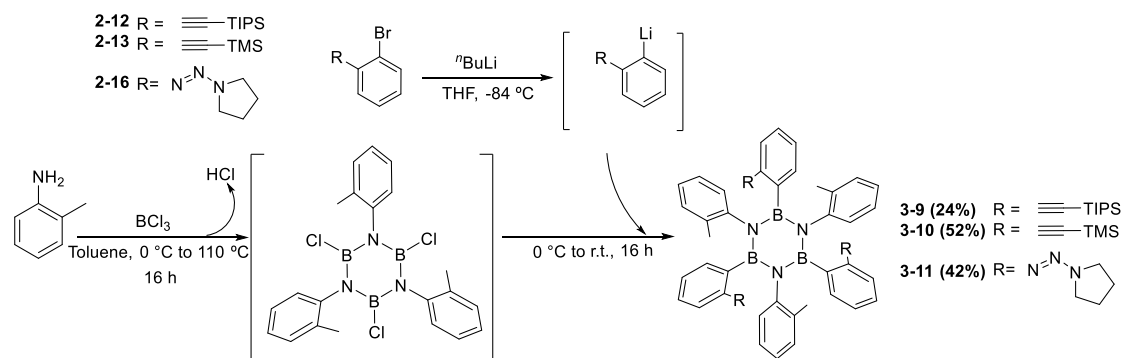


**Figure 3.9** – Crystal structure of borazine derivative **3-8**; (a) molecular structure; (b) crystal structure represented in *capped sticks*; (c) top view of the crystal structure represented in *spacefill*; (d) bottom view of the crystal structure represented in *spacefill*. Space group: *P n a 2*<sub>1</sub>. The crystal was grown by slow diffusion of MeOH in CH<sub>2</sub>Cl<sub>2</sub>. Colour code: grey: C, pink: B, red: O and blue: N. Hydrogen were omitted for the sake of clarity.

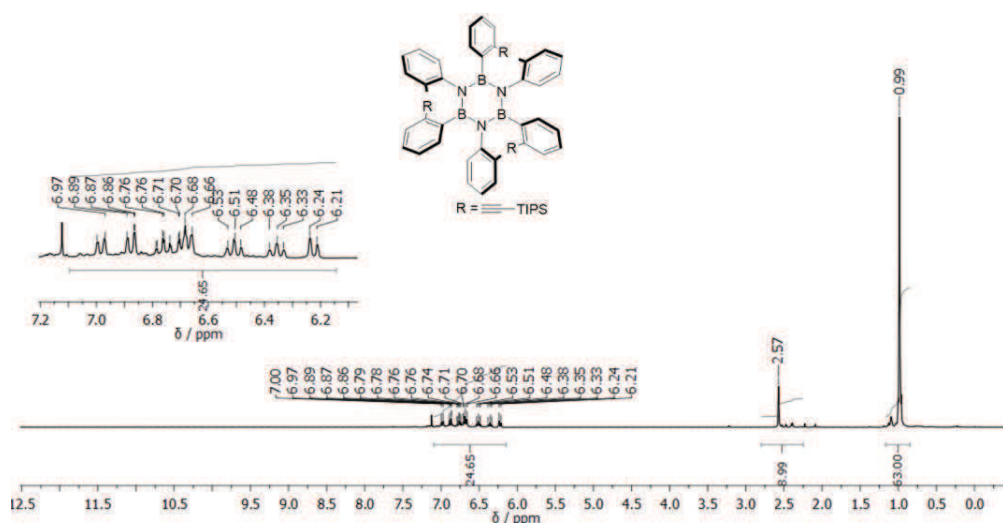
### 3.3.2.a.3 Functionalisation with mono long-range *ortho*-substituted aryl species

The reaction has also been investigated with mono long-range *ortho*-substituted *ArLi* compounds. In particular, using 2-methylaniline as amino precursor for the formation of the borazine core and the corresponding lithium species of compounds **2-12**, **2-13** and **2-16** for the functionalisation, borazines **3-9**, **3-10** and **3-11** were successfully synthesised in 24%, 52% and 42% yield, respectively (Scheme 3.9).



**Scheme 3.9** – Synthesis of borazine derivatives **3-9**, **3-10** and **3-11**.

All compounds have been fully characterised by  $^1\text{H}$   $^{13}\text{C}$  and  $^{11}\text{B}$ -NMR spectroscopy and HRMS spectrometry.  $^1\text{H}$ -NMR spectrum of molecule **3-9** shows the prevalence of one isomer (isomer  $\text{N}^{\text{cc}}:\text{B}^{\text{cc}}$ , in 70%) with respect to the other 7 isomers (see Scheme **3.5**). This attribution was done taking in consideration the main signal of the Me groups at around 2.5 ppm, and the main peak for the TIPS centred at 1 ppm (Figure **3.10**). In fact, additional weak peaks in intensity are visible in the aliphatic region of the spectrum, and they have been associated to the minor formation of the other isomers (30%). The mentioned isomer  $\text{N}^{\text{cc}}:\text{B}^{\text{cc}}$  was identified as the one in which the three methyl groups placed in the *ortho*-position of the *N*-aryl moieties are pointing in the same direction, while the three acetylene TIPS of the *B*-aryl groups are pointing in the opposite one. Anyway it is noteworthy to underline that such  $^1\text{H}$ -NMR profile can also be attributed to the isomer  $\text{N}^{\text{cc}}:\text{B}^{\text{cc}}$  in which the six substituents are pointing in the same direction. However, this possibility has been discarded for steric reasons. This suggests that only of *B,B',B''*-trichloro-*N,N',N''*-tri[2-(methyl)phenyl]-borazine, isomer *cc* was successfully functionalised with the *o*-acetylene-TIPS-*ArLi* derivative to yield **3-9**. Additionally, the addition/elimination reaction follows the same route presented for borazine **2-14** in previous Chapter 2.

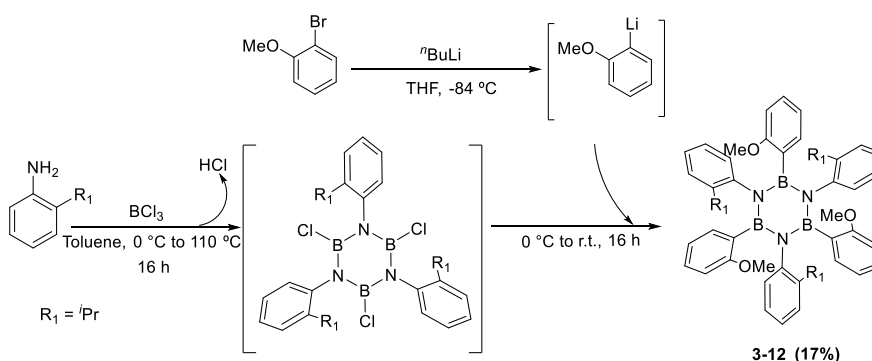


**Figure 3.10** –  $^1\text{H}$ -NMR of borazine **3-9** in  $\text{CDCl}_3$  (solvent residual peak: 7.26 ppm), where it can be observed one main peak in the region corresponding to methyl groups (2.57 ppm), and one main peak for the hydrogen of the TIPS moieties (0.99 ppm).

Concerning the case of molecules **3-10** and **3-11**, <sup>1</sup>H-NMR analysis in CDCl<sub>3</sub> showed that the final borazine was not enriched in any isomer, and a mixture of different isomers was obtained. Probably, as TMS acetylene and triazene substituents have a lower steric effect than the TIPS acetylene, the nucleophilic substitution reaction is not that much stereoselective, and the two initial isomers *cc* and *ct* of *B,B',B''*-trichloro-*N,N',N''*-tri[2-(methyl)phenyl]-borazine obtained are able to equally react with the corresponding nucleophiles. This is also reflected on the yield of the reaction, which almost are two times higher for **3-10** (52%) and **3-11** (42 %) with respect to borazine **3-9**.

## 3.3.2.b Formation of the BN-core from 2-isopropylaniline as Amino Precursor

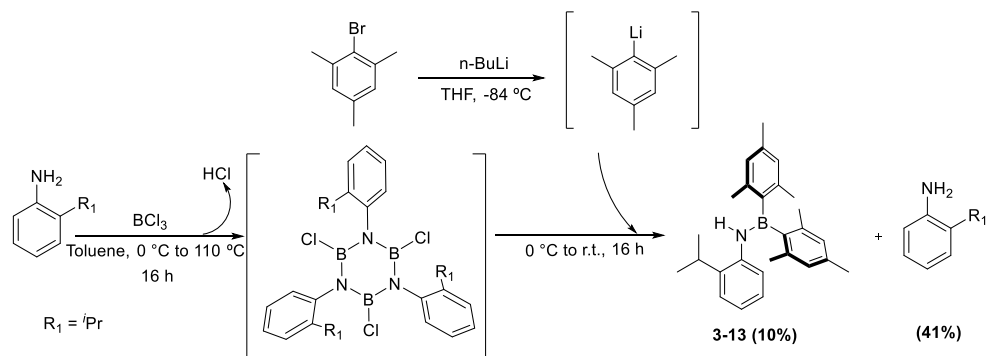
The reaction toward the formation of the borazine core using 2-isopropylaniline (A-value = 2.21 kcal/mol) as amino precursor has been explored and followed by  $^{11}\text{B}$ -NMR spectroscopy. Similarly to the study performed with 2-methylaniline, 2-isopropylaniline was reacted with  $\text{BCl}_3$  in toluene and two aliquots of the reaction mixture have been analysed, one before and one after heating at 110 °C. Before heating,  $^{11}\text{B}$ -NMR spectrum shows a peak at 6.58 ppm, corresponding to the formation of the BN-adduct. After heating, a new peak appeared at 32.12 ppm. The product formed during this step is not stable, therefore, a further functionalisation step was developed. This functionalisation has firstly been studied using a mono short-range aryl derivative, such as 2-bromoanisole for the halogen-lithium exchange (OMe, A-value = 0.55-0.75 kcal/mol) (Scheme 3.10). Borazine **3-12** has been successfully obtained in 17% yield, and fully characterised by  $^1\text{H}$   $^{13}\text{C}$  and  $^{11}\text{B}$ -NMR spectroscopy and HRMS spectrometry. HRMS spectrometry shows peak at 754.4497 for  $[\text{M}+\text{H}]^+$  ( $\text{C}_{48}\text{H}_{55}\text{B}_3\text{N}_3\text{O}_3$  calc. 754.4545).

Scheme 3.10 – Synthesis of molecule **3-12**.

It has been noticed that with the increment of the steric effect of the *ortho*-substituent on the aniline ring ( $\text{iPr}$ , A-value = 2.21 kcal/mol, Me A-value = 1.74 kcal/mol), the yield decreases quite considerably (65% for **3-6**, 17% for **3-12**). Most probably, the larger steric effect of  $\text{iPr}$  on the *N*-aryl rings impedes the attack of the  $\text{ArLi}$  derivative to  $B,B',B''$ -trichloro- $N,N',N''$ -tri[2-(isopropyl)phenyl]-borazine, or even the ability of the latter to form the 'ate complex' once the  $\text{ArLi}$  derivative has attacked. In any case, no restriction towards the formation of any isomer was observed, and a mixture of different isomers was observed by  $^1\text{H}$ -NMR spectroscopy.

The functionalisation was further explored with bis short-range *ortho*-substituted  $\text{ArLi}$  derivatives (e.g. 2-bromomesitylene, Me A-value = 1.74 kcal/mol). Reaction of  $\text{MesLi}$  and  $B,B',B''$ -trichloro- $N,N',N''$ -tri[2-(isopropyl)phenyl]-borazine led to the formation of a complex mixture

in which borazine was not detected (Scheme 3.11). Starting material 2-isopropylaniline was recovered (41%). In addition, it was possible to isolate and characterise aminoborane **3-13**.



Scheme 3.11 – Synthesis of molecule **3-13**.

The presence of molecule **3-13** can be due to two different possibilities: (i) decomposition of the BN-core or (ii) functionalisation of a BN-pair, which did not participate in the cyclisation towards the formation of the BN-ring. The latter is more plausible as the boron atom is substituted by two mesityl moieties, meaning that before, two chlorine moieties were placed on that boron atom. This molecule **3-13** has been obtained in low yield (10%), namely, the amount of amino-borane that does not cyclise is very poor. Hence, the rest could participate in the formation of *B,B',B''*-trichloro-*N,N',N''*-tri[2-(isopropyl)phenyl]-borazine, but the functionalisation step with *MesLi* cannot take place due to the steric effect of the *N*-isopropyl groups and the two methyl groups of the *ArLi*. Consequently, *B,B',B''*-tri(chloro)-*N,N',N''*-tri[2-(isopropyl)phenyl]-borazine decomposes during the workup, yielding starting aniline as major product.

The chemical identity of aminoborane **3-13** was unambiguously confirmed by X-Ray analysis. Suitable crystals of molecule **3-13** were grown by slow evaporation from pentane solution (Figure 3.11).

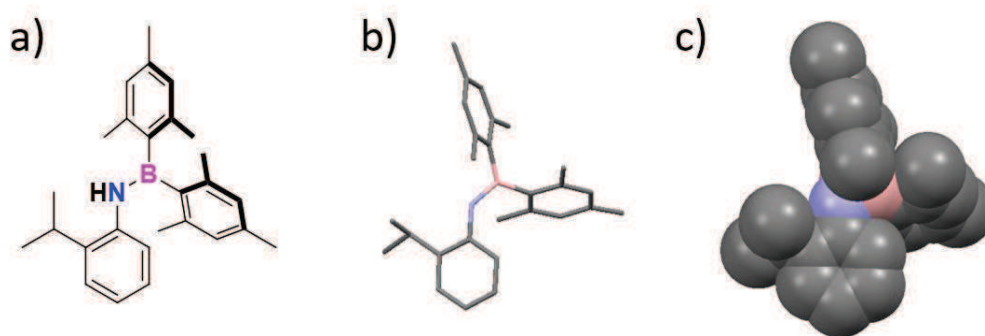
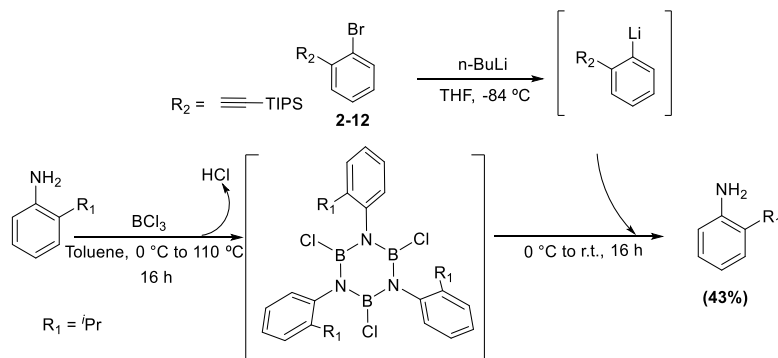


Figure 3.11 – Crystal structure of boron-nitrogen derivative **3-13**; (a) molecular structure; (b) crystal structure represented in *capped sticks*; (c) crystal structure represented in *spacefill*. Space group:  $P n a 2_1$ . The crystal was grown by slow evaporation of pentane. Color code: grey: C, pink: B, and Blue: N. Hydrogen atoms were omitted for the sake of clarity.

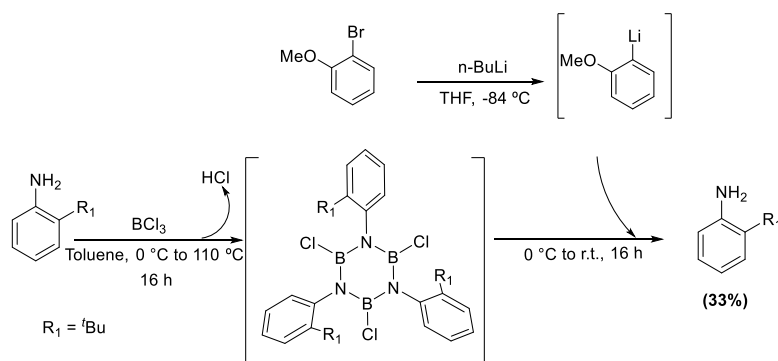
The functionalisation reaction was finally tested using a mono long-range substituent, such as **2-12**, for the halogen-lithium exchange. Also in this case, borazine was not obtained and just starting aniline was recovered (43%) (Scheme 3.12).



**Scheme 3.12** – Failed reaction toward the functionalisation of *B,B',B''*-tri(chloro)-*N,N',N''*-tri[2-(isopropyl)phenyl]-borazine with mono long-range *ortho*-substituted aryl moieties.

### 3.3.2.c Study of the Formation of the BN-core from 2-*tert*-butylaniline as Amino Precursor

The study was also developed using 2-*tert*-butylaniline as amino source (*tert*-butyl A-value = 4.7-4.9 kcal/mol). To commence, 2-*tert*-butylaniline was reacted with BCl<sub>3</sub> in toluene at 110 °C for 16 h. Analogously to the previous studies, the reaction was monitored by <sup>11</sup>B-NMR spectroscopy. <sup>11</sup>B-NMR analysis of the reaction mixture after heating shows a peak at 32.20 ppm. As already described, the intermediate is not stable, and has to be further functionalised toward the formation of stable borazine derivatives. Scheme 3.13 depicts the functionalisation of the BN-core with a mono short-range *ortho*-substituted *ArLi*, such as *o*-OMePhLi. No formation of final borazine was detected, and starting aniline (33%) was recovered from a complex mixture of by-products.



**Scheme 3.13** – Failed reaction toward the functionalisation of *B,B',B''*-tri(chloro)-*N,N',N''*-tri[2-(*tert*-butyl)phenyl]-borazine with mono short-range *ortho*-substituted aryl moieties.

The absence of the final borazine can be due to two main reasons: (i) there was no formation of the initial BN-ring, or (ii) the formation of initial *B,B',B''*-trichloro-*N,N',N''*-tri[2-(*tert*-butyl)phenyl]-borazine cycle occurred. However, this BN-cycle was not accessible for further functionalisation, due to the presence of the hindered *ortho*-substituents on the *N*-aryl moieties. Having in mind the results achieved with 2-methylaniline and 2-isopropylaniline, the formation of the initial cycle could successfully be achieved, obtaining both isomers (*cc* and *ct*) (Scheme 3.12). In particular, for *cc* isomer, the three bulky substituents (*tert*-butyl groups) would be pointing in the same direction, for example, below the ring. During the addition/elimination step, the attack of the nucleophile would be from the less hindered side, to wit, the opposite one (top face). This attack entails the formation of the 'ate complex', in which the boron-nitrogen cycle loses the planarity. The substituents on the adjacent nitrogen atoms would not be anymore placed perpendicular to the plane, but slightly below with respect to the initial conformation, involving an approach between those R bulky groups and to the borazine core. This conformation in which the two R substituents of the *N*-aryl rings are disposed close one to the other, and to the borazine core, cannot be adopted when the R groups has a large steric effect (like in the case of *tert*-butyl groups, A-value = 4.7-4.9 kcal/mol). Therefore, the nucleophilic substitution does not occur (Figure 3.12), which was proved by the formation of a complex mixture and the recovering of the starting material.

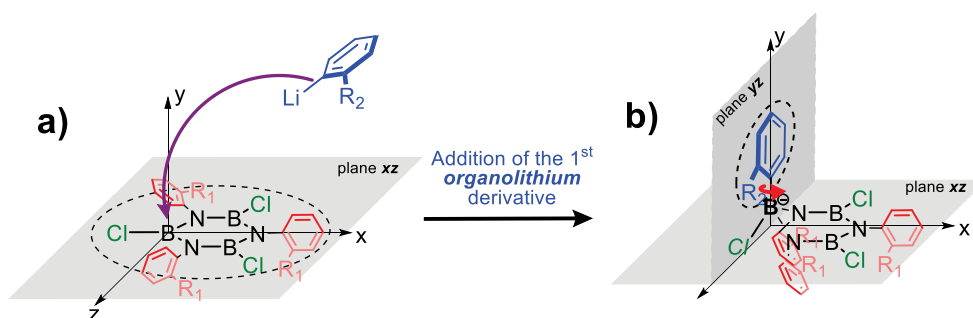


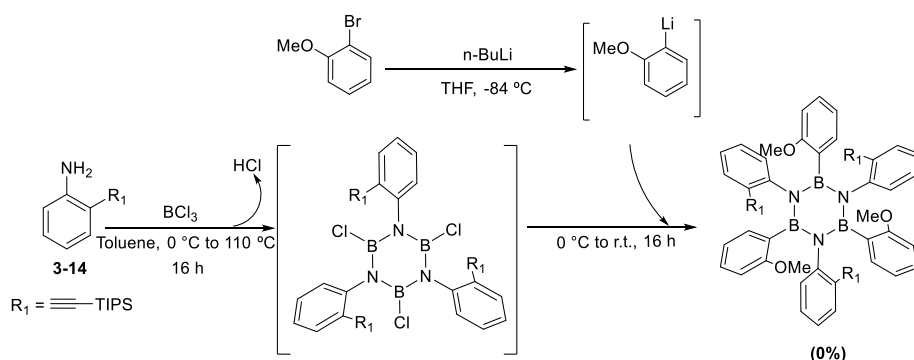
**Figure 3.12** – Addition of the first *organolithium* derivative to a borazine cycle with *ortho*-substituted aniline moieties. Isomer *cc*.

In the same way, the functionalisation at the boron site in *ct* isomer does not occur. The attack of the first *ArLi* would be from the less hindered side of the cycle, namely, the side that contains just one out of the three *tert*-butyl substituent, and it would occur at the furthest boron atom with respect to the R group. Thus, as before, the adjacent *N*-aryl moieties slightly moves down, involving an approach between the R bulky groups and to the borazine core, which does not occur when R groups has a large steric effect (like *tert*-butyl groups).

Therefore, the initial cycle, regardless the isomer (*cc* or *ct*), is not suitable for further functionalisation, and the final borazine derivative could not be obtained.

### 3.3.2.d Study of the Formation of the BN-core from mono long-range *ortho*-substituted Aniline as Amino Precursor

The reaction toward the formation of the borazine core has also been analysed using a mono long-range *ortho*-substituted aniline as amino precursor. In particular, aniline **3-14** bearing a TIPS acetylene in *ortho*-position was firstly obtained in quantitative yield by Sonogashira cross-coupling reaction from 2-iodoaniline and (triisopropylsilyl) acetylene at room temperature for 16 h, using  $[\text{PdCl}_2(\text{PPh}_3)_2]$  as catalyst. Subsequently, the reaction toward the synthesis of the BN-cycle was performed using the standard protocol. The reaction was monitored by  $^{11}\text{B}$ -NMR spectroscopy.  $^{11}\text{B}$ -NMR analysis shows the formation of a peak at 32.16 ppm after heating **3-14** and  $\text{BCl}_3$  at 110 °C for 16 h. However, further functionalisation in the presence of *ArLi* bearing an OMe *ortho*-substituent did not produce the expected borazine (Scheme 3.14).

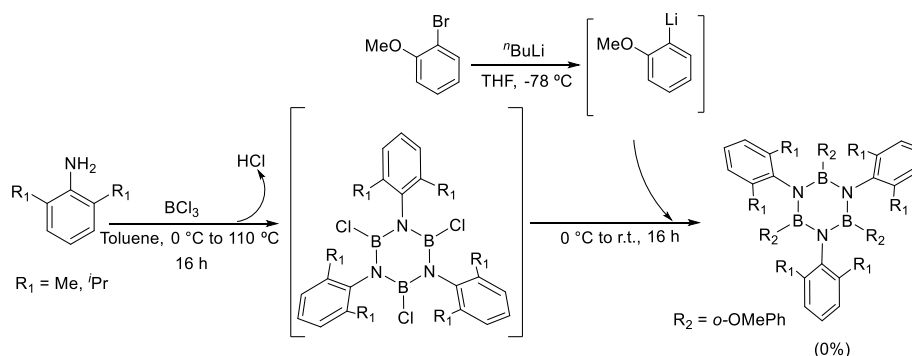


**Scheme 3.14** – Failed synthesis for the formation of borazine rings containing mono long-range *ortho*-substituted aryl moieties.

Similarly to the reaction with 2-*tert*-butylaniline, we can conclude that either there is no formation of the BN-core or the BN-core intermediate is not suitable for further functionalisation. Nevertheless, this is just a hypothesis and the formation or not of the initial cycle cannot be fully confirmed, as  $^1\text{H}$ ,  $^{13}\text{C}$  and  $^{11}\text{B}$ -NMR studies gives insufficient information in this regard.

### 3.3.3 Study of the formation of the BN-core from bis-substituted Anilines as Amino Precursor

In this last subsection, the results obtained using bis short-range *ortho*-substituted aniline species are presented. In particular, the reaction has been performed with commercially available 2,4,6-trimethylaniline (A-value = 1.74 kcal/mol) and 2,6-diisopropylaniline (A-value = 2.21 kcal/mol) which were reacted with BCl<sub>3</sub> in toluene at 110 °C for 16 h. <sup>11</sup>B-NMR of the reaction mixture after heating shows the formation of a peak around 32 ppm (31.97 and 32.40 ppm, respectively). However, the consecutive functionalisation reaction with *o*-OMePhLi did not produce the final stable borazines (Scheme 3.15).

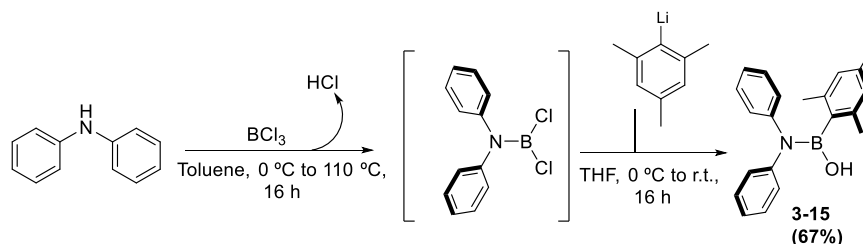


**Scheme 3.15** – Failed synthesis for the formation of borazine rings from bis substituted aniline species.

From our previous studies, we have demonstrated that in the presence of Me or *i*Pr groups in the *ortho*-position of the starting anilines, the formation of the BN-core occurs after reaction with BCl<sub>3</sub> (formation of isomers **cc** and **ct**). This was also corroborated by the isolation of final hexa-substituted borazines after the functionalisation step (**3-6** and **3-12**). Moreover, in Chapter 2 we studied that there is no restriction during the functionalisation of the BN-core using *o*-OMePhLi. Taking in consideration these two facts, it could be assumed that the formation of the initial BN-core does not occur.

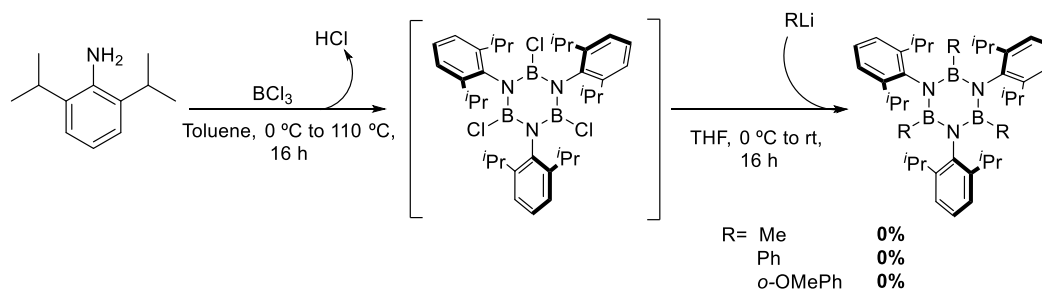
Nevertheless, <sup>11</sup>B-NMR analysis of both reaction mixtures shows the formation of a peak around 32 ppm, in the same region where the peak of molecule **1-3** appeared (see page 109). In order to further investigate the nature of this peak, BCl<sub>3</sub> was reacted with a secondary amine, instead of the primary amines used so far. Since with a secondary amine (*i.e.* diphenylamine), the initial BN-cycle cannot be formed, this can bring useful information for the attribution of the peak around 32 ppm to the formation of a BN-cycle or to the simple formation of the BN-bond. Analogously to the previous synthetic routes, diphenylamine was reacted with BCl<sub>3</sub> in toluene at 110 °C for 16 h. Aliquots of the reaction before and after heating have been submitted to <sup>11</sup>B-NMR analysis. In

particular, two peaks at around 32.42 and 8.08 ppm were observed before and after heating. In addition, two peaks low in intensity have appeared at 7.15 and 24.46 ppm. Therefore, it can be confirmed that the peak around 32 ppm is ascribable to a boron-nitrogen bond, but not necessary to the BN-cycle, as it has been presumably accepted before. To complete the study, addition of the nucleophile for the addition/elimination reaction has been also accomplished, obtaining the corresponding stable amino-borane **3-15** in 67% yield (Scheme 3.16).



**Scheme 3.16** – Synthesis of aminoborane **3-15** starting with diphenylamine.

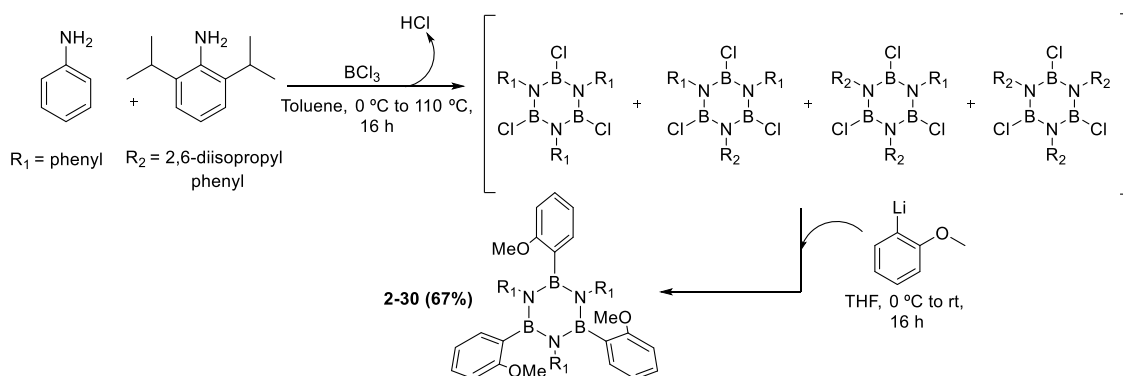
With the aim of finding more clues for the formation (or not) of the BN-cycle when using bis-substituted aniline molecules, the reaction was carried out under the same conditions but using less hindered *ArLi* reagents for the functionalisation step, such as an unsubstituted aryl ring (*PhLi*) or the smallest alkyl one (*MeLi*) (Scheme 3.17). In those cases, special attention is deserved during the workup, as the boron atoms of the expected borazines would not be sterically protected, and the molecule could hydrolyse. However, none of the expected borazine derivatives were obtained (Scheme 3.17).



**Scheme 3.17** – Failed synthesis for the obtaining of final borazine derivatives with bis-*ortho*-substituted anilines, using *MeLi*, *PhLi* or *o*-OMePhLi.

The last experiment developed towards the study of the formation of the cycle with bis-substituted aniline moieties consists of the submission of a mixture of different substituted aniline species to the reaction conditions. The purpose of this experiment was to observe if a less hindered BN-cycle intermediate could be formed by the combination of the two different aniline moieties. In fact, a mixture of an already studied aniline suitable either for the formation of the BN-ring, either for further functionalisation, and a bis *ortho*-substituted aniline was submitted to the reaction with

$\text{BCl}_3$  and the following functionalisation of that BN-cycle has been accomplished. In particular, aniline and 2,6-diisopropylaniline were reacted with  $\text{BCl}_3$  for 16 h at 110 °C (Scheme 3.18). The products that could be obtained after this reaction are: (i) the B-N cycle formed from aniline as amino precursor, (ii) BN-cycle formed from a combination of 2 eq. of aniline and 1 eq. of 2,6-diisopropylaniline, (iii) B-N cycle formed from 1 eq. of aniline and 2 eq. of 2,6-diisopropylaniline; and (iv) the already discarded B-N cycle formed from 3 eq. of 2,6-diisopropylaniline (Scheme 3.18). Afterwards, the functionalising step using *o*-OMePhLi was developed towards the synthesis of stable hexa-functionalised borazines. After purification by precipitation with MeOH,  $^1\text{H}$ -NMR analysis reveals the formation of borazine **2-30**, formed from only aniline as amino precursor and no formation of borazine with 2,6-disoproylaniline was detected. For molecule **2-30** (68%), both isomers were obtained, as usual in this borazine derivative (*cc:ct* 1:5). The yield is in accordance to the one usually obtained during the pure synthesis of molecule **2-30**, which can be an efficient proof of the total absence of a combined initial BN-cycle composed by aniline and 2,6-diisopropylaniline, that after could not be functionalised. Therefore, no positive proof was obtained for the confirmation of a borazine ring that contains bis *ortho*-substituted aniline moieties.



**Scheme 3.18** – Schematic representation of the study developed when using two different aniline moieties for the formation of the borazine ring. Aniline is well known to be suitable for the formation of the BN-cycle, and for further functionalisation at the boron place, while the second aniline moiety, 2,6-diisopropylaniline, is the object of study.

### 3.4 Conclusions

Along this Chapter, the study of the reaction between *ortho*-substituted aniline species and  $\text{BCl}_3$  has been carried out, obtaining crucial information about the importance of the steric effect of different substituents on the formation of the borazine core and the consecutive functionalisation. In particular, with 2-methylaniline (Me, A-value = 1.74 kcal/mol), it was possible to synthesise different borazine derivatives when changing the *ArLi* reagent (mono short-range *ortho*-substituted, bis short-range *ortho*-substituted and mono long-range *ortho*-substituted aryl moieties) (Figure 3.13). The same study was developed when increasing the steric effect of the groups placed in the aniline moiety. However, with 2-isopropylaniline, stable borazine was formed only when using a mono short-range *ortho*-substituted compound for the functionalisation step (Figure 3.13). Moreover, 2-*tert*-butylaniline (*tert*-butyl A-value = 4.7-4.9 kcal/mol) was also submitted to the reaction with  $\text{BCl}_3$ , and further functionalisation, but the desired product was not produced. The same methodology was applied for the study with mono long-range *ortho*-substituted anilines, but no desired borazine was formed (Figure 3.13). Finally, with bis short range-*ortho*-substituted aniline moieties (2,4,6-trimethylaniline and 2,6-diisopropylaniline) no evidence of formation of a borazine cycle were found (Figure 3.13).

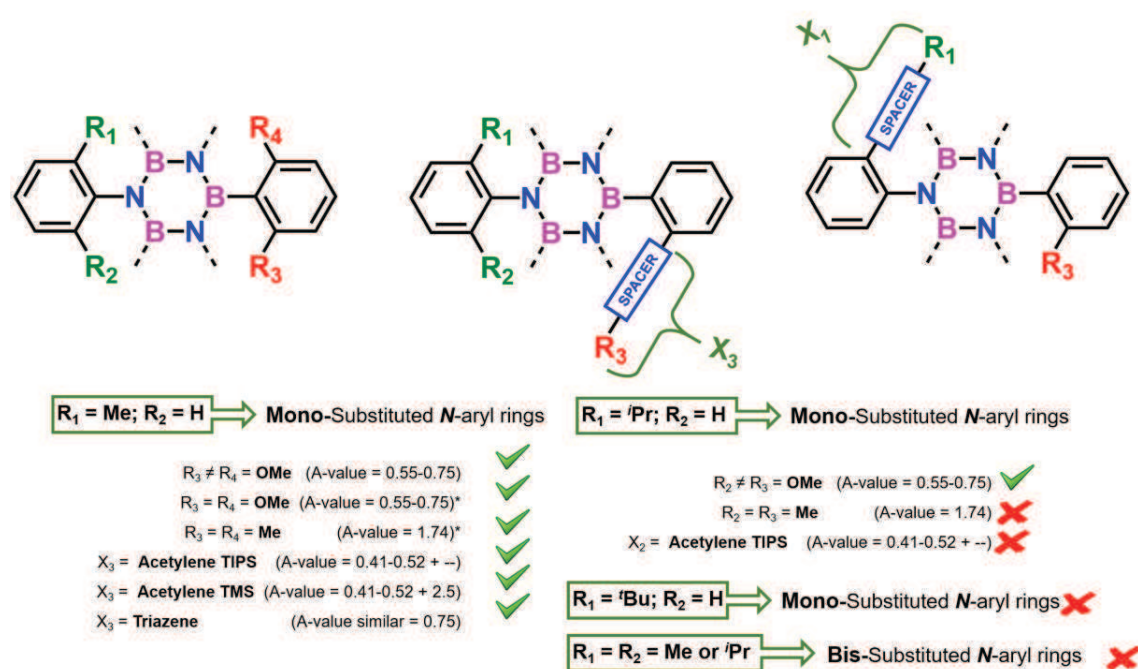


Figure 3.13 – Summarised results for the synthesis of borazines obtained in this Chapter.

### 3.5 References

- [1] A. Thozet, S. Allaoud, T. Zaïr, A. Karim, B. Frange, *J. Organomet. Chem.* **1991**, 406, 269.
- [2] S. Allaoud, B. Frange, *Inorg. Chem.* **1985**, 24, 2520.
- [3] W. Schwarz, D. Lux, H. Hess, *Cryst. Struct. Commun.* **1977**, 6, 431.
- [4] E. V. Steuber, G. Elter, M. Noltemeyer, H.-G. Schmidt, A. Meller, *Organometallics* **2000**, 19, 5083.
- [5] W. G. Henderson, E. F. Mooney, **1969**, p. 219.
- [6] H. Nöth, H. Vahrenkamp, *Chem. Ber.* **1966**, 99, 1049.
- [7] P. N. Gates, E. J. McLauchlan, E. F. Mooney, *Spectrochim. Acta* **1965**, 21, 1445.
- [8] V. Stepanenko, M. Ortiz-Marciales, C. E. Barnes, C. Garcia, *Tetrahedron Lett.* **2006**, 47, 7603.



## CHAPTER 4

### Experimental Part

#### 4.1 Instrumentation

**Thin layer chromatography** (TLC) was conducted on pre-coated aluminum sheets with 0.20 mm Merk Millipore Silica gel 60 with fluorescent indicator F254.

**Column chromatography** was carried out using *Merck Gerduran silica gel 60* (particle size 40-63  $\mu\text{m}$ ).

**Melting points** (M.P.) were measured on a *Büchi Melting Point B-545* or were measured on a *Gallenkamp* apparatus. All of the melting points have been measured in open capillary tubes and have not been corrected.

**Nuclear magnetic resonance** (NMR)  $^1\text{H}$ ,  $^{11}\text{B}$ ,  $^{13}\text{C}$ , and  $^{19}\text{F}$  spectra were obtained on a 300 MHz NMR (*Bruker Fourier*), 400 MHz NMR (*Jeol JNM EX-400* or *Bruker AVANCE III HD*), and 500 MHz NMR (*Jeol JNM EX-500R*). Chemical shifts were reported in ppm according to tetramethylsilane using the solvent residual signal as an internal reference ( $\text{CDCl}_3$ :  $\delta_{\text{H}} = 7.26$  ppm,  $\delta_{\text{C}} = 77.16$  ppm,  $\text{CD}_2\text{Cl}_2$ :  $\delta_{\text{H}} = 5.32$  ppm,  $\delta_{\text{C}} = 53.84$  ppm, Coupling constants ( $J$ ) were given in Hz and were averaged. Resonance multiplicity was described as *s* (singlet), *d* (doublet), *t* (triplet), *m* (multiplet), *br* (broad signal), *dd* (doublet of doublets), *dt* (doublet of triplets). Carbon, fluorine and boron spectra were acquired with a complete

decoupling for the proton. All spectra were recorded at 25 °C unless specified otherwise. Signals observed in  $^1\text{H}$  spectra at 1.27 ppm and 0.8 ppm are traces of grease.

**Infrared spectra** (IR) were recorded on a *Perkin-Elmer Spectrum II FT-IR System UATR*, mounted with a diamond crystal, on a *BIO-RAD FTS-165 apparatus*, or on a *Shimadzu IR Affinity 1S FTIR spectrometer* in ATR mode with a diamond mono-crystal. Selected absorption bands are reported in wavenumber ( $\text{cm}^{-1}$ ).

**ESI-High resolution mass spectrometry** (ESI-HRMS). ESI-HRMS was performed by the *Fédération de Recherche; ICOA/CBM (FR2708)* platform of Orléans in France, on a Bruker maXis Q-TOF in the positive ion mode. The analytes were dissolved in a suitable solvent at a concentration of 1 mg/mL and diluted 200 times in methanol ( $\approx 5$  ng/mL). The diluted solutions (1  $\mu\text{L}$ ) were delivered to the ESI source by a Dionex Ultimate 3000 RSLC chain used in FIA (Flow Injection Analysis) mode at a flow rate of 200  $\mu\text{L}/\text{min}$  with a mixture of  $\text{CH}_3\text{CN}/\text{H}_2\text{O}+0.1\%$  of  $\text{HCO}_2\text{H}$  (65/35). ESI conditions were as follows: capillary voltage was set at 4.5 kV; dry nitrogen was used as nebulizing gas at 0.6 bars and as drying gas set at 200 °C and 7.0 L/min. ESI-MS spectra were recorded at 1 Hz in the range of 50-3000  $m/z$ . Calibration was performed with ESI-TOF Tuning mix from Agilent and corrected using lock masses at  $m/z$  299.294457 (methyl stearate) and 1221.990638 (HP-1221). Data were processed using Bruker Data Analysis 4.1 software. Besides, ESI-HRMS analysis were performed on a Waters LCT HR TOF mass spectrometer in the positive or negative ion mode, at *Cardiff University*.

**Matrix-Assisted Laser Desorption-Ionisation Time-of-Flight Mass Spectrometry analysis** (MALDI-TOF). MALDI-HRMS was performed by the *Centre de spectrométrie de masse* at the *Université de Mons* in Belgium, using the following instrumentation: Waters

QToF Premier mass spectrometer equipped with a nitrogen laser, operating at 337 nm with a maximum output of 500 mW delivered to the sample in 4 ns pulses at 20 Hz repeating rate. Time-of-flight analyses were performed in the reflectron mode at a resolution of about 10.000. The matrix, trans-2-[3-(4-tertbutyl-phenyl)-2-methyl-2-propenylidene]malonitrile (DCTB), was prepared as a 40 mg/mL solution in chloroform. The matrix solution (1  $\mu$ L) was applied to a stainless steel target and air dried. Analyte samples were dissolved in a suitable solvent to obtain 1 mg/mL solutions. 1  $\mu$ L aliquots of these solutions were applied onto the target area already bearing the matrix crystals, and air dried. For the recording of the single-stage MS spectra, the quadrupole (rf-only mode) was set to S3 pass ions from 100 to 1000 THz and all ions were transmitted into the pusher region of the time-offlight analyser where they were analysed with 1s integration time. Besides, High-resolution MALDI mass spectra (HRMS) were performed on a Waters Synapt G2-Si QTOF mass spectrometer, all this analysis were carried out at *Cardiff University*.

## 4.2 Material and General Methods

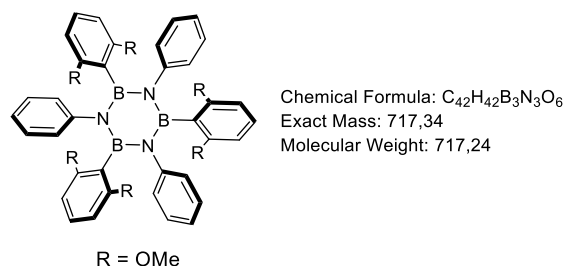
Chemicals were purchased from *Sigma Aldrich*, *Acros Organics*, *Fluorochem*, *TCI*, *aapptec*, *carbosynth*, and *ABCR*, and were used as received unless specified otherwise. Solvents were purchased from *Sigma Aldrich* and *Acros Organics*. Deuterated solvents were purchased from *Eurisotop*.

General solvents were distilled *in vacuo*. Anhydrous THF was distilled from Na/Benzophenone. Anhydrous Toluene was distilled from CaH<sub>2</sub>.

Low temperature baths were prepared using different solvent mixtures depending on the desired temperature: -196 °C with liquid N<sub>2</sub>, -84 °C with EtOAc/liquid N<sub>2</sub>, -78 °C Et<sub>2</sub>O/N<sub>2</sub> liquid, and 0 °C with ice/H<sub>2</sub>O.

Anhydrous conditions were achieved by drying *Schlenk* lines, 2-neck flasks or 3-neck flasks by flaming with a heat gun under vacuum and then purging with argon. The inert atmosphere was maintained using argon-filled balloons equipped with a syringe and needle that was used to penetrate the silicon stoppers used to close the flasks' necks. The addition of liquid reagents was done by means of dried plastic syringes or by cannulation.

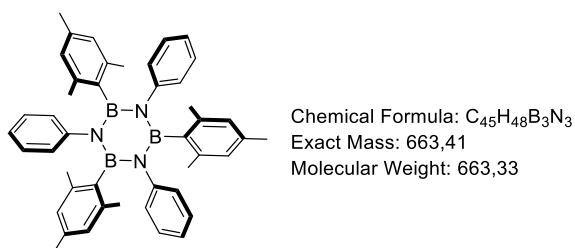
### 4.3 Experimental Procedures



#### ***B,B',B''*-Tri[2,6-(dimethoxy)phenyl]-*N,N',N''*-tri(phenyl)-borazine 2-3**

In a flame-dried 100-mL *Schlenk* flask, aniline (0.35 g, 3.76 mmol) was diluted with 6 mL of anhydrous toluene and cooled to -5 °C (ice-salt bath). A solution of BCl<sub>3</sub> (4.88 mL, 4.88 mmol, 1 M solution in heptane) was added dropwise. The septum was changed for a flame-dried condenser topped by a CaCl<sub>2</sub> tube and the resulting mixture refluxed for 16 h. The reaction solution was cooled down to 0 °C, the condenser was changed for a septum under argon, and the flask subjected to five *freeze-to-thaw* cycle to remove the remaining HCl. In parallel, to a flame-dried 100 mL *Schlenk* flask, 2,6-dimethoxybromobenzene (0.816 g, 3.76 mmol) was dissolved in 9 mL of anhydrous THF and *n*-BuLi (2.82 mL, 4.5 mmol, 1.6 M in hexane) added dropwise at -84 °C. The flask was allowed to warm up at 0 °C. *B,B',B''*-trichloro-*N,N',N''*-triphenyl-borazine **1-3** was cannulated dropwise to the *organolithium* solution at 0 °C and allowed to react at r.t. for 16 h. The reaction mixture was diluted with 15 mL of H<sub>2</sub>O, extracted with EtOAc (NOTE: It was not really soluble, and it remained as a white suspension) (3 × 20 mL) and then with CH<sub>2</sub>Cl<sub>2</sub> (2 × 20 mL) and the combined organic phases dried over MgSO<sub>4</sub> and the solvents removed under reduced pressure. The product was purified by precipitation in MeOH (0.73 g, **81%**) as a white solid. **M.P.:** 319 °C. **<sup>1</sup>H-NMR** (300 MHz, CDCl<sub>3</sub>): δ = 6.94-6.56 (*m*, 18 H), 6.02 (*d*, *J*<sub>1</sub> = 7.6 Hz, 6 H), 3.51 (*s*, 18 H) ppm (the <sup>13</sup>C resonance corresponding to the carbon atom bonded to

the boron atom is not observed due to the quadrupolar relaxation).  $^{11}\text{B}$ -NMR (128 MHz,  $\text{CDCl}_3$ ):  $\delta$  = 35.94 ppm.  $^{13}\text{C}$ -NMR (125 MHz,  $\text{CDCl}_3$ ):  $\delta$  = 160.90, 147.68, 129.01, 127.80, 125.55, 123.34, 102.15, 55.01 ppm. IR ( $\text{cm}^{-1}$ ):  $\nu$  = 422.41, 545.85, 696.30, 723.31, 744.52, 765.74, 1097.50, 1236.37, 1427.32, 1462.04, 1490.97, 1595.13, 2850.79, 2920.23. HRMS (MALDI): Found 717.2853  $[\text{M}]^+$ ,  $\text{C}_{42}\text{H}_{42}\text{B}_3\text{N}_3\text{O}_6$  requires = 717.3353.

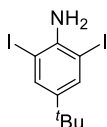


#### ***B,B',B''*-Tri(mesityl)-*N,N',N''*-tri(phenyl)-borazine 2-4**

In a flame-dried 100-mL *Schlenk* flask, aniline (1 g, 10.7 mmol) was diluted with 24 mL of anhydrous toluene and cooled to  $-5\text{ }^{\circ}\text{C}$  (ice-salt bath). A solution of  $\text{BCl}_3$  (13 mL, 13 mmol, 1 M solution in heptane) was added dropwise. The septum was changed for a flame-dried condenser topped by a  $\text{CaCl}_2$  tube and the resulting mixture refluxed for 16 h. The reaction solution was cooled down to  $0\text{ }^{\circ}\text{C}$ , the condenser was changed for a septum, and the flask subjected to five *freeze-to-thaw* cycle to remove the remaining HCl. In parallel, to a flame-dried 100 mL *Schlenk* flask, mesityl bromide (4.6 g, 16 mmol) was dissolved in 25 mL of anhydrous THF and *t*-BuLi (18 mL, 25 mmol, 1.7 M in hexane) added dropwise at  $-78\text{ }^{\circ}\text{C}$ . The flask was allowed to warm up at  $0\text{ }^{\circ}\text{C}$ . *B,B',B''*-trichloro-*N,N',N''*-triphenyl-borazine **1-3** was cannulated dropwise to the *organolithium* derivative solution at  $0\text{ }^{\circ}\text{C}$  and allowed to react at r.t. for 24 h. The reaction mixture was diluted with 20 mL of  $\text{H}_2\text{O}$ , extracted with EtOAc ( $3 \times 30\text{ mL}$ ), the combined organic phases dried over  $\text{MgSO}_4$  and the solvents

removed under reduced pressure. The product was purified by precipitation in MeOH (1.85 g, 75%) as a white solid.

**M.P.:** 262 °C. **<sup>1</sup>H-NMR** (400 MHz, CDCl<sub>3</sub>):  $\delta$  = 6.84-6.72 (*m*, 15 H), 6.33 (*s*, 6 H), 2.23 (*s*, 18 H) 1.97 (*s*, 9 H) ppm. **<sup>11</sup>B-NMR** (128 MHz, CDCl<sub>3</sub>):  $\delta$  = 36.80 ppm. **<sup>13</sup>C-NMR** (100 MHz, CDCl<sub>3</sub>):  $\delta$  = 146.42, 137.35, 136.17, 127.12, 126.81, 126.28, 124.27, 23.12, 21.15 ppm (the <sup>13</sup>C resonance corresponding to the carbon atom bonded to the boron atom is not observed due to the quadrupolar relaxation). **IR** (cm<sup>-1</sup>):  $\nu$  = 1308, 1356, 1491, 1597, 2856, 2915. **HRMS** (MALDI, matrix: DCTB, *m/z*): [M]<sup>+</sup> calc. for C<sub>45</sub>H<sub>48</sub>N<sub>3</sub>B<sub>3</sub>, 663.4127; found, 663.4138.



Chemical Formula: C<sub>10</sub>H<sub>13</sub>I<sub>2</sub>N  
Exact Mass: 400,91  
Molecular Weight: 401,03

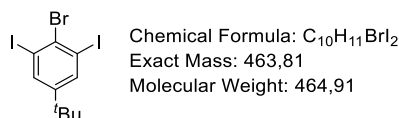
#### 4-(tert-butyl)-2,6-diiodoaniline 2-9

To a solution of 4-*tert*-butylaniline (5 g, 33.5 mmol) in MeOH (150 mL) and water (100 mL), 7.7 g (46.9 mmol) of KI and 5.5 g (23.4 mmol) of KIO<sub>3</sub> were added, resulting a suspension. Afterwards, 37 mL of HCl (1.5 M) were added dropwise over a period of 40 min. The mixture was stirred at r.t. under exclusion of light for 15 h. The reaction mixture was extracted with EtOAc (3 × 20 mL), the organic layer was washed with an aq. solution of Na<sub>2</sub>S<sub>2</sub>O<sub>3</sub> (50 mL), and dried over Na<sub>2</sub>SO<sub>4</sub>. Removal of the solvents under vacuum and purification of the crude by column chromatography (Eluent: CHX: EtOAc 9:1) yielded **2-9** (10.45 g, 79%) as a red oil.

**<sup>1</sup>H-NMR** (400 MHz, CDCl<sub>3</sub>):  $\delta$  = 7.61 (*s*, 2 H), 4.46 (*br s*, 2 H), 1.24 (*s*, 9 H) ppm.

**<sup>13</sup>C-NMR** (100 MHz, CDCl<sub>3</sub>):  $\delta$  = 144.80, 143.89, 136.68, 81.83, 33.86, 31.44 ppm. **IR** (cm<sup>-1</sup>):  $\nu$  = 551.59, 616.21, 701.94, 749.84, 822.24, 872.82, 1022.17, 1041.67, 1057.27,

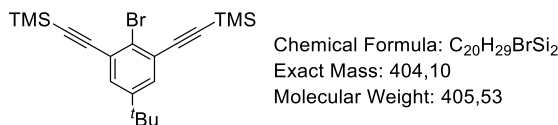
1202.6, 1245.84, 1256.32, 1286.43, 1361.15, 1387, 1460.71, 1526.47, 1572.09, 1604.06, 1758.34, 2863.43, 2956.57, 3361.33, 3456.62. **MS** (ESI-HRMS): Found 401.9207  $[M]^+$ ,  $C_{10}H_{14}I_2N$  requires = 400.9137.



### 2-bromo-5-(*tert*-butyl)-1,3-diiodobenzene **2-10**

To a solution of 4-(*tert*-butyl)-2,6-diiodoaniline **2-9** (5 g, 12.46 mmol) in dry  $CH_3CN$  (100 mL) was added  $CuBr_2$  (2.5 g, 11.37 mmol) followed by isopentyl nitrite (1.64 mL, 12.24 mmol) at 0 °C. After being stirred for 3 h at 0 °C, the reaction mixture was treated with a saturated aq. solution of  $NaHCO_3$  (50 mL). The reaction mixture was extracted with EtOAc (3 × 50 mL) and dried over  $Na_2SO_4$ . Removal of the solvents under vacuum and purification of the crude by column chromatography (Eluent: Pet. Et 100%) yielded **2-10** as a white solid (3.89 g, **75%**).

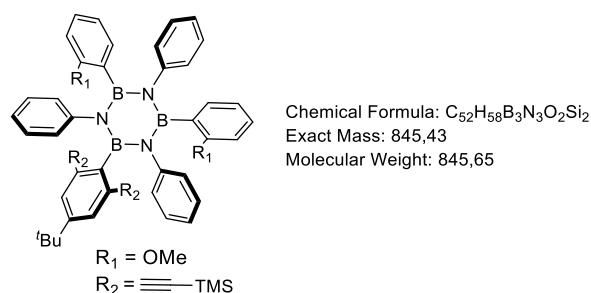
**M.P.:** 278 °C.  **$^1H$ -NMR** (400 MHz,  $CDCl_3$ ):  $\delta$  = 7.80 (s, 2 H), 1.24 (s, 9 H) ppm.  **$^{13}C$ -NMR** (100 MHz,  $CDCl_3$ ):  $\delta$  = 153.72, 137.83, 136.51, 99.88, 34.43, 31.02 ppm. IR ( $cm^{-1}$ ):  $\nu$  = 605.99, 690.47, 704.23, 719.96, 763.46, 853.96, 872.81, 925.38, 1002.34, 1112.05, 1143.57, 1170.6, 1215.26, 1258.48, 1349.83, 1363.55, 1376.52, 1394.46, 1403.31, 1475.23, 1518.37, 1536.79, 1562.42, 1759.08, 2867.37, 2961.76. **MS** (ESI-HRMS): Found  $[M]^+$  463.8125,  $C_{10}H_{12}I_2Br$ , requires 463.8133.



**((2-bromo-5-(*tert*-butyl)-1,3-phenylene)bis(ethyne-2,1-diyl))bis(trimethylsilane) 2-8**

To a degassed solution of dry  $Et_3N$  (12 mL) and THF (12 mL), 2-bromo-5-(*tert*-butyl)-1,3-diiodobenzene **2-10** (3 g, 6.45 mmol),  $[PdCl_2(PPh_3)_2]$  (0.45 g, 0.64 mmol), and  $CuI$  (0.031 g, 0.16 mmol) were added and the mixture degassed a second time. Finally, (trimethylsilyl)acetylene (1.83 mL, 12.9 mmol) was added, the reaction mixture degassed one last time and the final mixture stirred overnight at r.t. under argon. The resulting mixture was filtered over celite and washed with  $CH_2Cl_2$  (20 mL) and  $EtOAc$  (20 mL). Removal of the solvents under vacuum and purification of the crude by column chromatography (eluent:  $CHX$  100%) yielded **2-8** (2.82 g, **95%**) as a white-yellow solid.

**M.P.:** 238 °C. **<sup>1</sup>H-NMR** (400 MHz,  $CDCl_3$ ):  $\delta$  = 7.44 (s, 2 H), 1.28 (s, 9 H), 0.28 (s, 18 H) ppm. **<sup>13</sup>C-NMR** (100 MHz,  $CDCl_3$ ):  $\delta$  = 150.01, 130.84, 125.90, 125.66, 103.67, 99.19, 34.62, 31.08, 0.00 ppm. **IR** ( $cm^{-1}$ ):  $\nu$  = 454.13, 584.22, 629.5, 652.94, 688.55, 717.82, 758.69, 837.37, 882.19, 932.58, 993.36, 1031.15, 1139.29, 1248.84, 1309.92, 1364.32, 1393.43, 1410.52, 1465.33, 1561.32, 2155.96, 2900.57, 2960.74. **MS** (ESI-HRMS): Found 404.0991  $[M]^+$ ,  $C_{20}H_{29}BrSi_2$  requires = 404.0991.

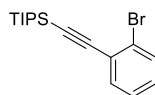


**B,B'-bis[2-(dimethoxy)phenyl]-B''-[4-(*tert*-butyl)-2,6-(trimethylsilyl)ethynyl]phenyl-N,N',N''-tri(phenyl)-borazine 2-11**

In a flame-dried 100-mL *Schlenk* flask, aniline (0.366 g, 3.9 mmol) was diluted with 10 mL of anhydrous toluene and cooled to -5 °C (ice-salt bath). A solution of  $BCl_3$  (5.1 mL, 5.1 mmol, 1 M solution in heptane) was added dropwise. The septum was changed for a flame-dried condenser topped by a  $CaCl_2$  tube and the resulting mixture refluxed for 16 h. The reaction solution was cooled down to 0 °C, the condenser was changed for a septum under argon, and the flask subjected to five *freeze-to-thaw* cycle to remove the remaining HCl. In parallel, to a flame-dried 100 mL *Schlenk* flask, molecule **2-10** (1.58 g, 3.9 mmol) was dissolved in 16 mL of anhydrous THF and *n*-BuLi (2.92 mL, 4.68 mmol, 1.6 M in hexane) added dropwise at -84 °C. The flask was allowed to warm up at 0 °C. *B,B',B''*-trichloro-*N,N',N''*-triphenyl-borazine **1-3** was cannulated dropwise to the *organolithium* solution at 0 °C and allowed to react at r.t. for 16 h. After that time, the second *organolithium* derivative was prepared in another flame-dried 100 mL *Schlenk* flask from 2-bromoanisole (0.729 g, 3.9 mmol) in 16 mL of anhydrous THF and *n*-BuLi (2.92 mL, 4.68 mmol, 1.6 M in hexane), added dropwise at -84 °C. The flask was allowed to warm up at 0 °C. The previous reaction mixture was cannulated dropwise to this *ArLi* solution at 0 °C and allowed to react again at r.t. for 16 h. The reaction mixture was diluted with 30 mL of  $H_2O$ , extracted with EtOAc (3 × 30 mL) and then with  $CH_2Cl_2$  (2 × 20 mL), the combined organic phases dried over

MgSO<sub>4</sub> and the solvents removed under reduced pressure. The product was purified by precipitation in MeOH (0.31 g, **20%**) as a white solid. Both isomer *c* and *t* were obtained and the characterisation here reported corresponds to the mixture.

**M.P.:** 324 °C. **<sup>1</sup>H-NMR** (300 MHz, CDCl<sub>3</sub>):  $\delta$  = 7.18-6.67 (*m*, 21 H), 6.53 (*t*, *J* = 7.6 Hz, 2 H), 6.28 (*d*, *J* = 7.6 Hz, 2 H), 3.44-3.43 (*m*, 6 H), 1.03 (*s*, 9 H), 0.51-0.50 (*m*, 18 H) ppm. **<sup>11</sup>B-NMR** (128 MHz, CDCl<sub>3</sub>):  $\delta$  = 35.84 ppm. **<sup>13</sup>C-NMR** (75 MHz, CDCl<sub>3</sub>):  $\delta$  = 160.12, 160.03, 149.49, 146.66, 146.58, 132.65, 128.90, 128.18, 126.65, 119.26, 108.41, 107.93, 95.37, 95.32, 95.23, 54.36, 34.60, 30.89, 0.46, 0.26, 0.10 ppm (some peaks missing due to overlap). **IR** (cm<sup>-1</sup>):  $\nu$  = 696.30, 750.31, 763.81, 842.89, 997.20, 1028.06, 1238.30, 1261.45, 1274.95, 1377.17, 1429.25, 1454.33, 1490.97, 1598.99, 2148.70, 2358.94. **MS** (AP-HRMS): Found 868.4288 [M+Na], C<sub>52</sub>H<sub>58</sub>B<sub>3</sub>N<sub>3</sub>NaO<sub>2</sub>Si<sub>2</sub> requires = 868.4347.

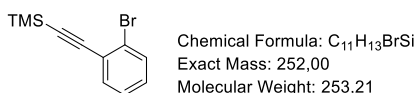


Chemical Formula: C<sub>17</sub>H<sub>25</sub>BrSi  
Exact Mass: 336.09  
Molecular Weight: 337.37

## 2-((triisopropylsilyl)ethynyl)bromobenzene **2-12**

To a degassed solution of 2-bromo-iodobenzene (5 g, 17.6 mmol) in *i*Pr<sub>2</sub>NH (40 mL), [PdCl<sub>2</sub>(PPh<sub>3</sub>)<sub>2</sub>] (0.370 g, 0.528 mmol) and CuI (0.101 g, 0.528 mmol) were added and the resulting solution degassed a second time. Finally, (triisopropylsilyl) acetylene (3.21 g, 17.6 mmol) was added, the reaction mixture degassed one last time and the final mixture stirred overnight at r.t. under argon. The resulting mixture was filtered over celite and washed with CH<sub>2</sub>Cl<sub>2</sub> (20 mL) and EtOAc (20 mL). Removal of the solvents under vacuum and purification of the crude by column chromatography (eluent: CHX 100%) yielded **2-12** (5.9 g, **99%**) as a pallid yellow liquid.

**<sup>1</sup>H-NMR** (400 MHz, CDCl<sub>3</sub>):  $\delta$  = 7.58 (*dd*,  $J_1$  = 7.6 Hz,  $J_2$  = 1.2 Hz, 1 H), 7.51 (*dd*,  $J_1$  = 7.6 Hz,  $J_2$  = 1.6 Hz, 1 H), 7.25 (*dd*,  $J_1$  = 7.6 Hz,  $J_2$  = 1.2, 1 H), 7.16 (*dt*,  $J_1$  = 7.6,  $J_2$  = 1.6, 1 H), 1.15 (m, 21 H) ppm. **<sup>13</sup>C-NMR** (100 MHz, CDCl<sub>3</sub>):  $\delta$  = 133.94, 132.43, 129.43, 126.91, 125.83, 125.75, 104.88, 96.27, 18.75, 11.39 ppm. **IR** (cm<sup>-1</sup>):  $\nu$  = 464.76, 482.65, 501.87, 548.18, 558.52, 634.18, 672.1, 711.66, 751.03, 832.95, 881.88, 919.28, 943.81, 996.01, 1017.14, 1027.54, 1046.22, 1072.33, 1119.04, 1219.87, 1257.73, 1366.27, 1383.31, 1433.84, 1463.92, 1558.05, 2160.56, 2864.15, 2891.17, 2941.97. **MS** (MALDI-HRMS): Found 336.0913 [M]<sup>+</sup>, C<sub>17</sub>H<sub>25</sub>BrSi requires = 336.0909.

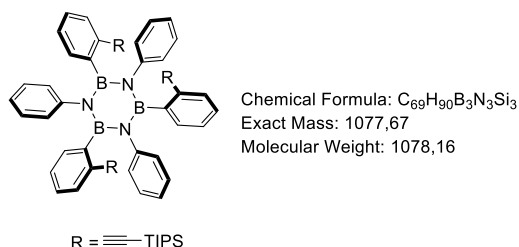


### 2-((trimethylsilyl)ethynyl)bromo-benzene 2-13

To a degassed solution of 2-bromiodobenzene (5 g, 17.6 mmol) in *i*Pr<sub>2</sub>NH (40 mL), [PdCl<sub>2</sub>(PPh<sub>3</sub>)<sub>2</sub>] (0.370 g, 0.528 mmol) and CuI (0.101 g, 0.528 mmol) were added and the resulting solution degassed a second time. Finally, (trimethylsilyl) acetylene (1.72 g, 17.6 mmol) was added, the reaction mixture degassed one last time and the final mixture stirred overnight at r.t. under argon. The resulting mixture was filtered over celite and washed with CH<sub>2</sub>Cl<sub>2</sub> (20 mL) and EtOAc (20 mL). Removal of the solvents under vacuum and purification of the crude by column chromatography (eluent: CHX 100%) yielded **2-16** (4.4 g, **98%**) as a pallid yellow liquid.

**<sup>1</sup>H-NMR** (400 MHz, CDCl<sub>3</sub>):  $\delta$  = 7.57 (*dd*,  $J_1$  = 8.0 Hz,  $J_2$  = 1.2 Hz, 1 H), 7.49 (*dd*,  $J_1$  = 7.7 Hz,  $J_2$  = 1.6 Hz, 1 H), 7.25 (*dd*,  $J_1$  = 7.7 Hz,  $J_2$  = 1.6 Hz, 1 H), 7.17 (*dt*,  $J_1$  = 8 Hz,  $J_2$  = 1.2 Hz, 1 H), 0.27 (s, 9 H) ppm. **<sup>13</sup>C-NMR** (100 MHz, CDCl<sub>3</sub>):  $\delta$  = 133.70, 132.44, 129.64, 126.96, 125.85, 125.33, 103.10, 99.73, -0.08 ppm. **IR** (cm<sup>-1</sup>):  $\nu$  = 548.7, 593.55, 640.34,

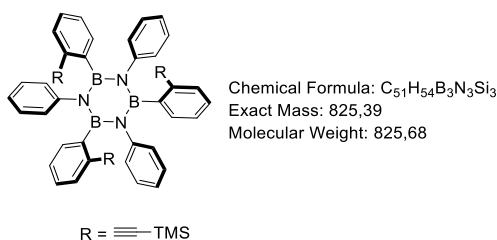
669.8, 699.84, 711.12, 750.42, 838.38, 860.89, 944.79, 1027.1, 1045.93, 1120.06, 1220.22, 1248.97, 1423.44, 1434.11, 1465.39, 1558.3, 1585.59, 2163.05, 2898.17, 2959.5. **MS** (MALDI-HRMS): Found 251.9961 [M]<sup>+</sup>, C<sub>17</sub>H<sub>25</sub>BrSi requires = 251.9970.



### ***B,B',B''*-tri[2-((triisopropylsilyl)ethynyl)phenyl]-*N,N',N''*-tri(phenyl)-borazine 2-14**

In a flame-dried 100-mL *Schlenk* flask, aniline (0.375g, 4 mmol) was diluted with 6 mL of anhydrous toluene and cooled to -5 °C (ice-salt bath). A solution of BCl<sub>3</sub> (5.2 mL, 5.2 mmol, 1 M solution in heptane) was added dropwise. The septum was changed for a flame-dried condenser topped by a CaCl<sub>2</sub> tube and the resulting mixture refluxed for 16 h. The reaction solution was cooled down to 0 °C, the condenser was changed for a septum under argon, and the flask subjected to five *freeze-to-thaw* cycle to remove the remaining HCl. In parallel, to a flame-dried 100 mL *Schlenk* flask, compound **2-12** (1.45 g, 4.29 mmol) was dissolved in 9 mL of anhydrous THF and *n*-BuLi (3 mL, 4.8 mmol, 1.6 M in hexane) added dropwise at -84 °C. The flask was allowed to warm up at 0 °C. *B,B',B''*-trichloro-*N,N',N''*-triphenylborazine **1-3** was cannulated dropwise to the *organolithium* derivative solution at 0 °C and allowed to react at r.t. for 24 h. The reaction mixture was diluted with 15 mL of H<sub>2</sub>O, extracted with EtOAc (3 × 20 mL) and the combined organic phases dried over MgSO<sub>4</sub> and the solvents removed under reduced pressure. The product was purified by precipitation in MeOH (0.57 g, **40%**) as a white solid (isomer *ct*).

**M.P.:** 261 °C. **<sup>1</sup>H-NMR** (400 MHz, CDCl<sub>3</sub>):  $\delta$  = 7.23–6.68 (*m*, 27 H), 1.33 (*m*, 21 H), 1.23 (*m*, 42 H) ppm. **<sup>11</sup>B-NMR** (128 MHz, CDCl<sub>3</sub>):  $\delta$  = 34.68 ppm. **<sup>13</sup>C-NMR** (100 MHz, CDCl<sub>3</sub>):  $\delta$  = 145.80, 145.60, 133.08, 131.82, 131.62, 130.80, 128.99, 128.74, 126.98, 126.83, 126.71, 126.35, 126.27, 126.21, 125.15, 125.10, 124.27, 124.24, 110.35, 110.24, 91.27, 91.03, 19.10, 19.04, 19.01, 11.74 ppm (some peaks missing due to overlap). **IR** (cm<sup>-1</sup>):  $\nu$  = 462.18, 499.55, 532.33, 547.82, 564.93, 604.26, 639.4, 661.64, 675.05, 694.31, 710.33, 756.62, 814.77, 851.84, 882.01, 918.69, 995.2, 1072.77, 1313.68, 1368.35, 1432.48, 1463.04, 1493.11, 1596.24, 2148.41, 2864.24, 2941.55, 3393.57. **MS** (ESI-HRMS): Found 1078.682344 [M+H]<sup>+</sup>, C<sub>69</sub>H<sub>91</sub>B<sub>3</sub>N<sub>3</sub>Si<sub>3</sub> requires = 1078.67.

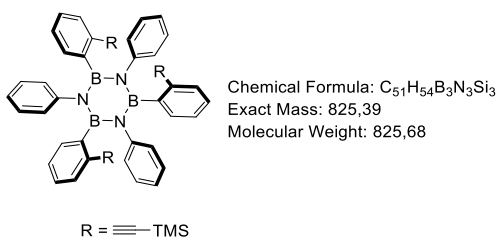


***B,B',B''*-tri[2-((trimethylsilyl)ethynyl)phenyl]-*N,N',N''*-tri(phenyl)-borazine 2-15 (isomer *cc*)**

In a flame-dried 100-mL *Schlenk* flask, aniline (0.7 g, 7.51 mmol) was diluted with 11 mL of anhydrous toluene and cooled to -5 °C (ice-salt bath). A solution of BCl<sub>3</sub> (9.77 mL, 9.77 mmol, 1 M solution in heptane) was added dropwise. The septum was changed for a flame-dried condenser topped by a CaCl<sub>2</sub> tube and the resulting mixture refluxed for 16 h. The reaction solution was cooled down to 0 °C, the condenser was changed for a septum under argon, and the flask subjected to five *freeze-to-thaw* cycle to remove the remaining HCl. In parallel, to a flame-dried 100 mL *Schlenk* flask, compound **2-13** (2.09 g, 8.26 mmol) was dissolved in 6 mL of anhydrous THF and *n*-BuLi (5.65 mL, 8.22 mmol, 1.6 M in hexane)

added dropwise at -84 °C. The flask was allowed to warm up at 0 °C. *B,B',B''*-trichloro-*N,N',N''*-triphenyl-borazine **1-3** was cannulated dropwise to the *organolithium* derivative solution at 0 °C and allowed to react at r.t. for 24 h. The reaction mixture was diluted with 15 mL of H<sub>2</sub>O, extracted with EtOAc (3 × 20 mL) and the combined organic phases dried over MgSO<sub>4</sub> and the solvents removed under reduced pressure. The product was purified by precipitation in MeOH (1.3 g, **63%**) as a white solid (isomer *cc*).

<sup>1</sup>H-NMR (500 MHz, CDCl<sub>3</sub>) δ = 6.52-6.11 (*m*, 27 H), 0.31 (*s*, 27 H) ppm. <sup>13</sup>C-NMR (125 MHz, CDCl<sub>3</sub>): δ = 145.80, 132.75, 132.62, 130.78, 129.00, 127.36, 126.58, 126.44, 126.17, 125.25, 123.94, 107.55, 94.66, 0.77 ppm (the <sup>13</sup>C resonance corresponding to the carbon atom bonded to the boron atom is not observed due to the quadrupolar relaxation).



### ***B,B',B''*-tri[2-((trimethylsilyl)ethynyl)phenyl]-*N,N',N''*-tri(phenyl)borazine 2-15**

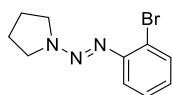
(isomer *ct*)

This isomer was obtained after heating isomer *cc* up to 60 °C (then, isomer *ct* being more stable than *cc*, no inverse isomerisation is observed when the temperature is back to 25 °C).

**M.P.:** 241-243 °C. <sup>1</sup>H-NMR (400 MHz, CDCl<sub>3</sub>) δ = 7.12-6.57 (*m*, 27 H), 0.47 (*s*, 9 H), 0.38 (*s*, 18 H) ppm. <sup>11</sup>B-NMR (128 MHz, CDCl<sub>3</sub>): δ = 34.61 ppm. <sup>13</sup>C-NMR (100 MHz, CDCl<sub>3</sub>): δ = 145.77, 145.62, 131.98, 131.92, 131.14, 130.32, 129.83, 129.19, 128.88, 126.91, 126.87, 126.57, 126.43, 124.76, 124.51, 124.34, 124.25, 108.14, 108.08, 95.12, 94.60, 0.67, 0.54 ppm (some peaks missing due to overlap). **IR** (cm<sup>-1</sup>): ν = 533.26, 548.08, 561.03,

644.94, 694.3, 709.91, 756.83, 837.99, 867.68, 1027.9, 1073.19, 1215.11, 1248.31, 1261.03, 1313.7, 1369.8, 1434.87, 1452.02, 1492.87, 1595.88, 2152.93, 2957.09, 3365.77.

**MS** (ESI-HRMS): found 826.3995  $[M+H]^+$ ,  $C_{51}H_{55}B_3N_3Si_3$  requires= 826.3983.

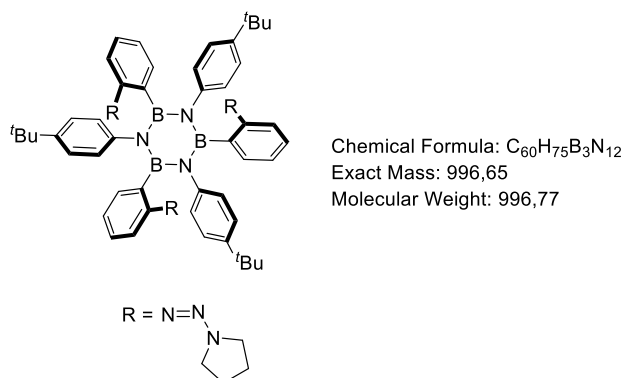


Chemical Formula:  $C_{10}H_{12}BrN_3$   
Exact Mass: 253.02  
Molecular Weight: 254.13

### (E)-1-((2-bromophenyl)diazenyl)pyrrolidine 2-16

To a suspension of 2-bromoaniline (2 g, 11.62 mmol) in conc. HCl at 0 °C (14 mL, 37% in  $H_2O$ ), a solution of  $NaNO_2$  (0.88 g, 12.78 mmol) in cold water (1.5 mL) was added dropwise. After 1 hour, the diazonium salt was formed and a solution (20 mL) of pyrrolidine (7.76 mL, 93 mmol) in aqueous solution of  $K_2CO_3$  (12.8 g, 93 mmol) was added, stirred for 1.5 h. Target molecule **2-14** was obtained after filtration as an orange solid (2.38 g, **70%**).

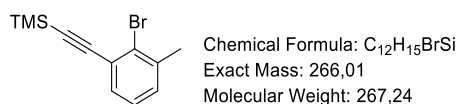
**M.P.:** 93 °C.  **$^1H$ -NMR** (300 MHz,  $CDCl_3$ ):  $\delta$ = 7.58 (*dd*,  $J_1$  = 8.0,  $J_2$  = 1.3 Hz, 1 H), 7.41 (*dd*,  $J_1$  = 8.1,  $J_2$  = 1.6 Hz, 1 H), 7.24 (*dd*,  $J_1$  = 8.1,  $J_2$  = 1.3 Hz, 1 H), 7.00 (*td*,  $J_1$  = 7.7,  $J_2$  = 1.6 Hz, 1 H), 3.85 (*s*, 4 H), 2.05 (*s*, 4 H) ppm.  **$^{13}C$ -NMR** (75 MHz,  $CDCl_3$ ):  $\delta$ = 148.77, 133.08, 127.87, 126.11, 119.45, 118.66, 51.35, 23.77 ppm. **IR** ( $cm^{-1}$ ):  $\nu$  = 561.29, 651.94, 669.30, 721.38, 752.24, 856.39, 1024.20, 1219.01, 1267.23, 1313.52, 1340.53, 1404.18, 1463.97, 2341.58, 2358.94, 2872.01, 2974.23. **MS** (ESI-HRMS): Found = 253.0215  $[M]^+$ ,  $C_{10}H_{12}BrN_3$  requires = 253.0215.



***B,B',B''*-tri[2-(pyrrolidin-1-yl-diazenyl)phenyl]-*N,N',N''*-tri[4-*tert*-butyl]phenyl]-borazine 2-17**

In a flame-dried 100-mL *Schlenk* flask, 4-*tert*-butylaniline (0.617 g, 3.93 mmol) was diluted with 9 mL of anhydrous toluene and cooled to -5 °C (ice-salt bath). A solution of BCl<sub>3</sub> (9 mL, 9 mmol, 1 M solution in heptane) was added dropwise. The septum was changed for a flame-dried condenser topped by a CaCl<sub>2</sub> tube and the resulting mixture refluxed for 16 h. The reaction solution was cooled down to 0 °C, the condenser was changed for a septum under argon, and the flask subjected to five *freeze-to-thaw* cycle to remove the remaining HCl. In parallel, to a flame-dried 100 mL *Schlenk* flask, **2-16** (1.2 g, 4.72 mmol) was dissolved in 20 mL of anhydrous THF and *n*-BuLi (3.24 mL, 5.18 mmol, 1.6 M in hexane) added dropwise at -84 °C. The flask was allowed to warm up at 0 °C. *B,B',B''*-trichloro-*N,N',N''*-tri[(4-*tert*-butyl)phenyl]-borazine was cannulated dropwise to the *organolithium* derivative solution at 0 °C and allowed to react at r.t. for 24 h. The reaction mixture was diluted with 15 mL of H<sub>2</sub>O, extracted with EtOAc (3 × 20 mL) and then with CH<sub>2</sub>Cl<sub>2</sub> (2 × 20 mL), the combined organic phases dried over MgSO<sub>4</sub> and the solvents removed under reduced pressure. The product was purified by precipitation in MeOH (0.52 g, **55%**) as a white solid (isomer *cc*).

**M.P.:** 195 °C. **<sup>1</sup>H-NMR** (400 MHz, CD<sub>2</sub>Cl<sub>2</sub>):  $\delta$  = 6.97 (*dd*,  $J$  = 7.2,  $J$  = 1.3 Hz, 4 H), 6.81–6.79 (*m*, 6 H), 6.76–6.62 (*m*, 10 H), 6.60 (*s*, 4 H), 3.80 (*s*, 12 H), 2.02–1.98 (*m*, 12 H), 1.02 (*s*, 27 H) ppm. **<sup>11</sup>B-NMR** (128 MHz, CD<sub>2</sub>Cl<sub>2</sub>):  $\delta$  = 35.41 ppm. **<sup>13</sup>C-NMR** (100 MHz, CD<sub>2</sub>Cl<sub>2</sub>):  $\delta$  = 153.28, 146.45, 145.84, 133.94, 129.37, 127.72, 124.36, 123.75, 117.54, 34.63, 31.92, 24.91 ppm. **IR** (cm<sup>-1</sup>):  $\nu$  = 403.12, 742.59, 750.31, 763.81, 769.60, 1022.27, 1267.23, 1319.31, 1419.61, 2358.94. **MS** (ESI-HRMS): Found 1019.6473 [M+Na]<sup>+</sup>, C<sub>60</sub>H<sub>75</sub>B<sub>3</sub>N<sub>12</sub>Na requires = 1019.6415.

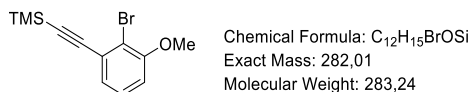


### **((2-bromo-3-methylphenyl)ethynyl)trimethylsilane 2-20**

To a degassed solution of 2-bromo-3-iodotoluene (1.2 g, 4.04 mmol) in *i*Pr<sub>2</sub>NH (25 mL), [PdCl<sub>2</sub>(PPh<sub>3</sub>)<sub>2</sub>] (50 mg, 0.07 mmol) and CuI (40 mg, 0.21 mmol) were added and the resulting solution degassed a second time. Finally, (trimethylsilyl) acetylene (0.417 g, 4.24 mmol) was added, the reaction mixture degassed one last time and the final mixture stirred overnight at r.t. under nitrogen. The resulting mixture was filtered over celite and washed with CH<sub>2</sub>Cl<sub>2</sub> (20 mL) and EtOAc (20 mL). Removal of the solvents under vacuum and purification of the crude by column chromatography (eluent: Pet. Et. 100%) yielded **2-19** (1 g, **94%**) as a pallid yellow liquid.

**<sup>1</sup>H-NMR** (300 MHz, CDCl<sub>3</sub>):  $\delta$  = 7.35 (*dd*,  $J_1$  = 8.0 Hz,  $J_2$  = 1.2 Hz, 1 H), 7.19 (*dd*,  $J_1$  = 7.7 Hz,  $J_2$  = 1.6 Hz, 1 H), 7.15 (*t*,  $J_1$  = 7.7 Hz, 1 H), 2.41 (*s*, 3 H), 0.28 (*s*, 9 H) ppm. **<sup>13</sup>C-NMR** (75 MHz, CDCl<sub>3</sub>):  $\delta$  = 138.84, 131.33, 130.74, 128.03, 126.72, 125.79, 103.90, 99.23, 23.97, 0.01 ppm. **IR** (cm<sup>-1</sup>):  $\nu$  = 408.91, 418.55, 659.66, 669.30, 709.80, 750.31, 763.81,

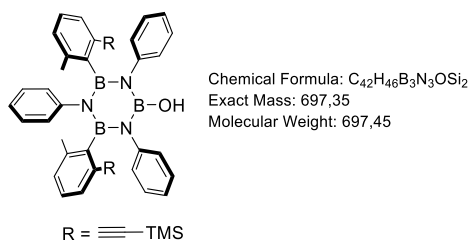
842.89, 937.40, 1029, 1259.52, 1274.95, 1398.39, 1460.11, 2154.49, 2341.58, 2360.87, 2958.80, 3005.10, 3628.10, 3649.32, 3676.32, 3853.77. **MS** (ESI-HRMS): Found 266.0130  $[M]^+$ ,  $C_{12}H_{15}BrSi$  requires = 266.0126.



### Synthesis of ((2-bromo-3-methoxyphenyl)ethynyl)trimethylsilane 2-21

To a degassed solution of 2-bromo-3-iodoanisole (1 g, 3.19 mmol) in  $iPr_2NH$  (15 mL),  $[PdCl_2(PPh_3)_2]$  (50 mg, 0.3 mmol) and CuI (50 mg, 0.528 mmol) were added and the resulting solution degassed a second time. Finally, (trimethylsilyl) acetylene (0.47 mL, 3.55 mmol) was added, the reaction mixture degassed one last time and the final mixture stirred overnight at r.t. under argon. The resulting mixture was filtered over celite and washed with  $CH_2Cl_2$  (20 mL) and EtOAc (20 mL). Removal of the solvents under vacuum and purification of the crude by column chromatography (eluent: Pet. Ether 100%) yielded **2-22** (0.90 g, **99%**) as a pallid yellow liquid.

**$^1H$ -NMR** (300 MHz,  $CDCl_3$ ):  $\delta$  = 7.22 (*t*,  $J$  = 8.0 Hz, 1 H), 7.13 (*dd*,  $J_1$  = 8 Hz,  $J_2$  = 1.8 Hz, 1 H), 6.86 (*dd*,  $J_1$  = 8 Hz,  $J_2$  = 1.8 Hz, 1 H), 3.89 (*s*, 3 H), 0.28 (*s*, 9 H) ppm.  **$^{13}C$ -NMR** (75 MHz,  $CDCl_3$ ):  $\delta$  = 156.29, 127.80, 126.80, 125.80, 115.36, 111.93, 103.17, 99.75, 56.50, -0.02 ppm (some peaks missing due to overlap). **IR** ( $cm^{-1}$ ):  $\nu$  = 659.66, 702.09, 750.31, 844.82, 931.62, 1035.77, 1074.35, 1249.87, 1300.02, 1423.47, 1465.90, 1562.34, 2958.80. **MS** (MALDI-HRMS): Found 282.0081  $[M]^+$ ,  $C_{12}H_{15}BrOSi$  requires = 282.0076.

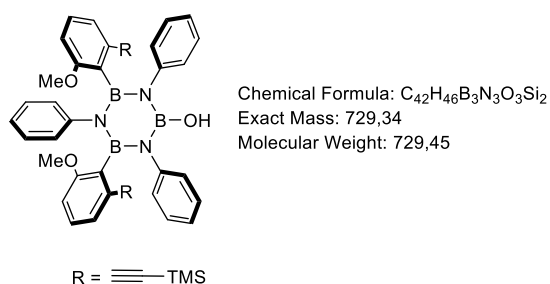


**B,B'-Bis-[2-(methyl)-6-((trimethylsilyl)ethynyl)phenyl]-B''-hydroxy-N,N',N''-tri(phenyl)-borazine 2-24**

In a flame-dried 100-mL *Schlenk* flask, aniline (0.14 g, 1.5 mmol) was diluted with 3 mL of anhydrous toluene and cooled to -5 °C (ice-salt bath). A solution of BCl<sub>3</sub> (1.95 mL, 1.95 mmol, 1 M solution in heptane) was added dropwise. The septum was changed for a flame-dried condenser topped by a CaCl<sub>2</sub> tube and the resulting mixture refluxed for 16 h. The reaction solution was cooled down to 0 °C, the condenser was changed for a septum under argon, and the flask subjected to five *freeze-to-thaw* cycle to remove the remaining HCl. In parallel, to a flame-dried 100 mL *Schlenk* flask, molecule **2-20** (0.4 g, 1.5 mmol) was dissolved in 6 mL of anhydrous THF and *n*-BuLi (1.125 mL, 1.8 mmol, 1.6 M in hexane) added dropwise at -84 °C. The flask was allowed to warm up at 0 °C. *B,B',B''*-trichloro-*N,N',N''*-triphenyl-borazine **1-3** was cannulated dropwise to the *organolithium* derivative solution at 0 °C and allowed to react at r.t. for 16 h. The reaction mixture was diluted with 15 mL of H<sub>2</sub>O, extracted with EtOAc (3 × 10 mL), the combined organic phases dried over MgSO<sub>4</sub> and the solvents removed under reduced pressure. The product was purified by precipitation in MeOH (0.140 g, **40%**) as a white solid. Just isomer *t* was obtained.

**M.P.:** 228 °C. **<sup>1</sup>H-NMR** (300 MHz, CDCl<sub>3</sub>): δ = 7.32-7.27 (*m*, 3 H), 7.25-6.94 (*m*, 10 H), 6.80-6.60 (*m*, 8 H), 3.50 (*s*, 1 H), 2.18 (*s*, 6 H), 0.41 (*s*, 18 H) ppm. **<sup>11</sup>B-NMR** (128 MHz, CDCl<sub>3</sub>): δ = 35.98, 25.72 ppm. **<sup>13</sup>C-NMR** (75 MHz, CDCl<sub>3</sub>): δ = 145.72, 143.50, 137.42, 128.21, 128.06, 127.72, 126.72, 126.68, 126.57, 125.22, 124.47, 124.20, 108.43, 94.95,

22.48, -0.01 ppm. **IR** ( $\text{cm}^{-1}$ ):  $\nu = 403.12, 412.77, 420.48, 518.85, 617.22, 653.87, 669.30, 887.26, 1006.84, 1026.13, 1072.42, 1122.57, 1209.37, 1452.40, 1587.42, 1597.06, 2140.99, 2360.87, 2956.87$ . **MS** (ES-HRMS): Found 698.3558  $[\text{M}+\text{H}]^+$ ,  $\text{C}_{42}\text{H}_{47}\text{B}_3\text{N}_3\text{OSi}_2$  requires = 698.3555.

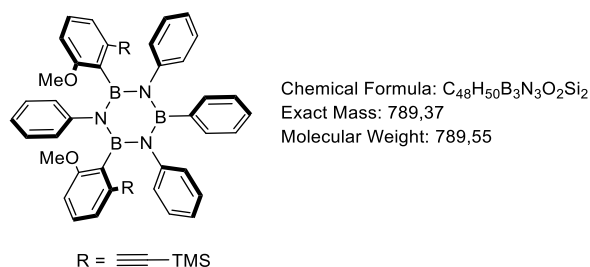


**B,B'-Bis-[2-(methoxy)-6-((trimethylsilyl)ethynyl)phenyl]-B''-hydroxy-*N,N',N''*-tri(phenyl)borazine 2-25**

In a flame-dried 100-mL *Schlenk* flask, aniline (0.14 g, 1.5 mmol) was diluted with 3 mL of anhydrous toluene and cooled to  $-5\text{ }^{\circ}\text{C}$  (ice-salt bath). A solution of  $\text{BCl}_3$  (1.95 mL, 1.95 mmol, 1 M solution in heptane) was added dropwise. The septum was changed for a flame-dried condenser topped by a  $\text{CaCl}_2$  tube and the resulting mixture refluxed for 16 h. The reaction solution was cooled down to  $0\text{ }^{\circ}\text{C}$ , the condenser was changed for a septum under argon, and the flask subjected to five *freeze-to-thaw* cycle to remove the remaining HCl. In parallel, to a flame-dried 100 mL *Schlenk* flask, compound **2-21** (0.42 g, 1.5 mmol) was dissolved in 6 mL of anhydrous THF and *n*-BuLi (1.125 mL, 1.8 mmol, 1.6 M in hexane) added dropwise at  $-84\text{ }^{\circ}\text{C}$ . The flask was allowed to warm up at  $0\text{ }^{\circ}\text{C}$ . *B,B',B''*-trichloro-*N,N',N''*-triphenyl-borazine **1-3** was cannulated dropwise to the *organolithium* derivative solution at  $0\text{ }^{\circ}\text{C}$  and allowed to react at r.t. for 16 h. The reaction mixture was diluted with 15 mL of  $\text{H}_2\text{O}$ , extracted with EtOAc ( $3 \times 10\text{ mL}$ ) and the combined organic

phases dried over  $\text{MgSO}_4$  and the solvents removed under reduced pressure. The product was purified by precipitation in MeOH (0.140 g, **39%**) as a white solid. Just isomer **t** was obtained.

**M.P.:** 251 °C.  **$^1\text{H}$ -NMR** (300 MHz,  $\text{CDCl}_3$ ):  $\delta$  = 7.32 (*s*, 1 H), 7.12–6.62 (*m*, 18 H), 6.35 (*d*,  $J$  = 7.6 Hz, 2 H), 3.60 (*s*, 6 H), 3.54 (*s*, 1 H), 0.45 (*s*, 18 H) ppm.  **$^{11}\text{B}$ -NMR** (128 MHz,  $\text{CDCl}_3$ ):  $\delta$  = 35.40, 25.77 ppm.  **$^{13}\text{C}$ -NMR** (75 MHz,  $\text{CDCl}_3$ ):  $\delta$  = 159.38, 146.28, 144.08, 128.04, 127.86, 127.44, 127.24, 126.11, 125.02, 124.98, 123.95, 122.85, 109.05, 106.97, 94.70, 54.62, 0.00 ppm (the  $^{13}\text{C}$  resonance corresponding to the carbon atom bonded to the boron atom is not observed due to the quadrupolar relaxation). **IR** ( $\text{cm}^{-1}$ ):  $\nu$  = 401.19, 522.17, 559.36, 570.93, 653.87, 781.17, 800.46, 889.70, 908.47, 931.62, 1028.06, 1120.64, 1168.86, 1290.38, 1431.18, 1456.26, 1490.97, 1558.48, 1593.20, 2144.84. **MS** (ESI-HRMS): Found 730.3457  $[\text{M}+\text{H}]^+$ ,  $\text{C}_{42}\text{H}_{47}\text{B}_3\text{N}_3\text{O}_3\text{Si}_2$  requires = 730.3485.

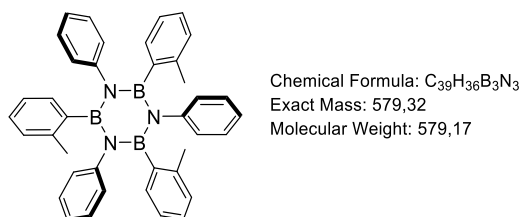


### **B,B'-Bis-[2-methoxy-6-((trimethylsilyl)ethynyl)phenyl]-B''-(phenyl)-N,N',N''-tri-(phenyl)-borazine 2-26**

In a flame-dried 100-mL *Schlenk* flask, aniline (0.14 g, 1.5 mmol) was diluted with 3 mL of anhydrous toluene and cooled to -5 °C (ice-salt bath). A solution of  $\text{BCl}_3$  (1.95 mL, 1.95 mmol, 1 M solution in heptane) was added dropwise. The septum was changed for a flame-dried condenser topped by a  $\text{CaCl}_2$  tube and the resulting mixture refluxed for 16 h.

The reaction solution was cooled down to 0 °C, the condenser was changed for a septum under argon, and the flask subjected to five *freeze-to-thaw* cycle to remove the remaining HCl. In parallel, to a flame-dried 100 mL *Schlenk* flask, compound **2-21** (0.42 g, 1.5 mmol) was dissolved in 6 mL of anhydrous THF and *n*-BuLi (1.125 mL, 1.8 mmol, 1.6 M in hexane) added dropwise at -84 °C. The flask was allowed to warm up at 0 °C. *B,B',B''*-trichloro-*N,N',N''*-triphenyl-borazine **1-3** was cannulated dropwise to the *organolithium* derivative solution at 0 °C and allowed to react at r.t. for 16 h. Finally, the reaction was quenched with *PhLi* (5 mL) and left to react at r.t. for 4 h. The reaction mixture was diluted with 15 mL of H<sub>2</sub>O, extracted with EtOAc (3 × 10 mL) and the combined organic phases dried over MgSO<sub>4</sub> and the solvents removed under reduced pressure. The product was purified by precipitation in MeOH (0.153 g, **37%**) as a white solid (isomer *t*).

**M.P.:** 253 °C. **<sup>1</sup>H-NMR** (300 MHz, CDCl<sub>3</sub>):  $\delta$  = 7.19 (*d*, *J* = 8 Hz, 2 H), 6.96 (*t*, *J* = 8 Hz, 4 H), 6.87-6.54 (*m*, 18 H), 6.35 (*d*, *J* = 8 Hz, 2 H), 3.61 (*s*, 6 H), 0.49 (*s*, 18 H) ppm. **<sup>11</sup>B-NMR** (128 MHz, CDCl<sub>3</sub>):  $\delta$  = 35.32 ppm. **<sup>13</sup>C-NMR** (75 MHz, CDCl<sub>3</sub>):  $\delta$  = 159.63, 147.00, 146.59, 132.92, 128.85, 128.27, 128.22, 127.43, 127.03, 126.79, 126.44, 126.22, 125.21, 124.43, 124.17, 123.12, 109.36, 107.34, 94.98, 54.95, 0.40 ppm (the <sup>13</sup>C resonance corresponding to the carbon atom bonded to the boron atom is not observed due to the quadrupolar relaxation). **IR** (cm<sup>-1</sup>):  $\nu$  = 405.05, 424.34, 433.98, 696.30, 750.31, 763.81, 842.89, 1078.21, 1259.52, 1274.95, 1377.17, 1456.26, 1490.97, 1558.48, 1595.13, 2341.58, 2358.94. **MS** (ES-HRMS): Found 790.3881 [M+H]<sup>+</sup>, C<sub>48</sub>H<sub>51</sub>B<sub>3</sub>N<sub>3</sub>O<sub>2</sub>Si<sub>2</sub> requires = 790.3822.

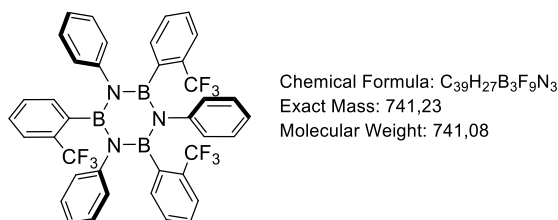


### ***B,B',B''*-Tri[2-(methyl)phenyl]-*N,N',N''*-tri(phenyl)borazine 2-27**

In a flame-dried 100-mL *Schlenk* flask, aniline (0.7 g, 7.5 mmol) was diluted with 11 mL of anhydrous toluene and cooled to -5 °C (ice-salt bath). A solution of  $BCl_3$  (9.77 mL, 9.77 mmol, 1 M solution in heptane) was added dropwise. The septum was changed for a flame-dried condenser topped by a  $CaCl_2$  tube and the resulting mixture refluxed for 16 h. The reaction solution was cooled down to 0 °C, the condenser was changed for a septum under argon, and the flask subjected to five *freeze-to-thaw* cycle to remove the remaining HCl. In parallel, to a flame-dried 100 mL *Schlenk* flask, 2-bromotoluene (1.33 g, 8.22 mmol) was dissolved in 17 mL of anhydrous THF and *n*-BuLi (5.65 mL, 9.06 mmol, 1.6 M in hexane) added dropwise at -84 °C. The flask was allowed to warm up at 0 °C. *B,B',B''*-trichloro-*N,N',N''*-triphenyl-borazine **1-3** was cannulated dropwise to the *organolithium* derivative solution at 0 °C and allowed to react at r.t. for 24 h. The reaction mixture was diluted with 15 mL of  $H_2O$ , extracted with EtOAc (NOTE: It was not really soluble, and it remained as a white suspension) ( $3 \times 20$  mL) and then with  $CH_2Cl_2$  ( $2 \times 20$  mL) and the combined organic phases dried over  $MgSO_4$  and the solvents removed under reduced pressure. The product was purified by precipitation in MeOH (0.60 g, **69%**) as a white solid. Two isomers were obtained (*cc:ct* 1:3). The characterisation here reported corresponds to both isomers together.

**M.p.** 329 °C.  **$^1H$ -NMR** (300 MHz,  $CDCl_3$ ):  $\delta$  = 7.10-6.59 (*m*, 108 H), 2.24 (*s*, 9 H), 2.18 (*s*, 18 H), 2.11 (*s*, 9 H) ppm.  **$^{11}B$ -NMR** (128 MHz,  $CDCl_3$ ):  $\delta$  = 36.47 ppm.  **$^{13}C$ -NMR**

(75 MHz,  $\text{CDCl}_3$ ):  $\delta$  = 146.39, 146.33, 146.12, 137.93, 137.83, 137.73, 132.41, 132.12, 131.84, 129.67, 128.73, 128.05, 127.24, 127.20, 127.06, 126.77, 124.25, 123.65, 123.53, 123.43, 23.16, 23.04, 22.92 ppm (some peaks missing due to overlap). **IR** ( $\text{cm}^{-1}$ ):  $\nu$  = 406.98, 418.55, 559.36, 696.30, 729.09, 748.38, 763.81, 1026.13, 1072.42, 1261.45, 1276.88, 1309.67, 1363.67, 1489.05, 1597.06. **MS** (ES-HRMS): Found 602.3105  $[\text{M}+\text{Na}]^+$ ,  $\text{C}_{39}\text{H}_{36}\text{B}_3\text{N}_3\text{Na}$  requires = 602.3086.

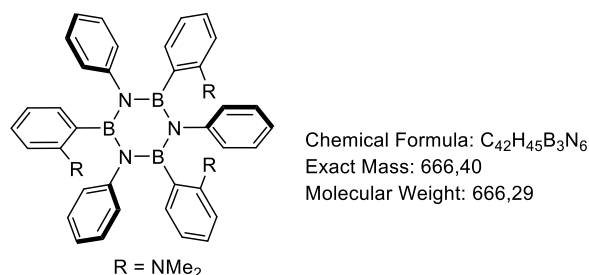


### ***B,B',B''*-Tri[2-(trifluoromethyl)phenyl]-*N,N',N''*-tri(phenyl)-borazine 2-28**

In a flame-dried 100-mL *Schlenk* flask, aniline (0.7 g, 7.5 mmol) was diluted with 11 mL of anhydrous toluene and cooled to  $-5\text{ }^{\circ}\text{C}$  (ice-salt bath). A solution of  $\text{BCl}_3$  (9.77 mL, 9.77 mmol, 1 M solution in heptane) was added dropwise. The septum was changed for a flame-dried condenser topped by a  $\text{CaCl}_2$  tube and the resulting mixture refluxed for 16 h. The reaction solution was cooled down to  $0\text{ }^{\circ}\text{C}$ , the condenser was changed for a septum under argon, and the flask subjected to five *freeze-to-thaw* cycle to remove the remaining  $\text{HCl}$ . In parallel, to a flame-dried 100 mL *Schlenk* flask, 2-bromobenzotrifluoride (1.85 g, 8.22 mmol) was dissolved in 17 mL of anhydrous THF and *n*-BuLi (5.65 mL, 9.06 mmol, 1.6 M in hexane) added dropwise at  $-84\text{ }^{\circ}\text{C}$ . The flask was allowed to warm up at  $0\text{ }^{\circ}\text{C}$ . *B,B',B''*-trichloro-*N,N',N''*-triphenyl-borazine **1-3** was cannulated dropwise to the *organolithium* derivative solution at  $0\text{ }^{\circ}\text{C}$  and allowed to react at r.t. for 24 h. The reaction mixture was diluted with 15 mL of  $\text{H}_2\text{O}$ , extracted with EtOAc (NOTE: It was not really soluble, and it

remained as a white suspension) ( $3 \times 20$  mL) and then with  $\text{CH}_2\text{Cl}_2$  ( $2 \times 20$  mL), the combined organic phases dried over  $\text{MgSO}_4$  and the solvents removed under reduced pressure. The product was purified by precipitation in MeOH (1.15 g, **51%**) as a white solid. Two isomers were obtained (*cc:ct* 1:3). The characterisation here reported corresponds to both isomers together.

**M.p.** 346 °C.  **$^1\text{H}$ -NMR** (300 MHz,  $\text{CDCl}_3$ ):  $\delta$  = 7.24-6.63 (m, 108 H) ppm.  **$^{11}\text{B}$ -NMR** (128 MHz,  $\text{CDCl}_3$ ):  $\delta$  = 36.55 ppm.  **$^{13}\text{C}$ -NMR** (75 MHz,  $\text{CDCl}_3$ ):  $\delta$  = 145.49, 145.18, 132.78, 132.36, 131.99, 129.41, 129.36, 129.21, 129.09, 129.00, 128.24, 128.10, 127.87, 127.40, 127.18, 126.18, 124.97 ppm (some peaks missing due to overlap).  **$^{19}\text{F}$ -NMR** (470 MHz):  $\delta$  = -58.80, -58.83 ppm. **IR** ( $\text{cm}^{-1}$ ):  $\nu$  = 420.48, 443.63, 457.13, 549.71, 700.16, 715.59, 752.24, 765.74, 1049.28, 1114.43, 1153.43, 1321.24, 1373.32, 1489.05. **MS** (ESI-HRMS): Found 742.2460  $[\text{M}]^+$ ,  $\text{C}_{39}\text{H}_{28}\text{B}_3\text{F}_3\text{N}_3$  requires = 742.2438.



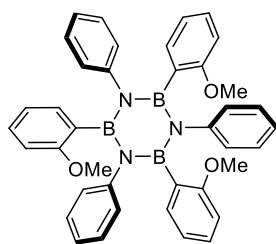
### ***B,B',B''*-Tri(2-*N,N*-dimethylaniline)-*N,N',N''*-tri(phenyl)-borazine 2-29**

In a flame-dried 100-mL *Schlenk* flask, aniline (0.7 g, 7.5 mmol) was diluted with 11 mL of anhydrous toluene and cooled to -5 °C (ice-salt bath). A solution of  $\text{BCl}_3$  (9.77 mL, 9.77 mmol, 1 M solution in heptane) was added dropwise. The septum was changed for a flame-dried condenser topped by a  $\text{CaCl}_2$  tube and the resulting mixture refluxed for 16 h. The reaction solution was cooled down to 0 °C, the condenser was changed for a septum

under argon, and the flask subjected to five *freeze-to-thaw* cycle to remove the remaining HCl. In parallel, to a flame-dried 100 mL *Schlenk* flask, 2-bromoN,N-dimethylaniline (1.44 g, 8.22 mmol) was dissolved in 17 mL of anhydrous THF and *n*-BuLi (5.65 mL, 9.06 mmol, 1.6 M in hexane) added dropwise at -84 °C. The flask was allowed to warm up at 0 °C. *B,B',B''*-trichloro-*N,N',N''*-triphenyl-borazine **1-3** was cannulated dropwise to the *organolithium* derivative solution at 0 °C and allowed to react at r.t. for 24 h.

The reaction mixture was filtered off, washed with MeOH (20 mL), H<sub>2</sub>O (20 mL), and again MeOH (20mL) to yield compound **2-28** as a white solid (0.7 g, **47%**). Two isomers were obtained (*cc:ct* 1:3). The characterisation here reported corresponds to both isomers.

**M.P.:** 189 °C. **<sup>1</sup>H-NMR** (300 MHz, CDCl<sub>3</sub>):  $\delta$  = 7.11-6.15 (*m*, 108 H), 2.77 (*s*, 18 H), 2.71 (*s*, 36 H), 2.61 (*s*, 18 H) ppm. **<sup>11</sup>B-NMR** (128 MHz, CDCl<sub>3</sub>):  $\delta$  = 36.25 ppm. **<sup>13</sup>C-NMR** (75 MHz, CDCl<sub>3</sub>):  $\delta$  = 154.33, 154.12, 153.94, 146.66, 146.58, 146.32, 135.06, 134.85, 134.63, 130.27, 129.69, 129.56, 128.89, 127.95, 126.33, 126.07, 125.94, 123.81, 123.71, 123.56, 117.62, 117.42, 117.24, 114.29, 114.18, 43.17, 43.03, 43.00 ppm. **IR** (cm<sup>-1</sup>):  $\nu$  = 418.55, 439.77, 505.35, 667.37, 690.52, 1008.77, 1028.06, 1043.49, 1099.43, 1261.45, 1429.25, 1570.06, 1595.13, 2791.00, 2833.43, 2866.22, 2949.16, 2985.81. **MS** (ESI-HRMS): Found 667.4023 [M+H]<sup>+</sup>, C<sub>42</sub>H<sub>46</sub>B<sub>3</sub>N<sub>6</sub> requires = 667.4035.



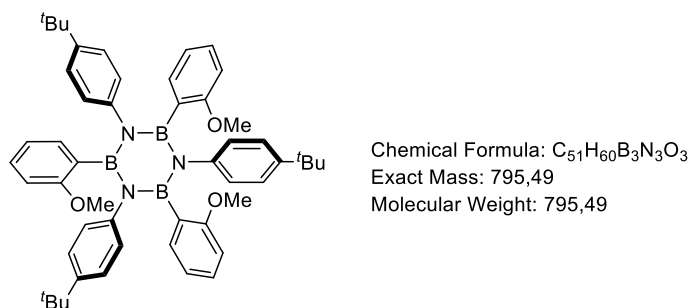
Chemical Formula:  $C_{39}H_{36}B_3N_3O_3$   
 Exact Mass: 627,30  
 Molecular Weight: 627,16

### ***B,B',B''*-Tri[2-(methoxy)phenyl]-*N,N',N''*-tri(phenyl)-borazine 2-30**

In a flame-dried 100-mL *Schlenk* flask, aniline (0.7 g, 7.5 mmol) was diluted with 11 mL of anhydrous toluene and cooled to -5 °C (ice-salt bath). A solution of  $BCl_3$  (9.77 mL, 9.77 mmol, 1 M solution in heptane) was added dropwise. The septum was changed for a flame-dried condenser topped by a  $CaCl_2$  tube and the resulting mixture refluxed for 16 h. The reaction solution was cooled down to 0 °C, the condenser was changed for a septum under argon, and the flask subjected to five *freeze-to-thaw* cycle to remove the remaining HCl. In parallel, to a flame-dried 100 mL *Schlenk* flask, 2-bromoanisole (1.54 g, 8.22 mmol) was dissolved in 17 mL of anhydrous THF and *n*-BuLi (5.65 mL, 9.06 mmol, 1.6 M in hexane) added dropwise at -84 °C. The flask was allowed to warm up at 0 °C. *B,B',B''*-trichloro-*N,N',N''*-triphenyl-borazine **1-3** was cannulated dropwise to the *organolithium* derivative solution at 0 °C and allowed to react at r.t. for 24 h. The reaction mixture was diluted with 15 mL of  $H_2O$ , extracted with EtOAc (NOTE: It was not soluble, and it remained as a white suspension) ( $3 \times 20$  mL) and then with  $CH_2Cl_2$  ( $2 \times 20$  mL) and the combined organic phases dried over  $MgSO_4$  and the solvents removed under reduced pressure. The product was purified by precipitation in MeOH (1.02 g, **69%**) as a white solid. Two isomers were obtained (*cc:ct* 1:5). The characterisation here reported corresponds to both isomers together.

**M.P.:** 298 °C.  **$^1H$ -NMR** (300 MHz,  $CDCl_3$ ):  $\delta$  = 6.99-6.65 (*m*, 126 H), 6.53 (*t*,  $J$  = 7.6 Hz, 18 H), 6.30 (*d*,  $J$  = 7.6 MHz, 18 H), 3.45 (*s*, 15 H), 3.42 (*s*, 30 H), 3.37 (*s*, 9 H) ppm.

**$^{11}\text{B}$ -NMR** (128 MHz,  $\text{CDCl}_3$ ):  $\delta = 35.98$  ppm.  **$^{13}\text{C}$ -NMR** (75 MHz,  $\text{CDCl}_3$ ):  $\delta = 160.16$ , 160.04, 159.93, 147.05, 146.98, 132.78, 128.55, 128.13, 126.38, 123.62, 119.28, 119.24, 108.54, 108.48, 108.41, 54.53 ppm (some peaks missing due to overlap). **IR** ( $\text{cm}^{-1}$ ):  $\nu = 406.98$ , 418.55, 532.35, 694.37, 744.52, 761.88, 1024.20, 1043.49, 1261.45, 1274.95, 1313.52, 1375.25, 1429.25, 1452.40, 1571.99, 1597.06, 2314.58, 2347.37. **MS** (ESI-HRMS): Found 628.3124  $[\text{M}+\text{H}]^+$ ,  $\text{C}_{39}\text{H}_{37}\text{B}_3\text{N}_3\text{O}_3$  requires = 628.3114.

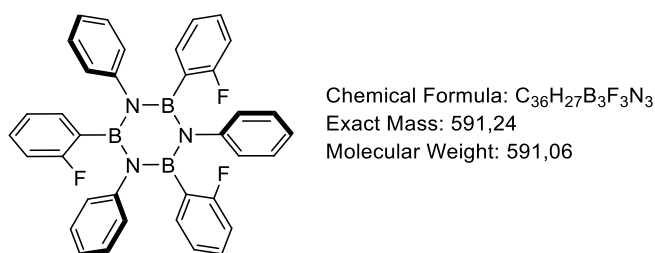


### ***B,B',B''*-Tri[2-(methoxy)phenyl]-*N,N',N''*-tri[4-(*tert*-butyl)phenyl]-borazine 2-32**

In a flame-dried 100-mL *Schlenk* flask, 4-*tert*-butylaniline (0.35 g, 2.2 mmol) was diluted with 6 mL of anhydrous toluene and cooled to  $-5\text{ }^{\circ}\text{C}$  (ice-salt bath). A solution of  $\text{BCl}_3$  (2.85 mL, 2.85 mmol, 1 M solution in heptane) was added dropwise. The septum was changed for a flame-dried condenser topped by a  $\text{CaCl}_2$  tube and the resulting mixture refluxed for 16 h. The reaction solution was cooled down to  $0\text{ }^{\circ}\text{C}$ , the condenser was changed for a septum under argon, and the flask subjected to five *freeze-to-thaw* cycle to remove the remaining HCl. In parallel, to a flame-dried 100 mL *Schlenk* flask, 2-bromoanisole (0.27 g, 2.2 mmol) was dissolved in 9 mL of anhydrous THF and *n*-BuLi (1.55 mL, 2.65 mmol, 1.6 M in hexane) added dropwise at  $-84\text{ }^{\circ}\text{C}$ . The flask was allowed to warm up at  $0\text{ }^{\circ}\text{C}$ . *B,B',B''*-trichloro-*N,N',N''*-tri[(4-*tert*-butyl)phenyl]-borazine was cannulated dropwise to the *organolithium* derivative solution at  $0\text{ }^{\circ}\text{C}$  and allowed to react at r.t. for 24 h. The reaction

mixture was diluted with 15 mL of H<sub>2</sub>O, extracted with EtOAc (3 × 20 mL) and the combined organic phases dried over MgSO<sub>4</sub> and the solvents removed under reduced pressure. The product was purified by precipitation in MeOH (0.42 g, **74%**) as a white solid. Two isomers were obtained (*cc:ct* 1:5). The characterisation here reported corresponds to both isomers together.

**M.P.:** 293 °C. **<sup>1</sup>H-NMR** (300 MHz, CDCl<sub>3</sub>):  $\delta$  = 6.87-6.62 (*m*, 110 H), 6.51-6.46 (*m*, 24 H), 6.26-6.23 (*m*, 20 H), 3.31 (*s*, 15 H), 3.28 (*s*, 30 H), 3.26 (*s*, 9 H), 1.06 (*s*, 162 H) ppm. **<sup>11</sup>B-NMR** (128 MHz, CDCl<sub>3</sub>):  $\delta$  = 36.02 ppm. **<sup>13</sup>C-NMR** (75 MHz, CDCl<sub>3</sub>):  $\delta$  = 160.46, 160.36, 160.24, 145.85, 145.76, 144.52, 144.40, 133.32, 128.12, 127.93, 122.99, 119.25, 108.54, 54.74, 54.65, 54.58, 34.02, 31.43 ppm (some peaks missing due to overlap). **IR** (cm<sup>-1</sup>):  $\nu$  = 418.55, 590.22, 669.30, 704.02, 738.74, 750.31, 794.67, 839.03, 1024.20, 1045.42, 1082.07, 1109.07, 1126.43, 1161.15, 1180.44, 1236.37, 1265.30, 1313.52, 1431.18, 1485.19, 1516.05, 1573.91, 2341.58, 2833.43. **MS** (ESI-HRMS): Found 796.5077 [M+H]<sup>+</sup>, C<sub>51</sub>H<sub>61</sub>B<sub>3</sub>N<sub>3</sub>O<sub>3</sub> requires = 796.4992.

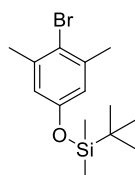


### ***B,B',B''*-Tri[2-(fluoro)phenyl]-*N,N',N''*-tri(phenyl)borazine 2-33**

In a flame-dried 100-mL *Schlenk* flask, aniline (0.35 g, 3.76 mmol) was diluted with 6 mL of anhydrous toluene and cooled to -5 °C (ice-salt bath). A solution of BCl<sub>3</sub> (4.88 mL, 4.88 mmol, 1 M solution in heptane) was added dropwise. The septum was changed for a

flame-dried condenser topped by a CaCl<sub>2</sub> tube and the resulting mixture refluxed for 16 h. The reaction solution was cooled down to 0 °C, the condenser was changed for a septum under argon, and the flask subjected to five *freeze-to-thaw* cycle to remove the remaining HCl. In parallel, to a flame-dried 100 mL *Schlenk* flask, 2-bromofluorobenzene (0.72 g, 4.12 mmol) was dissolved in 9 mL of anhydrous THF and *n*-BuLi (2.82 mL, 4.515 mmol, 1.6 M in hexane) added dropwise at -84 °C. *B,B',B''*-trichloro-*N,N',N''*-triphenyl-borazine **1-3** was cannulated dropwise to the *organolithium* solution at -84 °C and allowed to react at that temperature for 3 h, then stirred 3 h at 0 °C, and finally 12 h at r.t. The reaction mixture was diluted with 15 mL of H<sub>2</sub>O, extracted with EtOAc (3 × 20 mL), the combined organic phases dried over MgSO<sub>4</sub> and the solvents removed under reduced pressure. The product was purified by precipitation in MeOH (0.34 g, **46%**) as a white solid. Two isomers were obtained (*cc:ct* 5:1). The characterisation here reported corresponds to both isomers together.

**M.P.:** > 320 °C. **<sup>1</sup>H-NMR** (300 MHz, CDCl<sub>3</sub>): δ = 7.12-7.07 (*m*, 2 H), 6.98 – 6.64 (*m*, 22 H), 6.56-6.49 (*m*, 3 H) ppm. **<sup>11</sup>B-NMR** (128 MHz, CDCl<sub>3</sub>): δ = 34.84 ppm. **<sup>13</sup>C-NMR** (125 MHz, CDCl<sub>3</sub>): δ = 163.81 (*t*, *J* = 3.9 Hz), 161.92 (*t*, *J* = 2.7 Hz), 146.08, 146.02, 132.87 (*d*, *J* = 9.9 Hz), 129.25 (*d*, *J* = 8.1 Hz), 128.96 – 128.57 (*m*), 128.57 – 128.10 (*m*), 128.00 (*d*, *J* = 10.6 Hz), 127.63 (*d*, *J* = 9.7 Hz), 127.13 (*d*, *J* = 9.3 Hz), 124.75 (*d*, *J* = 3.5 Hz), 122.75 (*d*, *J* = 2.4 Hz), 113.77 (*d*, *J* = 4.3 Hz), 113.52 (*d*, *J* = 15.8 Hz) ppm. **<sup>19</sup>F-NMR** (470 MHz): δ = -102.25, -102.55, -102.85 ppm. **IR** (cm<sup>-1</sup>): ν = 418.55, 459.06, 526.57, 557.43, 694.37, 725.23, 754.17, 808.17, 842.89, 937.40, 1026.13, 1072.42, 1153.43, 1211.30, 1246.02, 1257.59, 1313.52, 1436.97, 1490.97, 1595.13, 1612.49, 2962.66, 3026.31, 3059.10. **MS** (ES-HRMS): Found 591.2565 [M]<sup>+</sup>, C<sub>36</sub>H<sub>27</sub>B<sub>3</sub>F<sub>3</sub>N<sub>3</sub> requires = 591.2436.

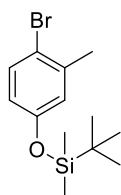


Chemical Formula: C<sub>14</sub>H<sub>23</sub>BrOSi  
Exact Mass: 314,07  
Molecular Weight: 315,32

#### (4-bromo-3,5-dimethylphenoxy)(*tert*-butyl)dimethylsilane 2-35

To a solution of 4-bromo-3,5-dimethylphenol (10.0 g, 49.8 mmol) in DMF (60 mL), TBDMS-Cl (10.5 g, 69.7 mmol), and imidazol (10.2 g, 150 mmol) were added and stirred at 50 °C for 16 h. The resulting mixture was diluted with EtOAc (200 mL), washed with water (3 × 200 mL) and brine (1 × 150 mL), and dried over MgSO<sub>4</sub>. Removal of the solvents and the excess of *tert*-butyl-dimethylsilyl under reduced pressure yielded compound **2-35** as a yellow oil (15.5 g, **99%**).

<sup>1</sup>H-NMR (400 MHz, CDCl<sub>3</sub>): δ = 6.58 (s, 6 H), 2.35 (s, 6 H), 0.98 (s, 9 H), 0.18 (s, 6 H) ppm. <sup>13</sup>C-NMR (100 MHz, CDCl<sub>3</sub>): δ = 154.22, 139.09, 120.00, 119.07, 25.76, 23.98, 18.26, -4.34 ppm. IR (cm<sup>-1</sup>): ν = 460.87, 469.72, 496.95, 524.01, 569.33, 673.42, 695.61, 778.72, 834.13, 864.97, 939.08, 977.96, 1005.73, 1019.95, 1031.36, 1052.62, 1166.6, 1252.45, 1321.15, 1361.9, 1390.06, 1409.75, 1464.27, 1581.86, 2857.62, 2896.32, 2929.33, 2954.99. MS (ESI-HRMS): Found 315.0774 [M+H]<sup>+</sup>, C<sub>14</sub>H<sub>24</sub>BrOSi requires= 314.0780.



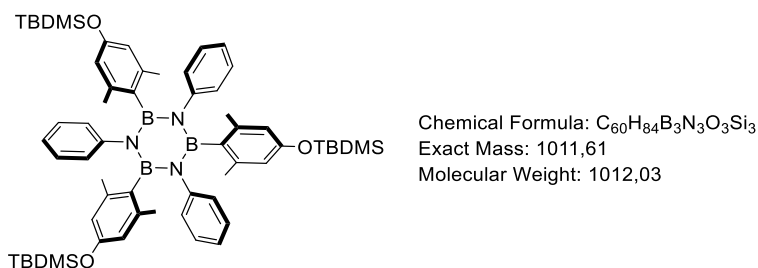
Chemical Formula: C<sub>13</sub>H<sub>21</sub>BrOSi  
Exact Mass: 300,05  
Molecular Weight: 301,30

#### (4-bromo-3-methylphenoxy)(*tert*-butyl)dimethylsilane 2-36

To a solution of 4-bromo-3-methylphenol (5.5 g, 29.8 mmol) in DMF (32 mL), TBDMS-Cl (6.2 g, 41.5 mmol), and imidazol (6 g, 87.6 mmol) were added and stirred at 50 °C for

16 h. The resulting mixture was diluted with EtOAc (200 mL), washed with water ( $3 \times 200$  mL) and brine ( $1 \times 150$  mL), and dried over  $\text{MgSO}_4$ . Removal of the solvents and the excess of *tert*-butyl-dimethylsilyl under reduced pressure yielded compound **2-36** as a yellow oil (8.82 g, **99%**).

**$^1\text{H}$ -NMR** (400 MHz,  $\text{CDCl}_3$ ):  $\delta$  = 7.15 (*d*,  $J$  = 8.5 Hz, 1 H), 6.54 (*s*, 1 H), 6.36 (*d*,  $J$  = 8.5 Hz, 1 H), 2.14 (*s*, 3 H), 0.79 (*s*, 9 H), 0.00 (*s*, 6 H) ppm.  **$^{13}\text{C}$ -NMR** (125 MHz,  $\text{CDCl}_3$ ):  $\delta$  = 154.97, 138.91, 132.89, 122.74, 119.25, 116.32, 25.77, 23.17, 18.31, -4.33 ppm. **IR** ( $\text{cm}^{-1}$ ):  $\nu$  = 418.55, 443.63, 549.71, 580.57, 617.22, 669.30, 696.30, 779.24, 812.03, 867.97, 939.33, 966.34, 1028.77, 1029.99, 1118.71, 1168.86, 1242.16, 1290.38, 1361.74, 1398.39, 1471.69, 1570.06, 1595.13, 2341.58, 2360.87, 2858.51, 2895.15, 2929.87, 2954.95, 3595.31, 3628.10, 3691.75, 3726.47. **Ms** (ESI-HRMS): Found 300.0544  $[\text{M}+\text{H}]^+$ ,  $\text{C}_{13}\text{H}_{21}\text{BrOSi}$  requires = 300.0623.

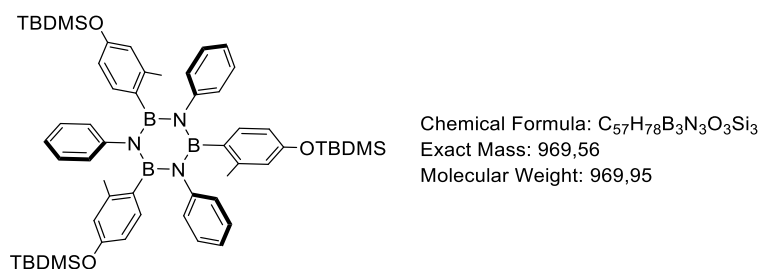


***B,B',B''*-tri[4-((*tert*-butyldimethylsilyl)oxy)-2,6-(dimethyl)phenyl]-*N,N',N''*-tri(phenyl)-borazine 2-37**

In a flame-dried 100-mL *Schlenk* flask, aniline (1 g, 10.7 mmol) was diluted with 24 mL of anhydrous toluene and cooled to  $-5\text{ }^\circ\text{C}$  (ice-salt bath). A solution of  $\text{BCl}_3$  (13 mL, 13 mmol, 1 M solution in toluene) was added dropwise. The septum was changed for a flame-dried condenser topped by a  $\text{CaCl}_2$  tube and the resulting mixture refluxed for 16 h. The reaction

solution was cooled down to 0 °C, the condenser was changed for a septum under argon, and the flask subjected to three *freeze-to-thaw* cycle to remove the remaining HCl. In parallel, to a flame-dried 100 mL *Schlenk* flask, **2-35** (4.6 g, 16 mmol) was dissolved in 25 mL of anhydrous THF and *t*-BuLi (18 mL, 25 mmol, 1.7 M in hexane) added dropwise at -84 °C. The flask was allowed to warm up at 0 °C. *B,B',B''*-trichloro-*N,N',N''*-triphenylborazine **1-3** was cannulated dropwise to the *organolithium* derivative solution at 0 °C and allowed to react at r.t. for 24 h. The reaction mixture was diluted with 20 mL of H<sub>2</sub>O, extracted with EtOAc (3 × 30 mL), the combined organic phases dried over MgSO<sub>4</sub>, and the solvents removed under reduced pressure. The product was purified by precipitation in MeOH (1.85 g, **52%**) as a white solid.

**M.P.**: 206 °C. **<sup>1</sup>H-NMR** (400 MHz, CDCl<sub>3</sub>): δ = 6.79-6.68 (*m*, 15 H), 6.06 (*s*, 6 H), 2.19 (*s*, 18 H) 0.84 (*s*, 27 H), -0.04 (*s*, 18 H) ppm. **<sup>11</sup>B-NMR** (128 MHz, CDCl<sub>3</sub>): δ = 36.05 ppm. **<sup>13</sup>C-NMR** (100 MHz, CDCl<sub>3</sub>): δ = 154.58, 146.23, 138.96, 133.15, 127.12, 126.70, 124.12, 117.60, 25.81, 23.07, 18.27, -4.50 ppm. **IR** (cm<sup>-1</sup>): ν = 470.11, 518.75, 565.09, 579.02, 617.95, 666.53, 683.96, 698.43, 736.54, 758.26, 778.53, 814.05, 835.76, 848.2, 848.51, 866.51, 904.69, 938.92, 967.82, 1005.57, 1037.98, 1074.67, 1087.19, 1150.76, 1191.84, 1251.38, 1303.38, 1356.81, 1452.53, 1462.76, 1471.67, 1491.27, 1562.22, 1597.15, 2857.3, 2929.15, 2955.44, 3039.83. **HRMS** (MALDI, matrix: DCTB, *m/z*): Found 1012.6193 [M+H]<sup>+</sup>, C<sub>60</sub>H<sub>85</sub>B<sub>3</sub>N<sub>3</sub>O<sub>3</sub>Si<sub>3</sub> requires = 1012.6178.

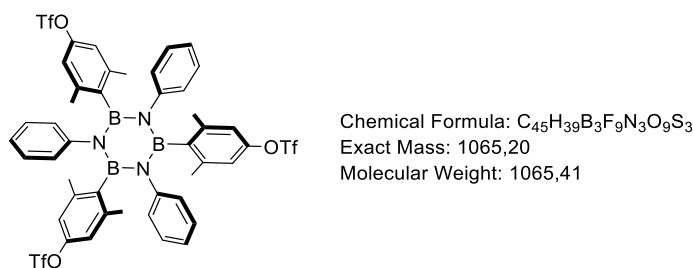


***B,B',B''*-tri[4-((*tert*-butyldimethylsilyl)oxy)-2-(dimethyl)phenyl]-*N,N',N''*-tri(phenyl)-borazine 2-38**

In a flame-dried 100-mL *Schlenk* flask, aniline (0.2 g, 2.19 mmol) was diluted with 4 mL of anhydrous toluene and cooled to -5 °C (ice-salt bath). A solution of  $BCl_3$  (2.62 mL, 2.62 mmol, 1 M solution in toluene) was added dropwise. The septum was changed for a flame-dried condenser topped by a  $CaCl_2$  tube and the resulting mixture refluxed for 16 h. The reaction solution was cooled down to 0 °C, the condenser was changed for a septum under argon, and the flask subjected to three *freeze-to-thaw* cycle to remove the remaining HCl. In parallel, to a flame-dried 100 mL *Schlenk* flask, **2-36** (0.73 g, 2.4 mmol) was dissolved in 12 mL of anhydrous THF and *n*-BuLi (1.8 mL, 2.84 mmol, 1.6 M in hexane) added dropwise at -84 °C. The flask was allowed to warm up at 0 °C. *B,B',B''*-trichloro-*N,N',N''*-triphenyl-borazine **1-3** was cannulated dropwise to the *organolithium* derivative solution at 0 °C and allowed to react at r.t. for 24 h. The reaction mixture was diluted with 20 mL of  $H_2O$ , extracted with EtOAc (3 × 30 mL), the combined organic phases dried over  $MgSO_4$ , and the solvents removed under reduced pressure. The product was purified by precipitation in MeOH (0.23 g, **32%**) as a white solid. Two isomers were formed (*cc:ct* 1:3). The characterisation here reported corresponds to the mixture of both isomers.

**M.P.:** 199 °C.  **$^1H$ -NMR** (400 MHz,  $CDCl_3$ ):  $\delta$ = 6.88-6.67 (*m*, 72 H), 6.29-6.12 (*m*, 24 H), 2.13 (*s*, 9 H), 2.07 (*s*, 18 H), 2.00 (*s*, 9 H), 0.84 (*s*, 108 H), 0.03 (*s*, 72 H) ppm.  **$^{11}B$ -NMR** (128 MHz,  $CDCl_3$ ):  $\delta$ = 36.05 ppm.  **$^{13}C$ -NMR** (100 MHz,  $CDCl_3$ ):  $\delta$ = 154.30, 154.28,

146.65, 146.59, 146.44, 139.71, 139.64, 139.58, 133.46, 133.18, 132.92, 129.69, 128.84, 127.55, 127.12, 127.04, 123.83, 120.15, 116.21, 116.09, 115.96, 25.87, 23.01, 22.92, 22.82, 18.34, 4.44 ppm (some peaks missing due to overlap). **IR** ( $\text{cm}^{-1}$ ):  $\nu$  = 435.27, 520.78, 559.36, 594.08, 646.15, 696.30, 3088.03, 713.66, 748.38, 763.81, 777.31, 815.89, 837.11, 856.39, 904.61, 939.33, 964.41, 1006.84, 1074.35, 1116.78, 1163.08, 1230.58, 1251.80, 1284.59, 1454.33, 1471.69, 1490.97, 1560.41, 1598.99, 2856.58, 2929.87, 2954.95, 3037.89, 3062.96. **MS** (ESI-HRMS): Found 970.5444  $[\text{M}+\text{H}]^+$ ,  $\text{C}_{57}\text{H}_{79}\text{B}_3\text{N}_3\text{O}_3\text{Si}_3$  requires = 970.5736.

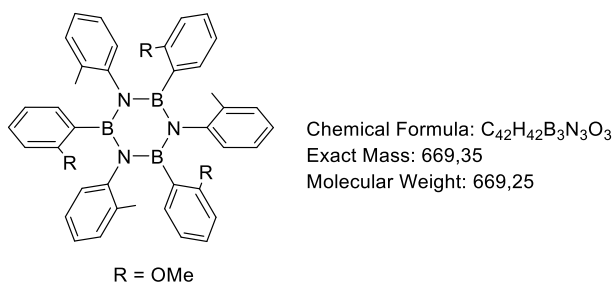


***B,B',B''*-tris[2,6-(dimethyl)-4-(((trifluoromethyl)sulfonyl)oxy)-phenyl]*N,N',N''*-tri(phenyl)-borazine 2-39**

To a solution of **2-37** in THF (30 mL) at 0 °C, TBAF (5.22 mL, 5.22 mmol) was added dropwise and stirred at 0 °C for 2 h. The resulting mixture was filtered off, dried under vacuum, and used directly for the next step by solution in pyridine (24 mL) and cooled at -5 °C. Addition of  $\text{Tf}_2\text{O}$  (2.82 mL, 17 mmol) dropwise lead to a red solution and stirred overnight at r.t. The resulting mixture was quenched with water, extracted with EtOAc ( $3 \times 20$  mL), and the combination of the organic layers dried over  $\text{MgSO}_4$ . Removal of the solvents under reduced pressure and purification of the compound by column

chromatography (eluent: CHX/EtOAc 9:1) yielded compound **2-39** (1.3 g, **78%**) as a white solid.

**M.P.:** 236-238 °C. **<sup>1</sup>H-NMR** (400 MHz, CDCl<sub>3</sub>):  $\delta$  = 6.81-6.74 (*m*, 15 H), 6.48 (*s*, 6 H), 2.31 (*s*, 18 H). **<sup>11</sup>B-NMR** (128 MHz, CDCl<sub>3</sub>):  $\delta$  = 35.68 ppm. **<sup>13</sup>C-NMR** (100 MHz, CDCl<sub>3</sub>):  $\delta$  = 149.18, 144.80, 140.32, 127.47, 126.37, 125.44, 120.22, 118.03, 27.00, 23.19 ppm. **<sup>19</sup>F-NMR** (376 MHz, CDCl<sub>3</sub>):  $\delta$  = -72.27 ppm. **IR** (cm<sup>-1</sup>):  $\nu$  = 531.51, 568.27, 582.87, 610.15, 648.01, 701.64, 748.68, 769.42, 813.16, 844.82, 870.17, 908.64, 945.78, 1012.81, 1075.81, 1120.98, 1141.01, 1207.06, 1239.85, 1310.89, 1364.41, 1418.87, 1492.23, 1590.18, 2924.08. **HRMS** (MALDI, matrix: DCTB, *m/z*): Found 1066.2067 [M+H]<sup>+</sup>, C<sub>45</sub>H<sub>40</sub>B<sub>3</sub>F<sub>9</sub>N<sub>3</sub>O<sub>9</sub>S<sub>3</sub> requires = 1066.2062.

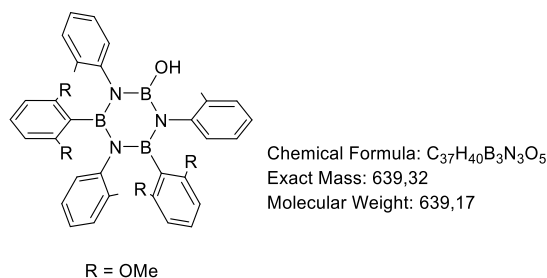


### ***B,B',B''*-tri[2-(methoxy)phenyl]-*N,N',N''*-tri[2-(methyl)phenyl]-borazine 3-6**

In a flame-dried 100-mL *Schlenk* flask, 2-methylaniline (0.403 g, 3.76 mmol) was diluted with 6 mL of anhydrous toluene and cooled to -5 °C (ice-salt bath). A solution of BCl<sub>3</sub> (4.88 mL, 4.88 mmol, 1 M solution in heptane) was added dropwise. The septum was changed for a flame-dried condenser topped by a CaCl<sub>2</sub> tube and the resulting mixture refluxed for 16 h. The reaction solution was cooled down to 0 °C, the condenser was changed for a septum under argon, and the flask subjected to five *freeze-to-thaw* cycle to remove the remaining HCl. In parallel, to a flame-dried 100 mL *Schlenk* flask,

2-bromoanisole (0.77 g, 4.136 mmol) was dissolved in 9 mL of anhydrous THF and *n*-BuLi (2.82 mL, 4.512 mmol, 1.6 M in hexane) added dropwise at -84 °C. The flask was allowed to warm up at 0 °C. *B,B',B''*-trichloro-*N,N',N''*-tri[2-(methyl)phenyl]-borazine was cannulated dropwise to the *organolithium* derivative solution at 0 °C and allowed to react at r.t. for 24 h. The reaction mixture was diluted with 15 mL of H<sub>2</sub>O, extracted with EtOAc (3 × 20 mL), the combined organic phases dried over MgSO<sub>4</sub> and the solvents removed under reduced pressure. The product was purified by precipitation in MeOH (0.540 g, **65%**) as a white solid. The product was composed by a mixture of isomers which separation was not possible. The characterisation here reported corresponds to the mixture of isomers.

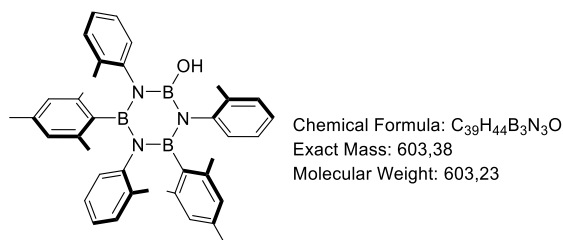
**M.P.:** > 320 °C. **<sup>1</sup>H-NMR** (300 MHz, CDCl<sub>3</sub>): δ = 7.16-6.20 (*m*, 24 H), 3.69-3.26 (*m*, 9 H), 2.32-2.06 (*m*, 9 H) ppm. **<sup>11</sup>B-NMR** (128 MHz, CDCl<sub>3</sub>): δ = 36.46 ppm. **<sup>13</sup>C-NMR** (100 MHz, CDCl<sub>3</sub>): δ = 160.24, 160.21, 160.14, 160.10, 160.02, 159.96, 159.88, 146.14, 146.06, 145.98, 145.88, 145.83, 145.76, 145.62, 134.87, 134.61, 134.47, 133.05, 132.75, 130.53, 130.07, 129.53, 129.05, 128.79, 128.69, 128.40, 128.30, 124.42, 124.27, 124.11, 123.75, 118.87, 108.13, 107.97, 54.63, 54.56, 54.09, 54.05, 53.57, 19.19, 19.12, 18.93, 18.86, 18.81, 18.67, 18.63, 18.50 ppm. **IR** (cm<sup>-1</sup>): ν = 443.63, 460.99, 493.78, 551.64, 584.43, 721.38, 752.24, 786.96, 806.25, 846.75, 931.62, 1026.13, 1047.35, 1080.14, 1112.93, 1128.36, 1161.15, 1178.51, 1232.51, 1267.23, 1305.81, 1363.67, 1427.32, 1448.54, 1485.19, 1571.99, 1597.06, 2829.57, 2926.01, 3014.74. **MS** (ESI-HRMS): Found 670.3657 [M+H]<sup>+</sup>, C<sub>42</sub>H<sub>43</sub>B<sub>3</sub>N<sub>3</sub>O<sub>3</sub> requires = 670.3604.



### **B,B'-Bis-[2,6-(dimethoxy)phenyl]-B''-hydroxy-*N,N',N''*-tri[2-(methyl)phenyl]-borazine 3-7**

In a flame-dried 100-mL *Schlenk* flask, 2-methylaniline (0.403 g, 3.76 mmol) was diluted with 6 mL of anhydrous toluene and cooled to  $-5\text{ }^{\circ}\text{C}$  (ice-salt bath). A solution of  $\text{BCl}_3$  (4.88 mL, 4.88 mmol, 1 M solution in heptane) was added dropwise. The septum was changed for a flame-dried condenser topped by a  $\text{CaCl}_2$  tube and the resulting mixture refluxed for 16 h. The reaction solution was cooled down to  $0\text{ }^{\circ}\text{C}$ , the condenser was changed for a septum under argon, and the flask subjected to five *freeze-to-thaw* cycle to remove the remaining HCl. In parallel, to a flame-dried 100 mL *Schlenk* flask, 2,6-dimethoxybromobenzene (0.90 g, 4.136 mmol) was dissolved in 9 mL of anhydrous THF and *n*-BuLi (2.82 mL, 4.512 mmol, 1.6 M in hexane) added dropwise at  $-84\text{ }^{\circ}\text{C}$ . The flask was allowed to warm up at  $0\text{ }^{\circ}\text{C}$ . *B,B',B''*-trichloro-*N,N',N''*-tri[2-(methyl)phenyl]-borazine was cannulated dropwise to the *organolithium* solution at  $0\text{ }^{\circ}\text{C}$  and allowed to react at r.t. for 24 h. The reaction mixture was diluted with 15 mL of  $\text{H}_2\text{O}$ , extracted with EtOAc ( $3 \times 20\text{ mL}$ ), the combined organic phases dried over  $\text{MgSO}_4$  and the solvents removed under reduced pressure. The product was purified by precipitation in MeOH (0.33 g, **39%**) as a white solid. The three possible isomers were found, and the characterisation here reported corresponds to the mixture of the three of them.

**M.P.:** 250 °C. **<sup>1</sup>H-NMR** (400 MHz, CDCl<sub>3</sub>):  $\delta$  = 7.23-6.58 (*m*, 12 H) 6.13-5.93 (*m*, 4 H) 3.80-3.40 (*m*, 12 H), 3.01 (*s*, 1 H), 2.50-2.22 (*m*, 9 H) ppm. **<sup>11</sup>B-NMR** (128 MHz, CDCl<sub>3</sub>):  $\delta$  = 35.66, 24.50 ppm. **<sup>13</sup>C-NMR** (100 MHz, CDCl<sub>3</sub>):  $\delta$  = 161.26, 161.22, 160.86, 160.85, 160.72, 160.68, 146.11, 146.09, 143.55, 143.51, 143.42, 135.41, 135.37, 135.33, 135.29, 135.13, 129.82, 129.60, 129.56, 129.19, 129.11, 129.02, 128.98, 128.50, 128.48, 128.42, 128.39, 125.56, 125.50, 125.34, 125.24, 125.16, 124.08, 124.03, 123.10, 101.87, 101.69, 101.65, 101.61, 54.81, 54.68, 54.30, 53.98, 53.93, 18.24, 17.92, 17.51, 17.45 ppm (some peaks missing due to overlap). **IR** (cm<sup>-1</sup>):  $\nu$  = 416.62, 474.49, 553.57, 578.64, 596.00, 721.38, 738.74, 759.95, 842.89, 1035.77, 1109.07, 1240.23, 1367.53, 1427.32, 1462.04, 1490.97, 1593.20, 2158.35, 2829.57, 2929.87, 2954.95. **MS** (ESI-HRMS): Found 640.3370 [M+H]<sup>+</sup>, C<sub>37</sub>H<sub>41</sub>B<sub>3</sub>N<sub>3</sub>O<sub>5</sub> requires = 640.3344.

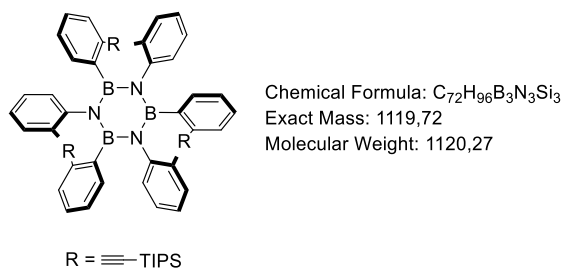


### **B,B'-Bis-(mesityl)-B''-hydroxy-*N,N',N''*-tri[2-(methyl)phenyl]-borazine 3-8**

In a flame-dried 100-mL *Schlenk* flask, 2-methylaniline (0.403 g, 3.76 mmol) was diluted with 6 mL of anhydrous toluene and cooled to -5 °C (ice-salt bath). A solution of BCl<sub>3</sub> (4.88 mL, 4.88 mmol, 1 M solution in heptane) was added dropwise. The septum was changed for a flame-dried condenser topped by a CaCl<sub>2</sub> tube and the resulting mixture refluxed for 16 h. The reaction solution was cooled down to 0 °C, the condenser was changed for a septum under argon, and the flask subjected to five *freeze-to-thaw* cycle to

remove the remaining HCl. In parallel, to a flame-dried 100 mL *Schlenk* flask, 2-bromomesitylene (0.823 g, 4.136 mmol) was dissolved in 9 mL of anhydrous THF and *n*-BuLi (2.82 mL, 4.512 mmol, 1.6 M in hexane) added dropwise at -84 °C. The flask was allowed to warm up at 0 °C. *B,B',B''*-trichloro-*N,N',N''*-tri-[2-(methyl)phenyl]-borazine was cannulated dropwise to the *organolithium* solution at 0 °C and allowed to react at r.t. for 24 h. The reaction mixture was diluted with 15 mL of H<sub>2</sub>O, extracted with EtOAc (3 × 20 mL) and the combined organic phases dried over MgSO<sub>4</sub> and the solvents removed under reduced pressure. The product was purified by precipitation in MeOH (0.17 g, **20%**) as a white solid. The mixture was enriched in isomer *cc*.

**M.P.:** 295 °C. **<sup>1</sup>H-NMR** (300 MHz, CDCl<sub>3</sub>):  $\delta$  = 7.11 (*d*, *J* = 7.5 Hz, 2 H), 7.05 (*d*, *J* = 7.7 Hz, 1 H), 6.99-6.83 (*m*, 6 H), 6.77 (*d*, *J* = 7.4 Hz, 1 H), 6.71-6.58 (*m*, 2 H), 6.51 (*s*, 2 H), 6.25 (*s*, 2 H), 3.40 (*s*, 1 H), 2.59 (*s*, 6 H), 2.52 (*s*, 6 H), 2.32 (*s*, 3 H), 2.00 (*s*, 6 H), 1.94 (*s*, 6 H) ppm. **<sup>11</sup>B-NMR** (128 MHz, CDCl<sub>3</sub>):  $\delta$  = 37.33, 24.92 ppm. **<sup>13</sup>C-NMR** (100 MHz, CDCl<sub>3</sub>):  $\delta$  = 144.84, 142.46, 138.25, 138.11, 135.96, 133.97, 133.79, 130.40, 129.54, 128.62, 128.15, 126.64, 126.43, 126.14, 125.62, 124.52, 124.35, 24.35, 23.54, 21.08, 19.52, 18.79 ppm (the <sup>13</sup>C resonance corresponding to the carbon atom bonded to the boron atom is not observed due to the quadrupolar relaxation). **IR** (cm<sup>-1</sup>):  $\nu$  = 426.27, 464.84, 669.30, 723.31, 761.88, 848.68, 1083.99, 1114.86, 1168.86, 1365.60, 1392.61, 1435.04, 1489.05, 1610.56, 2341.58, 2358.94. **MS** (ESI-HRMS): Found 603.3807 [M]<sup>+</sup>, C<sub>39</sub>H<sub>44</sub>B<sub>3</sub>N<sub>3</sub>O requires = 603.3782.

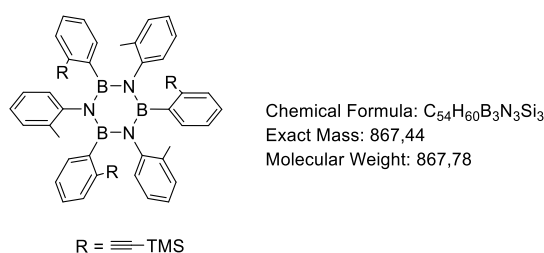


***B,B',B''*-tri[2-((triisopropylsilyl)ethynyl)phenyl]-*N,N',N''*-tri[2-(methyl)phenyl]-borazine 3-9**

In a flame-dried 100-mL *Schlenk* flask, 2-methylaniline (0.403 g, 3.76 mmol) was diluted with 6 mL of anhydrous toluene and cooled to -5 °C (ice-salt bath). A solution of  $BCl_3$  (4.88 mL, 4.88 mmol, 1 M solution in heptane) was added dropwise. The septum was changed for a flame-dried condenser topped by a  $CaCl_2$  tube and the resulting mixture refluxed for 16 h. The reaction solution was cooled down to 0 °C, the condenser was changed for a septum under argon, and the flask subjected to five *freeze-to-thaw* cycle to remove the remaining HCl. In parallel, to a flame-dried 100 mL *Schlenk* flask, compound **2-12** (1.39 g, 4.136 mmol) was dissolved in 9 mL of anhydrous THF and *n*-BuLi (2.82 mL, 4.512 mmol, 1.6 M in hexane) added dropwise at -84 °C. The flask was allowed to warm up at 0 °C. *B,B',B''*-trichloro-*N,N',N''*-tri[2-(methyl)phenyl]-borazine was cannulated dropwise to the organolithium solution at 0 °C and allowed to react at r.t. for 24 h. The reaction mixture was diluted with 15 mL of  $H_2O$ , extracted with EtOAc (3 × 20 mL), the combined organic phases dried over  $MgSO_4$  and the solvents removed under reduced pressure. The product was purified by precipitation in MeOH (0.33 g, **24%**) as a white solid. The mixture was enriched in isomer *cc/cc*.

**M.P.:** 225 °C.  **$^1H$ -NMR** (400 MHz,  $CDCl_3$ ):  $\delta$  = 6.96 (*dd*,  $J_1 = 14.3$ ,  $J_1 = 6.3$  Hz, 3 H), 6.87 (*d*,  $J = 7.7$  Hz, 3 H), 6.76 (*t*,  $J = 7.4$  Hz, 3 H), 6.72-6.64 (*m*, 6 H), 6.51 (*dd*,  $J_1 = 13.6$ ,

$J_2 = 6.4$  Hz, 3 H), 6.35 (*t*,  $J = 7.6$  Hz, 1 H), 6.22 (*d*,  $J = 7.8$  Hz, 1 H), 2.65-2.39 (*m*, 9 H), 1.03-0.94 (*m*, 63 H) ppm.  $^{11}\text{B}$ -NMR (128 MHz,  $\text{CDCl}_3$ ):  $\delta = 36.76$  ppm.  $^{13}\text{C}$ -NMR (100 MHz,  $\text{CDCl}_3$ ):  $\delta = 144.56, 136.18, 134.94, 134.44, 130.42, 130.16, 126.37, 125.77, 124.97, 124.28, 123.87, 110.51, 93.21, 21.32, 18.99, 11.84$  ppm (the  $^{13}\text{C}$  resonance corresponding to the carbon atom bonded to the boron atom is not observed due to the quadrupolar relaxation). IR ( $\text{cm}^{-1}$ ):  $\nu = 457.13, 511.14, 547.78, 648.08, 657.75, 723.31, 756.10, 833.25, 860.25, 1246.02, 1361.74, 1490.97, 2158.35, 2962.66$ . MS (ESI-HRMS): The mass found does not match with the desired compound, even though the formation of this compound was confirmed in the subsequent deprotection reaction.

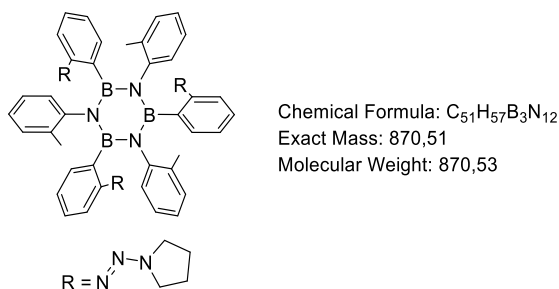


### ***B,B',B''*-tri[2-((trimethylsilyl)ethynyl)phenyl]-*N,N',N''*-tri[2-(methyl)phenyl]-borazine 3-10**

In a flame-dried 100-mL *Schlenk* flask, 2-methylaniline (0.30 g, 2.81 mmol) was diluted with 5 mL of anhydrous toluene and cooled to  $-5$  °C (ice-salt bath). A solution of  $\text{BCl}_3$  (3.6 mL, 3.6 mmol, 1 M solution in heptane) was added dropwise. The septum was changed for a flame-dried condenser topped by a  $\text{CaCl}_2$  tube and the resulting mixture refluxed for 16 h. The reaction solution was cooled down to  $0$  °C, the condenser was changed for a septum under argon, and the flask subjected to five *freeze-to-thaw* cycle to remove the remaining HCl. In parallel, to a flame-dried 100 mL *Schlenk* flask, compound **2-13** (0.7 g,

2.8 mmol) was dissolved in 8 mL of anhydrous THF and *n*-BuLi (1.92 mL, 3.08 mmol, 1.6 M in hexane) added dropwise at -84 °C. The flask was allowed to warm up at 0 °C. *B,B',B''*-trichloro-*N,N',N''*-tri[2-(methyl)phenyl]-borazine was cannulated dropwise to the *organolithium* solution at 0 °C and allowed to react at r.t. for 24 h. The reaction mixture was diluted with 15 mL of H<sub>2</sub>O, extracted with EtOAc (3 × 20 mL) and the combined organic phases dried over MgSO<sub>4</sub> and the solvents removed under reduced pressure. The product was purified by precipitation in MeOH (0.43 g, **52%**) as a white solid. A mixture of isomers was obtained and reported in the following characterisation.

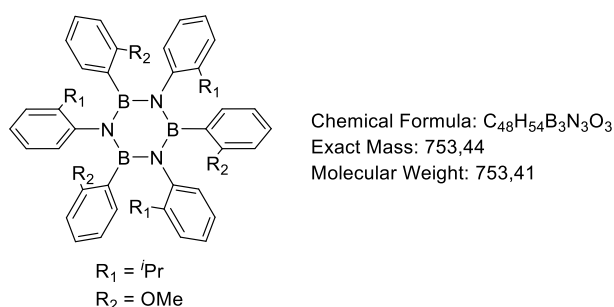
**M.P.:** 260 °C. **<sup>1</sup>H-NMR** (500 MHz, CDCl<sub>3</sub>):  $\delta$  = 7.10-6.42 (*m*, 24 H), 2.70-1.91 (*m*, 9 H), 0.52-0.08 (*m*, 27 H) ppm. **<sup>11</sup>B-NMR** (128 MHz, CDCl<sub>3</sub>):  $\delta$  = 36.31 ppm. **<sup>13</sup>C-NMR** (125 MHz, CDCl<sub>3</sub>):  $\delta$  = 144.50, 144.47, 136.31, 136.23, 134.13, 134.10, 133.80, 133.48, 133.18, 132.89, 132.49, 132.04, 130.98, 130.76, 130.14, 130.12, 128.61, 126.54, 126.43, 126.37, 126.07, 125.78, 125.25, 125.19, 124.70, 124.55, 124.46, 124.45, 124.38, 124.06, 123.99, 108.65, 108.03, 107.87, 95.62, 95.50, 95.34, 21.09, 20.80, 19.27, 1.17, 0.64, 0.60, 0.29 ppm. **IR** (cm<sup>-1</sup>):  $\nu$  = 412.77, 460.99, 503.42, 547.78, 572.86, 596.00, 698.23, 723.31, 856.10, 837.11, 866.04, 1074.35, 1107.14, 1247.94, 1261.45, 1311.28, 1429.25, 1489.05, 1489.34, 1589.34, 2152.56, 2956.87. **MS** (ESI-HRMS): Found 868.4478 [M+H]<sup>+</sup>, C<sub>54</sub>H<sub>61</sub>B<sub>3</sub>N<sub>3</sub>Si<sub>3</sub> requires = 868.4478.



***B,B',B''*-tri[2-(pyrrolidin-1-yl)diazenyl]phenyl-*N,N',N''*-tri[2-(methyl)phenyl]-borazine 3-11**

In a flame-dried 100-mL *Schlenk* flask, 2-methylaniline (0.403 g, 3.76 mmol) was diluted with 6 mL of anhydrous toluene and cooled to -5 °C (ice-salt bath). A solution of BCl<sub>3</sub> (4.88 mL, 4.88 mmol, 1 M solution in heptane) was added dropwise. The septum was changed for a flame-dried condenser topped by a CaCl<sub>2</sub> tube and the resulting mixture refluxed for 16 h. The reaction solution was cooled down to 0 °C, the condenser was changed for a septum under nitrogen, and the flask subjected to five *freeze-to-thaw* cycle to remove the remaining HCl. In parallel, to a flame-dried 100 mL *Schlenk* flask, compound **2-16** (0.955 g, 3.76 mmol) was dissolved in 9 mL of anhydrous THF and *n*-BuLi (2.82 mL, 2.82 mmol, 1.6 M in hexane) added dropwise at -84 °C. The flask was allowed to warm up at 0 °C. *B,B',B''*-trichloro-*N,N',N''*-tri[2-(methyl)phenyl]-borazine was cannulated dropwise to the organolithium solution at 0 °C and allowed to react at r.t. for 24 h. The reaction mixture was diluted with 15 mL of H<sub>2</sub>O, extracted with EtOAc (3 × 20 mL) and the combined organic phases dried over MgSO<sub>4</sub> and the solvents removed under reduced pressure. The product was purified by precipitation in MeOH (0.458 g, **42%**) as a white-yellow solid. A mixture of isomers was obtained and reported in the following characterisation.

**M.P.:** 220 °C. **<sup>1</sup>H-NMR** (400 MHz, CDCl<sub>3</sub>):  $\delta$  = 7.22-6.57 (*m*, 24 H), 3.88-3.79 (*m*, 12 H), 2.37-2.24 (*m*, 9 H), 2.07-2.01 (*m*, 12 H) ppm. **<sup>11</sup>B-NMR** (128 MHz, CDCl<sub>3</sub>):  $\delta$  = 36.65 ppm. **<sup>13</sup>C-NMR** (100 MHz, CDCl<sub>3</sub>):  $\delta$  = 153.01, 152.86, 152.21, 145.72, 145.48, 145.40, 135.50, 135.39, 134.40, 133.10, 133.07, 131.43, 131.23, 130.59, 129.41, 129.26, 128.46, 128.36, 127.46, 127.29, 124.11, 123.96, 123.86, 123.38, 123.31, 115.76, 115.38, 24.26, 24.16 19.44, 19.28, 19.15 ppm. **IR** (cm<sup>-1</sup>):  $\nu$  = 414.70, 460.99, 503.42, 547.78, 580.57, 655.80, 725.23, 758.02, 835.18, 858.32, 1028.06, 1105.21, 1157.29, 1207.44, 1261.45, 1359.82, 1415.75, 1490.97, 1591.27, 2160.27, 2866.22, 2960.73, 3057.17. **MS** (ESI-HRMS): Found 871.5253 [M+H]<sup>+</sup>, C<sub>51</sub>H<sub>58</sub>B<sub>3</sub>N<sub>12</sub> requires = 871.5210.

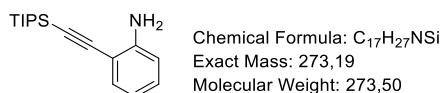


### ***B,B',B''*-tri[2-(isopropyl)phenyl]-*N,N',N''*-tri[2-(methyl)phenyl]-borazine 3-12**

In a flame-dried 100-mL *Schlenk* flask, 2-isopropylaniline (0.508 g, 3.76 mmol) was diluted with 6 mL of anhydrous toluene and cooled to -5 °C (ice-salt bath). A solution of BCl<sub>3</sub> (4.88 mL, 4.88 mmol, 1 M solution in heptane) was added dropwise. The septum was changed for a flame-dried condenser topped by a CaCl<sub>2</sub> tube and the resulting mixture refluxed for 16 h. The reaction solution was cooled down to 0 °C, the condenser was changed for a septum under argon, and the flask subjected to five *freeze-to-thaw* cycle to remove the remaining HCl. In parallel, to a flame-dried 100 mL *Schlenk* flask, 2-bromoanisole (0.77 g, 4.136 mmol) was dissolved in 9 mL of anhydrous THF and *n*-BuLi (2.82 mL, 4.512 mmol, 1.6 M

in hexane) added dropwise at -84 °C. The flask was allowed to warm up at 0 °C. *B,B',B''*-trichloro-*N,N',N''*-tri[2-(*iso*-propyl)phenyl]-borazine was cannulated dropwise to the organolithium solution at 0 °C and allowed to react at r.t. for 24 h. The reaction mixture was diluted with 15 mL of H<sub>2</sub>O, extracted with EtOAc (3 × 20 mL) and the combined organic phases dried over MgSO<sub>4</sub> and the solvents removed under reduced pressure. The product was purified by precipitation in MeOH (0.16 g, **17%**) as a white solid. The product was composed by a mixture of isomers which separation was not possible. The characterisation here reported corresponds to the mixture of isomers.

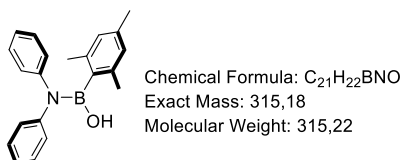
**M.P.:** >320 °C. **<sup>1</sup>H-NMR** (400 MHz, CDCl<sub>3</sub>):  $\delta$  = 7.23-6.24 (*m*, 24 H), 3.99-2.95 (*m*, 12 H), 1.33-0.70 (*m*, 18 H) ppm. **<sup>11</sup>B-NMR** (128 MHz, CDCl<sub>3</sub>):  $\delta$  = 35.98 ppm. **<sup>13</sup>C-NMR** (100 MHz, CDCl<sub>3</sub>):  $\delta$  = 160.36, 160.21, 160.16, 160.05, 159.95, 159.90, 145.02, 144.70, 144.52, 144.34, 144.30, 144.26, 144.03, 143.94, 143.57, 143.48, 143.38, 143.07, 143.00, 142.88, 134.73, 134.64, 134.38, 132.47, 131.63, 131.57, 131.41, 131.20, 130.02, 129.75, 129.69, 129.36, 129.20, 129.07, 128.63, 128.30, 128.25, 128.10, 128.07, 127.96, 124.97, 124.85, 124.79, 124.61, 124.43, 124.36, 124.23, 124.07, 123.96, 123.88, 123.78, 123.67, 123.45, 123.19, 123.01, 122.87, 122.78, 119.10, 119.01, 118.80, 118.78, 118.63, 118.60, 118.38, 108.35, 108.10, 108.04, 107.88, 107.77, 107.72, 107.68, 54.52, 53.84, 53.70, 53.63, 28.07, 27.94, 27.76, 27.06, 26.74, 26.65, 24.38, 24.25, 23.84, 23.76, 23.72, 23.59, 23.35, 23.22, 23.03, 22.94, 22.45 ppm. **IR** (cm<sup>-1</sup>):  $\nu$  = 418.55, 462.12, 528.51, 545.85, 640.37, 655.80, 698.23, 719.45, 725.24, 835.18, 862.18, 1029.99, 1147.31, 1178.51, 1244.09, 1303.88, 1427.32, 1446.61, 1485.19, 1571.99, 1597.06, 2866.22, 2929.87, 2958.80. **MS** (ESI-HRMS): Found 654.4545 [M+H]<sup>+</sup>, C<sub>48</sub>H<sub>55</sub>B<sub>3</sub>N<sub>3</sub>O<sub>3</sub> requires = 754.4497.



### 2-[(triisopropylsilyl)ethynyl]-aniline 3-14

To a degassed solution of 2-iodoaniline (2 g, 9.12 mmol) in *i*Pr<sub>2</sub>NH (20 mL), [PdCl<sub>2</sub>(PPh<sub>3</sub>)<sub>2</sub>] (0.190 g, 0.278 mmol) and CuI (0.050 g, 0.278 mmol) were added and the resulting solution degassed a second time. Finally, (triisopropylsilyl) acetylene (1.66 g, 9.12 mmol) was added, the reaction mixture degassed one last time and the final mixture stirred overnight at r.t. under nitrogen. The resulting mixture was filtered over celite and washed with CH<sub>2</sub>Cl<sub>2</sub> (20 mL) and EtOAc (20 mL). Removal of the solvents under vacuum and purification by column chromatography (Pet. Et. 100%) yielded **3-8** (2.39 g, **99%**) as a pallid yellow liquid.

**<sup>1</sup>H-NMR** (300 MHz, CDCl<sub>3</sub>):  $\delta$  = 7.33 (*dd*,  $J_1$  = 7.6 Hz,  $J_2$  = 1.3 Hz, 1 H), 7.15 (*dt*,  $J_1$  = 7.6 Hz,  $J_2$  = 1.3 Hz, 1 H), 6.71-6.65 (*m*, 2 H), 4.26 (*bs*, 2 H), 1.14 (*s*, 21 H) ppm. **<sup>13</sup>C-NMR** (75 MHz, CDCl<sub>3</sub>):  $\delta$  = 148.37, 132.54, 129.83, 117.83, 114.25, 108.38, 103.77, 96.01, 18.85, 11.39 ppm. **IR** (cm<sup>-1</sup>):  $\nu$  = 433.98, 723.31, 783.10, 840.96, 1111.00, 1240.23, 1315.45, 1278.34, 1460.11, 1489.05, 1612.49, 2142.91, 2341.58, 2360.87, 2864.29, 2954.95. **MS** (MALDI-HRMS): Found 274.1989 [M+H]<sup>+</sup>, C<sub>17</sub>H<sub>28</sub>NSi requires = 274.1991.



### 1-hydroxy-1-mesityl-N,N-diphenylboranamine 3-15

In a flame-dried 100-mL *Schlenk* flask, diphenylamine (0.636 g, 3.76 mmol) was diluted with 6 mL of anhydrous toluene and cooled to -5 °C (ice-salt bath). A solution of BCl<sub>3</sub>

(4.88 mL, 4.88 mmol, 1 M solution in heptane) was added dropwise. The septum was changed for a flame-dried condenser topped by a CaCl<sub>2</sub> tube and the resulting mixture refluxed for 16 h. The reaction solution was cooled down to 0 °C, the condenser was changed for a septum under argon, and the flask subjected to five *freeze-to-thaw* cycle to remove the remaining HCl. In parallel, to a flame-dried 100 mL *Schlenk* flask, 2-bromomesitylene (0.63 mL, 3.76 mmol) was dissolved in 9 mL of anhydrous THF and *n*-BuLi (2.82 mL, 2.82 mmol, 1.6 M in hexane) added dropwise at -84 °C. The flask was allowed to warm up at 0 °C. The first mixture was cannulated dropwise to the *organolithium* solution at 0 °C and allowed to react at r.t. for 24 h. The reaction mixture was diluted with 15 mL of H<sub>2</sub>O, extracted with EtOAc (3 × 20 mL) and the combined organic phases dried over MgSO<sub>4</sub> and the solvents removed under reduced pressure. The product was purified by chromatography column (0.128 g, **10%**) as a yellowish solid.

**M.P.:** 189 °C. **<sup>1</sup>H-NMR** (400 MHz, CDCl<sub>3</sub>):  $\delta$  = 7.49-7.21 (*m*, 5 H), 7.16-6.92 (*m*, 5 H), 6.78 (*s*, 2 H), 4.47 (*s*, 1 H), 2.41 (*s*, 6 H), 2.27 (*s*, 3 H) ppm. **<sup>11</sup>B-NMR** (128 MHz, CDCl<sub>3</sub>):  $\delta$  = 32.79 ppm. **<sup>13</sup>C-NMR** (75 MHz, CDCl<sub>3</sub>):  $\delta$  = 147.54, 146.37, 139.34, 137.87, 129.35, 128.27, 127.89, 127.30, 125.80, 125.42, 123.93, 22.14, 21.29 ppm (the <sup>13</sup>C resonance corresponding to the carbon atom bonded to the boron atom is not observed due to the quadrupolar relaxation). **IR** (cm<sup>-1</sup>):  $\nu$  = 414.70, 460.99, 503.42, 547.78, 580.57, 655.80, 725.23, 758.02, 835.18, 858.32, 1028.06, 1105.21, 1157.29, 1207.44, 1261.45, 1359.82, 1415.75, 1490.97, 1591.27, 2160.27, 2866.22, 2960.73, 3057.17. **MS** (ESI-HRMS): Found 316.1860 [M+H]<sup>+</sup>, C<sub>21</sub>H<sub>23</sub>BNO requires = 316.1873.

